PACIFIC EARTHQUAKE ENGINEERING
RESEARCH CENTER

Performance Improvement of Long Period Building Structures Subjected to Severe Pulse-Type Ground Motions

James C. Anderson
University of Southern California

Vitelmo V. Bertero
University of California, Berkeley

Raul D. Bertero
Universidad de Buenos Aires

Report to sponsors: CUREe/Kajima Corporation

PEER 1999/09
OCT. 1999

Performance Improvement of Long Period Building Structures Subjected to Severe Pulse-Type Ground Motions

James C. Anderson
University of Southern California

Vitelmo V. Bertero
University of California, Berkeley

Raul D. Bertero
Universidad de Buenos Aires

Report to sponsors CUREe/Kajima Corporation

PEER Report 1999/09
Pacific Earthquake Engineering Research Center
College of Engineering
University of California, Berkeley

October 1999

ABSTRACT

It has been known since the 1950s that under certain conditions, earthquake ground motions can consist of a limited number of strong acceleration pulses. These types of ground motions have come to be referred to as "pulse-type" ground motions. However, it has only been recently, following the Northridge earthquake (1994), that their importance for the earthquake resistant design of civil engineering structures has been recognized and introduced into the seismic provisions of building codes through the introduction of the near-source factor [UBC, 1991-1997]. In an earlier paper [Anderson and Bertero, 1987] it was shown that the deflections, including lateral displacement, interstory drift and inelastic rotation, in a mid-rise steel building were increased significantly when the moment frame was subjected to ground motions recorded in the near fault region during the Imperial Valley earthquake (1979). It has been shown that these types of ground motion can be particularly severe on the lower story levels causing increased drift demands and concern over increased second order P-Δ effects. Following the Northridge earthquake concerns were expressed for the safety of highrise buildings which may be subjected to pulse-type motions. Thus it was decided to conduct the current study of medium to tall buildings having long periods. In addition to considering the performance of the existing buildings, both traditional strategies and innovative procedures for improving the performance of these structural systems were investigated.

The results obtained for two steel buildings and two reinforced concrete buildings are reported in this paper. Three of the buildings are existing structures dating from as early as 1965. The buildings range in height from 15 stories to 41 stories with lateral resistance provided by moment resistant frames. Fundamental periods of vibration range from 1.78 seconds for the 30-story RC frame to 3.2 seconds for the 15-story RC frame to 5.4 seconds for the 41-story steel frame. The results of inelastic dynamic analyses using four recorded pulse-type ground motions indicated that the maximum interstory drift requirement for these structures was excessive, ranging between 3.5% and 5.4%. For these reasons it was decided to investigate strategies for improving the performance of these buildings.

The conventional strategy for improving the performance is to stiffen and strengthen the system. For steel frames, this usually implies the addition of lateral bracing in the form of diagonal bracing or chevron bracing. For the RC frames, the use of various shear wall configurations was considered for one and the application of steel joint jackets and confinement plates was considered for the other. These techniques did not prove to be very efficient for this group of longer period structures. The displacements were reduced but the inertia forces and story shears were increased significantly. Stiffening a longer period building shortens the period and shifts the structure to a higher acceleration level on the response spectrum of the input motion. Based on these results it was decided that some form of energy dissipation was required. An attractive means of accomplishing this appeared to be the use of supplemental (passive) damping.

It was recognized that for a single acceleration pulse, damping is not very effective in decreasing the response. However, in view of the fact that the peak value of the velocity pulse is very high and that the recorded pulse-type motions contain at least three severe pulses, it was decided to attempt the use of such a strategy. Manufacturers of fluid-viscous dampers claim that structural damping can be increased to 20% to 50% of critical damping through the use of a sufficient number of damping devices. For purposes of this study a damping of 30% of critical was used. Results of using supplemental damping proved very encouraging in these initial studies. The maximum interstory drift of 5.4% was reduced to 2.1% and the corresponding plastic rotation demands were reduced to 2.1%. Similar types of reductions in force and displacement demands, although not as dramatic, were attained for all of the structures. While it should be emphasized that these are the results of initial studies, the use of supplemental damping for improving the seismic performance of tall buildings subjected to pulse-type ground motions appears to be very promising.

ACKNOWLEDGMENTS

This report is based on the results of studies that have been conducted by the authors as part of the CUREe/Kajima Phase III study. These studies which are under the general heading of "Structural Design for Near-Field Effects," are part of the main research project on "Near Field Ground Motions." This research project has been supported by a grant provided by the Kajima Corporation and administered by CUREe (California Universities for Research in Earthquake Engineering). The financial support from Kajima is gratefully acknowledged. The assistance of Dr. Akira Endoh of Kajima in managing the project and of Professor Helmut Krawinkler in the overall direction of this section of the investigation are also appreciated. The analyses of the 15-Story RC Building that were conducted by Mr. Mehrdad Sasani, a graduate student at UC/Berkeley, are gratefully acknowledged.

This work made use of Pacific Earthquake Engineering Research Center Shared Facilities supported by the Earthquake Engineering Research Center Program of the National Science Foundation under Award Number EEC-9701568.

CONTENTS

LIST OF TABLES

LIST OF FIGURES

Section 5.3

Section 5.4

Section 6.2

Section 6.3

Section 6.5

Section 6.6

Section 6.7

1 Introduction

1.1 STATEMENT OF PROBLEM

Recent studies have shown that severe pulse-type ground motions may significantly increase the seismic lateral displacement and consequently the interstory drift and inelastic rotation demands on long period structures. In extreme cases, such demands, coupled with the action of the gravity load, may pose a collapse hazard. This is particularly true for certain frame-type structures in which the drift demand in the story levels near the base may be amplified by severe displacement pulses and P-delta effects. Special precautions will have to be taken to insure adequate performance at both the damage control and life safety levels. The use of just the traditional strategy of increasing the members' strength and/or stiffness alone may lead to inadequate and inefficient means of mitigating the problems. Thus it was decided to carry out the studies reported herein which have the following main objectives.

2 Objectives and Scope

2.1 MAIN OBJECTIVES

The main specific objectives of the study were as follows:

1. To conduct a survey of recorded severe pulse-type Earthquake Ground Motions (EQGMs).

2. To carry out parametric studies of the main dynamic characteristics of idealized as well as recorded severe pulse-type EQGMs.

3. To investigate the effects of severe pulse-type EQGMs on the dynamic response (seismic performance) of long period (medium to tall) building structures.

4. To investigate and determine the most promising changes that can be introduced in the structural system of existing medium to high rise buildings using traditional strategies in order to improve their performance under severe pulse-type base motions and possible periodic type of ground motions.

5. To investigate which types of passive energy dissipation devices are more promising for improving the performance of the structural system and to evaluate their effectiveness in modifying the building response to severe pulse-type EQGMs.

2.2 SCOPE

To achieve the above objectives, the following tasks were carried out:

Task 1. Survey recorded EQGMs containing severe acceleration and/or velocity and/or displacement pulses.

Task 2. Conduct linear and nonlinear time-history dynamic analysis of the response of Single-Degree-of-Freedom System to severe pulse-type EQGMs (idealized and recorded) to develop Linear and Nonlinear Response Spectra considering the effects of variation in ductility (μ) and damping (ξ) on the Seismic Coefficient (C_y = Pseudo Acceleration/g), Displacement (u), Input Energy (E_I/M), Hysteretic Energy (E_H/M), Damage Parameter (γ), and Interstory Drift Index (IDI).

Task 3. Review results of previous studies of medium and highrise building response to seismic ground motions and inventory the building systems that have been considered. Select buildings having representative lateral force systems for further study and develop models for nonlinear dynamic analyses.

Task 4. Conduct nonlinear dynamic analyses on the building models obtained from Task 3, considering the response of the buildings to the ensemble of near-fault ground motions obtained in Task 1, and an ensemble of frequent, periodic type ground motions. Compare behavior and identify those systems having the most promise for controlling the response.

Task 5. Investigate structural modifications to those framing systems indicating relatively poor performance under severe pulse-type base motions, using traditional strategies and techniques to improve performance.

Task 6. Investigate the addition of efficient supplemental passive energy dissipation devices to improve the response of the structural systems identified as having poor performance in Task 4.

3 Survey of Recorded Severe Pulse-Type Earthquake Ground Motions

3.1 INTRODUCTORY REMARKS

A critical and historical review of pulse-type EQGMs (which in the past were also frequently denominated as Impulse EQGMs) has been done by Bertero et al. in 1999 [*Proceedings*, 1999 SEI Structures Congress, 19-21, April, 1999]. A copy of this review is attached as **Appendix A**. Guided by these results, the authors decided to concentrate on the analysis of the following records: (1) the recorded near-fault EQGMs considered by the Seismology Committee of the Structural Engineers Association of California (SEAOC) in the development of the new strength design recommendations published in the Sixth Edition of the SEAOC Blue Book [1996] and reproduced in **Tables 3.1 through 3.3** and (2) the recorded EQGMs considered by Alavi and Krawinkler [1997] that are given in **Table 3.4**.

3.2 SELECTION OF SEVERE PULSE-TYPE EQGMs TO BE CONSIDERED IN THIS STUDY

In order to identify the severe pulse-type EQGMs critical to the seismic response of medium to highrise buildings (i.e., buildings with a $T \geq 1.5$ seconds), response spectra for Single-Degree-of Freedom-Systems (SDOFS) were investigated for different dynamic parameters so as to judge their damage potential considering the attainable ductility (μ) and additional damping (ξ) with which these buildings could be supplied.

Table 3.1 Pre-Northridge Earthquake Records Close to Fault Rupture (After SEAOC, 1996)

Instrument Name/ Location	Magnitude	Earthquake Name and Year
Pacoima Dam	M = 6.6	1971 San Fernando, CA earthquake
Karakyr Point	M_S = 7.0	1976 Gazli (Russia) earthquake
El Centro Array Nos. 5,6,7	M_L = 6.6	1979 Imperial Valley, CA earthquake
Tabas	M = 7.4	1979 Tabas (Iran) earthquake
Site 1	M_S = 6.9	1985 Nahanni (Canada) earthquake
Corralitos	M_S = 7.1	1989 Loma Prieta, CA earthquake
Cape Mendocino	M_S = 6.9	1992 Petrolia earthquake
Lucerne Valley	M_S = 7.5	1992 Landers, CA earthquake

Table 3.2 1994 Northridge Earthquake Records (Sites ≤ 15 km from Fault Rupture) (After SEAOC, 1996)

Instrument Station Information		Peak Response		Distance to Fault Rupture (km)
Name	Site	PGA (g)	$SA_{1.0}$ (g)	
Jensen Filter Plant - Generator Bldg.	N/A	0.98/0.56	> 0.90	0
Newhall - County Fire Station	Soil	0.63/0.61	> 0.90	0
Rinaldi Receiving Station	Soil	0.85/0.48	> 0.90	0
Sylmar Converter Station (East)	Rock	0.79/0.45	> 0.90	0
Sylmar Converter Station	Soil	0.90/0.61	> 0.90	0
Sepulveda VA Hospital	N/A	0.94/0.74	0.7	0
Sylmar County Hospital	Soil	0.91/0.61	0.75	2
Arleta - Nordhoff Ave. Fire Station	Soil	0.35/0.29	0.6	7
Pacoima - Kagel Canyon	Rock	0.44/0.30	0.45	9
Castaic - Old Ridge Route	Rock	0.59/0.54	0.35	10
Lake Hughes 12A	Soil	0.26/0.18	0.35	12
Energy Control Center	Rock	0.23/0.21	0.4	12
Santa Susana -ETEC	N/A	0.29/0.23	0.25	14

Table 3.3 1994 Northridge Earthquake Ground Motion Recorded Near-Fault Rupture

Recording Station			Site Geology	Distance from Fault (km)		Maximum Acceleration	
Name	Owner (Instrument No.)	Location		Epicenter	Fault Rupture	Comp.	PGA (g)
Sepulveda VA Hospital	VA (NSMP)	Ground level		7	10	360°	0.94
						Up	0.48
						270°	0.74
Rinaldi Receiving Station	LADWP (5968)	Free field	Alluvium	10	5	318°	0.48
						Up	0.85
						228°	0.84
Arleta Nordhoff Ave. Fire Station	CDMG (CSMIP 24087)	Ground level	Alluvium	10	15	90°	0.35
						Up	0.59
						360°	0.29
Jensen Filter Plant Generator Building	MWD (NSMP)	Ground level		12	5	022°	0.56
						Up	0.52
						292°	0.98

Recording Station			Site Geology	Distance from Fault (km)		Maximum Acceleration	
Name	Owner (Instrument No.)	Location		Epicenter	Fault Rupture	Comp.	PGA (g)
Sylmar Converter Station (SCS)	LADWP (306-3)	Free field	Alluvium	12	5	052°	0.61
						Up	0.64
						142°	0.90
Sylmar Converter Station East (SCSE)	LADWP (6273)	Free field	Rock	13	5	015°	0.83
						Up	0.38
						285°	0.49
Sylmar LA County Hospital	CDMG (CSMIP 24514)	Free field	Alluvium	16	5	360°	0.91
						Up	0.60
						90°	0.61
Newhall LA County Fire Station	CDMG (CSMIP 24279)	Ground level	Alluvium	20	5	90°	0.63
						Up	0.62
						360°	0.61

Table 3.4 Near Field Ground Motion Records [Alavi and Krawinkler, 1997]

NEAR-FIELD TIME HISTORIES
Fault-Normal Component

SAC Name	Earthquake	Mw	Mechanism[1]	R, km	Station	Site[2]	PGA, g's
Recorded:							
NF01	Tabas, 1978	7.4	th	1.2	Tabas	D	0.90
NF03	Loma Prieta, 1989	7.0	ob	3.5	Los Gatos	D_1	0.72
NF05	Loma Prieta, 1989	7.0	ob	6.3	Lex. Dam	D_1	0.69
NF07	C. Mendocino, 1992	7.1	th	8.5	Petrolia	D_1	0.64
NF09	Erzincan, 1992	6.7	ss	2.0	Erzincan	D	0.43
NF11	Landers, 1992	7.3	ss	1.1	Lucerne	D_1	0.71
NF13	Northridge, 1994	6.7	th	7.5	Rinaldi	D	0.89
NF15	Northridge, 1994	6.7	th	6.4	Olive View	D	0.73
NF17	Kobe, 1995	6.9	ss	3.4	Kobe JMA	D_1	1.09
NF19	Kobe, 1995	6.9	ss	4.3	Takatori	D	0.79
Simulated:							
NF21	Elysian Park 1	7.1	th	17.5		D_1	0.86
NF23	Elysian Park 2	7.1	th	10.7		D_1	1.01
NF25	Elysian Park 3	7.1	th	11.2		D_1	0.92
NF27	Elysian Park 4	7.1	th	13.2		D_1	1.80
NF29	Elysian Park 5	7.1	th	13.7		D_1	1.16
NF31	Palos Verdes 1	7.1	ss	1.5		D_1	0.97
NF33	Palos Verdes 2	7.1	ss	1.5		D_1	0.79
NF35	Palos Verdes 3	7.1	ss	1.5		D_1	0.97
NF37	Palos Verdes 4	7.1	ss	1.5		D_1	0.87
NF39	Palos Verdes 5	7.1	ss	1.5		D_1	0.92

1. Codes for mechanism:
   ss- strike-slip; ob- oblique; th- thrust
2. Codes for site:
   D- soil; D1- rock converted to soil

4 Linear and Nonlinear Time-History Analysis of the Response of SDOFS to Idealized and Recorded Severe Pulse-Type EQGMs

4.1 GENERAL REMARKS

According to results obtained in studies conducted prior to the 1989 Loma Prieta EQ, a review by Bertero et al. [1999], and the results of recent investigations conducted by Sasani and Bertero [1997], the authors decided that the main parameters controlling the elastic linear and particularly the nonlinear (inelastic) performance of long period building structures are the following:

- The required ***Seismic Coefficient*** C_s that in the case of the safety performance level is considered to be equal to the ***Yield Seismic Resistance Coefficient*** C_y and which is assumed to be equal to the Spectral Pseudo Acceleration (S_{pa}) divided by the acceleration of gravity (g). Thus there is a need to estimate the response spectra for this parameter.

- The expected or ***Demanded Displacement u*** and therefore its response spectra.

- The ***Interstory Drift Index (IDI)***. For long period (**T**) it can be expected that the inelastic displacement would be similar to the elastic displacement; it can also be expected that the inelastic $(IDI)_{in}$ would be similar to the elastic $(IDI)_{el}$. Thus only the response spectra for the elastic IDI were considered. However, the authors believe that while these assumptions might be acceptable for preliminary EQ-Resistant Design (EQ-RD), their validity can be seriously questioned for verifying the actual performance, particularly in the case of significant global inelastic deformation [global ductility, i.e., $(\mu_\delta)_{gl}$].

- ***The Input Energy*** (E_I) and particularly the ***Hysteretic Energy*** ($E_{H\mu}$), ***(or*** E_H ***to simplify the notation)*** that can be dissipated by inelastic (plastic) deformation, and the Hysteretic Energy ($E_{H\xi}$) that can be dissipated by damping (ξ).

- ***The Damage Index or Damage Parameter*** (γ) suggested by Fajfar [1992].

The linear elastic and nonlinear inelastic response spectra of SDOFSs with ductility μ equal to 1, 1.5, 2, 3, and 6 and for $\xi = 5\%$ and $\xi = 30\%$ were computed and plotted for T varying from 0 to 4 seconds considering the time history of idealized and recorded severe pulse-type EQGMs.

4.2 IDEALIZED SEVERE PULSE-TYPE EQGMS

In the studies conducted in the 1970s, Bertero and his research associates studied the effects of trapezoidal (near rectangular) severe acceleration pulses (Bertero et al, 1976). Sasani and Bertero [1997] carried out studies of the effects of a half sine cycle and one full sine cycle of acceleration pulses, and then one full sine cycle of sine velocity and displacement pulses on SDOFSs. These studies were repeated for a series of these severe pulses, up to 10, to get an idea of how their effects vary when they become periodical types of EQGMs. In 1997, Alavi and Krawinkler reported studies using three basic pulse shapes: one-directional pulse, two-directional pulse, and multiple pulses. In these basic pulses, the acceleration history is described by square waves. However, to consider the effects of rise time on response parameters, modified versions considering triangular types of pulses were also considered.

After reviewing the results obtained in the above studies, it was decided to simulate the possible effects of recorded severe pulse-type EQGMs by an idealized pulse-type history of acceleration consisting of three successive half sine individual pulses that lead to a full sine reversal cycle of velocity and half sine cycle of displacement as illustrated in **Figure 4.1**. The duration and intensity of these pulses were selected to match as close as possible the most severe cycle of pulses recorded at any specific site (station). The idealized acceleration pulses, shown in **Figure 4.1,** are originated by one positive half-sine pulse of 0.4 second, followed by a negative half-sine pulse of 0.8 seconds and another positive half-sine pulse of 0.4 seconds. These were created to fit the largest building (SDOFS) response to the recorded EQGMs at the Takatori station in the direction normal to the fault.

4.3 SELECTION OF NEAR-FAULT RECORDED EQGMs

The two horizontal components of the recorded EQGMs considered by Alavi and Krawinkler [1997], shown in Table 3.4, have been studied and their effects on the main response parameters discussed previously (Section 4.1) have been analyzed. Herein, only the results obtained under the horizontal fault normal component of the records obtained at the Los Gatos and Takatori stations are presented and discussed. These are the ones that give the higher displacement demands for buildings with T $\geq$ 1.5 seconds [Alavi and Krawinkler 1997] as shown in **Figure 4.2**.

4.4 LINEAR AND NONLINEAR RESPONSE SPECTRA OF IDEALIZED AND RECORDED SEVERE PULSE-TYPE EQGMs

4.4.1 Idealized Severe Pulse

Response spectra are shown in **Figure 4.3** for ξ = 5% and in **Figure 4.4** for ξ = 30%. The results presented in **Figure 4.3** clearly indicate the following: (1) the demanded displacements for a nonlinear system (μ > 1.0) are not the same as those demanded by a linear system (μ = 1.0), even in the case of long period (T > 1.5 sec) and (2) it will be very difficult to design and construct buildings with more than ten stories (H $\geq$ 30m) using conventional procedures if the IDI is required

to be smaller than 2%.

Comparison of response spectra given in **Figure 4.4** for $\xi = 30\%$ with those of **Figure 4.3** for $\xi = 5\%$ shows a significant reduction in the response when the ξ increases from 5% to 30%, particularly for low values of μ and a T close to that corresponding to the peak response. For example, the C_y at 1.5 sec for $\mu = 2$ decreases from a value of about 1.0 to 0.58. The larger the μ, the smaller the reduction due to an increase in ξ. Similar reduction is observed in the demanded displacement and IDI. The E_I and E_H are also reduced significantly. This reduction of response spectra with increase in ξ is a somewhat welcome surprise since from the results obtained in studies conducted using single acceleration pulse excitation, it has usually been assumed that for a single pulse an increase in damping will not be effective.

4.4.2 Recorded EQGMs

Takatori 1. The response spectra for $\xi = 5\%$ are shown in **Figure 4.5** and for $\xi = 30\%$ are given in **Figure 4.6**. Comparing these spectra with those for the idealized pulse of **Figures 4.3** and **4.4**, the following can be observed: (1) While the values of the C_y spectra are similar, those for the u (displacement) and the IDI are somewhat different, with the larger peak value due to the Takatori 1 record; (2) The E_I and E_H for the Takatori 1 ground motion have peak values higher than those for the idealized pulse; (3) The Takatori 1 spectra are more rugged than those corresponding to the idealized pulse; and (4) The reductions due to an increase in ξ are higher for the Takatori 1 record.

Los Gatos 1. The response spectra for $\xi = 5\%$ are illustrated in **Figure 4.7** and those for $\xi = 30\%$ in **Figure 4.8**. When the Los Gatos 1 spectra are compared to those corresponding to the Takatori 1 EQGM, it can be seen that there are significant differences as can be expected from analyses of the results obtained by Alavi and Krawinkler [1997] and shown in **Figure 4.2**. This comparison leads to the following observations: (1) Up to a period, T = 2.3 sec, the Takatori 1 EQGM demands a larger C_y; (2) For periods, $T \geq 2.4$ sec, the Los Gatos 1 record demands a higher value for the u, IDI, E_I, and E_H; and (3) The reduction in the spectra values due to an increase in ξ is somewhat higher for the Los Gatos 1 record.

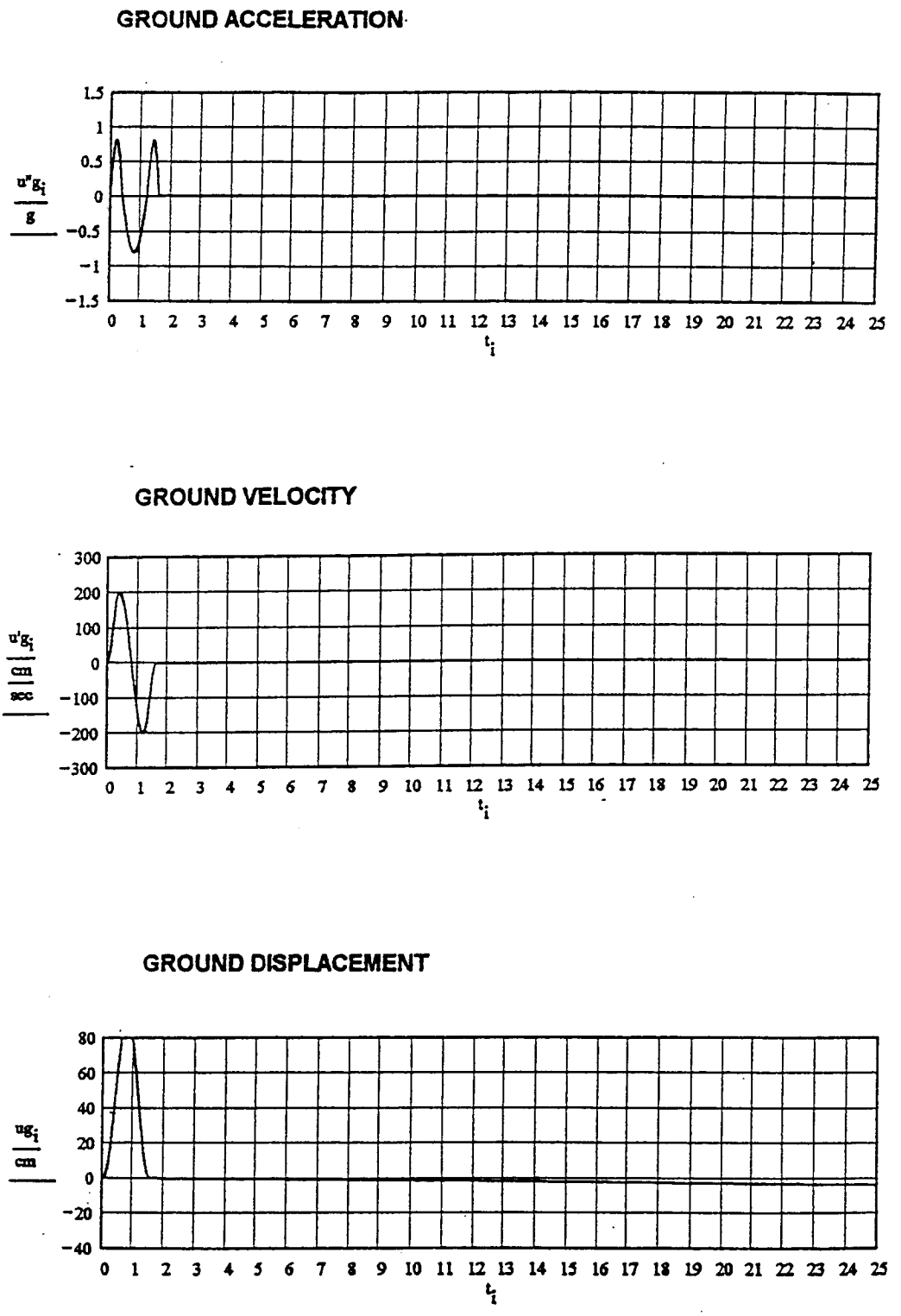

Figure 4.1 Idealized Pulse-Type Earthquake Ground Motion

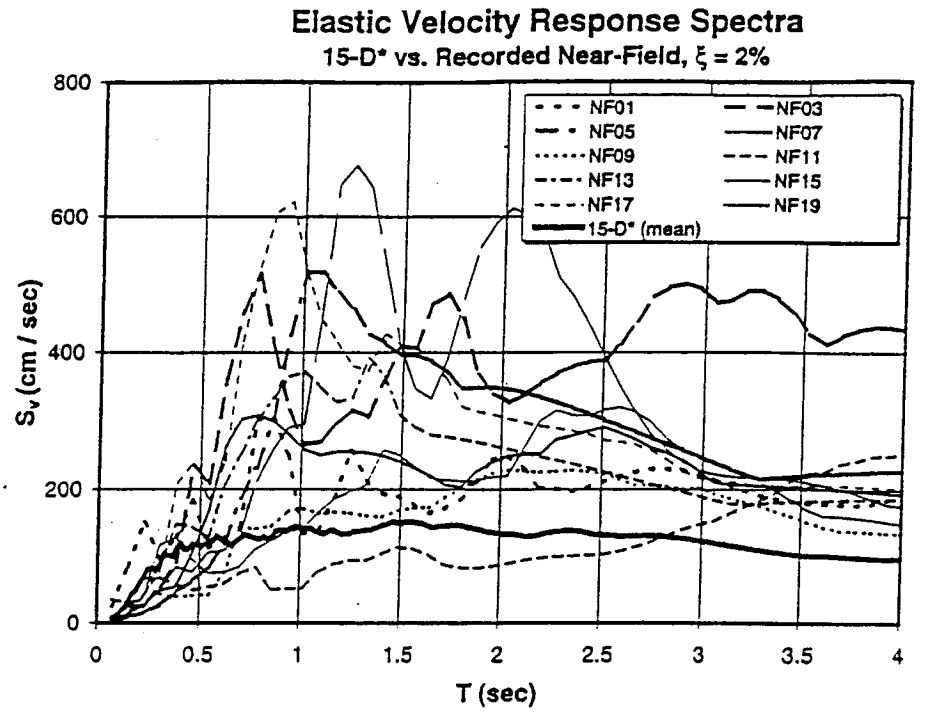

Velocity Response Spectra of Near Field and Reference Ground Motions

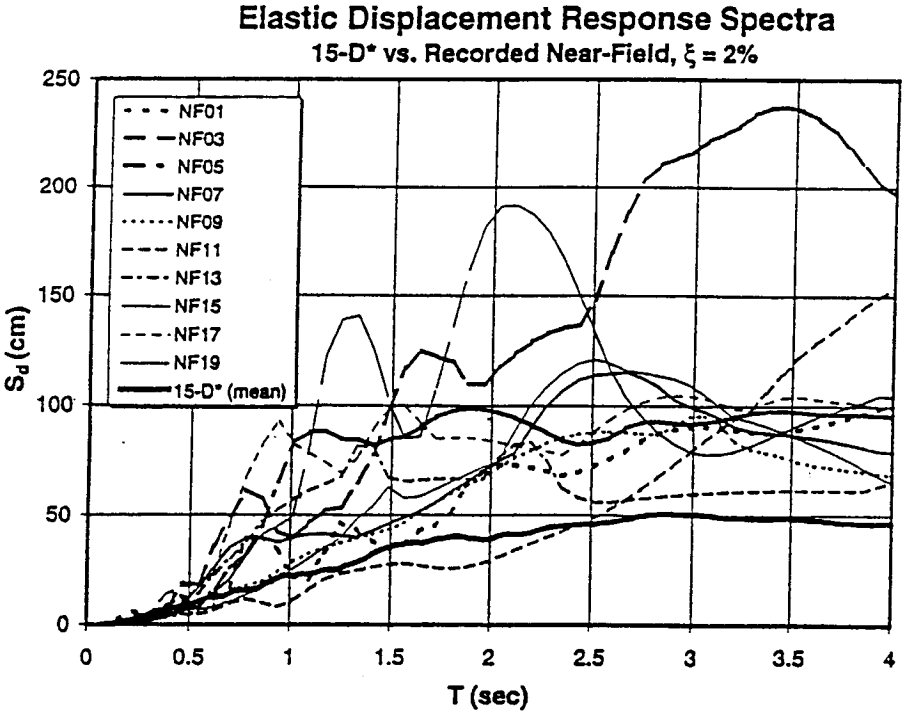

Displacement Response Spectra of Near Field and Reference Ground Motions

Figure 4.2 Spectra of Recorded Near Field Ground Motions (after Alavi and Krawinkler, 1997)

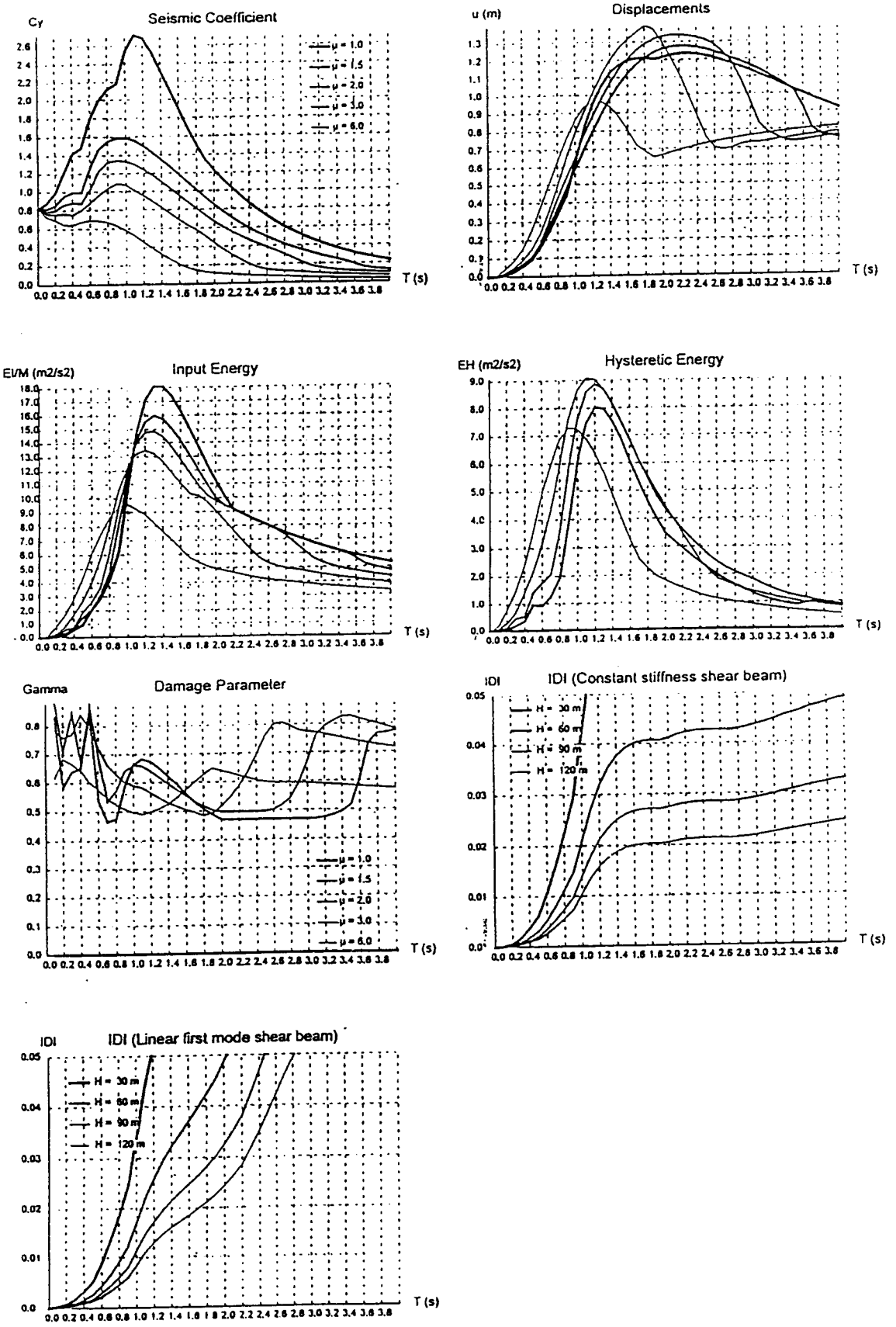

Figure 4.3 Linear and Nonlinear Response Spectra,
Idealized Pulse, ξ=5%

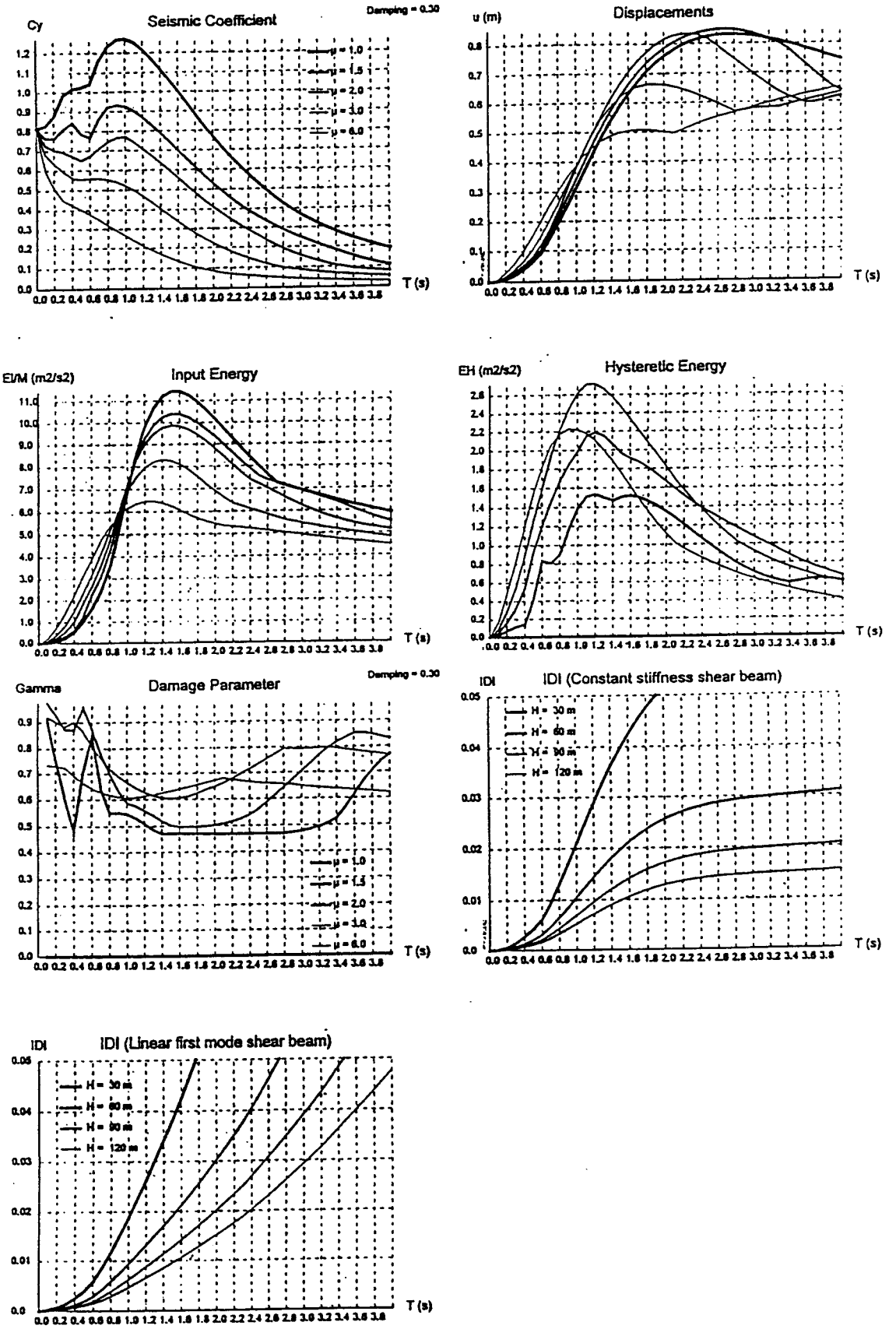

Figure 4.4 Linear and Nonlinear Response Spectra,
Idealized Pulse, ξ=30%

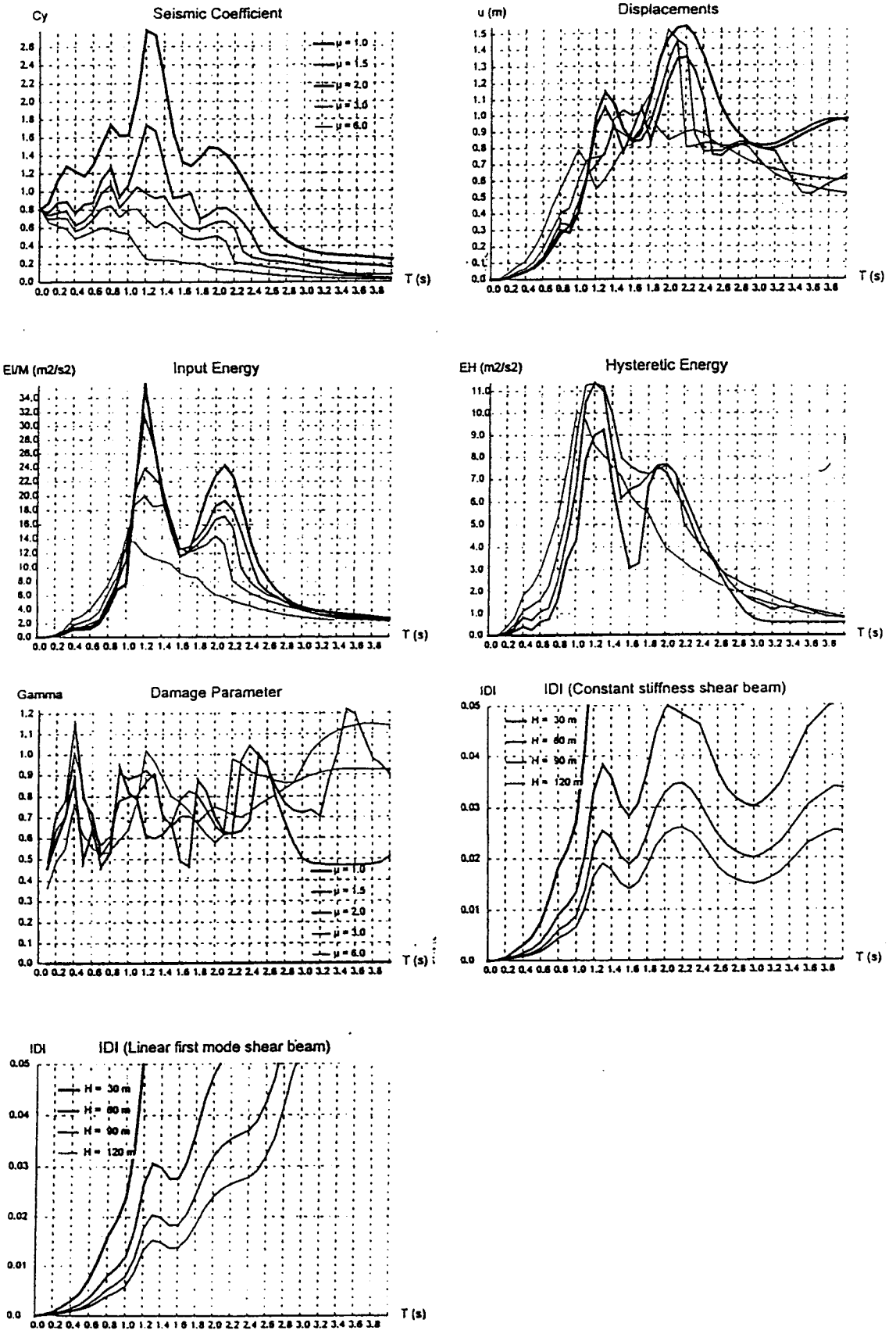

Figure 4.5 Linear and Nonlinear Response Spectra,
Takatori 1, ξ=5%

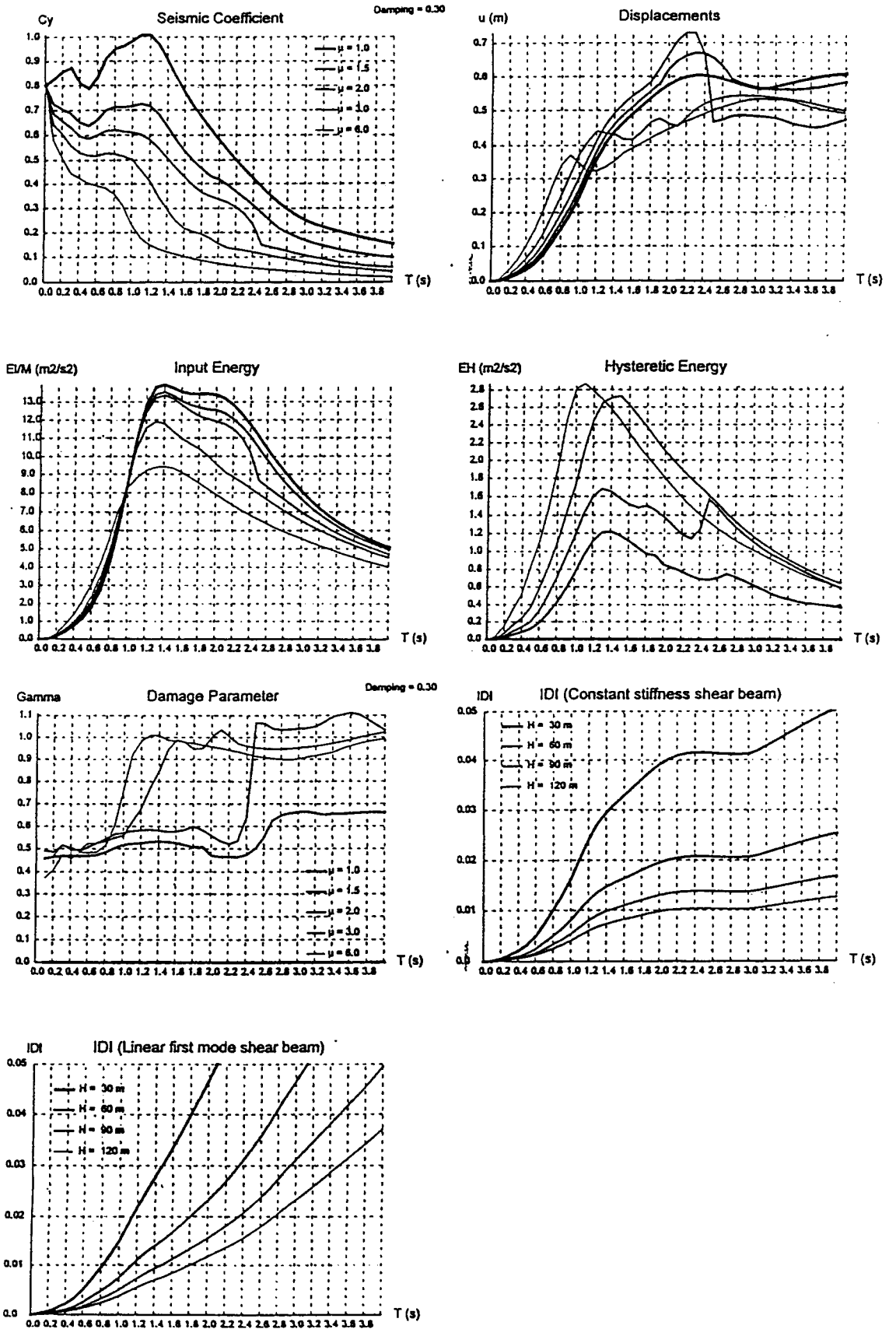

Figure 4.6 Linear and Nonlinear Response Spectra,
Takatori 1, ξ=30%

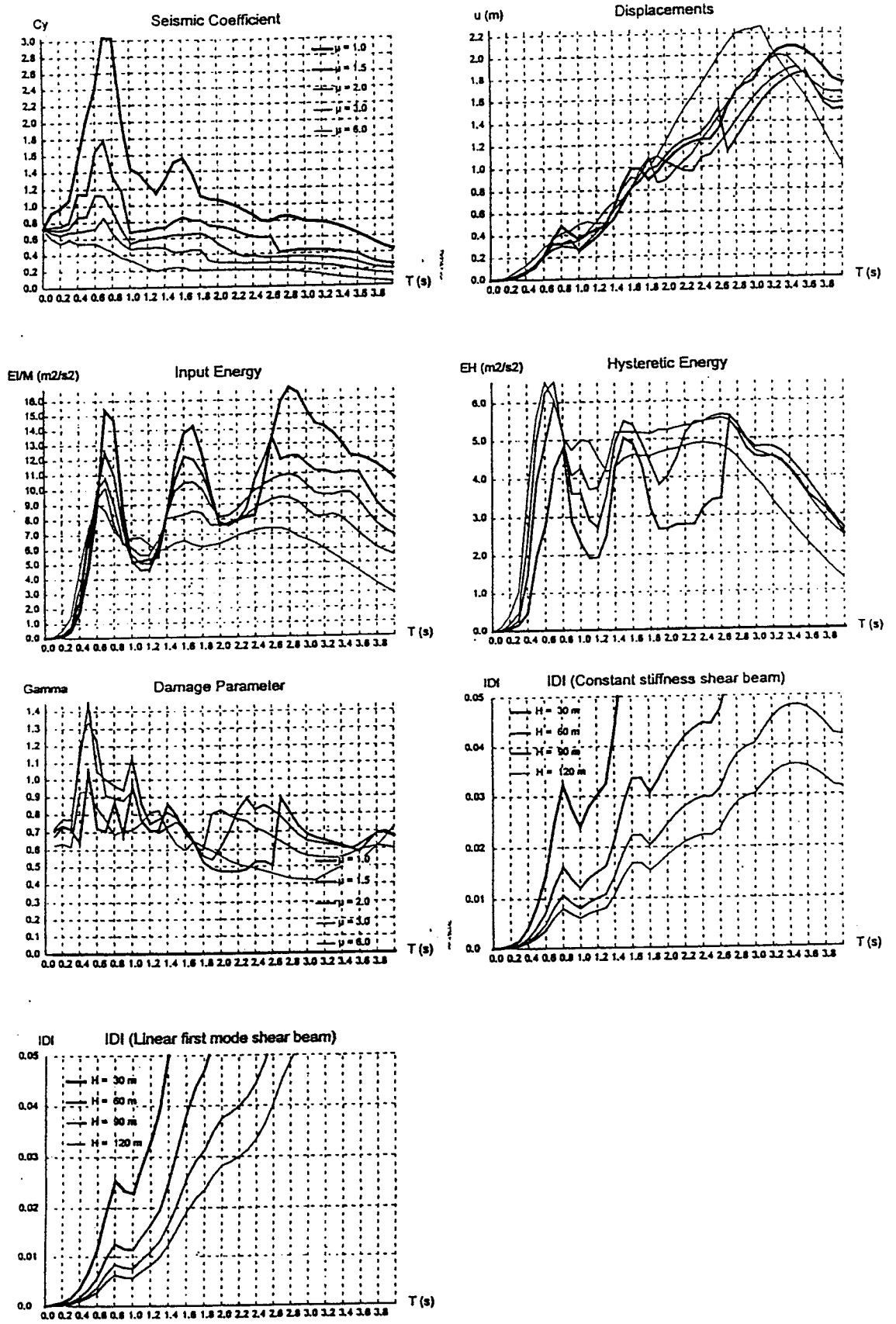

Figure 4.7 Linear and Nonlinear Response Spectra,
Los Gatos 1, ξ=5%

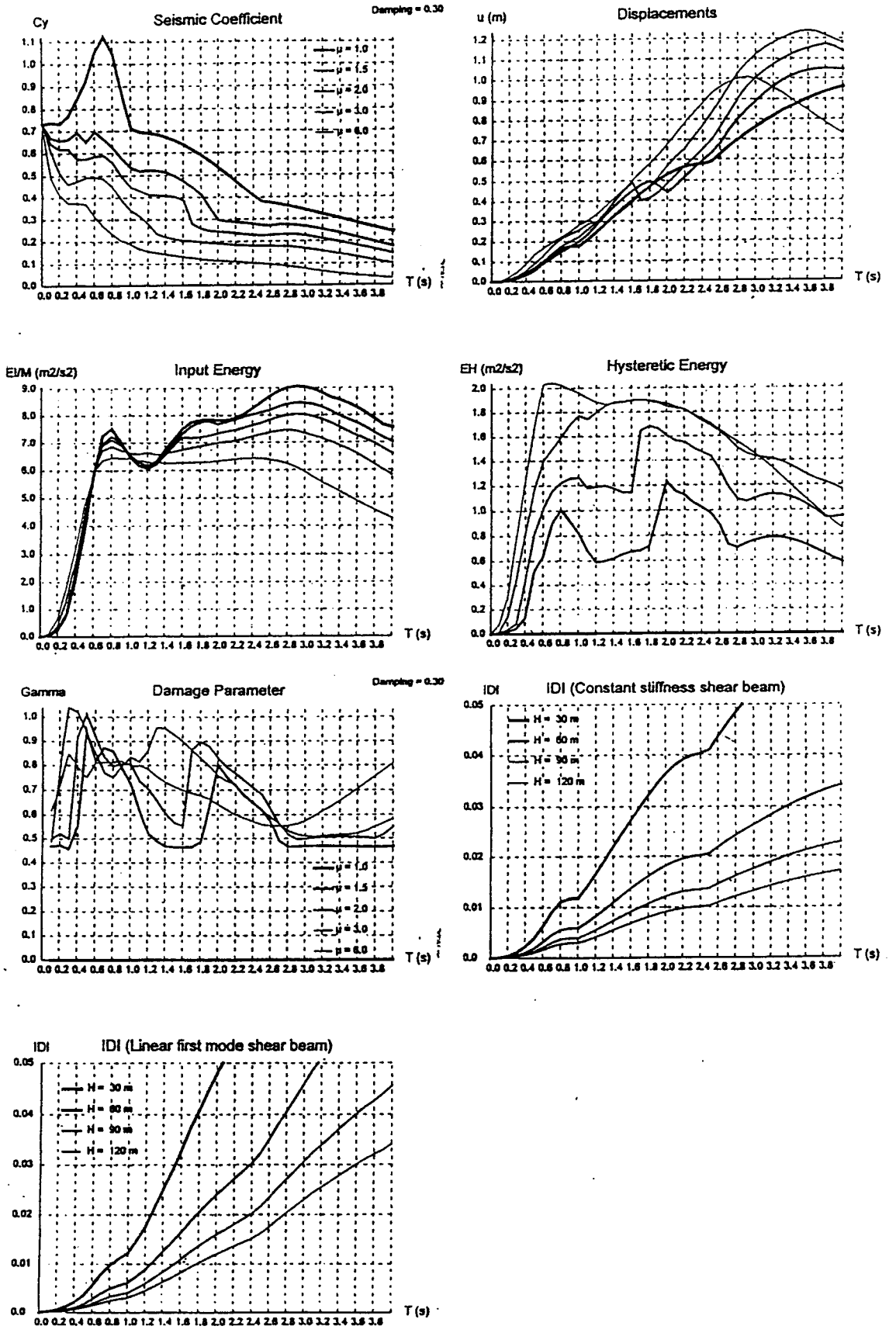

Figure 4.8 Linear and Nonlinear Response Spectra,
Los Gatos 1, ξ=30%

5 Effects of Severe Pulse-Type EQGMs on the Dynamic Response (Seismic Performance) of Long Period Building Structures

5.1 REVIEW OF RESULTS OF PREVIOUS STUDIES ON RESPONSE OF MEDIUM AND HIGHRISE BUILDINGS TO SEISMIC GROUND MOTIONS AND SELECT BUILDINGS FOR CONDUCTING ANALYSIS OF THE EFFECTS OF SEVERE PULSE-TYPE EQGMs

From a review of the different buildings which have been analyzed for seismic performance by the authors and from the results obtained in such analyses, it was decided to conduct additional analyses of the effects of severe pulse-type EQGMs on the following buildings.

- **30-Story RC S-K Building** redesigned using performance-based engineering through the Comprehensive Conceptual Approach [Bertero, R. D., and Bertero, V. V., 1992].
- **30-Story RC S-K Building** as built in 1983.
- **30-Story RC S-K Building** redesigned for UBC 1991 [Anderson and Chen, 1992].
- **15-Story RC Building** as built in 1965.
- **41-Story Steel Space Frame** as built in 1972 [Anderson and Bertero, 1998].
- **20-Story Steel Perimeter Frame** as designed for UBC 1994.

5.2 THE 30-STORY RC S-K BUILDING REDESIGNED USING PERFORMANCE-BASED ENGINEERING

5.2.1 General Configuration and Structural Layout

This building has the same configuration and structural layout as the original structure built in Japan. Typical floor plans are shown in **Figure 5.2.1** and elevations are shown in **Figure 5.2.2**. The building was redesigned using a comprehensive conceptual EQ-RD methodology [R. D. Bertero and V. V. Bertero, 1992] which is one of the approaches proposed in 1995 for Performance-Based Engineering [SEAOC Vision 2000 Committee, 1995]. The periods for the first 9 modes of the analyses are given in **Table 5.1**.

Table 5.1 Periods for the First 9 Modes

Mode	Period (sec.) e_{st}	Period (sec.) $e_{st} + e_{acc}$
1	1.70	1.78
2	1.69	1.69
3	1.63	1.56
4	0.59	0.62
5	0.59	0.59
6	0.57	0.54
7	0.34	0.35
8	0.34	0.34
9	0.32	0.31

5.2.2 Nonlinear Dynamic Time-History Analysis

Using the response spectra graphs developed for SDOF systems with constant ductility (μ = 1, 1.5, 2, 3, and 6) and for ξ = 5% and considering all the recorded severe pulse-type EQGMs shown in **Table 3.4**, it was estimated that for the computed periods given in **Table 5.1**, the following four recorded EQGMs result in the larger demands in strength (C_y), displacement (u), interstory drift index (IDI), and Energy (E_I and E_H): (1) Los Gatos 1; (2) Takatori 1; (3) JMA 1 (Kobe); and (4) Lexington Dam 1. The main values of the SDOF spectra at the fundamental period considering an expected global ductility (μ_{gl}) of the 30-story building are summarized in **Table 5.2a**.

The building frames used in the nonlinear analyses are identified in the plan view shown in **Figure 5.2.3**. These analyses were conducted using the DRAIN 2DX (1988) program for the model of the 30-story building illustrated in **Figure 5.2.4**. The results are presented in terms of the following parameters: (a) displacement envelope, (b) IDI envelope, (c) maximum plastic rotation, (d) maximum cumulative plastic rotation, and (e) maximum damage index.

Ground motion parameters (acceleration, velocity, and displacement) for the Los Gatos 1 ground motion are shown in **Figure 5.2.5**. Building response envelopes for this ground motion are shown in **Figures 5.2.6 to 5.2.8**. Ground motion parameters for Takatori 1 are shown in **Figure 5.2.9** and the corresponding building response envelopes are shown in **Figures 5.2.10 to 5.2.12**. Similar data for JMA 1(Kobe) and Lexington Dam 1 are shown in **Figures 5.2.13 to 5.2.20**. The ground motion parameters for the idealized pulse are shown in **Figure 5.2.21** and the corresponding building response parameters in **Figures 5.2.22 to 5.2.24**. The main results obtained are summarized in **Table 5.2b**. ***Hereafter, the earthquake records will be referred to as Los Gatos, Takatori, JMA and Lexington Dam since only one component was used.***

Table 5.2a Single-Degree-of-Freedom Response (for T_1 = 1.75s and μ = 3)

Record	Max Displac. u (m)=Δ	$\frac{E_I}{M}\left(\frac{m^2}{s^2}\right)$	$\frac{E_H}{M}\left(\frac{m^2}{s^2}\right)$	γ Damage Parameter	IDI Uniform Shear Beam (Elastic)	IDI Linear 1st Mode Shear Beam (Elastic)	$\frac{IDI\ H}{\Delta}$
Takatori 1	1.08	12.0	7.2	0.70	0.023	0.023	1.92
Los Gatos 1	1.00	8.2	5.2	0.60	0.021	0.030	1.89
Kobe JMA 1	0.54	4.5	3.0	0.85	0.018	0.030	3.00
Lexington Dam1	0.70	4.2	2.5	0.65	0.020	0.020	2.57
Idealized Pulse	1.35	10.2	5.5	0.50	0.027	0.026	1.80

Table 5.2b Maximum 30-Story Building Response Using DRAIN 2DX

Record	Max Displac. Δ=u (m)	Max IDI	Max Plastic Rotation Θ_p	Max Cumulative Plastic Rotation Θ_{pcum}	$\frac{\theta_p}{IDI_{max}}$	$\frac{\theta_{pcum}}{\theta_p}$	$\frac{IDI_{max}H}{\Delta}$
Takatori 1	1.40	0.0200	0.0214	0.0608	1.07	2.84	1.29
Los Gatos1	1.12	0.0204	0.0207	0.0395	1.01	1.91	1.64
Kobe JMA1	0.99	0.0192	0.0200	0.0492	1.04	2.46	1.75
Lexington Dam1	0.79	0.0169	0.0163	0.0215	0.96	1.32	1.93
Idealized Pulse	1.42	0.0210	0.0214	0.0309	1.02	1.44	1.33

5.2.3 Observations Regarding the Results Obtained

The following are some preliminary conclusions regarding the results obtained from the different analyses conducted:

- With the exception of the values for IDI reaching up to 0.0204 under Los Gatos, which is

larger than the original acceptable value of 1.5%, the demands of all the other main parameters considered are acceptable.

- The IDI values obtained using linear elastic modal analysis with a shear beam model are good approximations to the IDIs obtained from the nonlinear building analysis.

- For pulse-type ground motions such as those analyzed here, and for a buildings of 90m in height, it is necessary to reduce the fundamental period to near 1.0 sec in order to have IDI less than 0.015. Since this could be very difficult, either a larger IDI should be allowed, which may require isolating the partitions from the structure, or the structure will need to be modified.

- Of the two continuous shear beam models analyzed, the uniform (constant stiffness) shear beam model seems to produce better results. However, in the shear beam analysis, 5% damping was used for the building analysis, resulting in 10% damping for the second mode. Therefore, the higher mode effects are larger in the continuous shear beam model and a study with similar damping coefficients should be done. Note that the main differences between the two shear beam models occur in buildings having a fundamental period of more than 2 seconds due to the effects of higher modes that are much more important in the model with linear first mode.

- The Fajfar damage parameter γ seems to be a good parameter to classify ground motions as pulse-type. For a building with a fundamental period of 1.75 seconds, $\gamma \leq 0.85$ was obtained for all ground motions analyzed, with the lesser value of 0.50 obtained for the idealized pulse-type ground motion.

- The results under the Takatori ground motion and the artificial pulse are very similar, with the exception of the cumulative plastic hinge rotation that is larger in the case of Takatori.

- Plastic rotations and IDIs are very similar, with the exception of the top stories where additional coupling beams exist in the central frames of the building and in the bottom stories where plastic hinges form at the columns.

- Plastic hinges form at the columns due to the high values of tension load in the columns. For design, the axial load in the columns was computed using the formulas suggested by Paulay [1977]. The results obtained here suggest that the axial load in the external columns should be computed considering the ultimate bending capacity in the beams of all the stories. However, this conclusion should be investigated further.

- The Takatori 1 and the pulse-type ground motions have an IDI distribution that is close to the first mode and push-over distribution. An increased concentration of IDI around the 21st story and second mode participation in the response occurs for Los Gatos, Kobe JMA, and Lexington Dam ground motions.

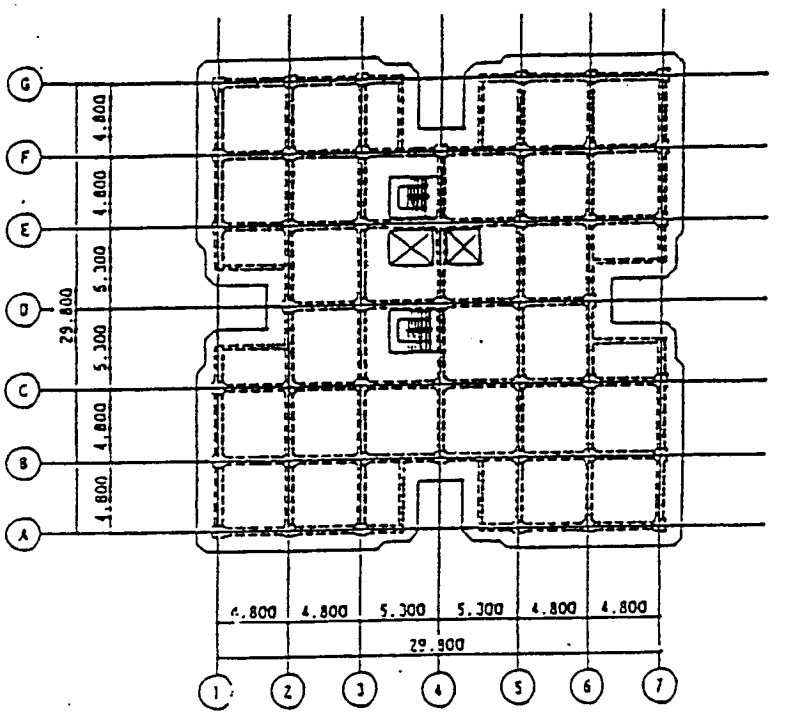

TYPICAL FLOOR PLAN

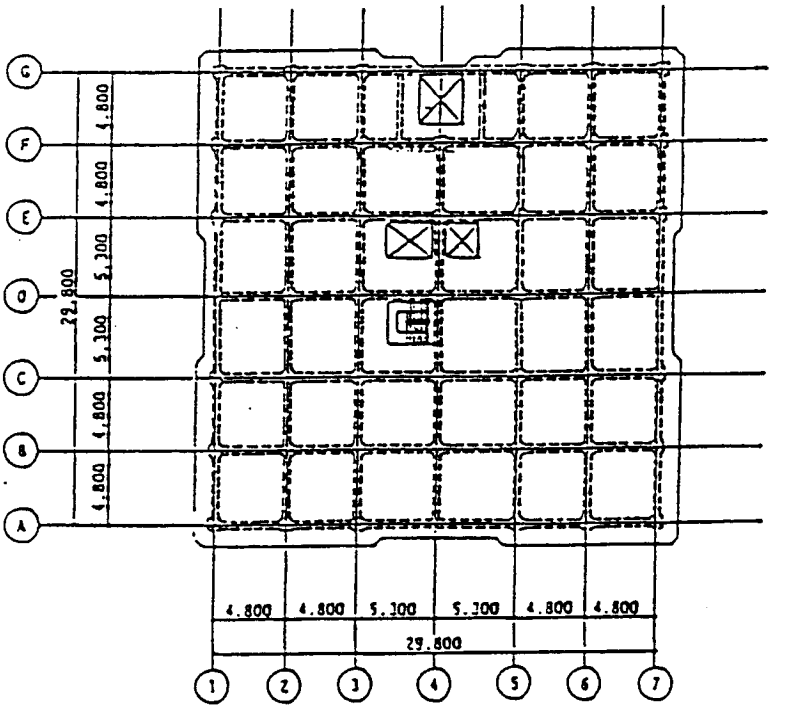

29TH,30TH AND ROOF FLOOR PLAN

Figure 5.2.1 S-K Building Floor Plans (units:m)

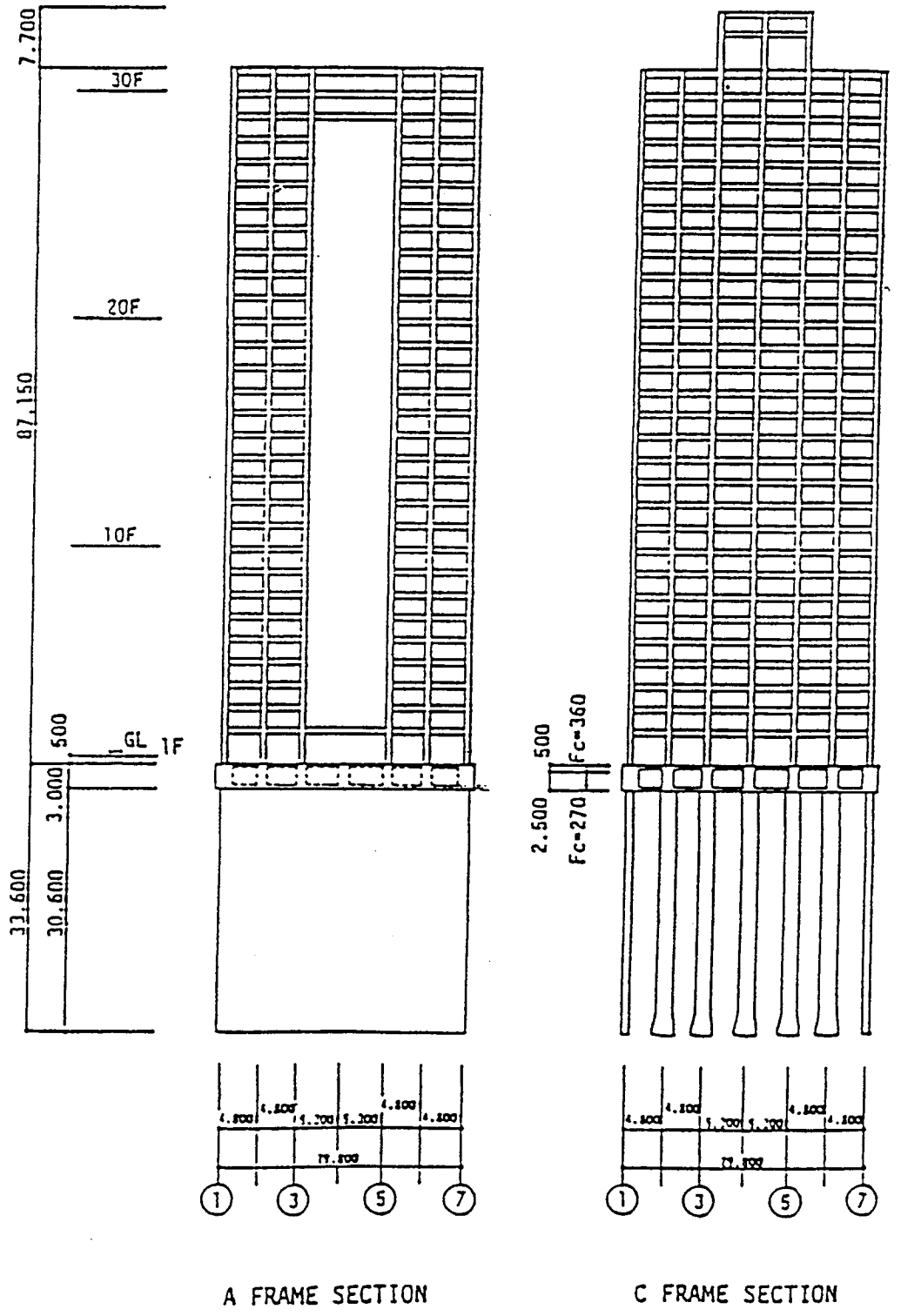

Figure 5.2.2 S-K Building Elevations (units:m)

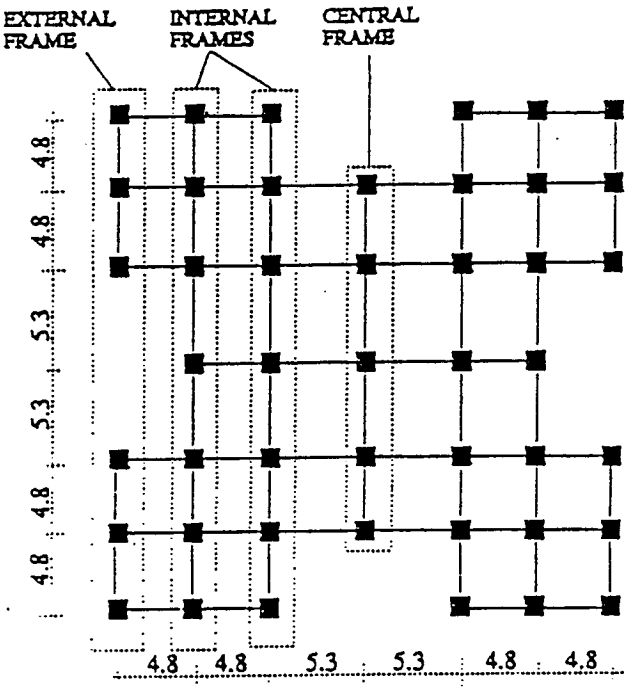

Figure 5.2.3 Identification of Building Frames (units:m)

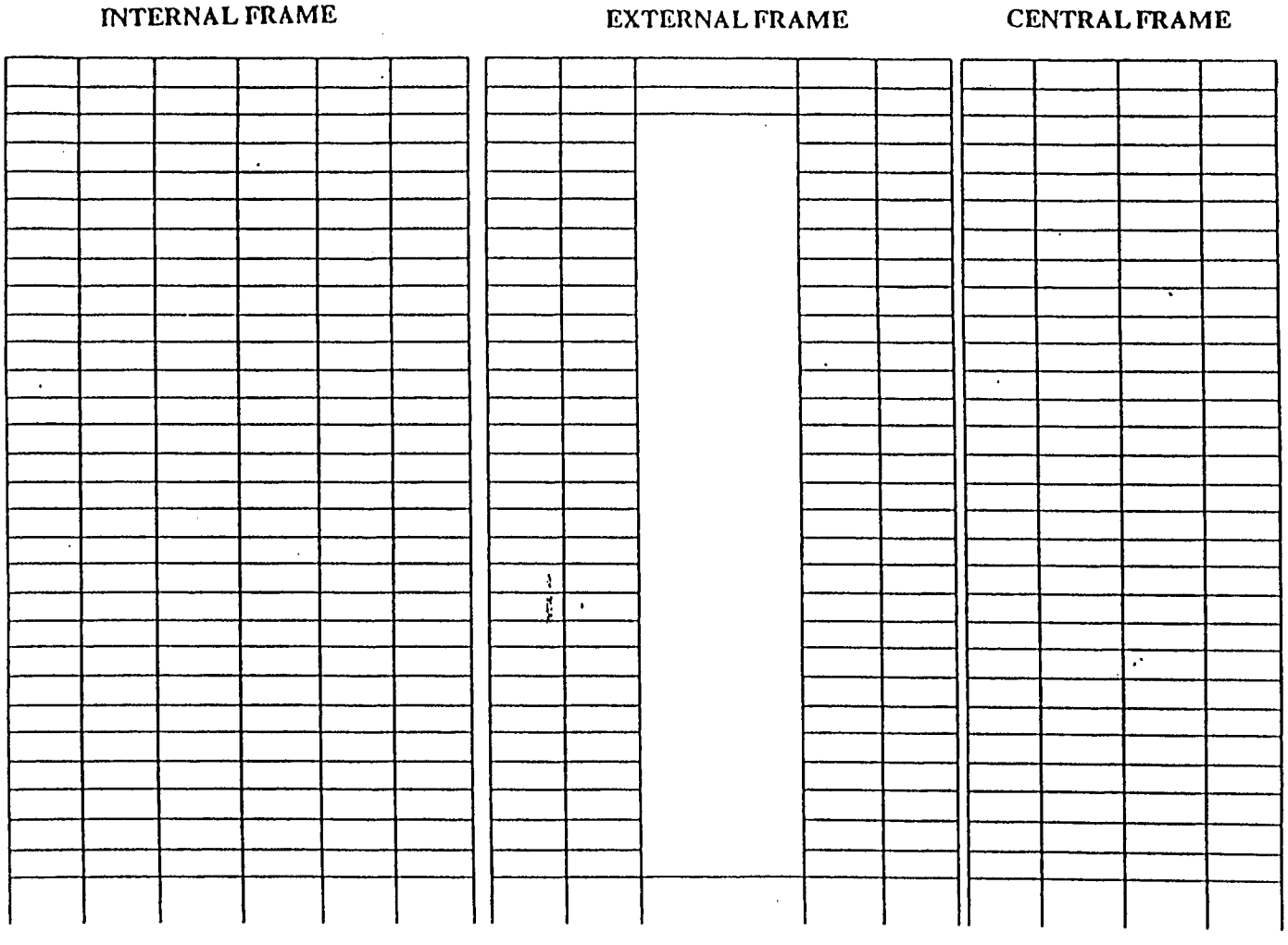

Figure 5.2.4 Frames Modeled for Nonlinear Analyses

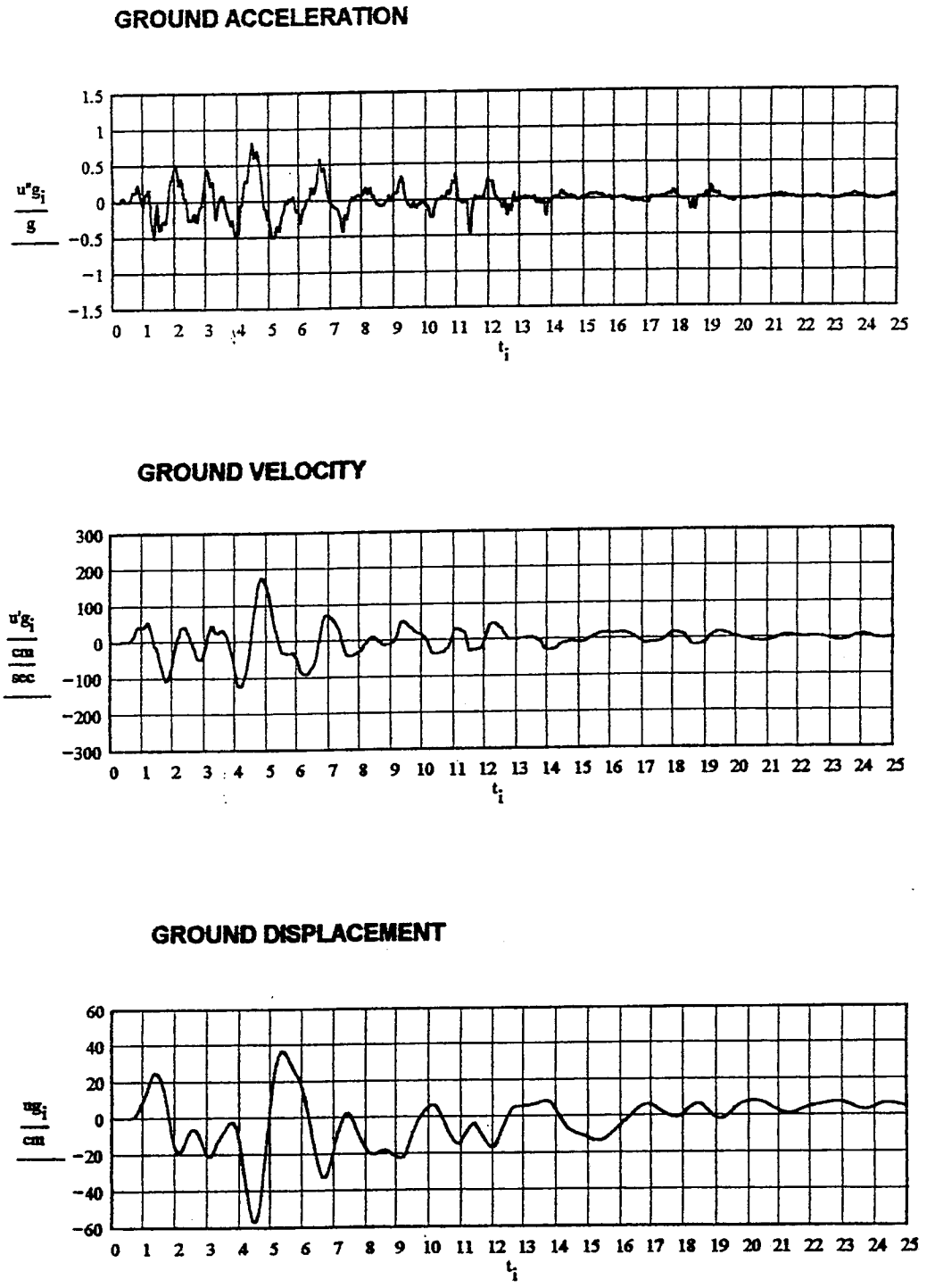

Figure 5.2.5 Ground Motion Parameters, Takatori

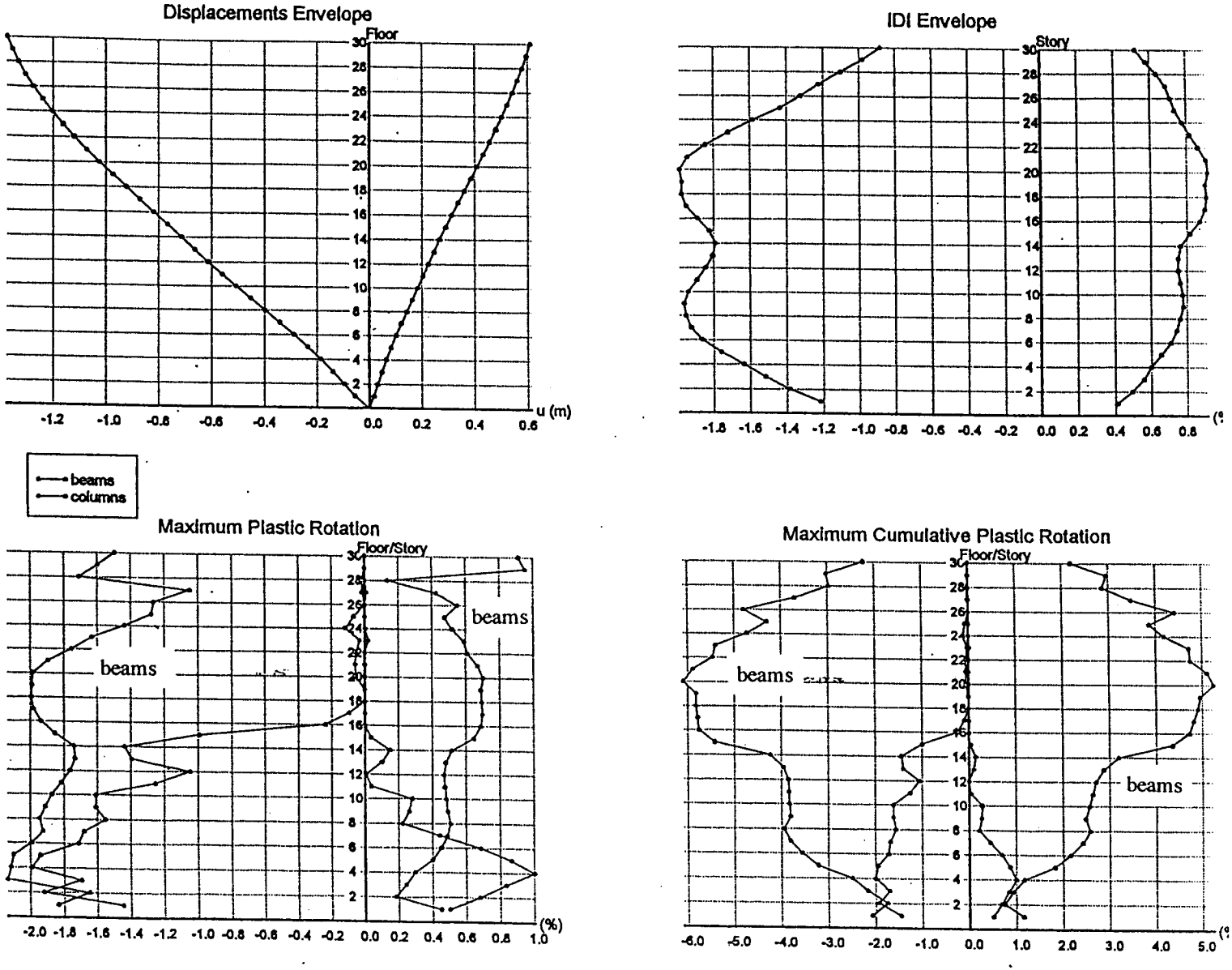

Figure 5.2.6 Building Response Envelopes, Takatori

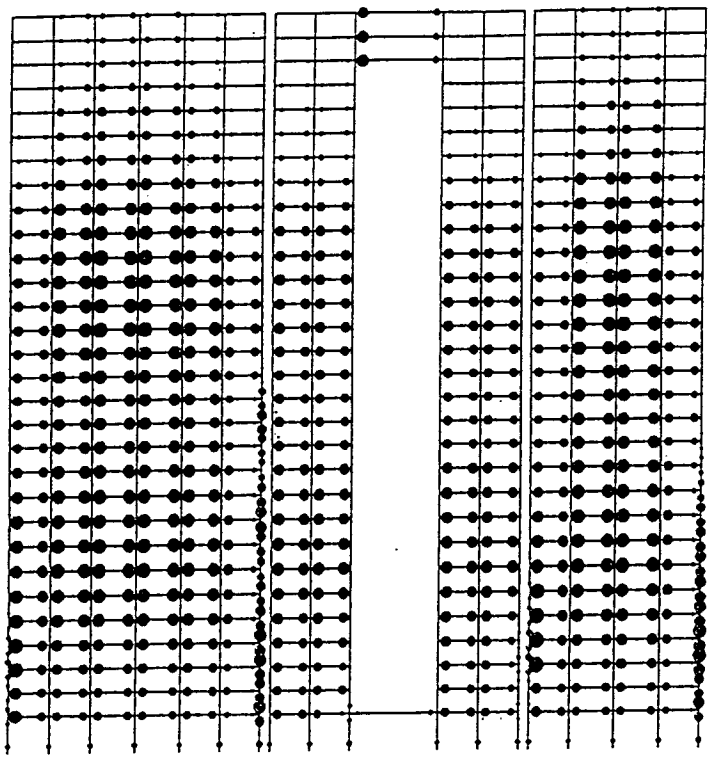

MAXIMUM PLASTIC ROTATION

θmax (beams) = 0.0214

θmax (columns) = 0.0199

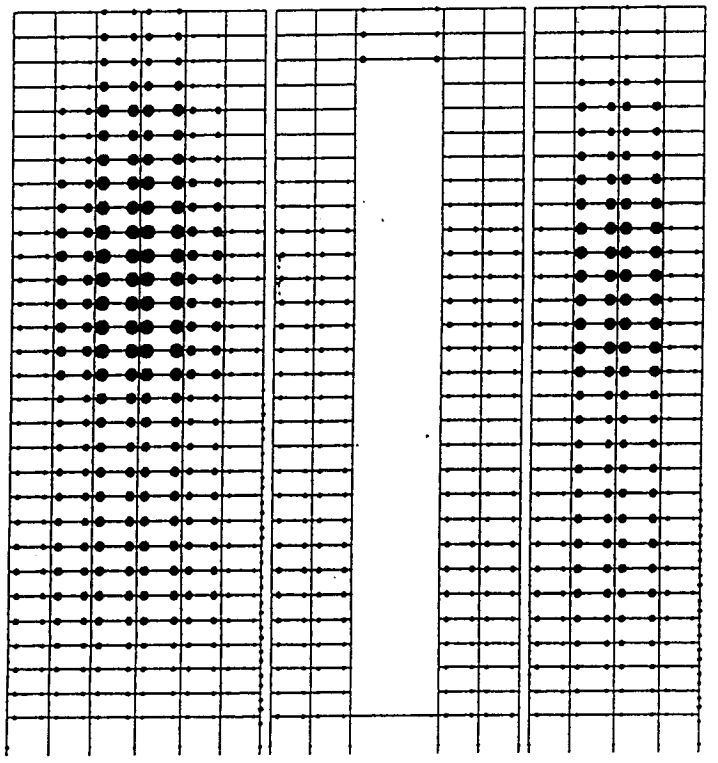

CUMULATIVE PLASTIC ROTATION

θcum (beams) = 0.0608

θcum (columns) = 0.0199

Figure 5.2.7 Plastic Hinge Rotations, Takatori

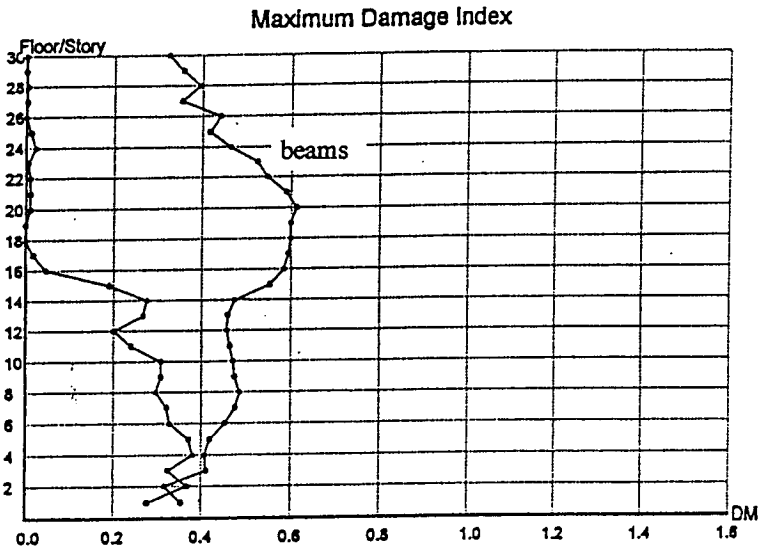

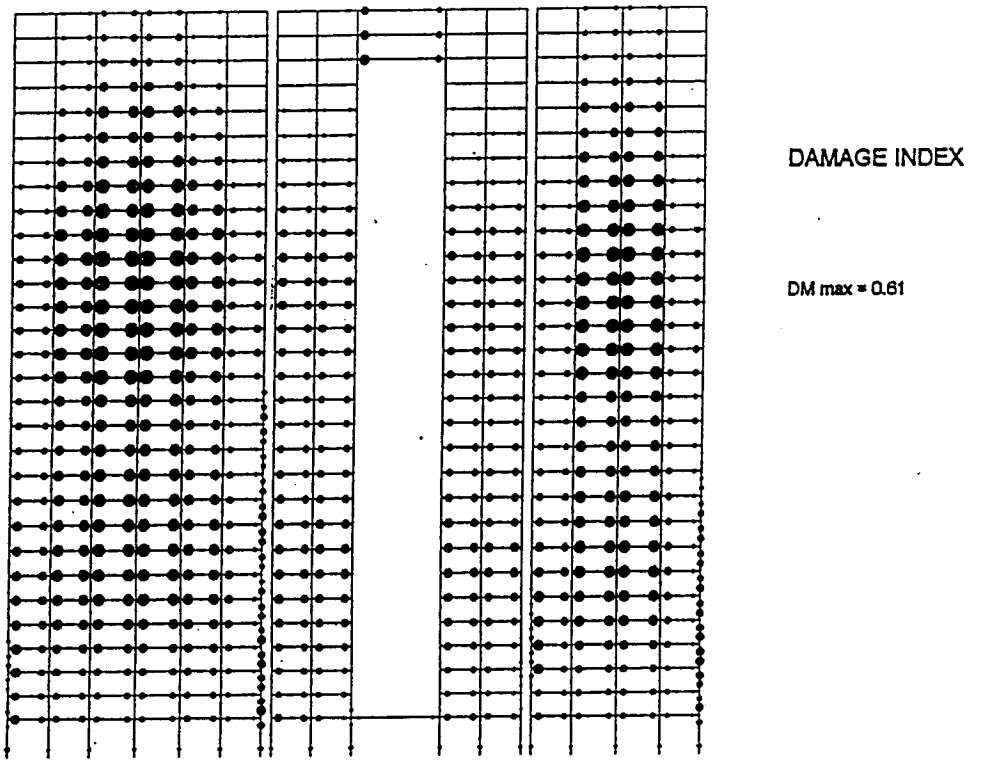

Figure 5.2.8 Damage Index, Takatori

GROUND ACCELERATION

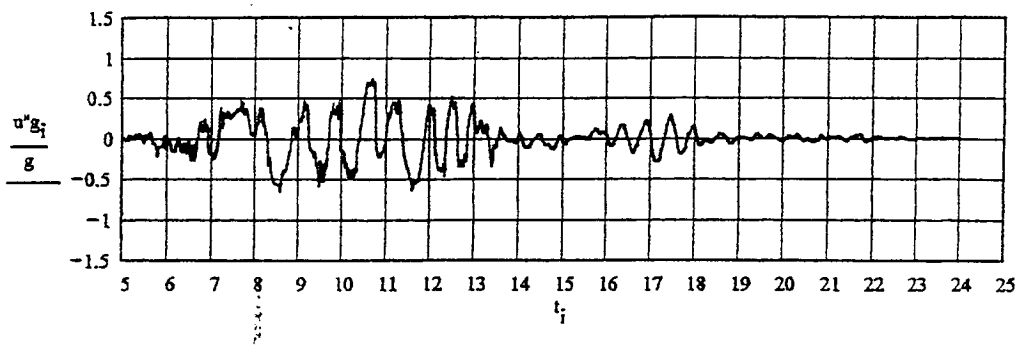

GROUND VELOCITY

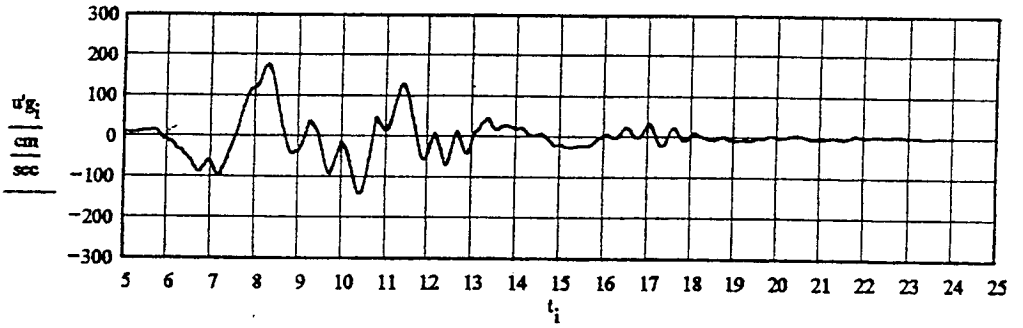

GROUND DISPLACEMENT

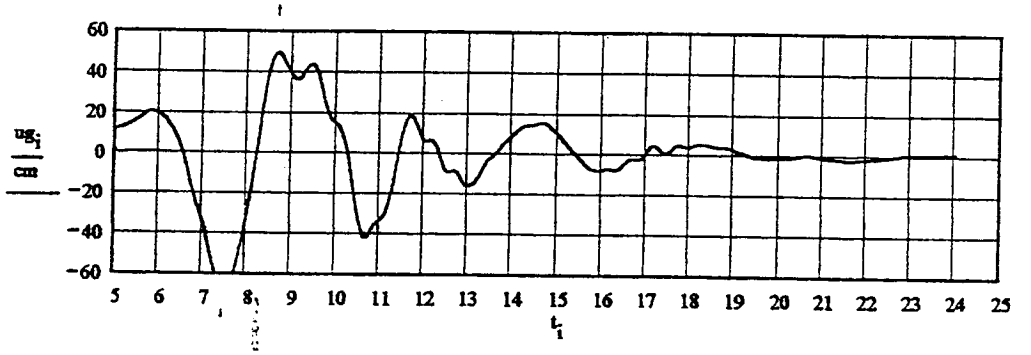

Figure 5.2.9 Ground Motion Parameters, Los Gatos

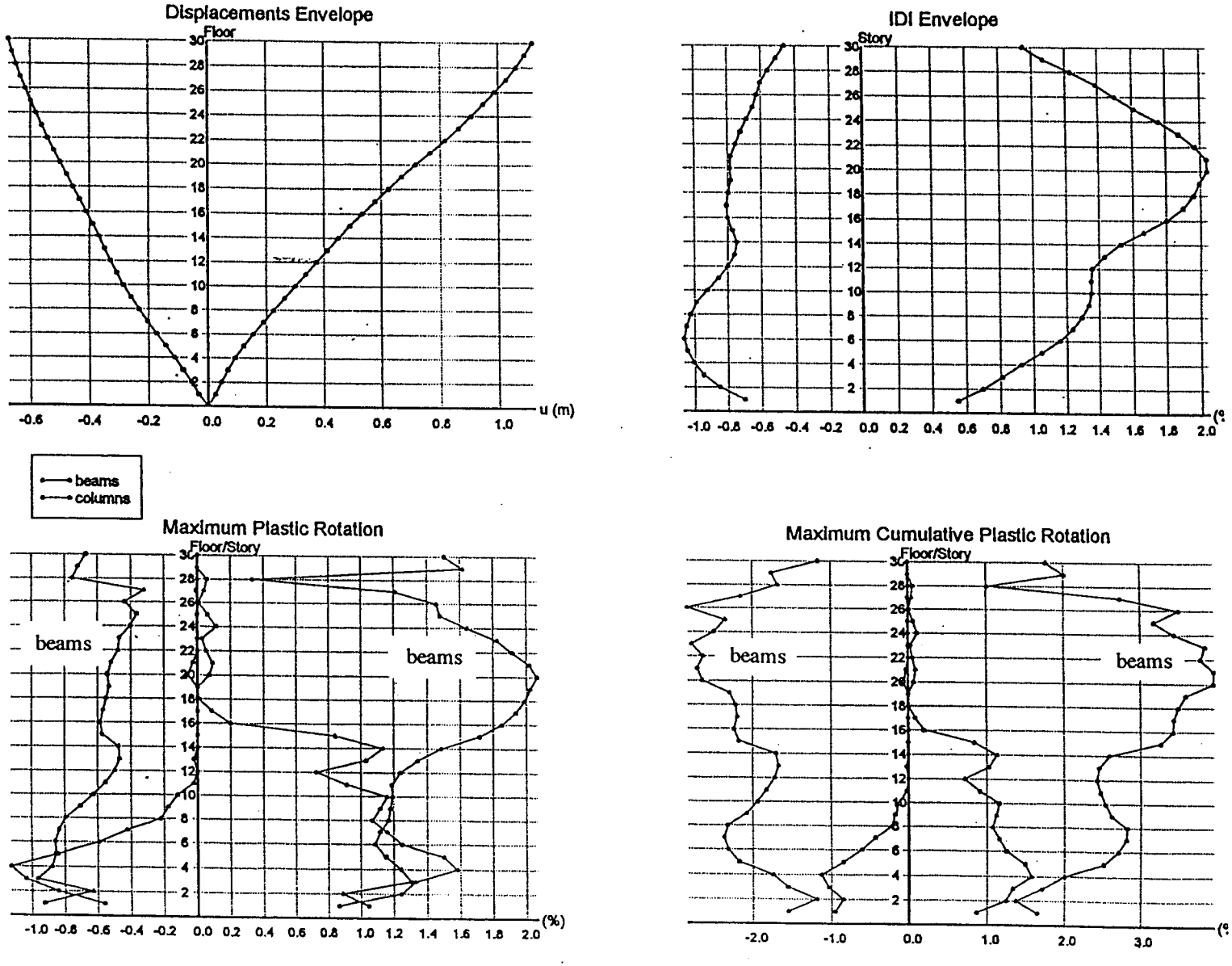

Figure 5.2.10 Building Response Envelopes, Los Gatos

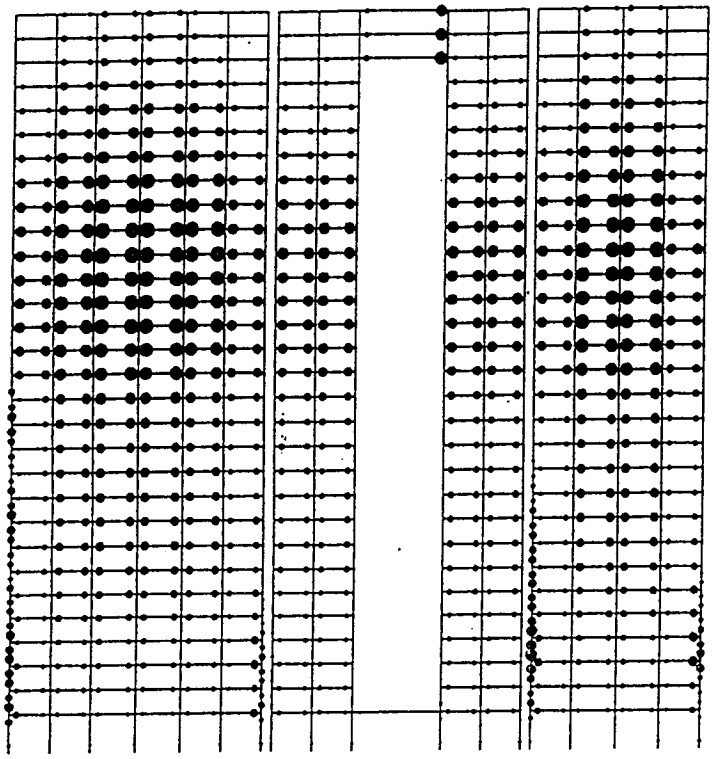

MAXIMUM PLASTIC ROTATION

θmax (beams) = 0.0207

θmax (columns) = 0.0158

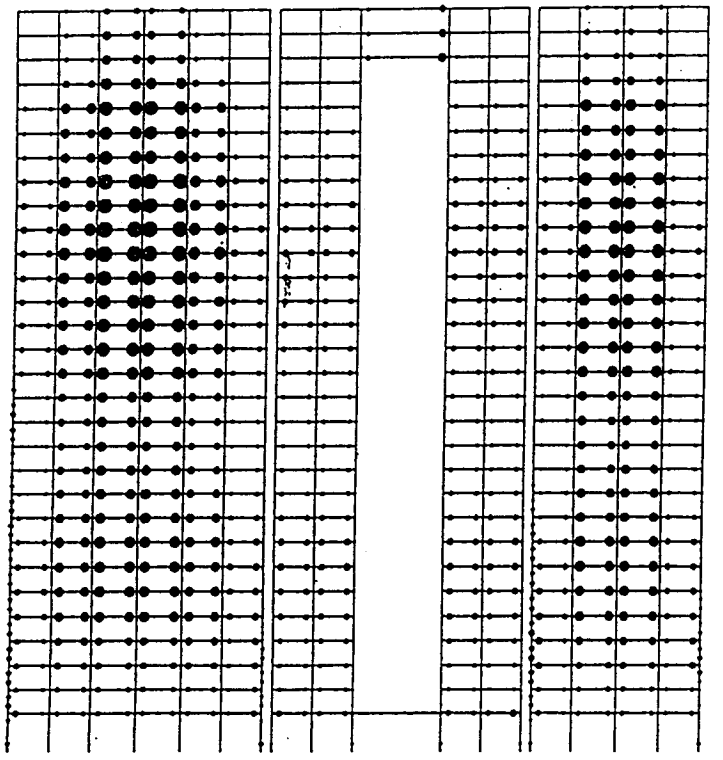

CUMULATIVE PLASTIC ROTATION

θcum (beams) = 0.0395

θcum (columns) = 0.0158

Figure 5.2.11 Plastic Hinge Rotations, Los Gatos

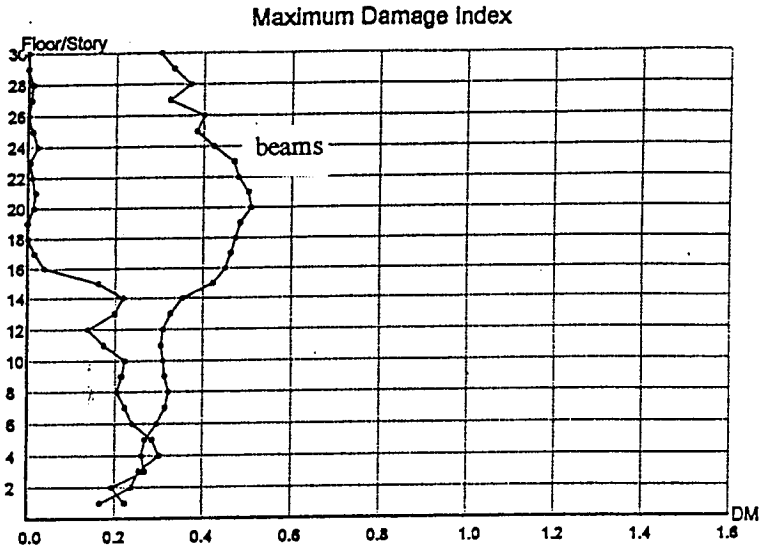

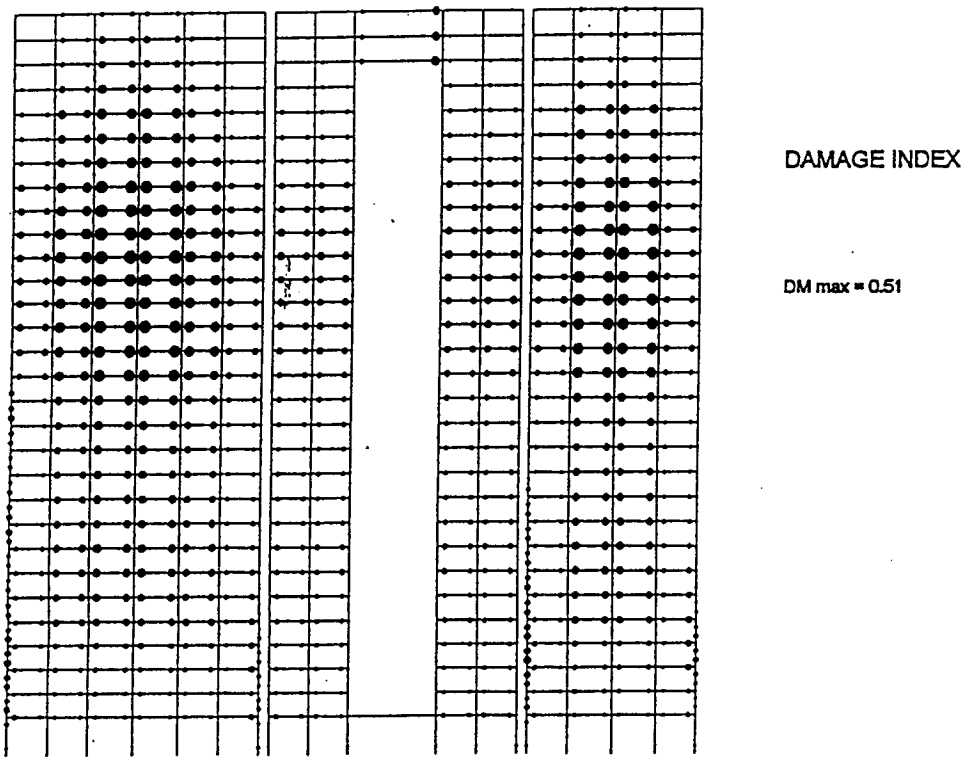

Figure 5.2.12 Damage Index, Los Gatos

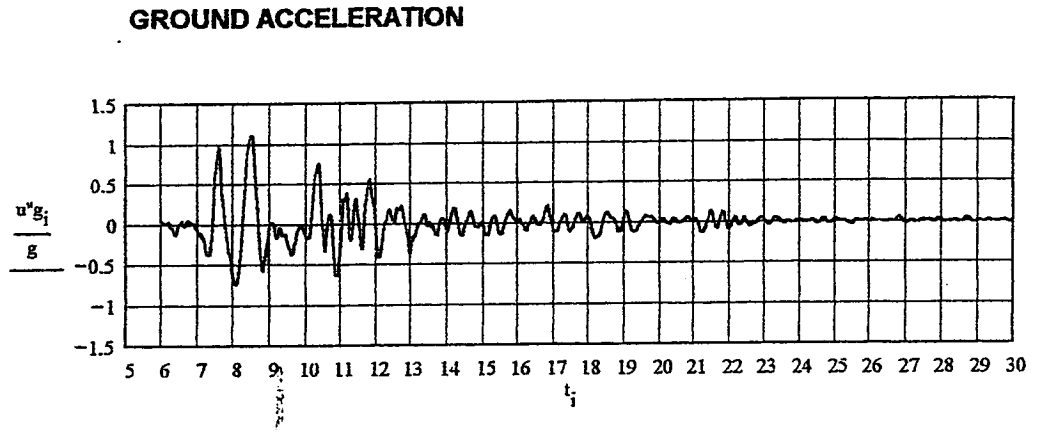

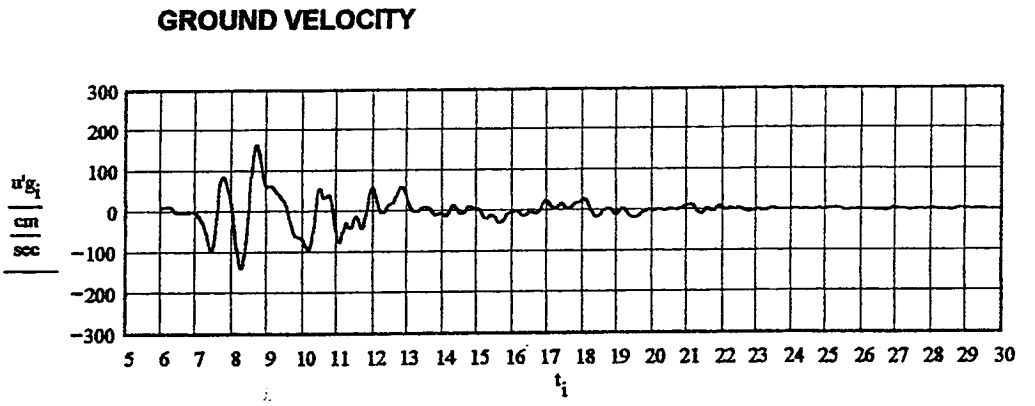

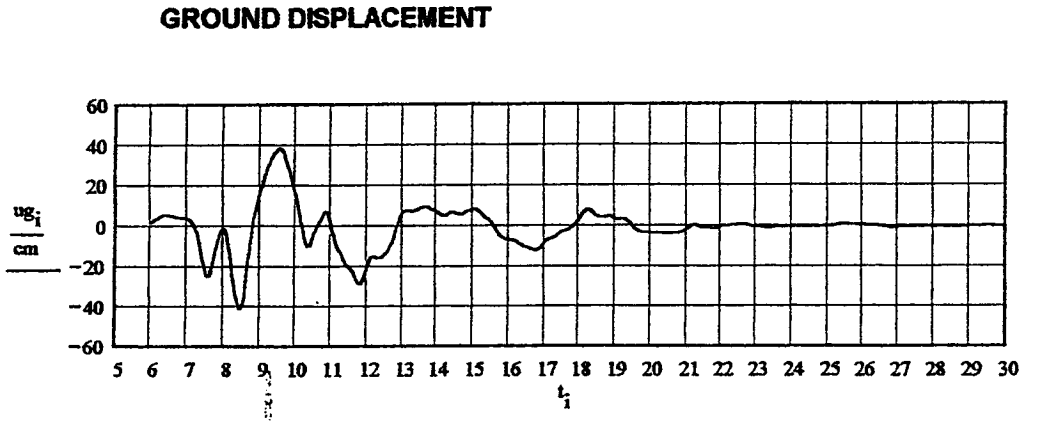

Figure 5.2.13 Ground Motion Parameters, JMA(Kobe)

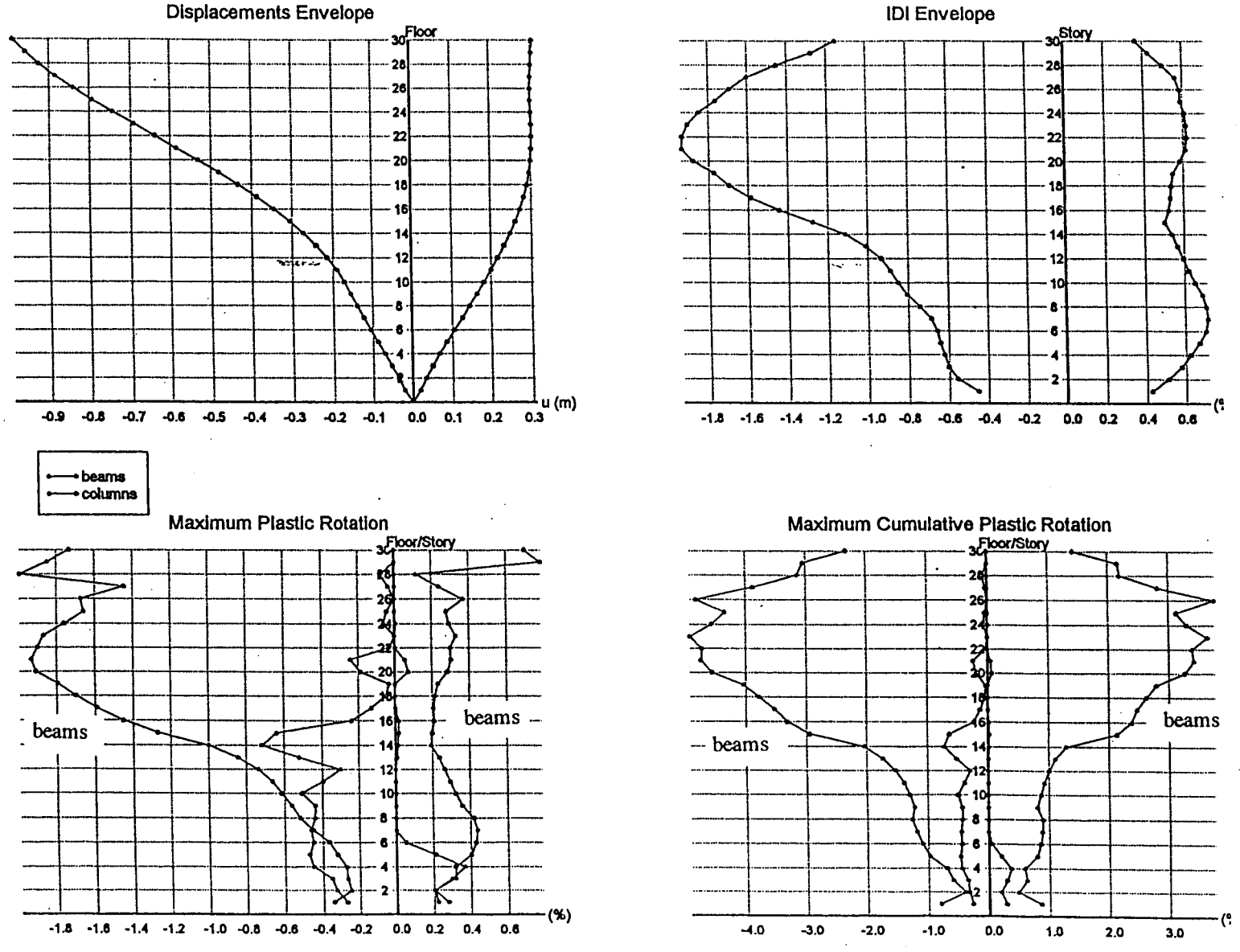

Figure 5.2.14 Building Response Envelopes, JMA

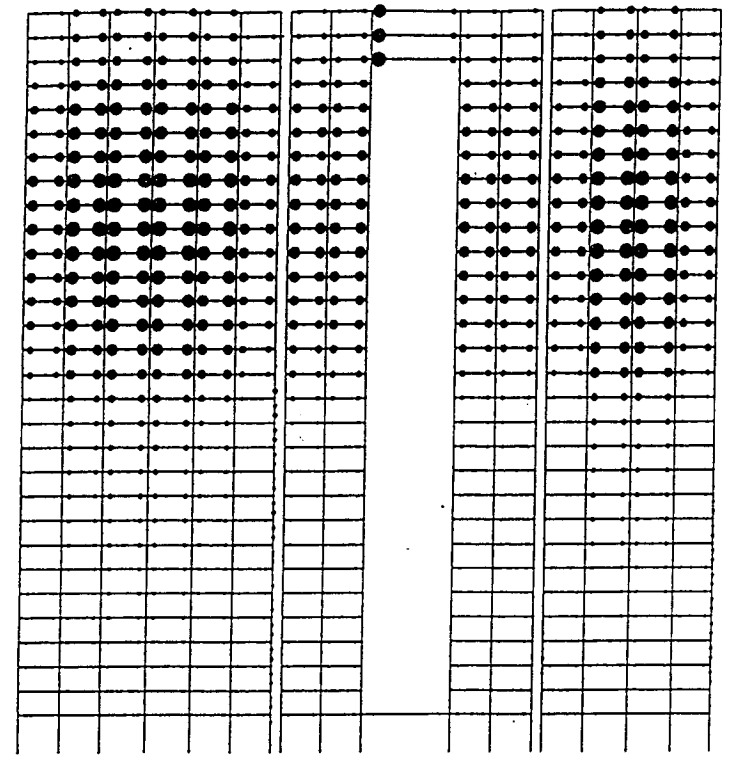

MAXIMUM PLASTIC ROTATION

θmax (beams) = 0.0200

θmax (columns) = 0.0072

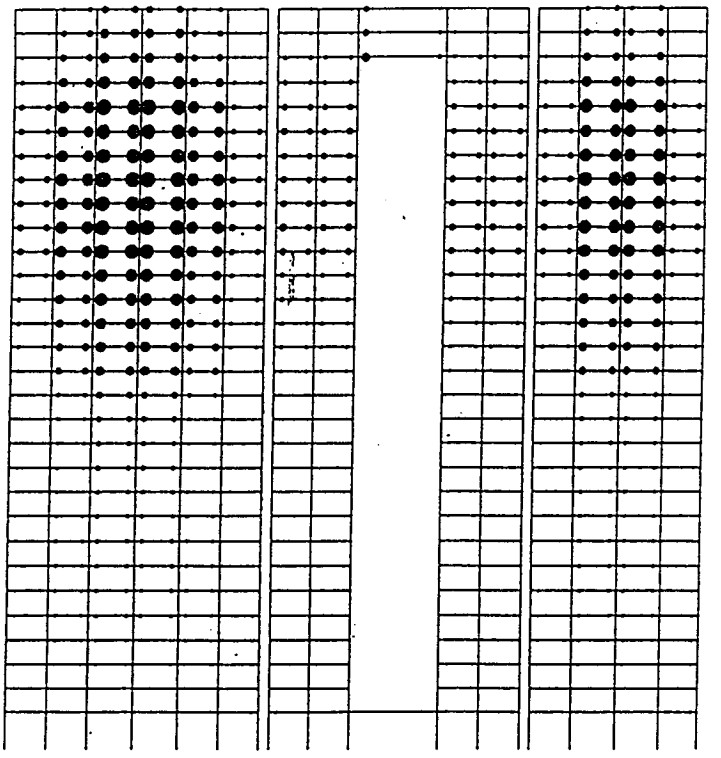

CUMULATIVE PLASTIC ROTATION

θcum (beams) = 0.0492

θcum (columns) = 0.0072

Figure 5.2.15 Plastic Hinge Rotations, JMA

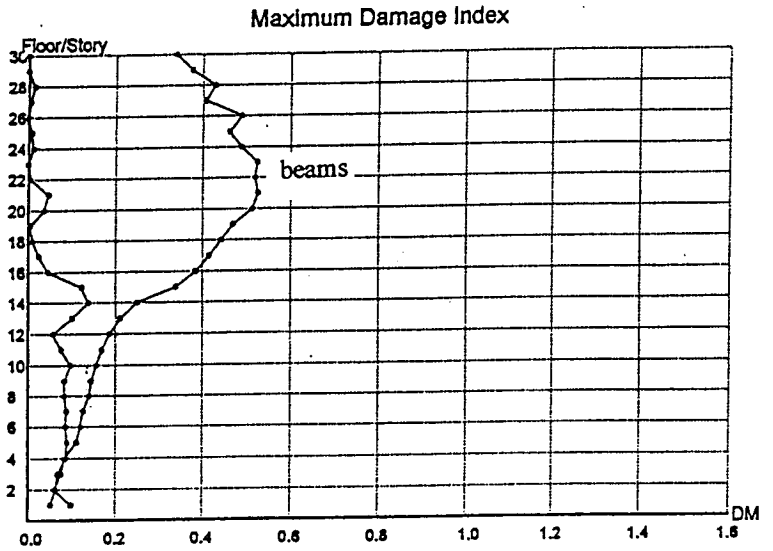

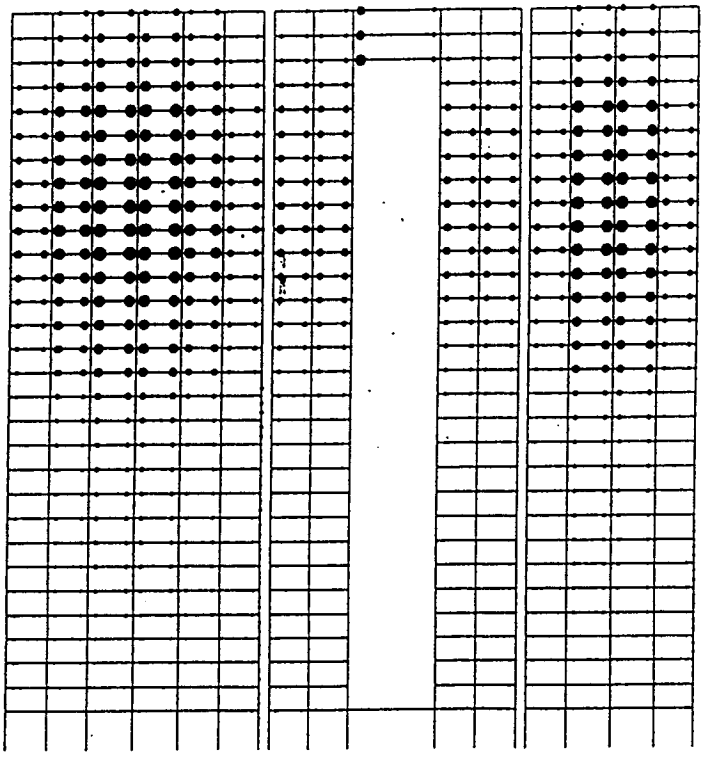

DAMAGE INDEX

DM max = 0.53

Figure 5.2.16 Damage Index, JMA

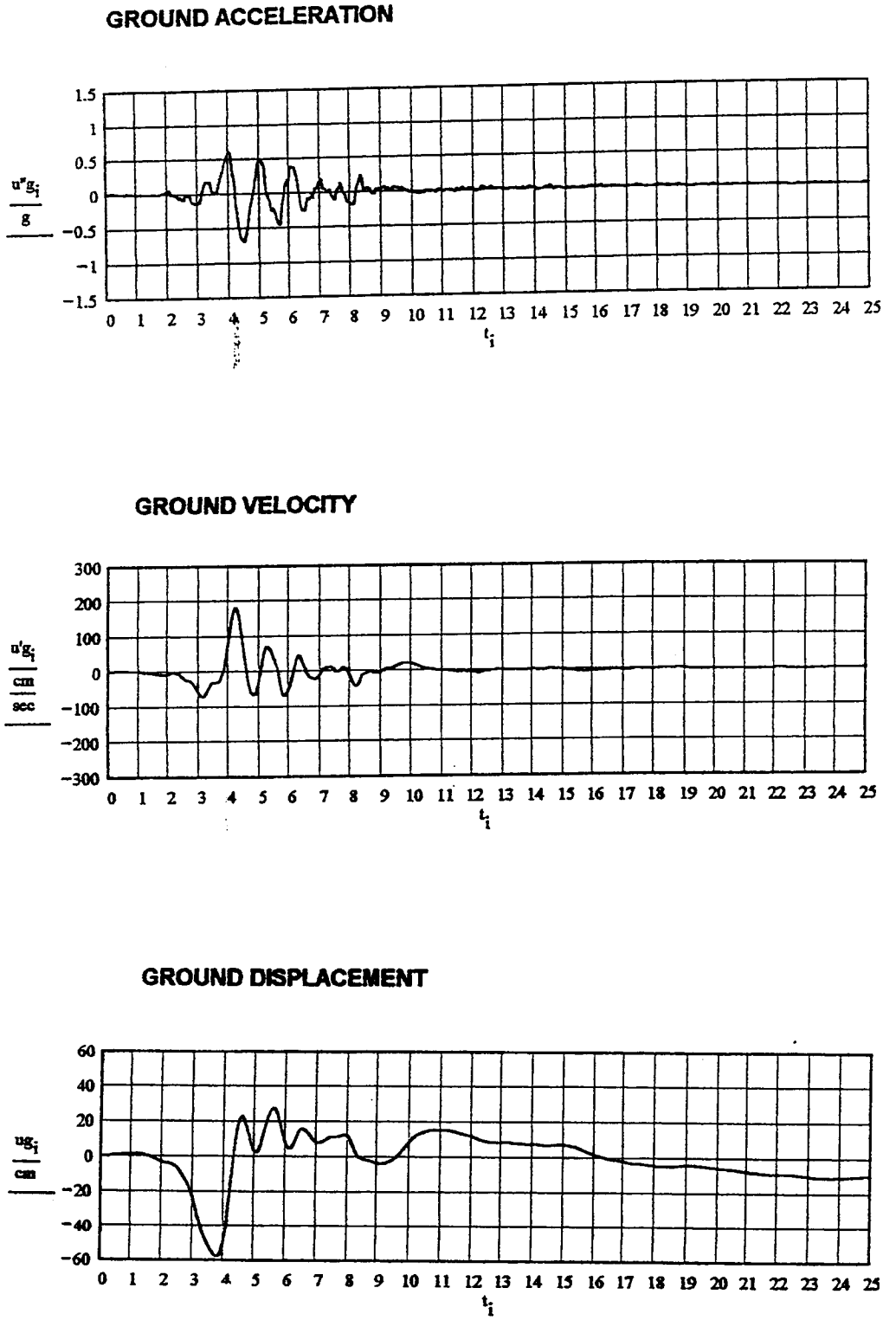

Figure 5.2.17 Ground Motion Parameters, Lexington Dam

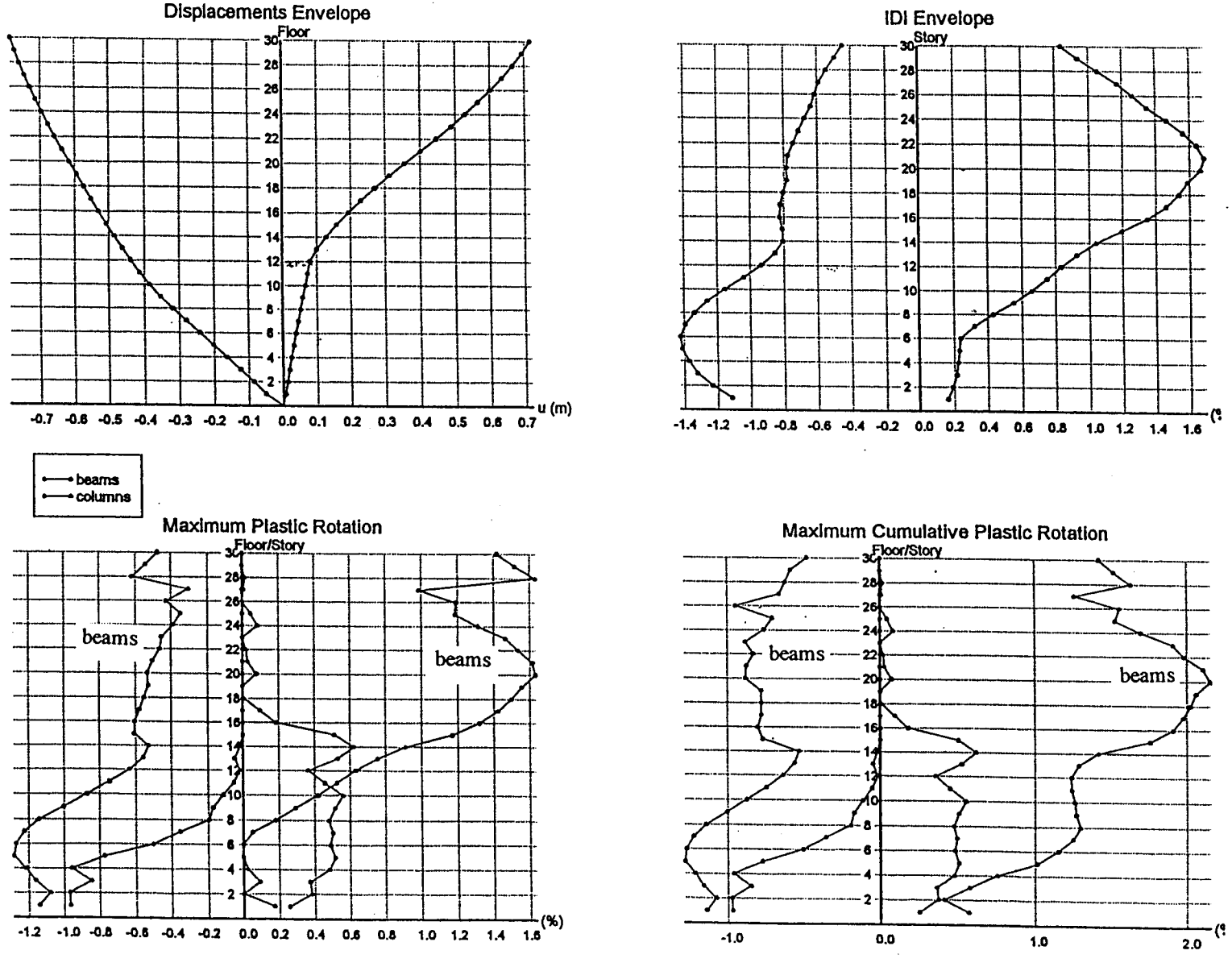

Figure 5.2.18 Building Response Envelopes, Lexington Dam

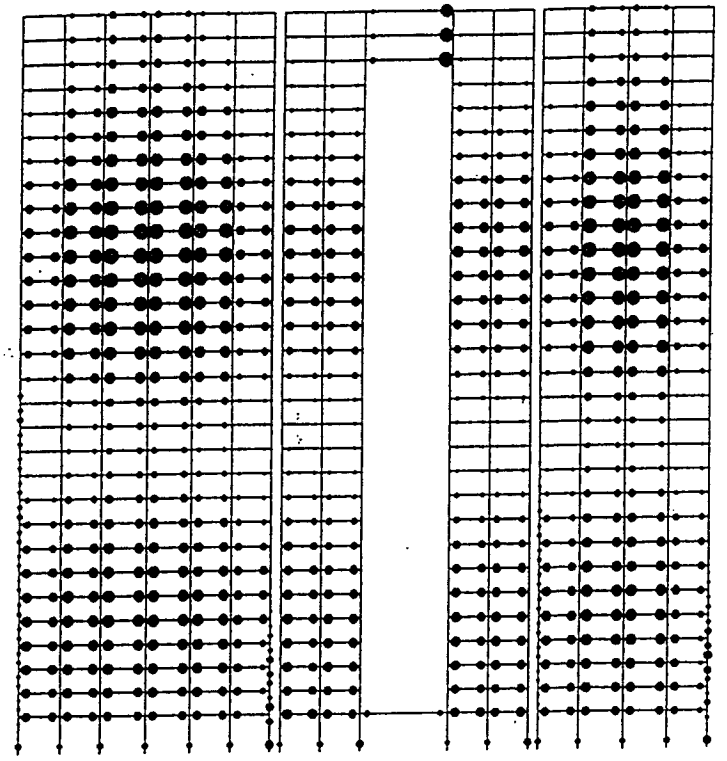

MAXIMUM PLASTIC ROTATION

θmax (beams) = 0.0163

θmax (columns) = 0.0097

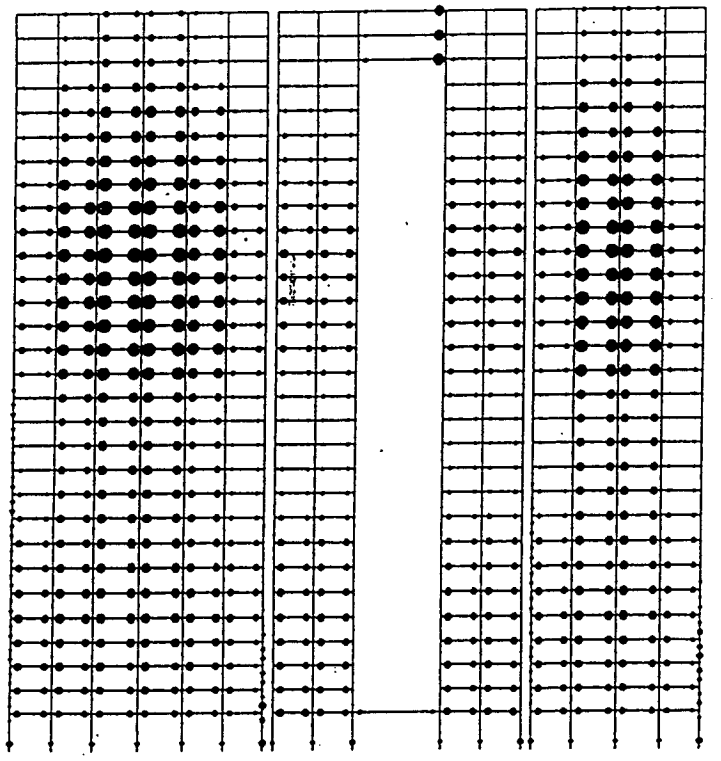

CUMULATIVE PLASTIC ROTATION

θcum (beams) = 0.0215

θcum (columns) = 0.0097

Figure 5.2.19 Plastic Hinge Rotations, Lexington Dam

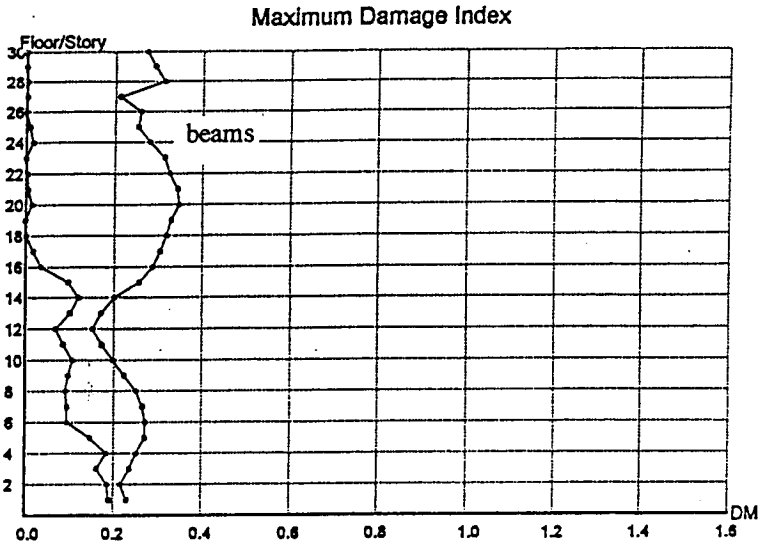

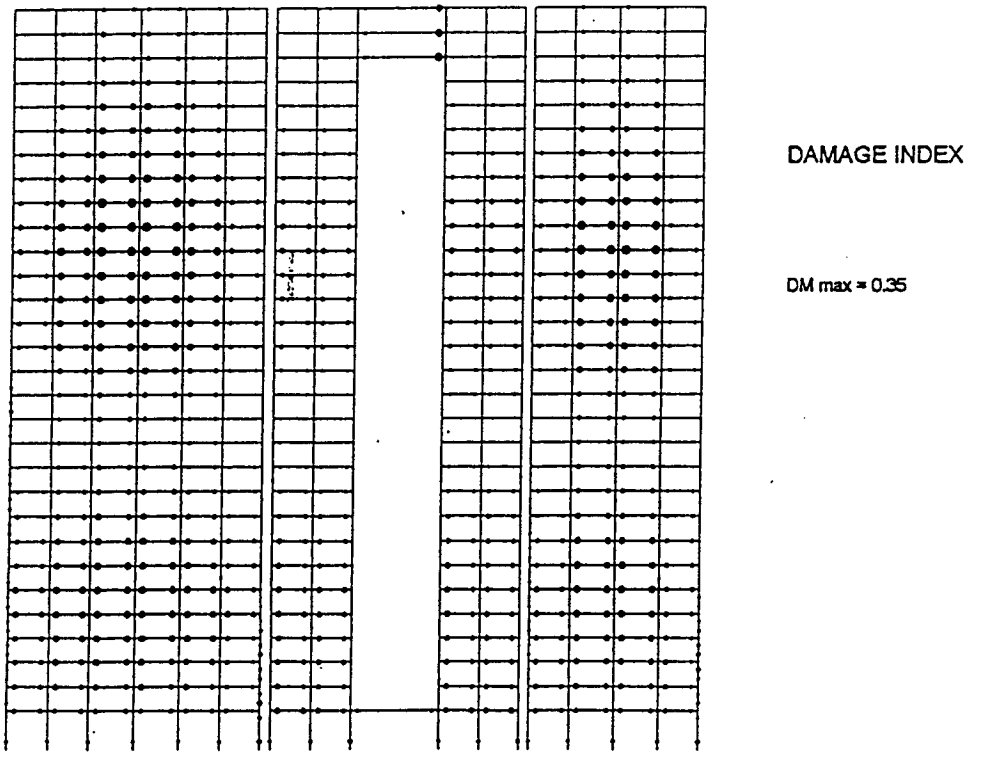

Figure 5.2.20 Damage Index, Lexington Dam

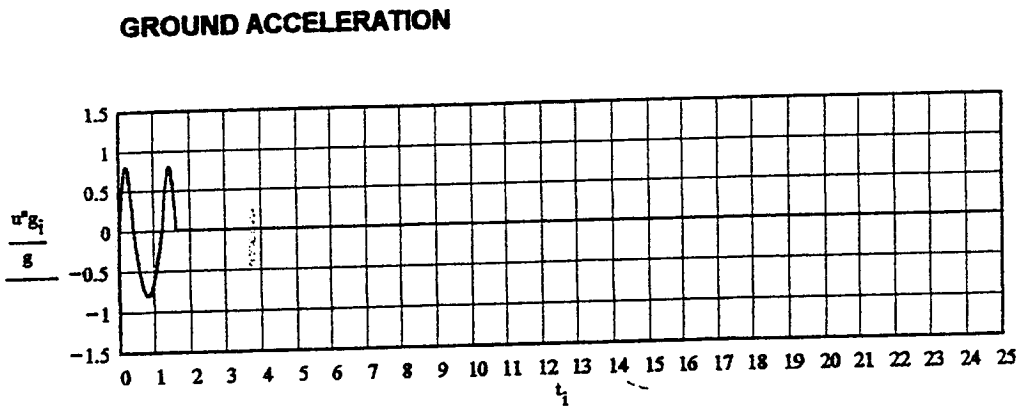

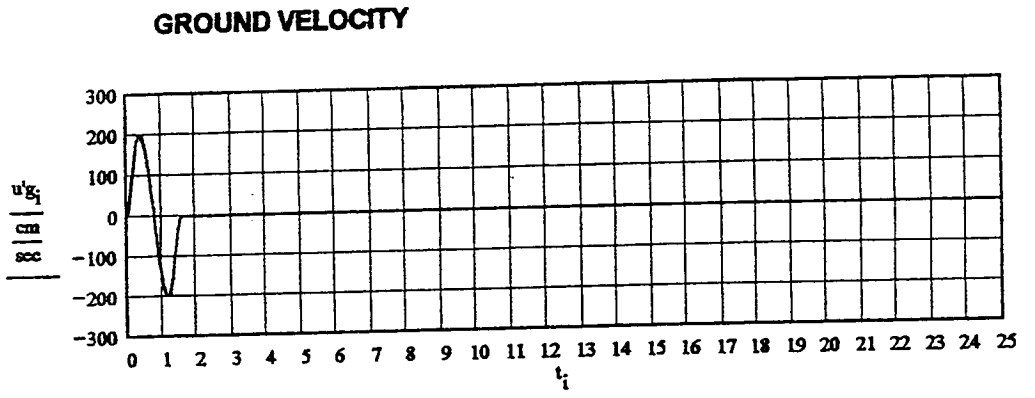

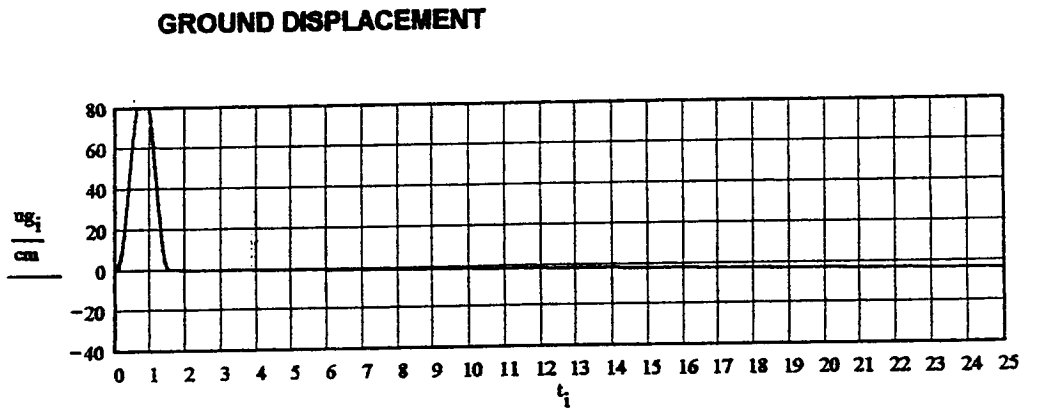

Figure 5.2.21 Ground Motion Parameters, Idealized Pulse

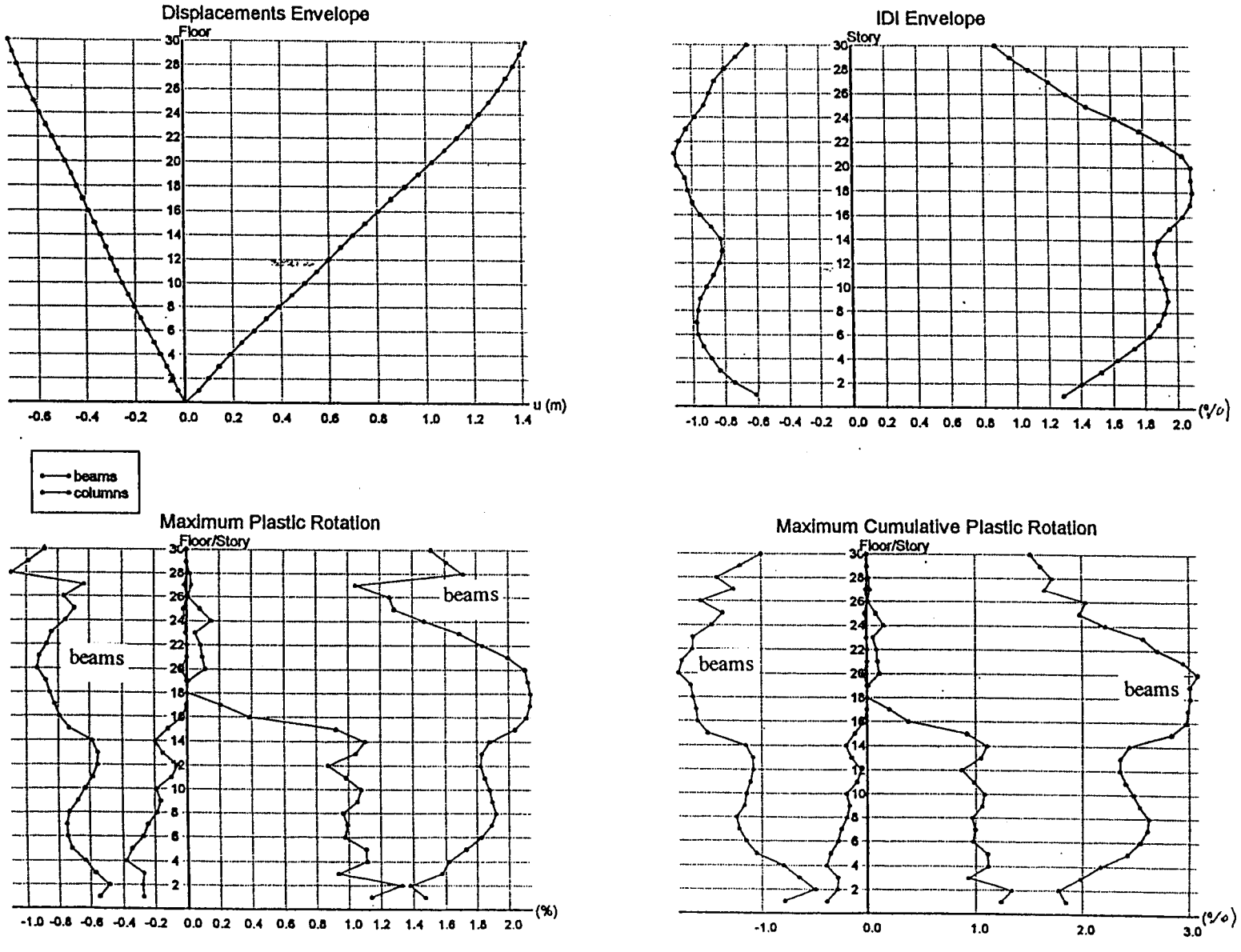

Figure 5.2.22 Building Response Envelopes, Idealized Pulse

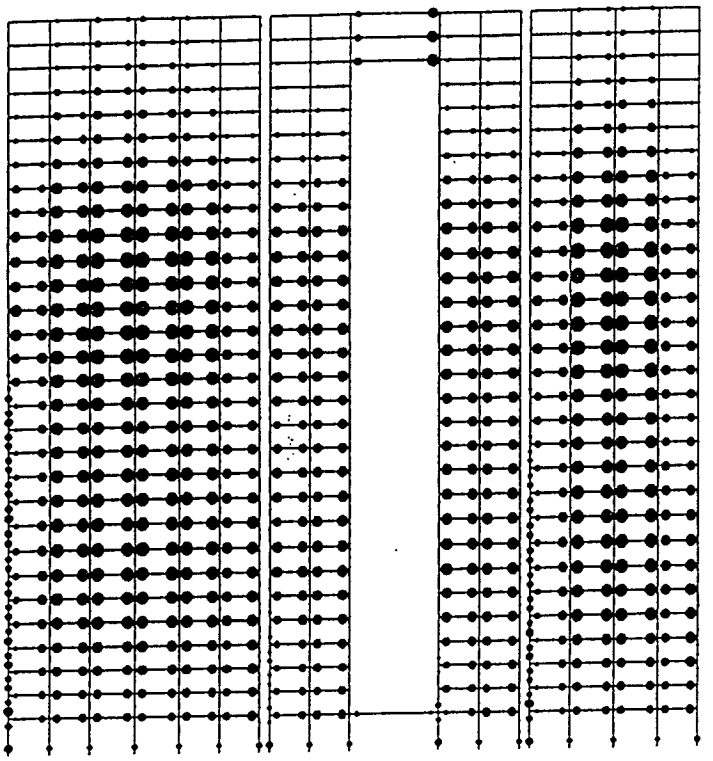

MAXIMUM PLASTIC ROTATION

θmax (beams) = 0.0214

θmax (columns) = 0.0133

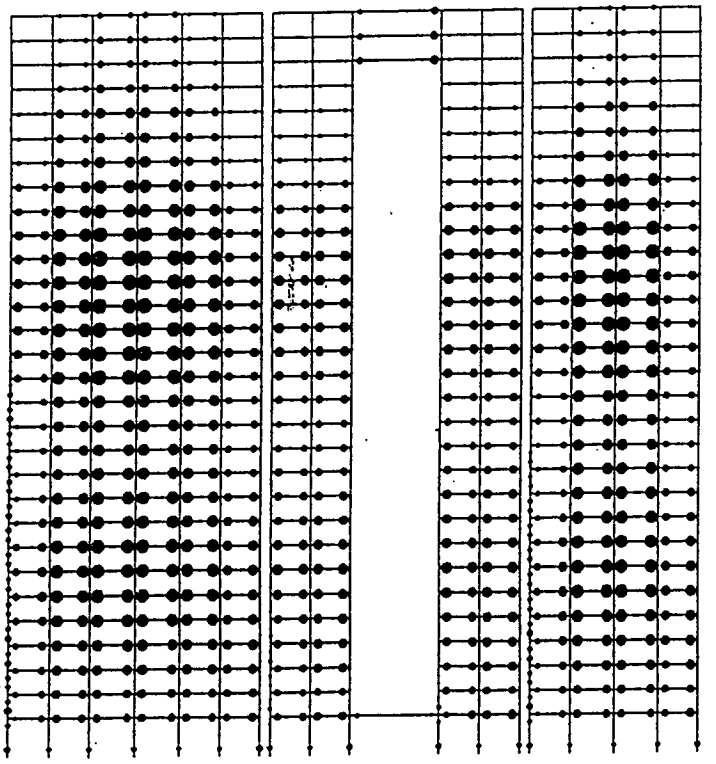

CUMULATIVE PLASTIC ROTATION

θcum (beams) = 0.0309

θcum (columns) = 0.0133

Figure 5.2.23 Plastic Hinge Rotations, Idealized Pulse

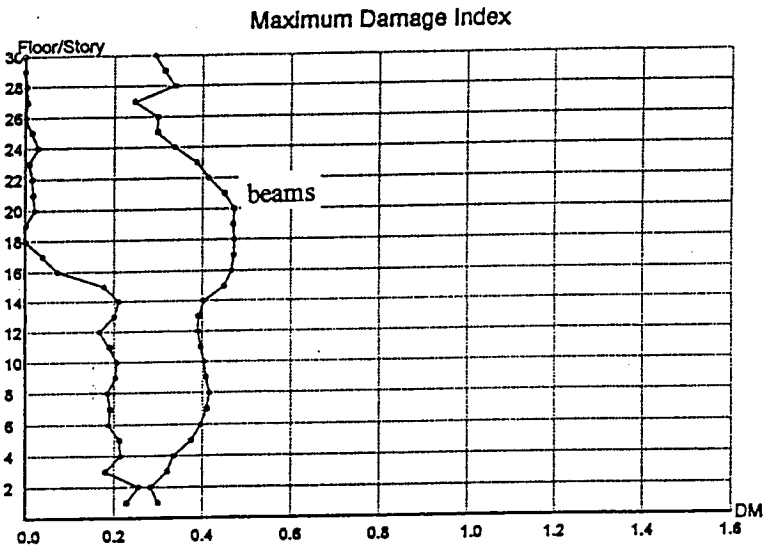

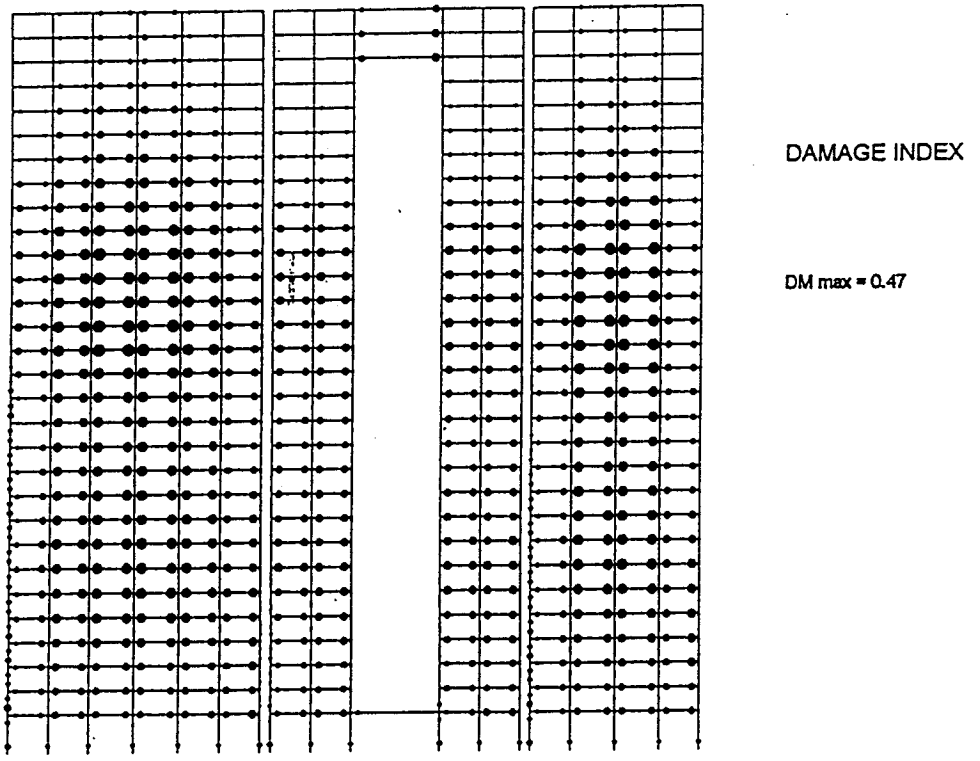

Figure 5.2.24 Damage Index, Idealized Pulse

5.3 THE 30-STORY S-K BUILDING AS BUILT

The configuration and structural layout of this building are the same as those of the conceptually designed building discussed in 5.2 and illustrated in **Figure 5.2.1**. A comparison of the main features (mechanical characteristics) is given in **Table 5.3**.

Table 5.3 Comparison of Conceptually Designed and Original (As-Built) S-K Buildings

	Conceptual	As Built
Total mass (ton.)	26095	29711
T_1 (sec)	1.75	2.15
T_2 (sec)	0.62	0.70
Shear Base Capacity (Constant Load Pattern) (kN)	78991	62652
Shear Base Capacity (Linear Load Pattern) (kN)	61244	48576
First Story Mechanism (kN)	104798	72109
Shear Base Capacity (Constant Load Pattern) (Weight)	0.31	0.21
Shear Base Capacity (Linear Load Pattern) (Weight)	0.24	0.17
First Story Mechanism (Weight)	0.41	0.25

Note that the as-built (S-K) building has 23% longer periods than the conceptually designed building because it has a 14% greater mass and 32% smaller lateral stiffness. The smaller stiffness is mainly because of the smaller columns in all the frames and the smaller beam sizes in the exterior frames. The main difference in the lateral strength capacities between these two S-K buildings is in the lateral resistance of the interior frame columns. In stories 6 to 10, the longitudinal steel reinforcement in the columns of the as-built S-K building is about 60% of that used in the conceptually designed S-K building. These observed main differences are illustrated in the graphs given in **Appendix B**.

5.3.1 Nonlinear Dynamic Time-History Analyses

Analyses similar to those conducted for the conceptually designed S-K building were conducted for the S-K as built. Only the Los Gatos 1 and Takatori 1 EQGMs (**hereafter called Los Gatos and Takatori**) were considered because an analysis of the response spectra obtained for all the recorded motions used in this study reveals that, for a fundamental period $T_1 = 2.15$ seconds and a $\mu = 3$ to 6, these are the critical EQGMs. The analytical model used for these analyses is shown in **Figure 5.3.1**. Envelopes of maximum building response under the Los Gatos ground motion are shown in **Figure 5.3.2**. Location of maximum plastic hinge rotations and damage indices are shown in **Figures 5.3.3 and 5.3.4,** respectively. Similar data for the Takatori ground motion are shown in **Figures 5.3.5 through 5.3.7**.

5.3.2 Observations Regarding the Results Obtained

- The responses with ξ = 5% of the S-K as-built building (as it also was for the S-K conceptually designed building) are very sensitive to the recorded severe pulse-type EQGMs. The displacement and IDI envelopes are quite different for Los Gatos and Takatori records. Maximum values occur at quite different floor or story levels. Similarly, the maximum plastic rotation and maximum cumulative plastic rotations occur at different beams and columns (compare graphs in Figures 5.3.2 and 5.3.3 with those in Figures 5.3.5 and 5.3.6).

- Except for the maximum cumulative plastic rotation in the beams, the Los Gatos EQGM is more demanding than the Takatori EQGM, and it resulted in a Damage Index (DI) of 0.8 in the beams and of 1.1 in the columns of the story levels 6 to 8.

- The Los Gatos demands an IDI of about 3.3% at stories 6, 7, and 8. This value is unacceptable, demanding plastic rotations of about 5.4% in the columns and 3.8% in the beams.

- An increase in the damping coefficient ξ from 5% to 30% significantly reduces the responses under Los Gatos and Takatori. The reductions for most of the response parameters are about 60%. Thus the response (performance) of the as-built S-K building will be acceptable if, by adding dampers, its effective ξ can be increased to 30%.

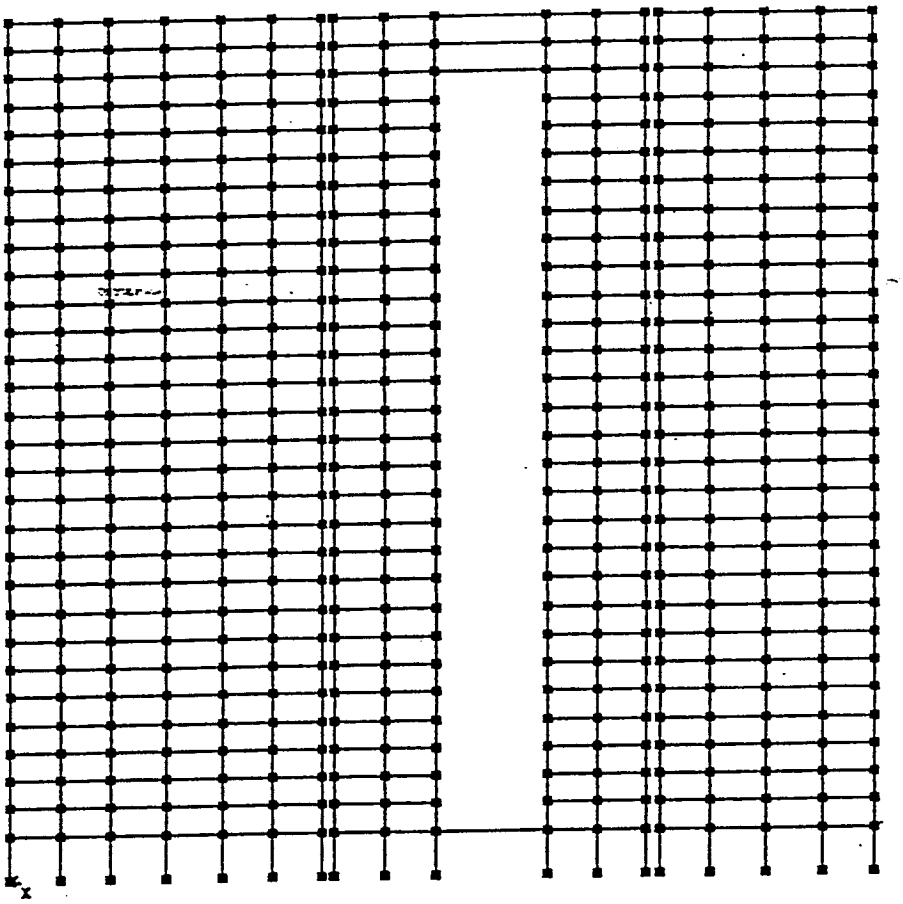

Figure 5.3.1 Analytical Model, S-K as Built

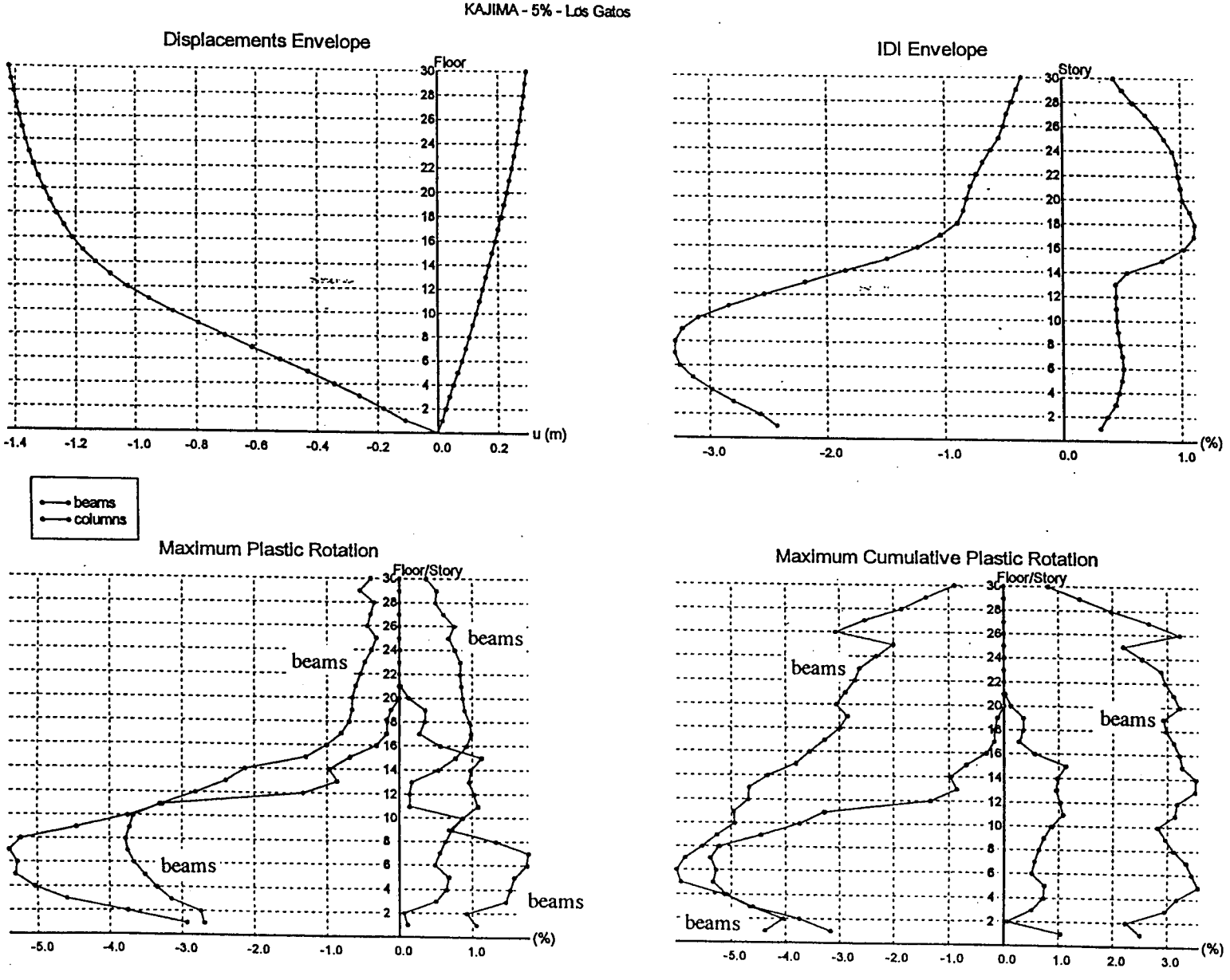

Figure 5.3.2 Building Response Envelopes, Los Gatos

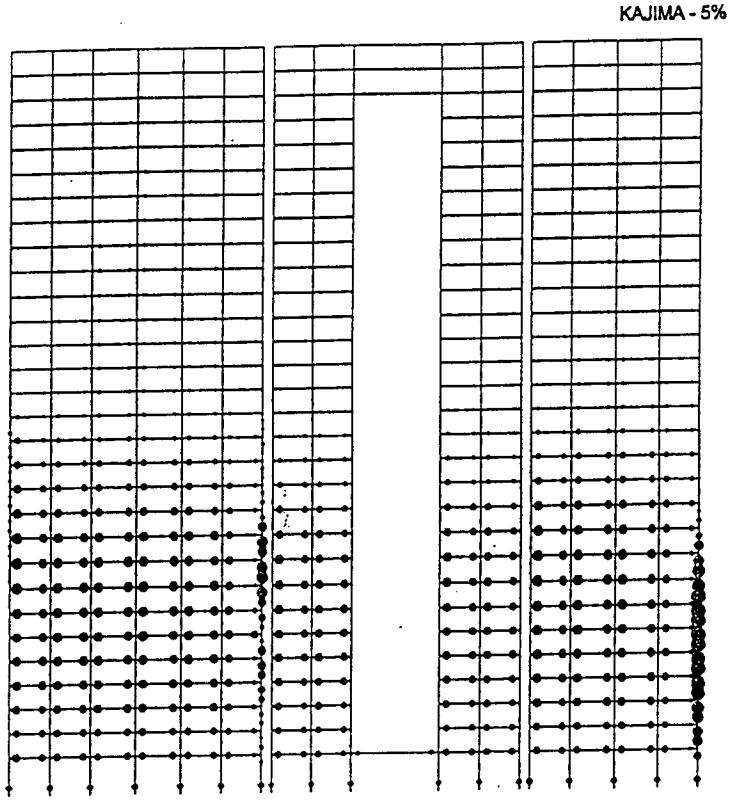

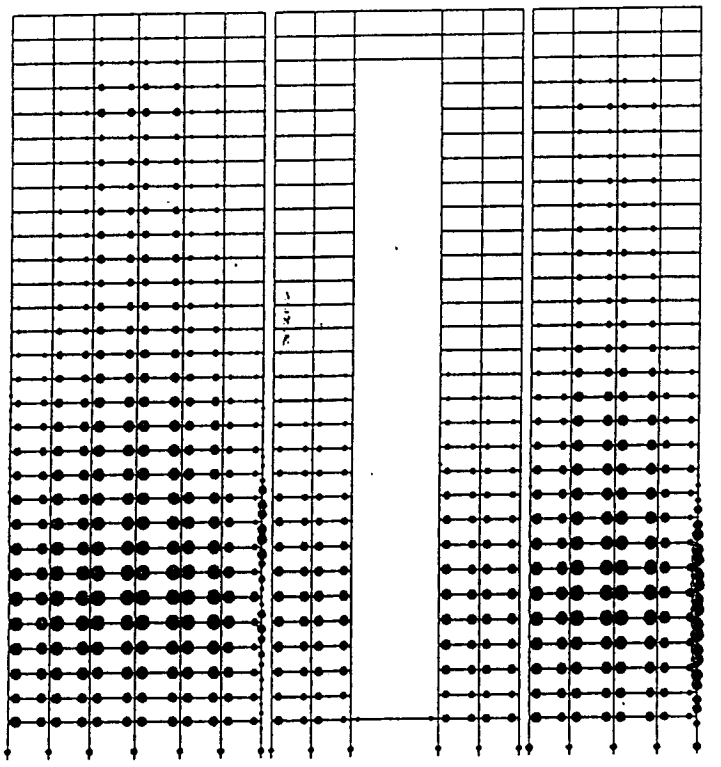

Figure 5.3.3 Plastic Hinge Rotations, Los Gatos

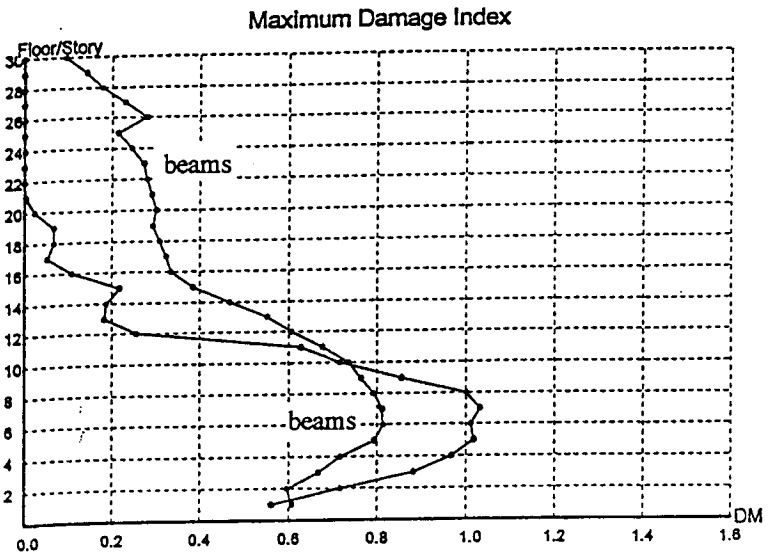

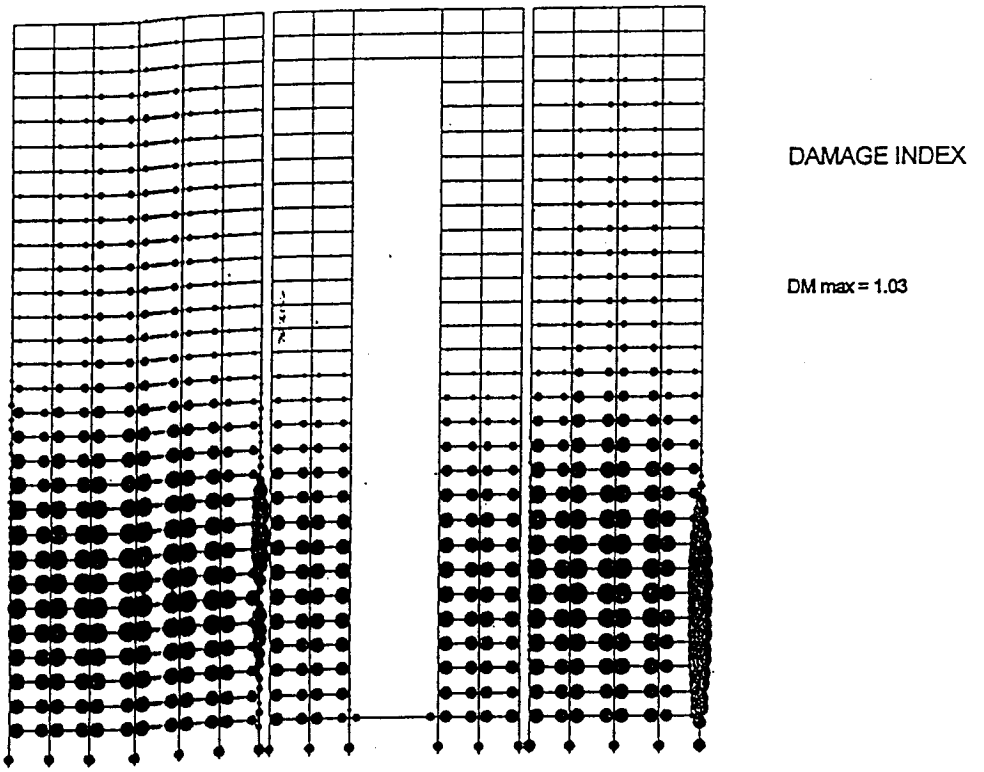

Figure 5.3.4 Damage Index, Los Gatos

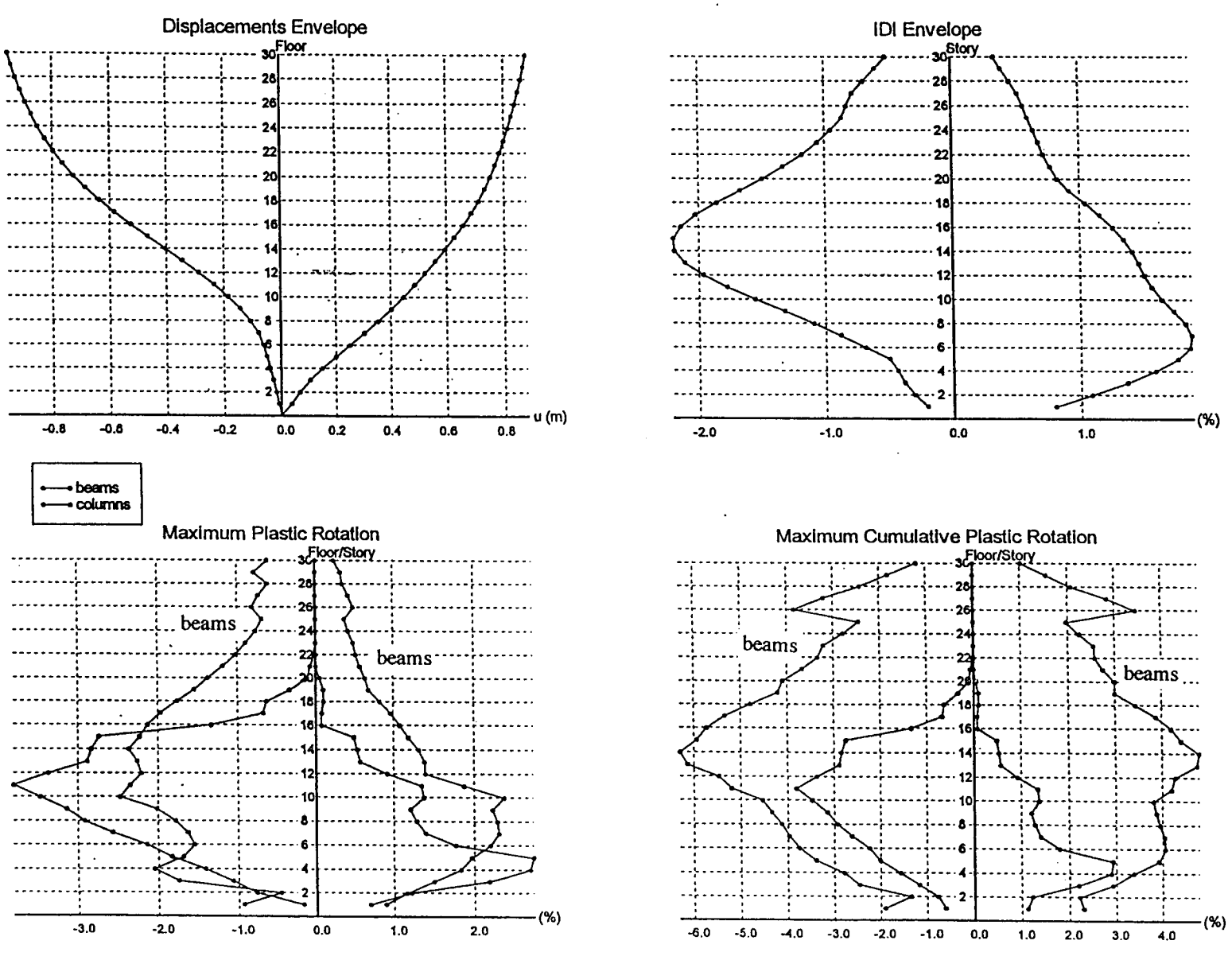

Figure 5.3.5 Building Response Envelopes, Takatori

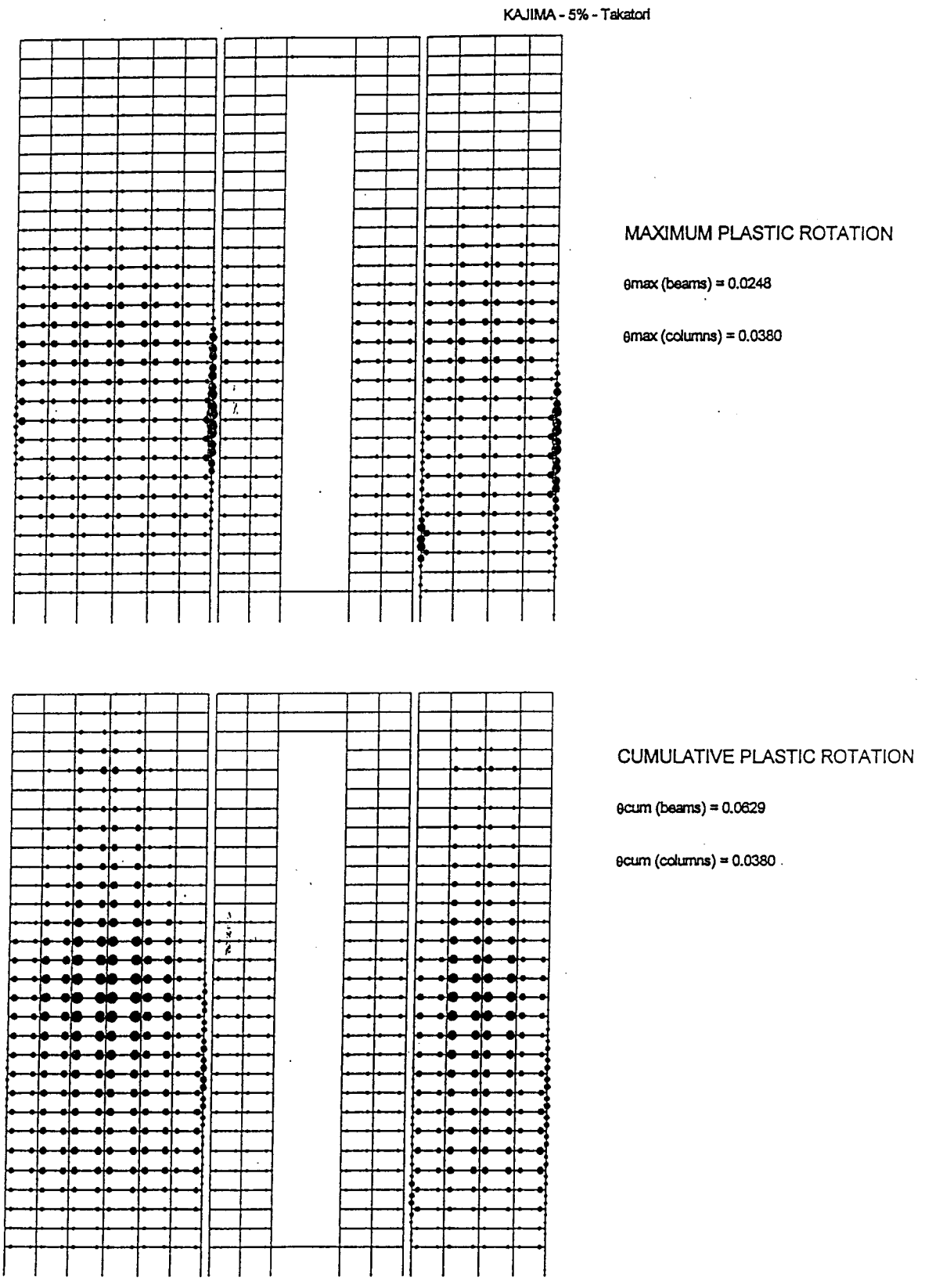

Figure 5.3.6 Plastic Hinge Rotations, Takatori

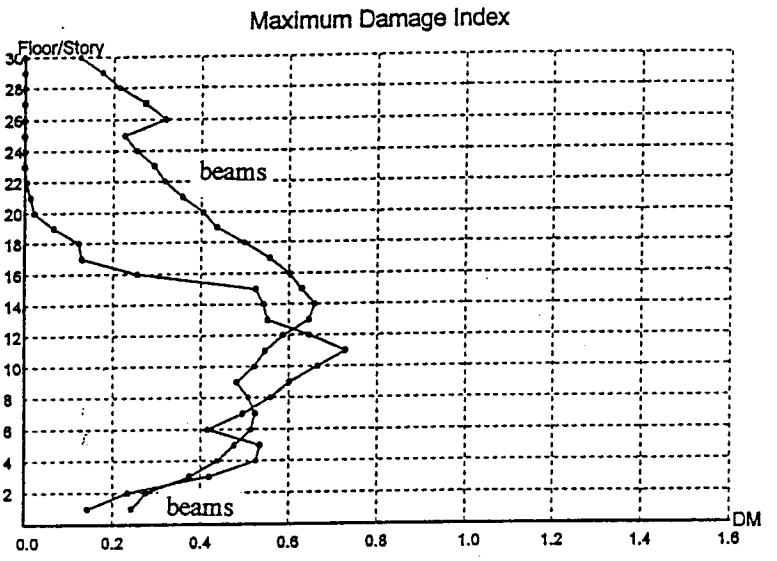

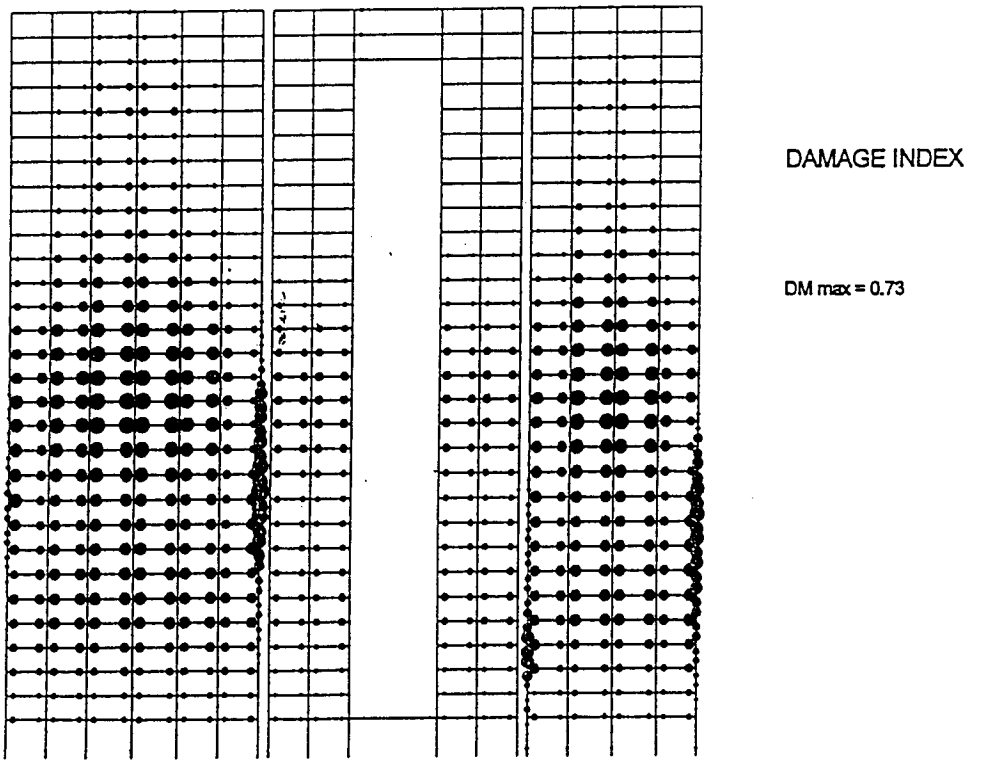

Figure 5.3.7 Damage Index, Takatori

5.4 THE 30-STORY S-K BUILDING REDESIGNED ACCORDING TO 1991 UBC

As part of an earlier CUREe/Kajima study [Anderson and Chen 1992], the S-K Building was redesigned according to the then current Uniform Building Code [ICBO 1991]. Due to the height of the building and its location in the equivalent of seismic zone 4, a dynamic analysis was used. Rather than use the normalized response spectrum given in the code, a site specific design spectrum [Bertero and Bertero, 1992] for soft soil sites was used. Orthogonal effects are considered by designing the structure for one hundred percent of the prescribed seismic forces in one direction plus thirty percent in the perpendicular direction. According to code, if the base shear determined by the dynamic analysis is different form that specified by the static lateral force procedure, the dynamic analysis results are scaled to agree with the base shear given by the static procedure. This resulted in a design base shear of 5% of the total weight of 51,600 kips (25,800 tons).

5.4.1 Dynamic Time-History Analyses

An isometric view of the three-dimensional model of the building used for the linear elastic analyses conducted with the ETABS Plus computer program [CSI,1992] is shown in **Figure 5.4.1**. The plan layouts used are summarized in **Figure 5.4.2** and the section sizes determined from the UBC design are summarized in **Figures 5.4.3** and **5.4.4.** Summaries of the reinforcement used in the individual members can be found in the original study [Anderson and Chen, 1992]. Elastic dynamic analyses were conducted using the ETABS program and the nonlinear dynamic analyses were conducted using an in-house program that is similar to DRAIN-2D. For the nonlinear analyses, only a typical frame on Line B was considered. The earthquake ground motions considered in the analyses included the motions recorded at Los Gatos, Lexington Dam, Takatori, and James Road, in addition to the idealized pulse discussed previously. The James Road (1979) record was used in the earlier study and was included as a basis for comparison with those results. Time histories of the recorded accelerations for these records and the resulting response spectra are shown in **Figures 5.4.5** and **5.4.6**. The periods for the first three translational modes of vibration for this building were calculated as 2.16, 0.68, and 0.34 seconds.

The displacement response envelopes obtained using elastic and nonlinear dynamic analyses for the four recorded ground motions are shown in **Figures. 5.4.7 - 5.4.10**. For the Los Gatos record, shown in **Figure 5.4.7**, the elastic and nonlinear displacement responses are quite different, particularly for the interstory drift index. The nonlinear response indicates an IDI demand at the fifth floor level of almost 3%. A similar pattern of displacement response is indicated in **Figure 5.4.8** for the Lexington Dam record where the nonlinear IDI demand reaches 2.8%. The elastic and inelastic displacement envelopes for the Takatori ground motion, shown in **Figure 5.4.9** are also different with the elastic response being approximately three times larger. The inelastic IDI demand is only 2% for this record and occurs at the 5-6 floor levels. The displacement response for the James Road record, shown in **Figure 5.4.10**, has an inelastic IDI demand of less than 1.5%. This was the controlling ground motion for the earlier study and for this reason, among others, the design was deemed to be adequate.

The results of a static pushover analysis (neglecting P-Δ) are shown in **Figure 5.4.11**. Plastic

hinge locations are shown in **Figure 5.4.11a**. From the displacement vs. base shear plot, **Figure 5.4.11b**, the yield base shear for the frame is estimated as 950 kips (4,225 kN). For the complete building, the yield base shear is estimated to be 6000 kips (26,700 kN). This results in a yield seismic resistance coefficient, C_y, of 0.12.

The displacement response envelopes for the nonlinear dynamic analyses are shown in **Figure 5.4.12**. It can be seen that the Los Gatos ground motion produces the most severe displacement response for this building. The results also indicate that the lateral displacement envelope for the idealized pulse is a close approximation to the envelope for the Takatori ground motion. The Lexington Dam record produces a displacement envelope of similar shape to that of Los Gatos but not as large. It is interesting to note that the James Road record, which produced the largest displacement response in the earlier study, results in the smallest response, which is less than 50% of the maximum response. Envelopes of girder ductility demand (curvature ductility) and girder plastic rotation demand are shown in **Figure 5.4.13**. The general shape of these envelopes are similar to those of the interstory drift index. Curvature ductility demand in excess of 20 is required for the Los Gatos and Lexington Dam records with plastic rotation demands of more than 4%. These values compare with demands of 12 and 2.4% for the James Road ground motion which are much more manageable. The displaced shape of the building and the distribution of the plastic hinges are shown in **Figures 5.4.14-5.4.18** for the four ground motions and the idealized pulse. Time histories of the base shear obtained from the nonlinear analyses are shown in **Figure 5.4.19**. The dotted lines indicate the yield value obtained from the pushover analysis.

5.4.2 Observations Regarding the Results Obtained

- The displacements obtained from elastic dynamic analyses do not necessarily provide a good estimate of the displacements obtained from the nonlinear dynamic analyses.

- The building response obtained from one of the strongest pulse-type motions available at the time of the previous study (James Road, 1992) produces displacement and ductility demands that are less than 50% of those required by more recent pulse-type ground motions (Los Gatos, Lexington Dam).

- The displacement and ductility demands on this building from the more recent earthquakes are unacceptable. This indicates that some building modification (retrofit) scheme will have to be used to reduce them.

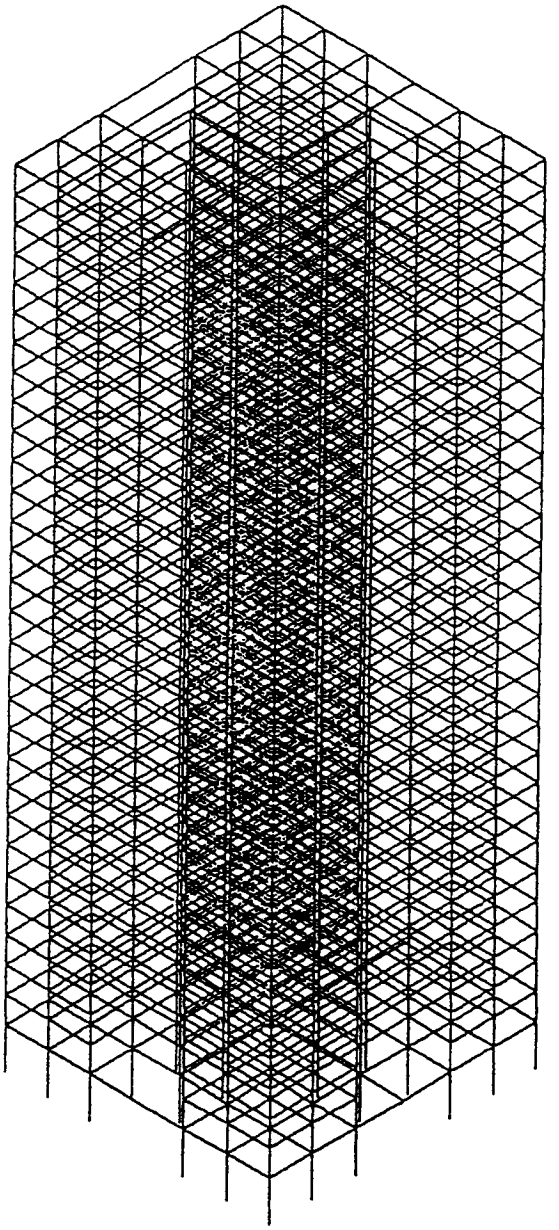

Figure 5.4.1 S-K Building, Elastic ETABS Model

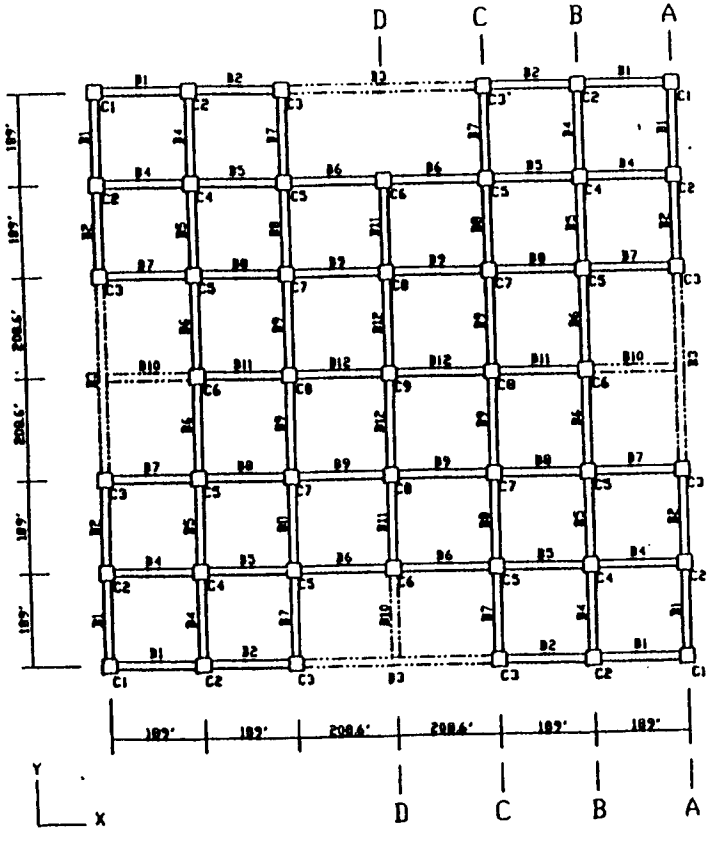

(a) Column and Beam Types

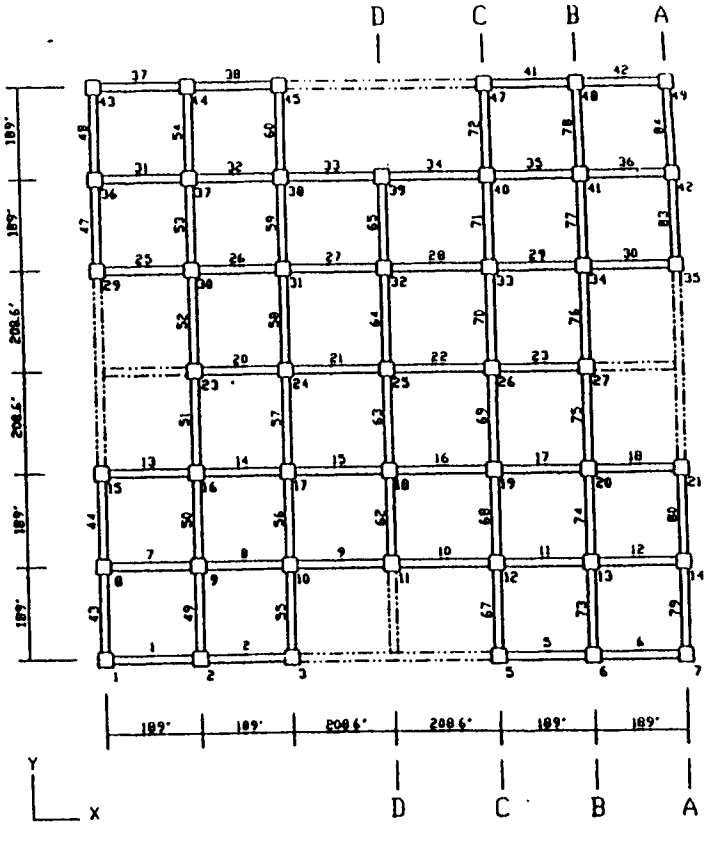

(b) Column Line and Bay Numbers

Figure 5.4.2 S-K, Typical Floor Plans, ETABS Model

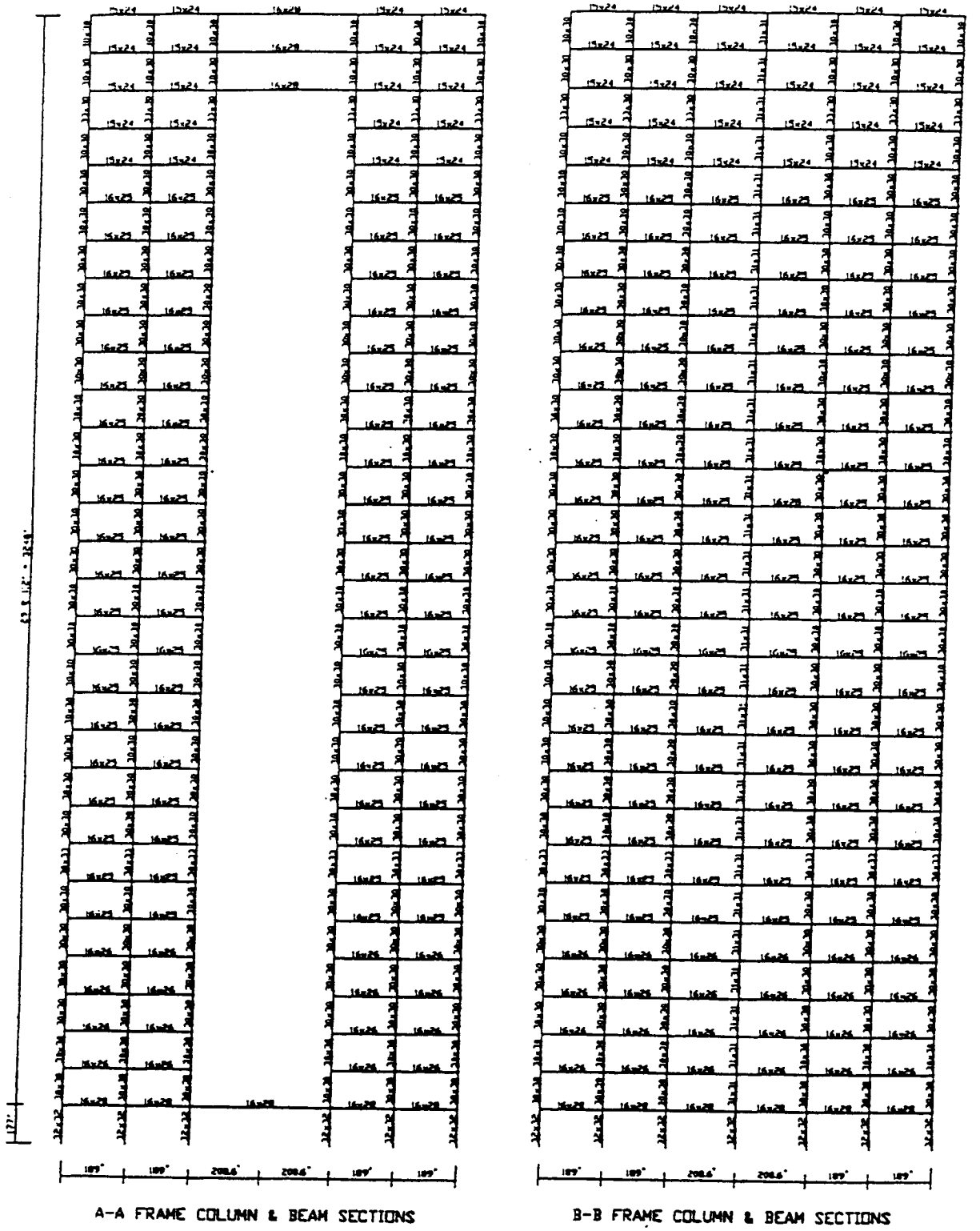

Figure 5.4.3 S-K Frame Lines A and B, Member Sizes, UBC

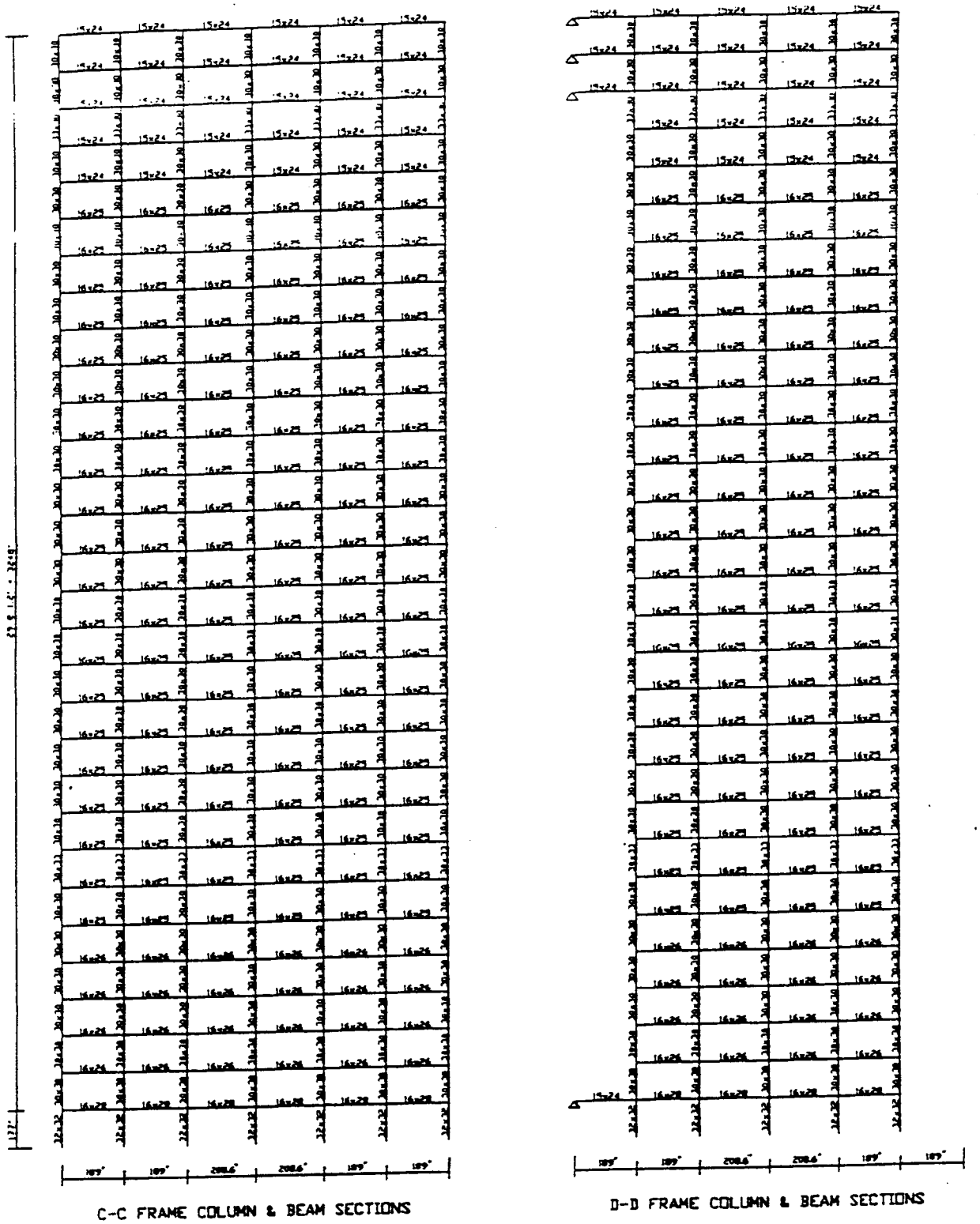

Figure 5.4.4 S-K Frame Lines C and D, Member Sizes, UBC

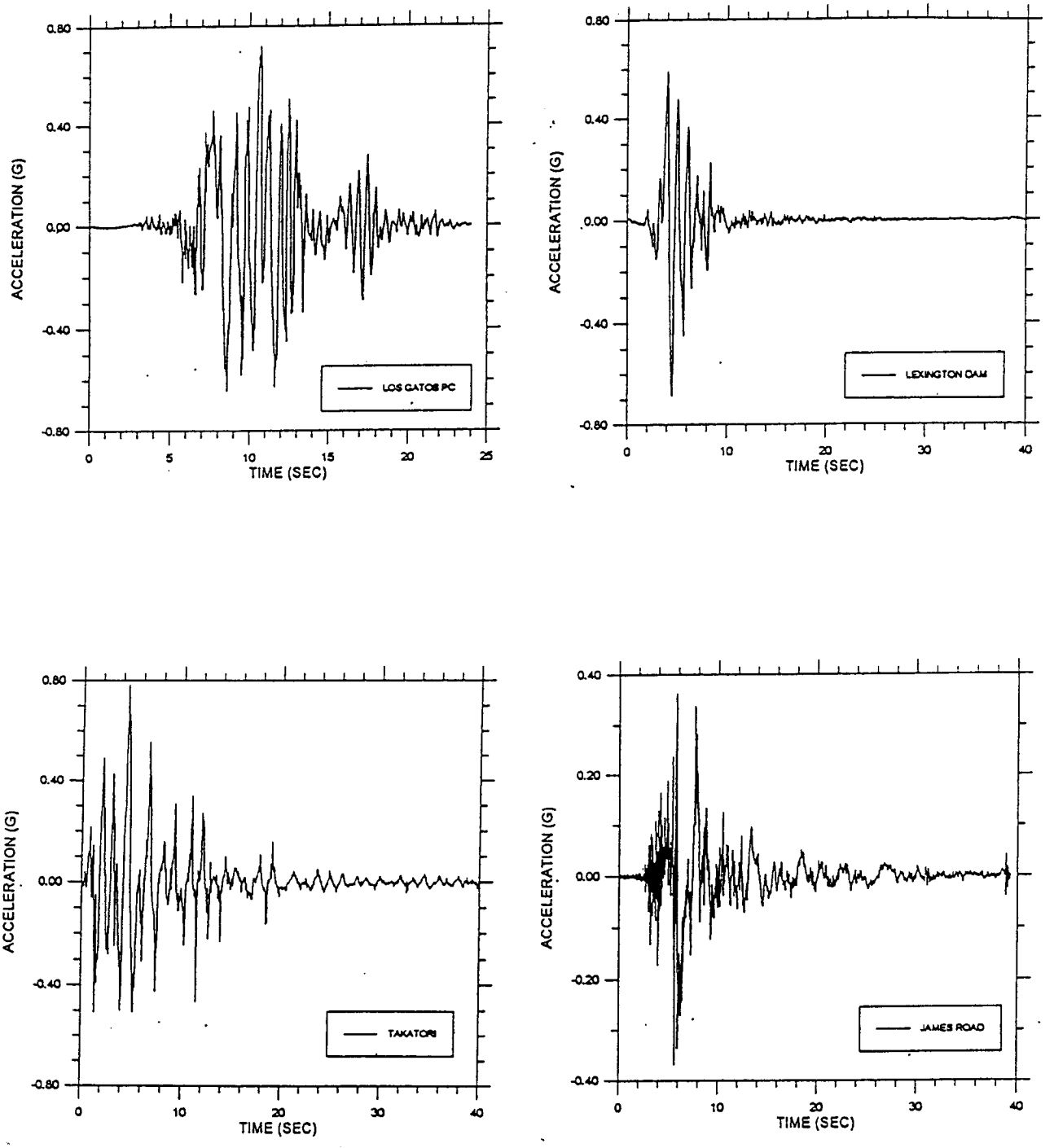

Figure 5.4.5 Pulse-Type Earthquake Acceleration Records

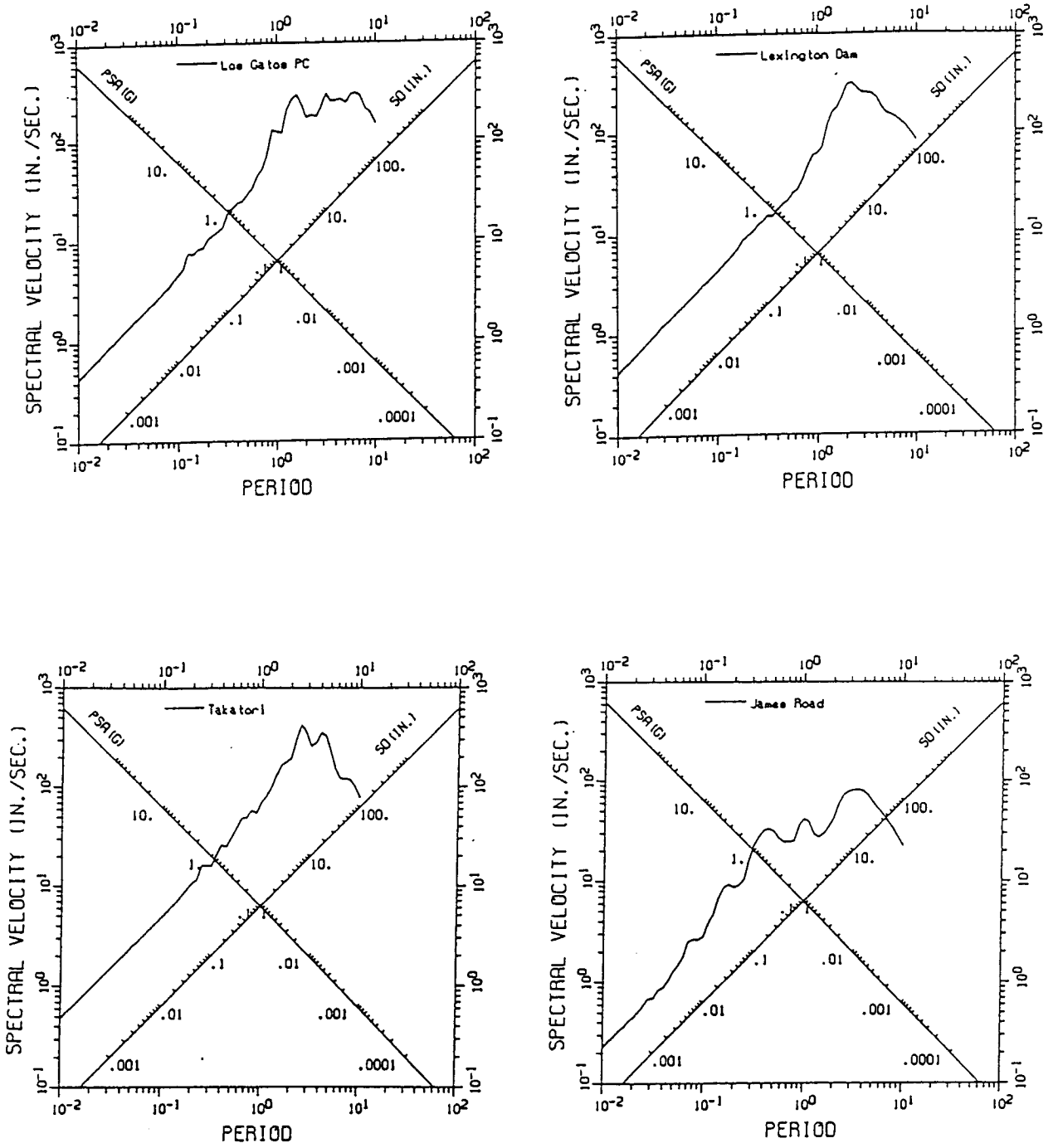

Figure 5.4.6 Pulse-Type Earthquake Elastic Spectra

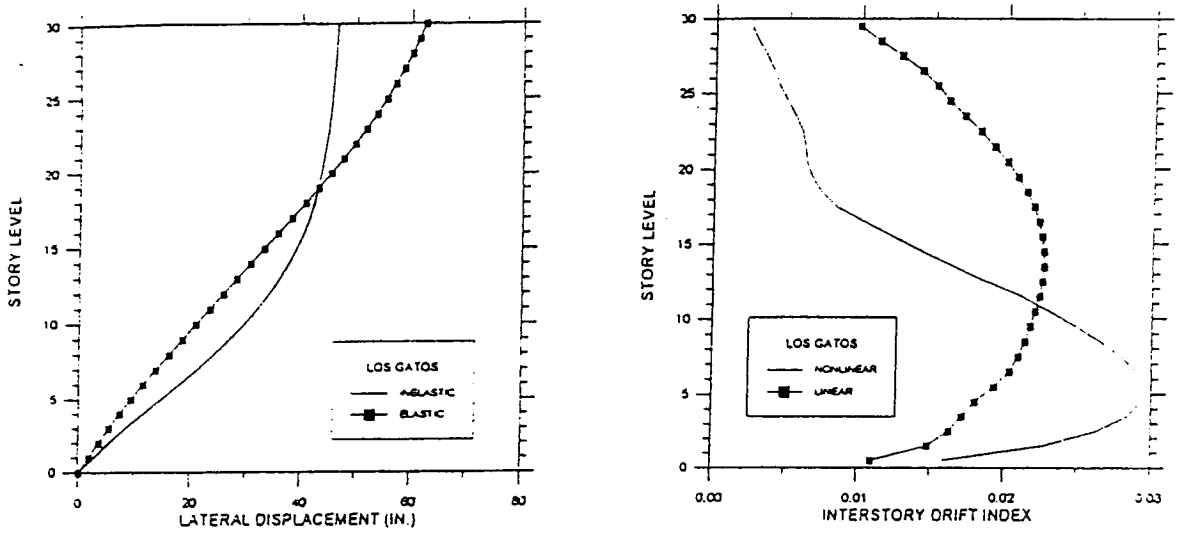

Figure 5.4.7 S-K (UBC) Elastic vs. Inelastic Displacement, Los Gatos

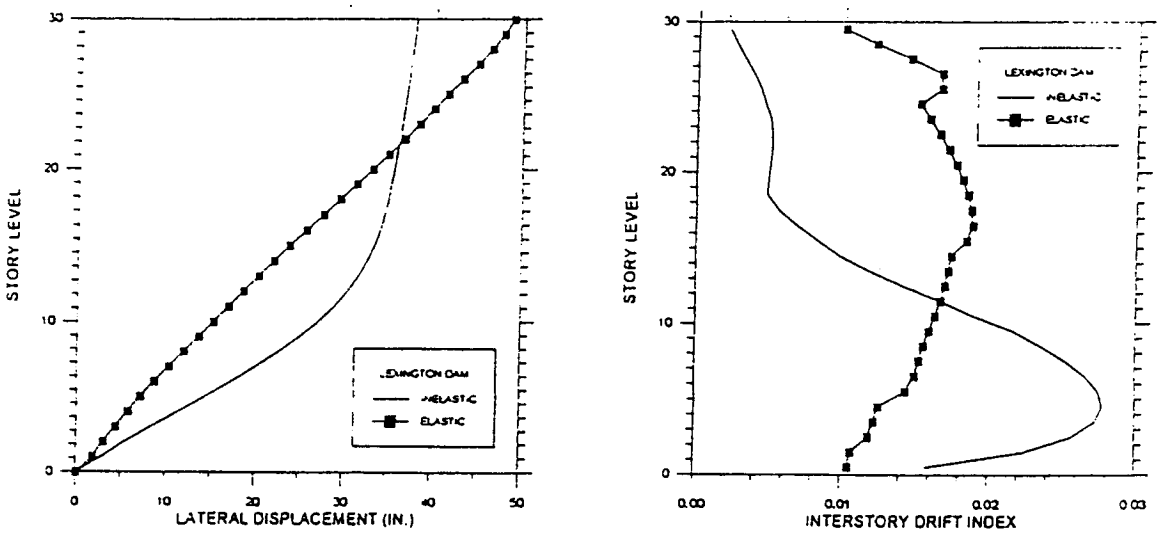

Figure 5.4.8 S-K (UBC) Elastic vs. Inelastic Displacement, Lexington Dam

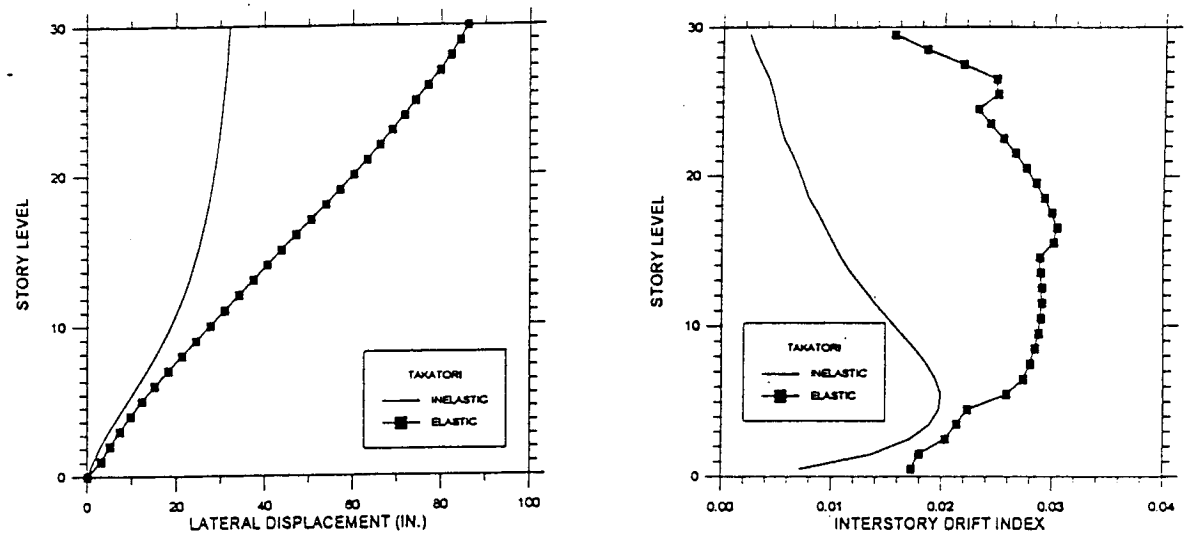

Figure 5.4.9 S-K (UBC) Elastic vs Inelastic Displacement, Takatori

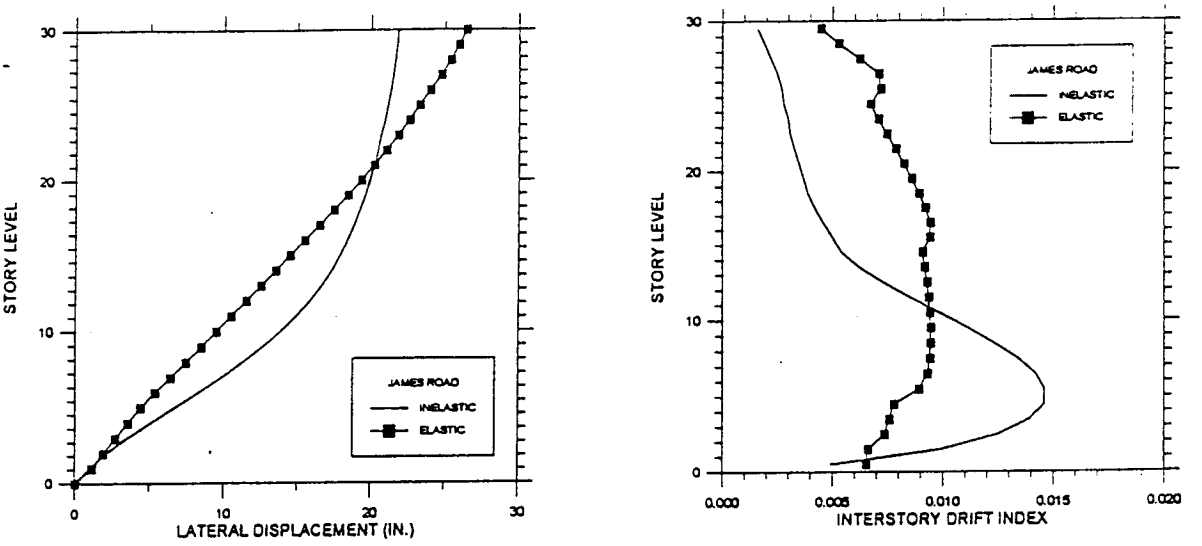

Figure 5.4.10 S-K (UBC) Elastic vs. Inelastic Displacement, James Road

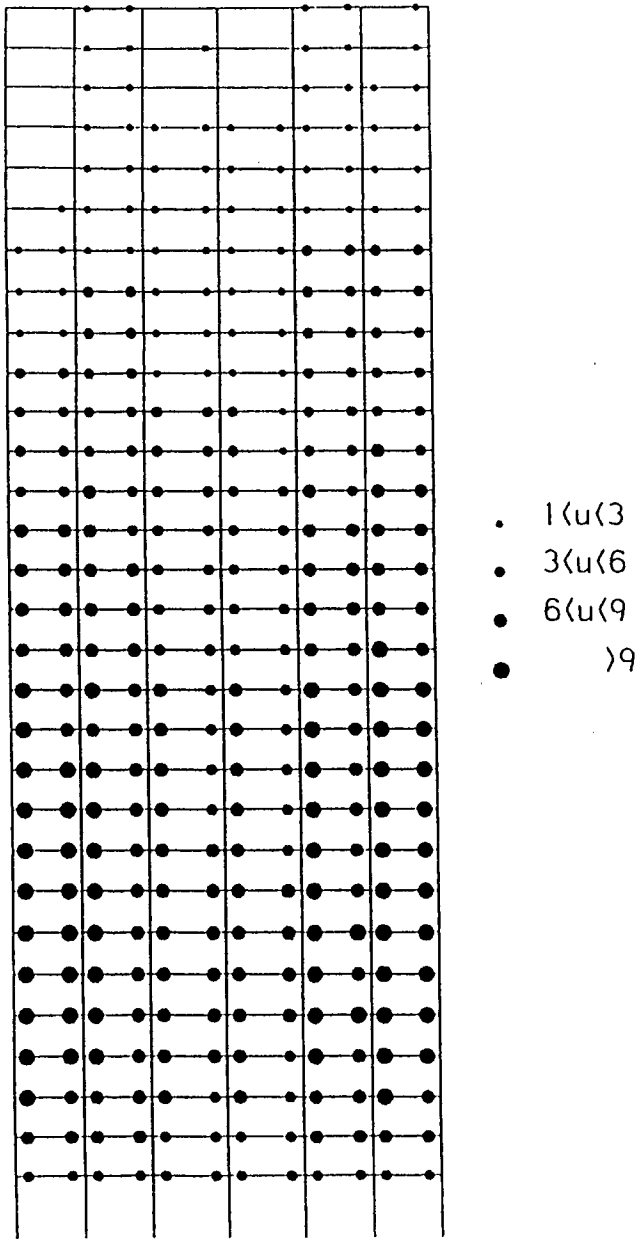

(a) Plastic Hinge Locations

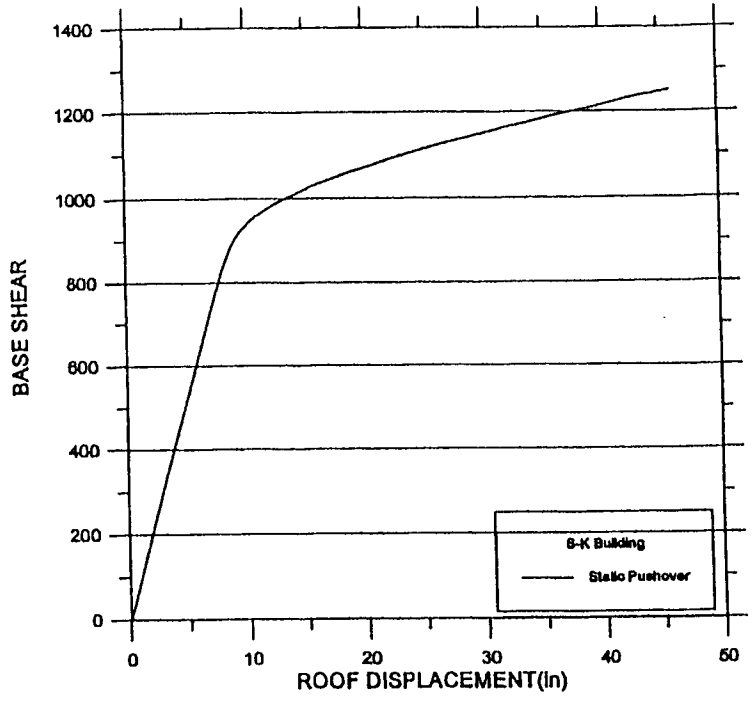

(b) Base Shear vs. Roof Displacement

Figure 5.4.11 Static Pushover, S-K (UBC) Building

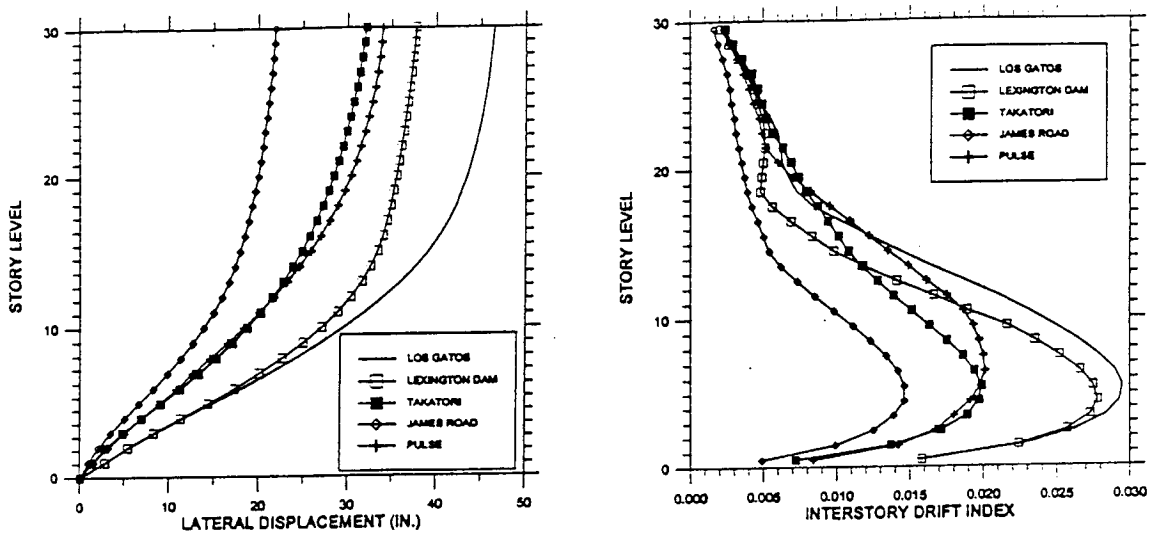

Figure 5.4.12 Displacement and Drift Demands, S-K Building, UBC

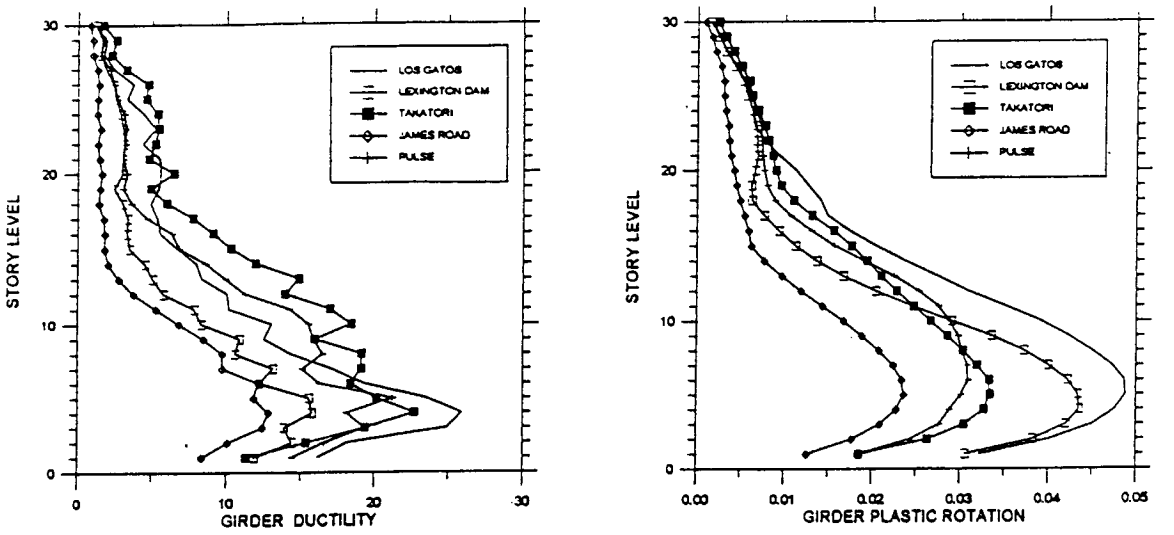

Figure 5.4.13 Ductility and Plastic Rotation Demands, S-K Building, UBC

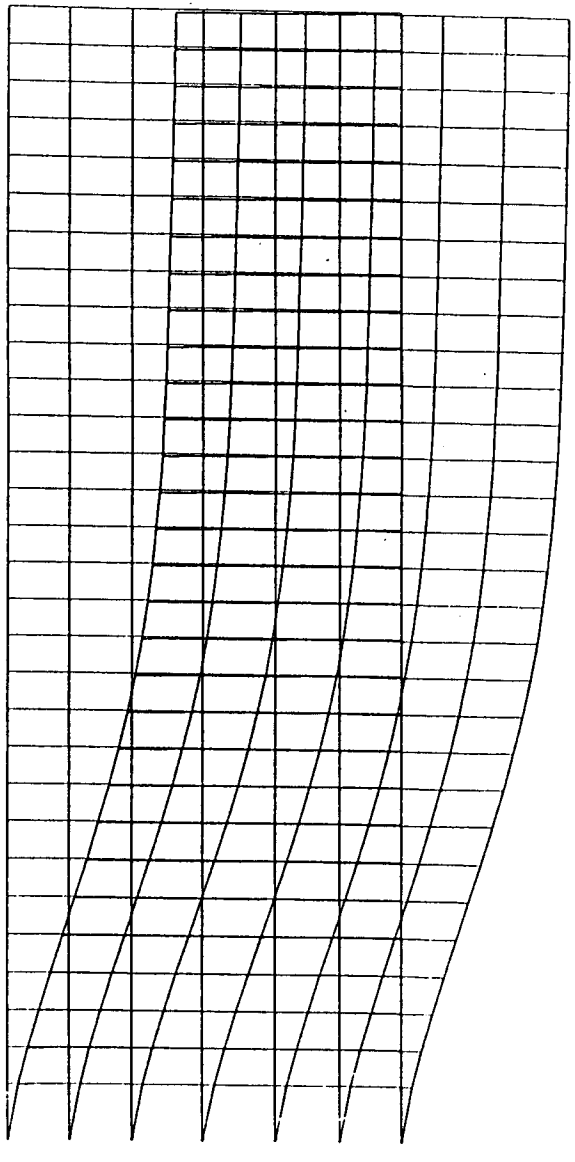

(a) Max. Displaced Shape, Δ_{Roof} = 47 inches

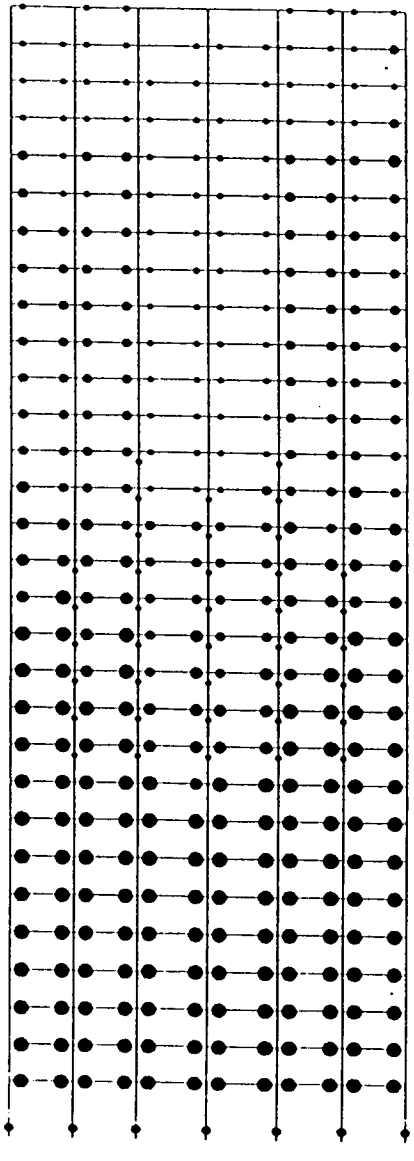

(b) Plastic Hinge Locations

Figure 5.4.14 S-K (UBC) Building Response, Los Gatos

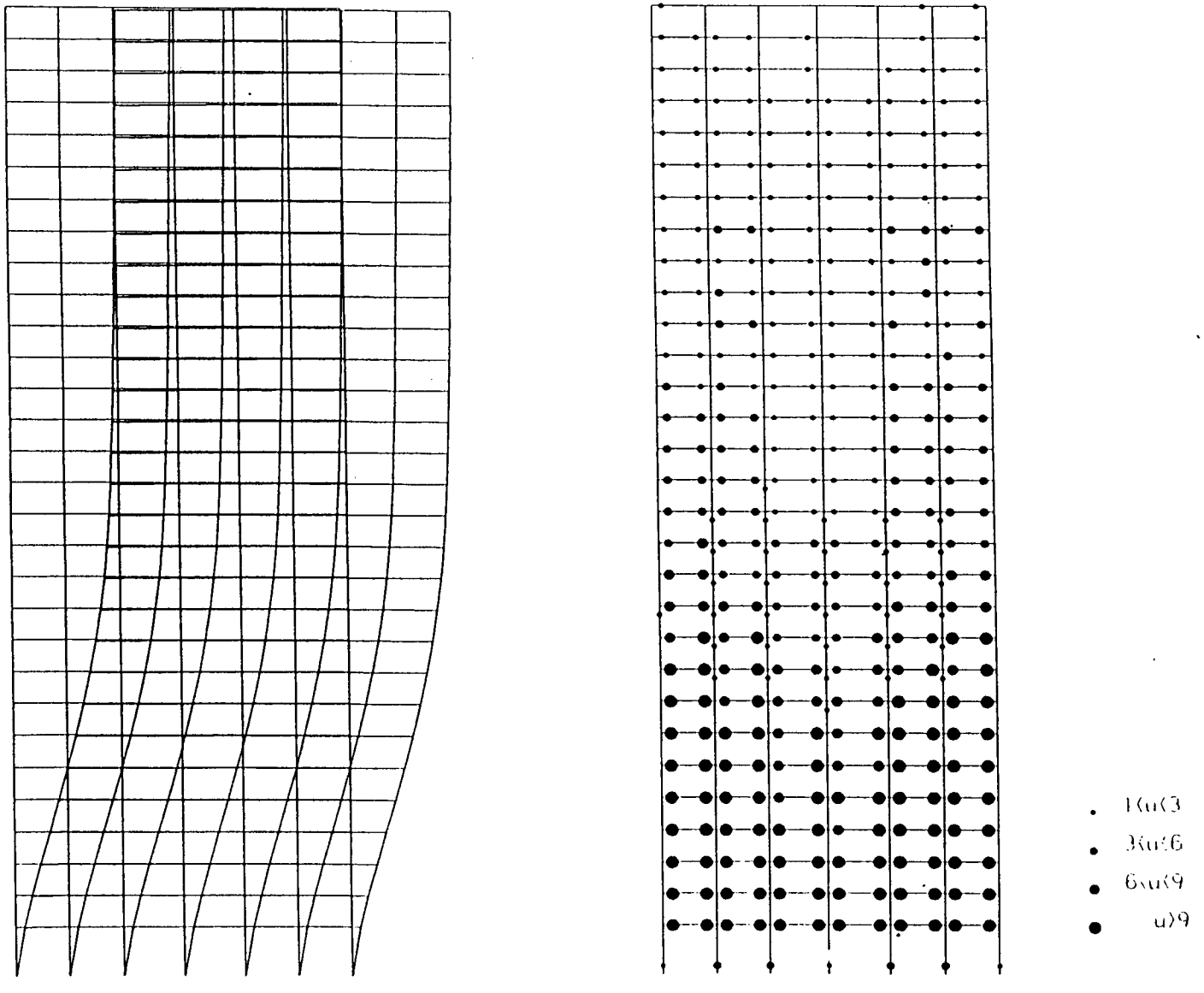

(a) Max. Displaced Shape, Δ_{Roof} = 38.4 inches

(b) Plastic Hinge Locations

Figure 5.4.15 S-K (UBC) Building Response, Lexington Dam

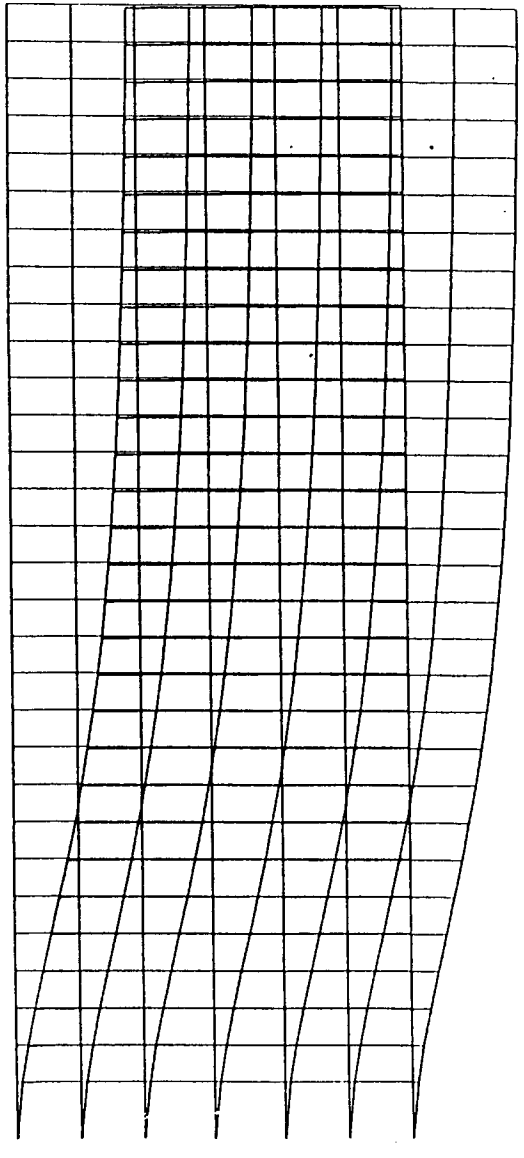

(a) Max. Displaced Shape, Δ_{Roof} = 32 inches

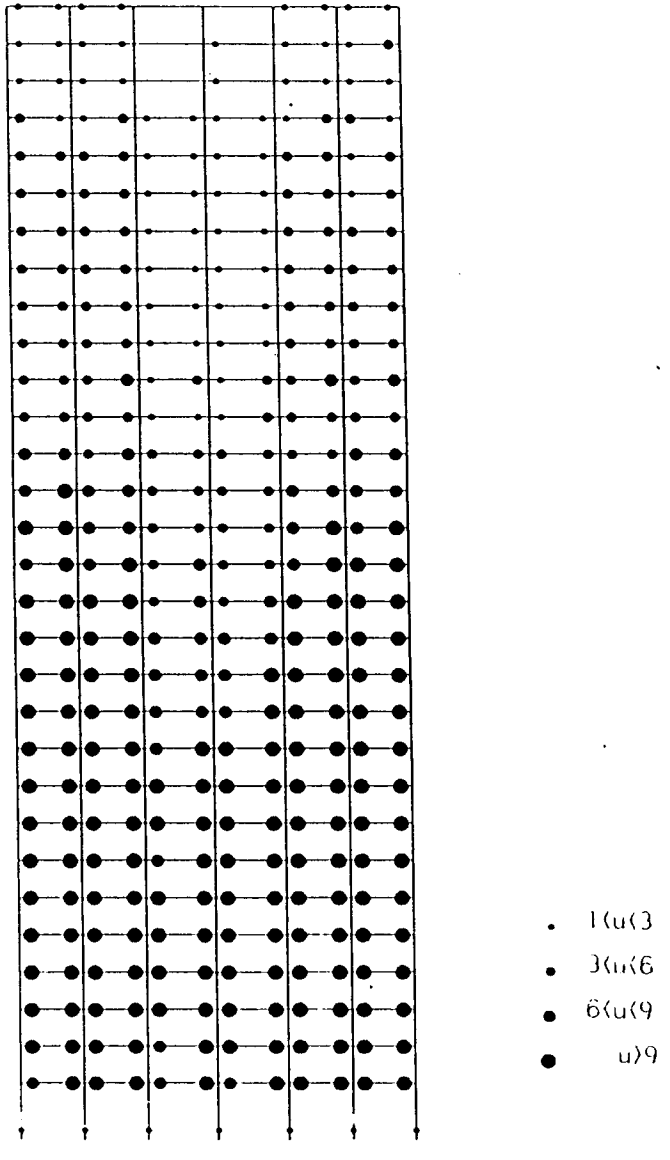

(b) Plastic Hinge Locations

Figures 5.4.16 S-K (UBC) Building Response, Takatori

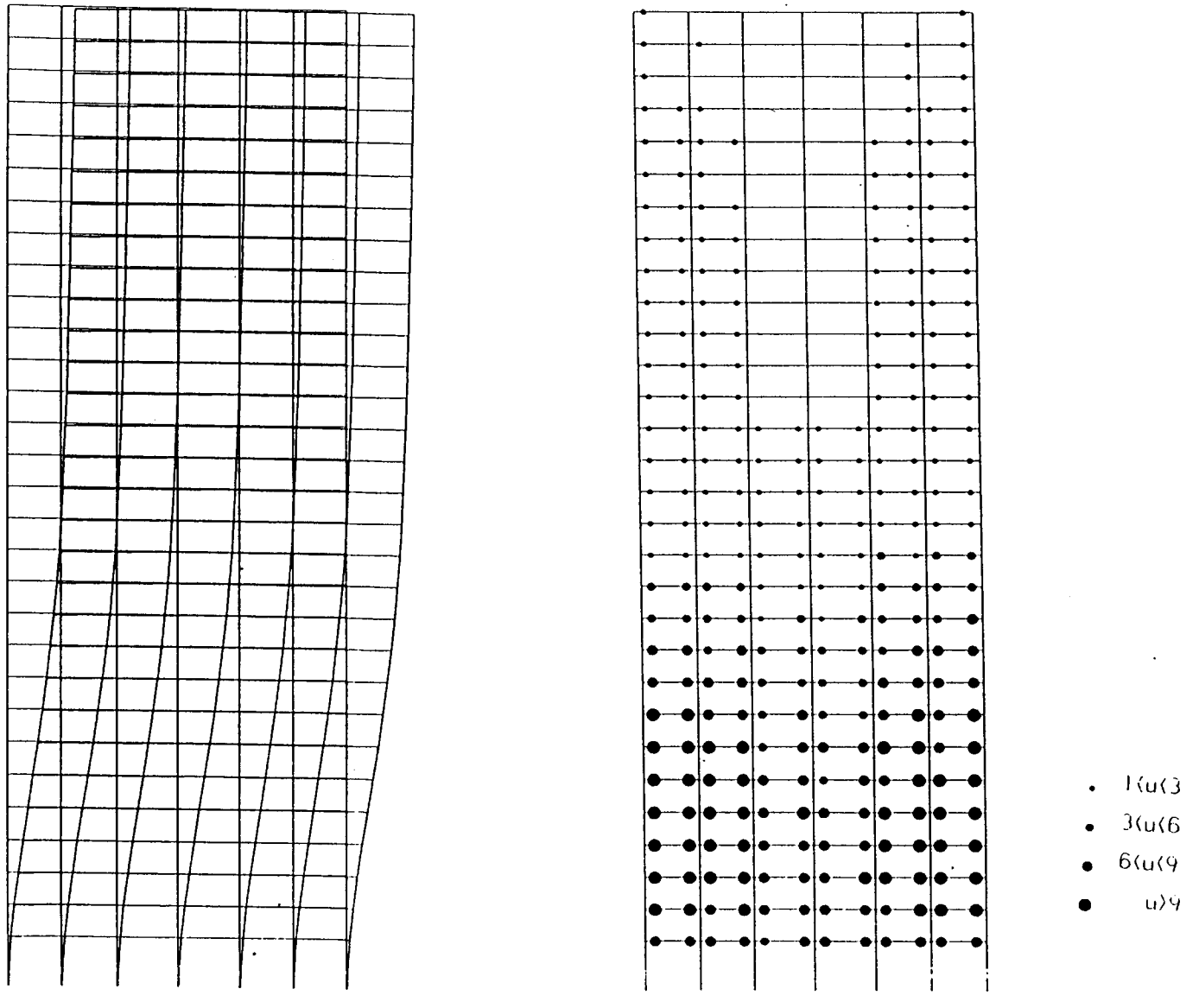

(a) Max. Displaced Shape, Δ_{Roof} = 22 inches

(b) Plastic Hinge Locations

Figure 5.4.17 S-K (UBC) Building Response, James Road

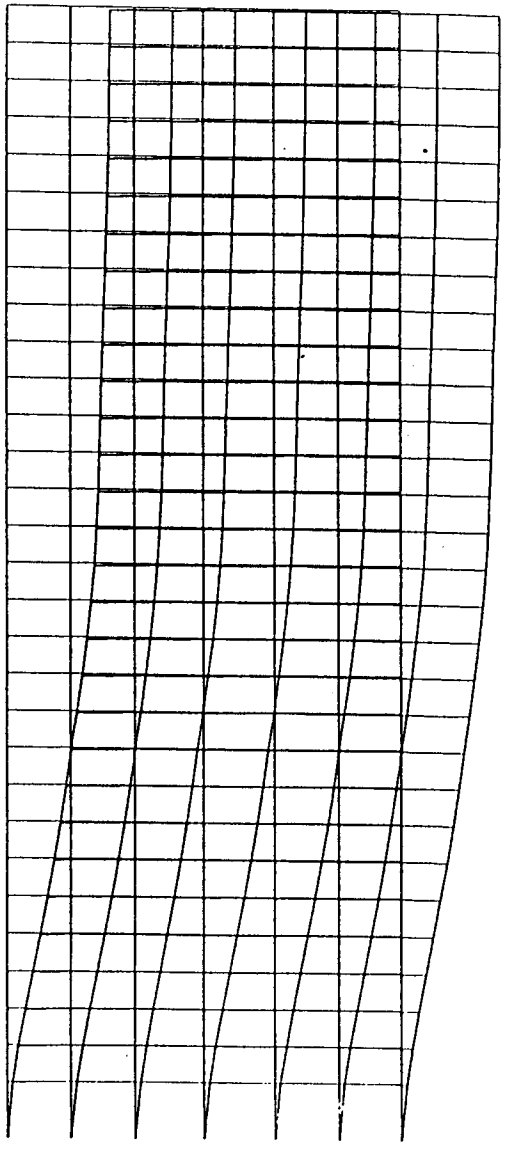

(a) Max. Displaced Shape, Δ_{Roof} = 33.5 inches

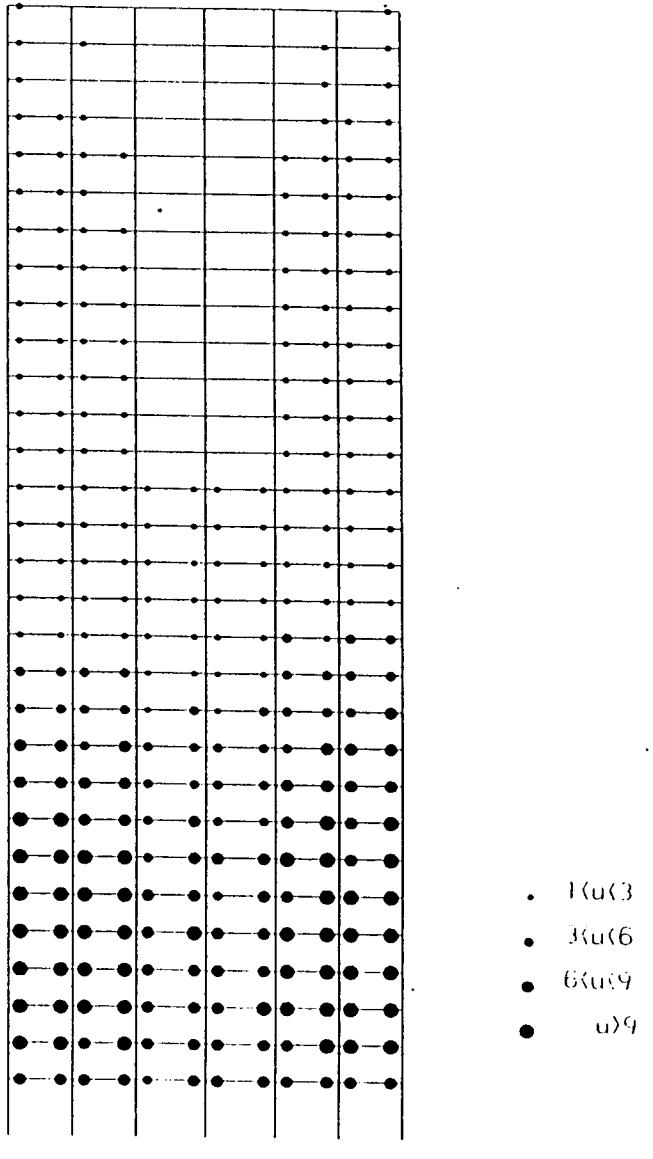

(b) Plastic Hinge Locations

Figure 5.4.18 S-K (UBC) Building Response, Idealized Pulse

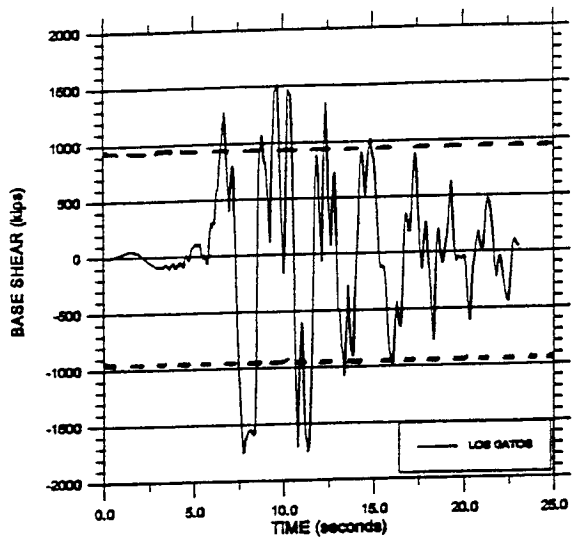

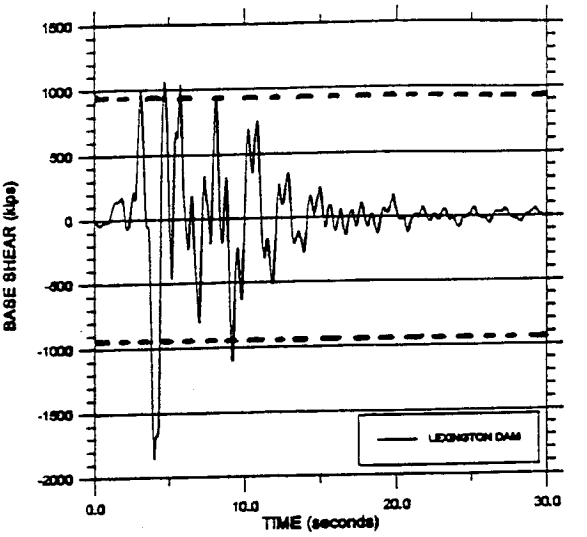

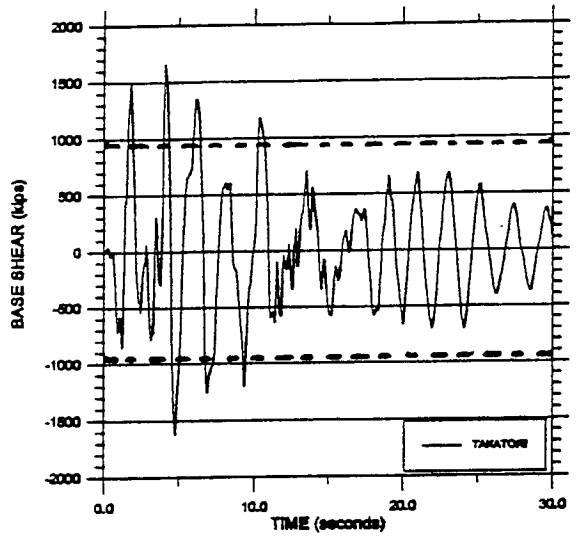

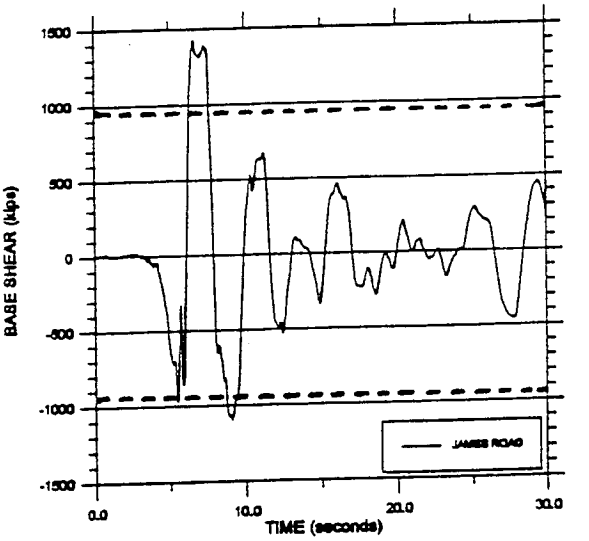

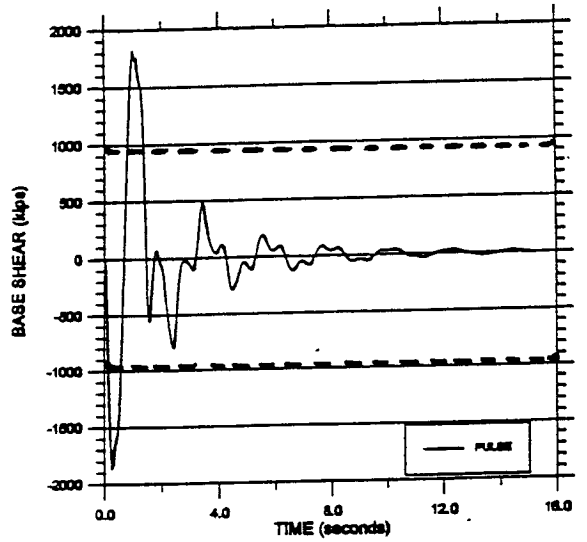

Figure 5.4.19 S-K (UBC) Base Shear Response

5.5 THE 15-STORY RC MOMENT-RESISTANT FRAME AS BUILT IN 1965

This building was designed in 1964 and built in 1965. The plan for a typical floor, shown in **Figure 5.5.1a**, indicates a building plan that is 75 feet wide and 193 feet long. The foundation plan, shown in **Figure 5.5.1b**, indicates the location of the cast-in-place piles. An elevation of a typical transverse section is shown in **Figure 5.5.2**. Thirteen story levels are above grade and the two which are below grade, are enclosed by shear walls. The total height above the first floor is 164 feet - 6 inches. The foundation consists of cast-in-place concrete piles that extend a distance of 34 feet below the sub-basement level. A review of the design and detailing of the reinforcement indicates that the existing structure, which is a RC moment-resistant frame, has several significant weaknesses regarding its resistance to even moderate EQGMs. These weaknesses include the following: (1) deficient amounts of transverse reinforcement along all the main components (columns, girders, and particularly the girder-column joints which contain no transverse reinforcement); (2) lack of adequate longitudinal reinforcement along the bottom of the girders as well as at the top near the midspan; (3) poor anchorage of the bottom longitudinal reinforcement in the girders at the columns; and (4) inadequate lap splicing of the longitudinal reinforcement. A detailed study of this building has been reported elsewhere [Sasani et al., 1999].

5.5.1 Linear and Nonlinear Analyses

From the results of a 3D linear elastic analysis of this building, it was determined that the fundamental period in the transverse direction (fixed base) was 2.6 seconds. However, when the flexibility of the two basements and rotation of the foundation were included, the period increased to 3.2 seconds. Using the response spectra developed for constant $\xi = 5\%$ and considering all the recorded severe pulse-type EQGMs shown in **Table 3.4**, it was estimated that for the computed periods, the two most probable critical EQGMs were the Los Gatos 1 and Takatori 1. Thus, the following nonlinear analyses were conducted.

(a) Nonlinear Static (Pushover) and Dynamic (Time-History) Analyses

These analyses were conducted using the DRAIN 2DX (1988) program considering the following two models: (1) fixed-base; and (2) flexibility of basements and rotation of foundation. The main results obtained are summarized in **Table 5.4**. Results of the pushover analysis are shown in **Figure 5.5.3** and results of the nonlinear dynamic analysis for the Los Gatos ground motion are shown in **Figure 5.5.4**. From these results, it becomes clear, assuming $\xi = 5\%$, that the maximum IDI for Los Gatos 1 (6.1% and 5.4% for the two above models) are significantly higher than the acceptable values. Thus, there is a need to seismically upgrade this building if it could be subjected to severe pulse-type EQGMs. Even if the ξ_{eff} is increased to 30%, the $(IDI)_{max}$ values will be unacceptable.

Table 5.4 As-Built Structure (W≈25000 kips)

Type of Supports	Response Parameters	Pushover Analysis[1]	Los Gatos Ground Motion (1989 Loma Prieta EQ)			Takatori Ground Motion (1995 Kobe EQ)		
			Spectral Response[2] (ξ=5%)	Dynamic Analysis[1] (ξ=5%)	Dynamic Analysis[1] (ξ=30%)	Spectral Response[2] (ξ=5%)	Dynamic Analysis[1] (ξ=5%)	Dynamic Analysis[1] (ξ=30%)
Basement & Foundation Flexibility Included (T=3.2 sec) (Δ_y≈18.5in)	Δ_{top} (in)	53 (μ=2.9)		69 (μ=3.7)	43		32 (μ=1.7)	30
	$\Delta_{2/3H}$ (in)	47	80	60	35	32	21	20
	IDI_{ave}	2.7%		3.5%	1.8%		1.6%	1.5%
	IDI_{max}	4.3%		5.4%	3.2%		2.8%	1.9%
	IDI(ratio)	1.6		1.5	1.8		1.8	1.3
	$Max\Delta_{found}$	0.4%		0.5%	0.5%		0.5%	0.5%
	IDI_{tang}	3.9%		4.9%	2.7%		2.3%	1.4%
	V_{base} (w%)	14%	21%[3]	20%[4]	23%[4]	20%[3]	18%[4]	19%[4]
Fixed –Base (T=2.6 sec) (Δ_y≈12.7 sec)	Δ_{top} (in)	45 (μ=3.5)		72 (μ=5.8)	35		31 (μ=2.4)	26
	$\Delta_{2/3H}$ (in)	41	79	67	31	31	20	20
	IDI_{ave}	2.3%		3.6%	1.7%		1.6%	1.3%
	IDI_{max}	3.8%		6.1%	3.1%		2.6%	1.9%
	IDI(ratio)	1.7		1.7	1.8		1.6	1.5
	V_{base} (w%)	14%	20%[3]	19%[4]	23%[4]	20%[3]	18%[4]	20%[4]

(1) P-Δ effects are included.
(2) Single-Degree-of-Freedom system is elastic perfectly plastic and P-Δ effect is not included (response for corresponding ductility).
(3) Viscous damping forces not included.
(4) Viscous damping forces included.

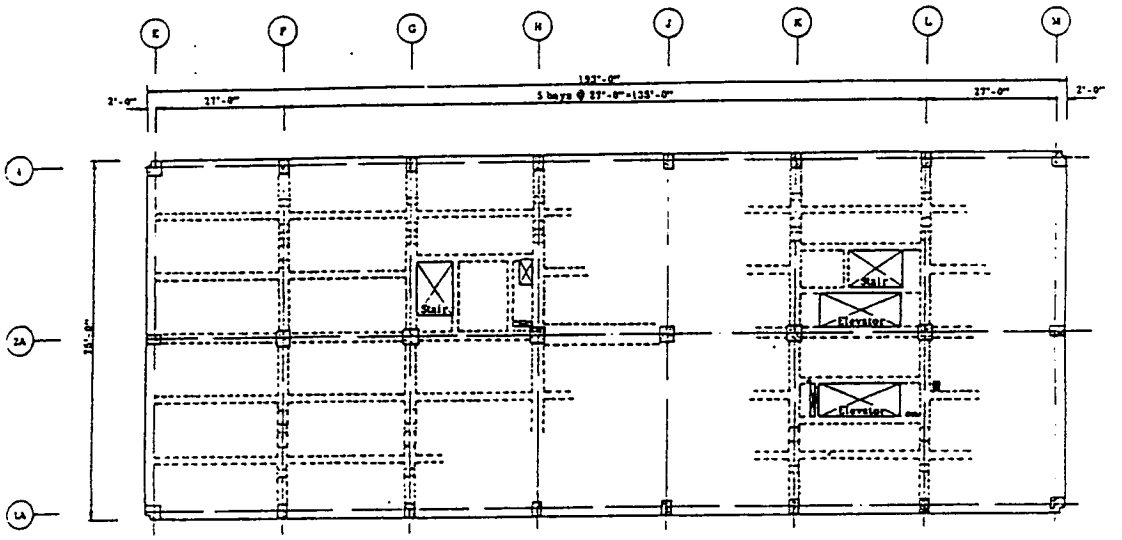

(a) Typical Floor Plan

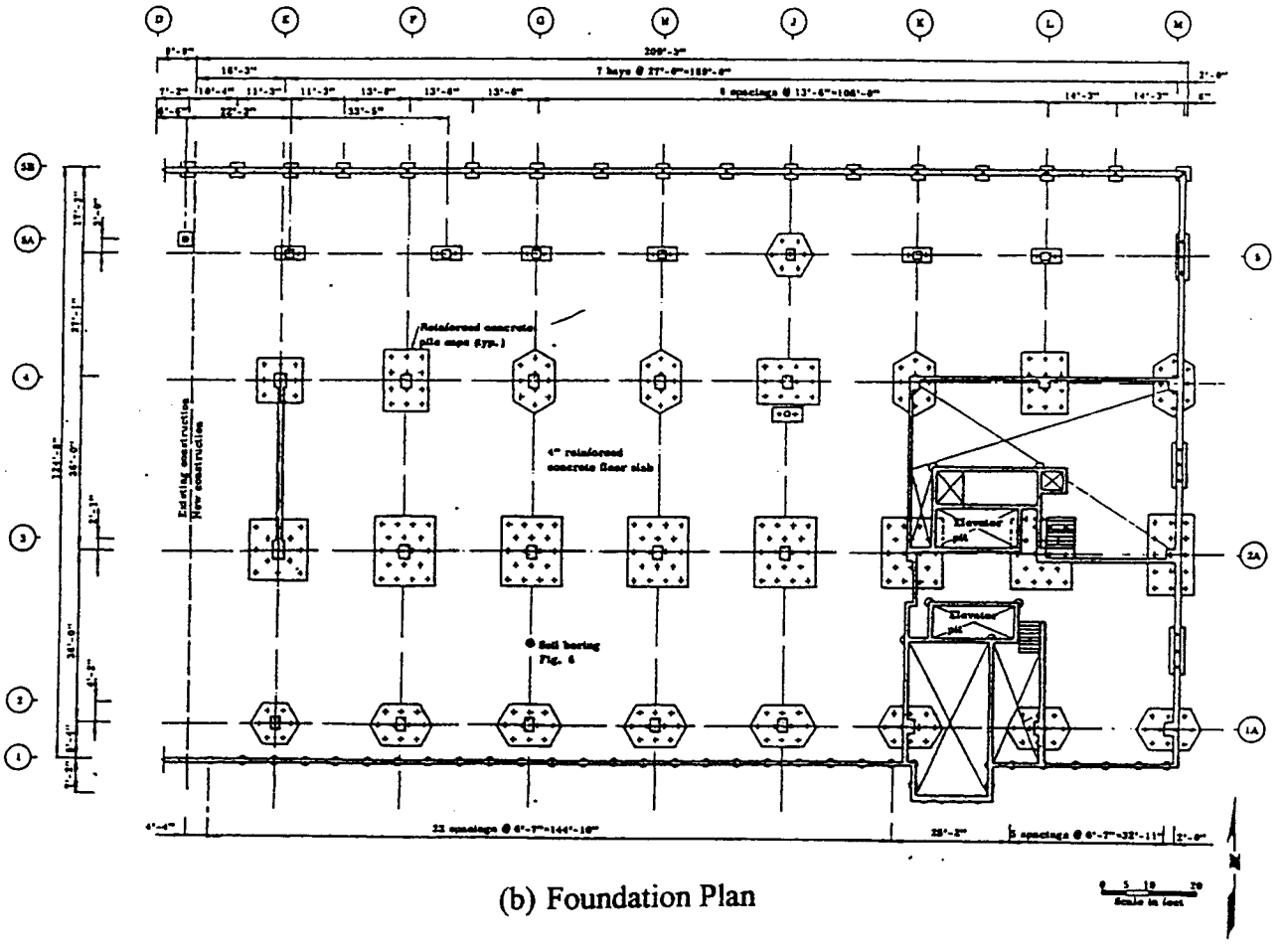

(b) Foundation Plan

Figure 5.5.1 Plan Views of the 15 Story RC Building

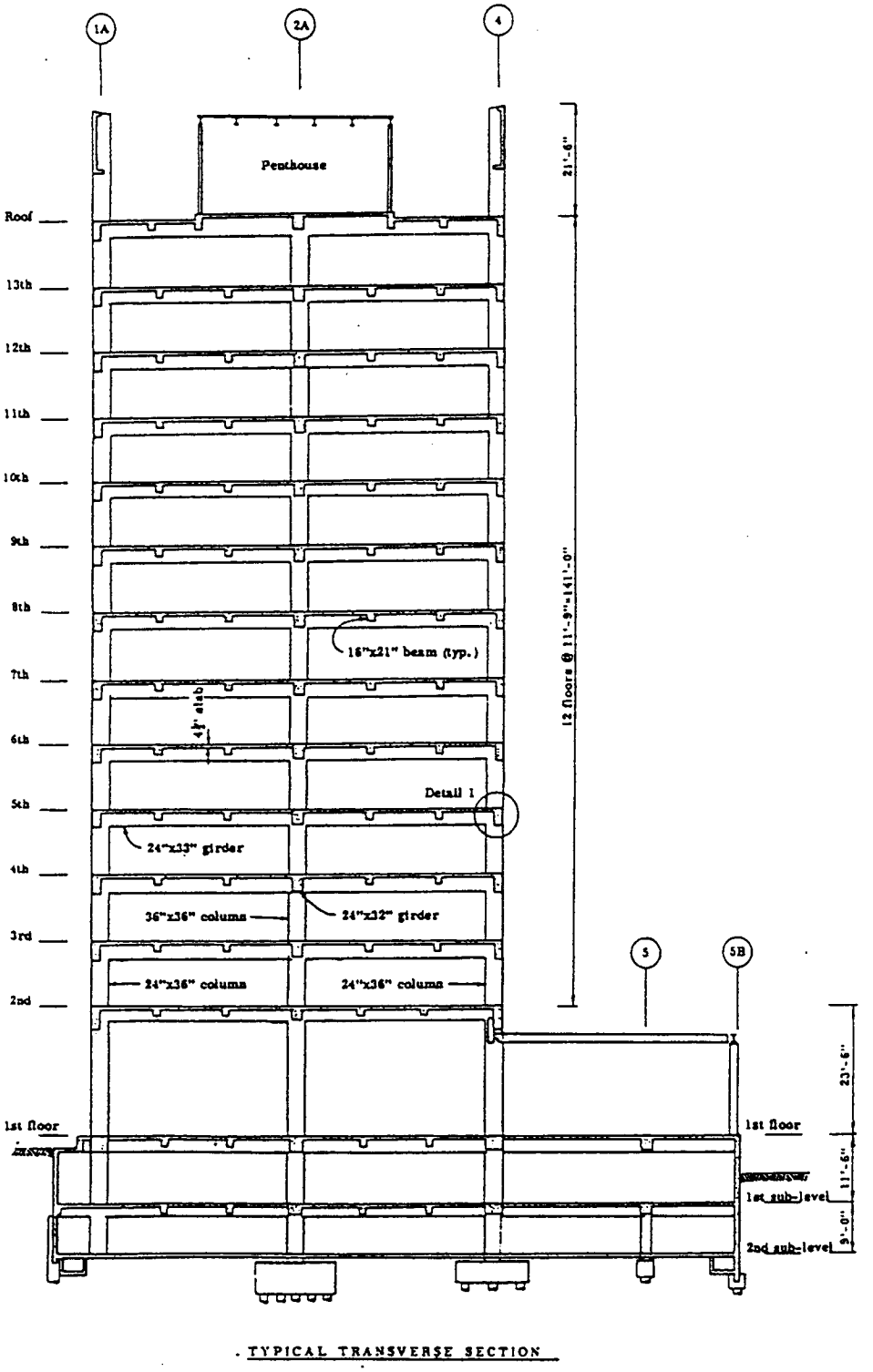

TYPICAL TRANSVERSE SECTION

Figure 5.5.2 Typical Elevation, 15 Story RC Building

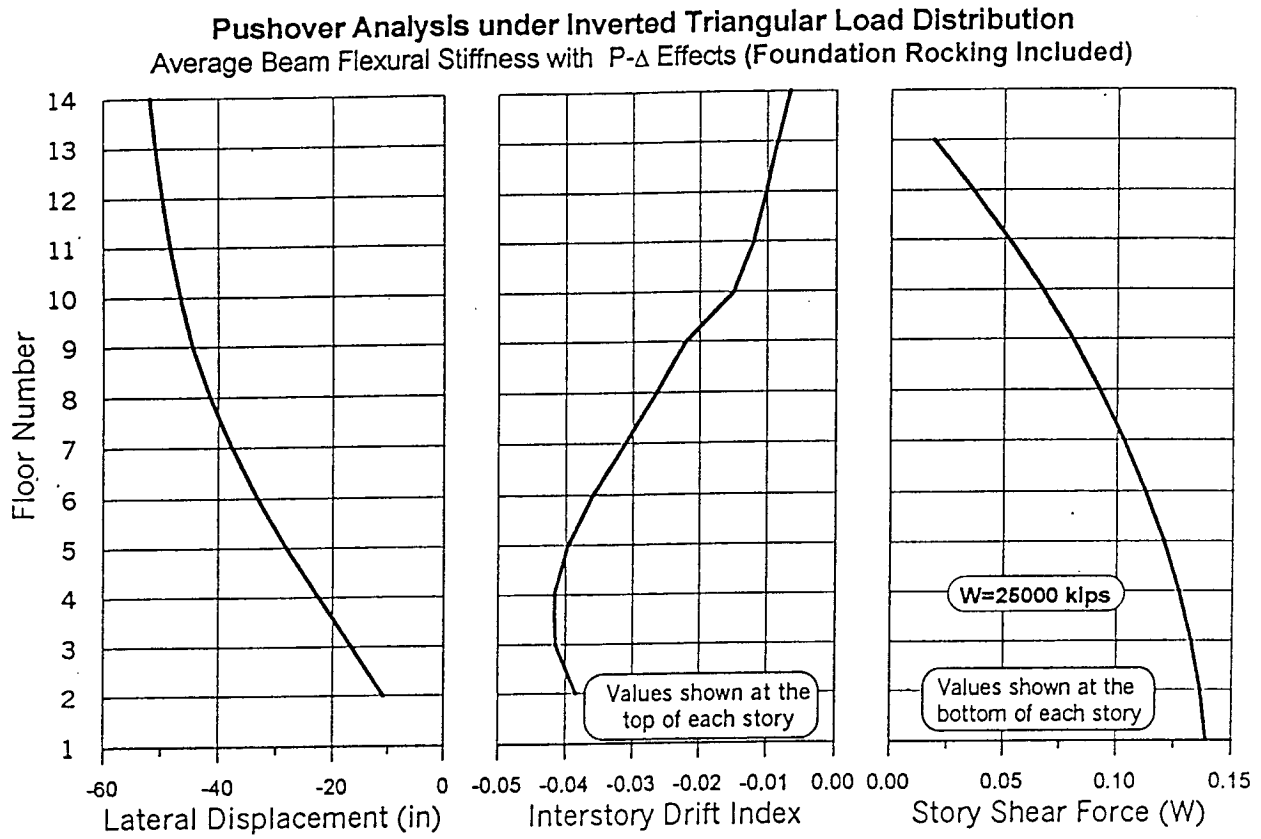

Figure 5.5.3 15 Story RC Building Behavior, Pushover

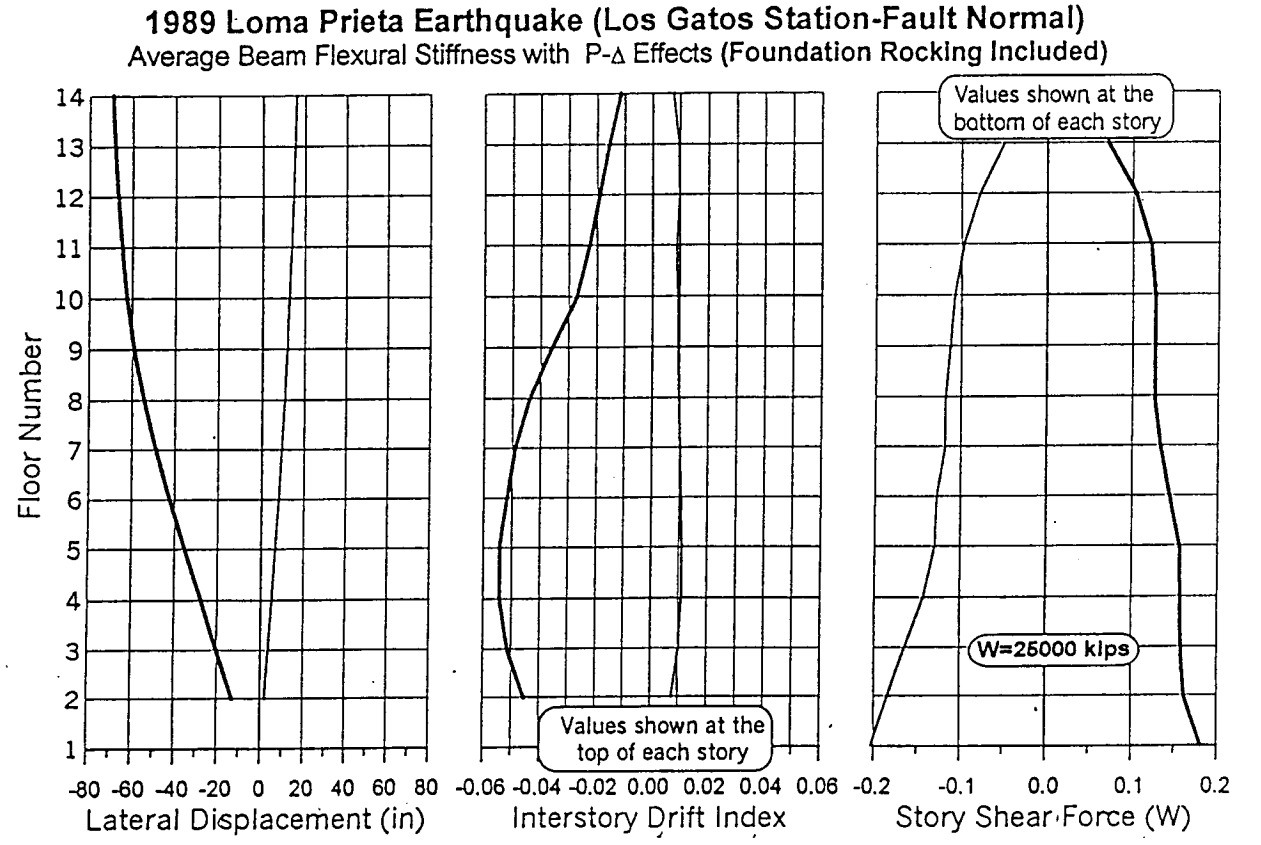

Figure 5.5.4 15 Story RC Building Response, $\xi = 5\%$

5.6 THE 41-STORY STEEL SPACE FRAME AS BUILT IN 1972

The 41-story office building which has a height of 550 feet (168m) was designed in 1972. The superstructure is a special moment-resistant space frame using rolled sections and built-up members for the beams and girders and welded box sections for the columns. Pile groups consisting of 13 to 25 piles are located under the 29 column lines that are interconnected by concrete tie beams. An isometric view of the seismic framing used in the elastic dynamic analyses is shown in **Figure 5.6.1a** and a typical floor plan (79'x151') is shown in **Figure 5.6.1b**. At the time of the Loma Prieta earthquake (1989) the building was instrumented with 14 strong motion accelerometers. Following the earthquake, the performance of the building was investigated [Anderson and Bertero, 1998]. Modal analysis indicated the periods of the first four lateral modes in the transverse direction to be 5.4, 1.8, 1.1, and 0.7 seconds, respectively. Corresponding values in the longitudinal direction were determined to be 5.1, 1.7, 1.0, and 0.7 seconds.

At the time of the design, the code lateral force requirement for this building was an equivalent static loading which was defined in terms of the base shear as V = (KC)W, where K=0.67, $C=0.05/(T)^{1/3}$ and T=0.1N where N is the number of stories. This results in a design seismic resistance coefficient of 0.021 (2.1%) and a base shear of 1312 kips (5,836 kN). In addition, the owner and the structural engineer decided to use a site-specific design spectrum and a dynamic analysis to determine the lateral design forces. The design criteria required that the structural frame should withstand the lateral forces due to the base design spectrum with stresses less than the yield stress. Based on this criteria, the design seismic resistance coefficient was 0.064 and the base shear was 4000 kips (17,800 kN).

5.6.1 Linear and Nonlinear Analyses (41-Story Steel Building)

The envelopes of elastic and inelastic dynamic displacement responses for the four recorded pulse-type ground motions are compared in **Figures 5.6.2** through **5.6.5**. For this building, the elastic displacement response represents a reasonable estimate of the inelastic displacement response.

The location of plastic hinges and the displaced shape of the building due to a static pushover using inverted triangular loading are shown in **Figure 5.6.6**. The corresponding base shear versus roof displacement curve is shown in **Figure 5.6.7**. Note the large elastic displacement of this structure. An evaluation of the pushover curve indicates that the yield seismic resistance coefficient is approximately 0.11.

The envelopes of maximum displacement for the five records used in the nonlinear dynamic analyses are shown in **Figure 5.6.8**. Of these, the Los Gatos record produces the largest displacement in the upper half of the building that occurs at the roof and reaches 90 inches (2.3m). In the lower half of the building, the largest lateral displacement is produced by the Takatori record and reaches a value of 30 inches (0.76m). The interstory drifts are not excessive in the lower twenty stories but become large in the upper half of the building under the Los Gatos and Takatori ground motions. The

maximum interstory drift occurs under the Los Gatos motion with a value of 3.8% at the 29th story. The Takatori record produces an IDI of 3% at the 33rd story. Since the excessive drifts occur primarily in the upper half of the structure, it is likely that they are influenced significantly by the contribution of the higher modes of vibration. The contribution of these modes could be reduced by the addition of supplemental damping. The curvature ductility and plastic rotation demands for the girders are shown in **Figure 5.6.9**. The shape of these two curves closely follows that of the IDI just discussed. The maximum curvature ductility demand (6.5) occurs in the 28th floor level and is due to the Los Gatos ground motion. This is not considered to be excessive provided proper care has been exercised in making the necessary moment connections. The ductility demands for the other ground motions are all less than 4.5 which is certainly attainable. The maximum plastic rotation demand is also due to the Los Gatos motion and occurs in the 29th floor level. The value of 2.4% is certainly attainable today with improved connection details, welding materials and welding procedures. However, it may be difficult to meet these demands considering the welding procedure and materials used at the time the building was constructed. After Los Gatos, the largest rotation demand is due to the Takatori record and is 1.6% at the 33rd floor, which should be attainable. Envelopes of maximum lateral displacement and locations of plastic hinges are shown in **Figures 5.6.10 – 5.6.13** for the four pulse-type motions. Time histories of the base shear obtained from the nonlinear analyses are shown in **Figure 5.6.14**. The dotted lines indicate the yield value obtained from the pushover analysis.

5.6.2 Observations Regarding the Results Obtained

- The Los Gatos ground motion is clearly the critical ground motion for this building, producing response demands around the 30-story level which are above acceptable values

- If the Los Gatos and Takatori ground motions are neglected, the building response demand is such that it can most likely be supplied by the structure; however, the IDI will still be above the 1.5% limitation.

- It is of interest to note that for the James Road ground motion, the base shear does not exceed the yield capacity determined from the static pushover analysis, indicating that for this motion the building has considerable reserve strength.

- The relatively good performance of this building is largely due to the use of a site-specific design spectrum which resulted in lateral design forces more than three times higher than required by the then current building code.

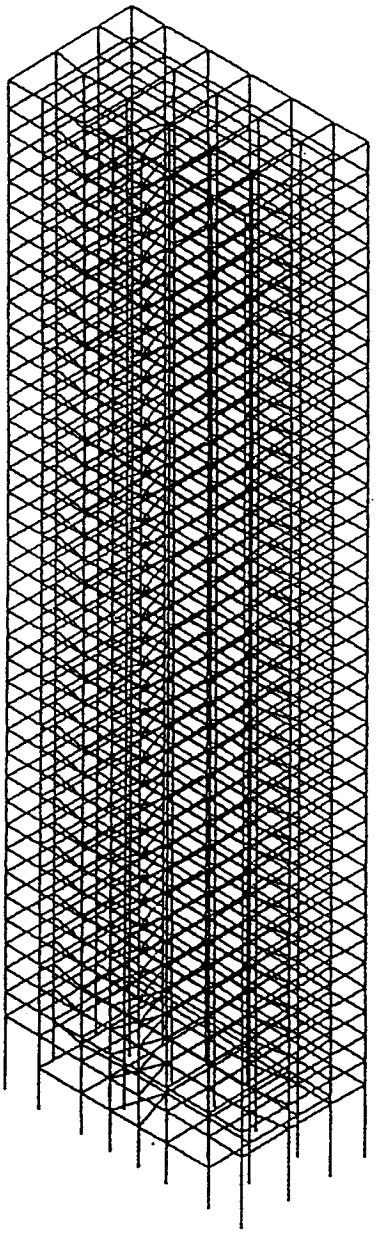

(a) Computer Model, ETABS

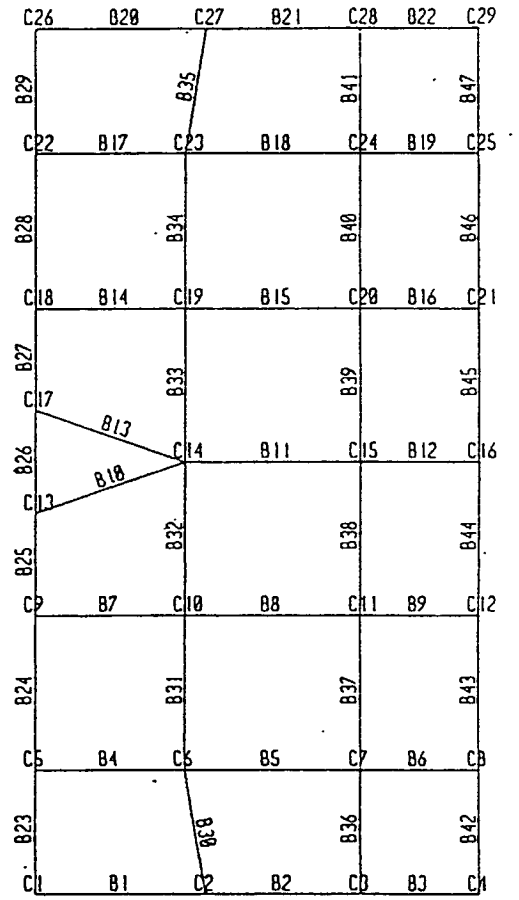

(b) Typical Floor Plan

Figure 5.6.1 41 Story Steel Space Frame

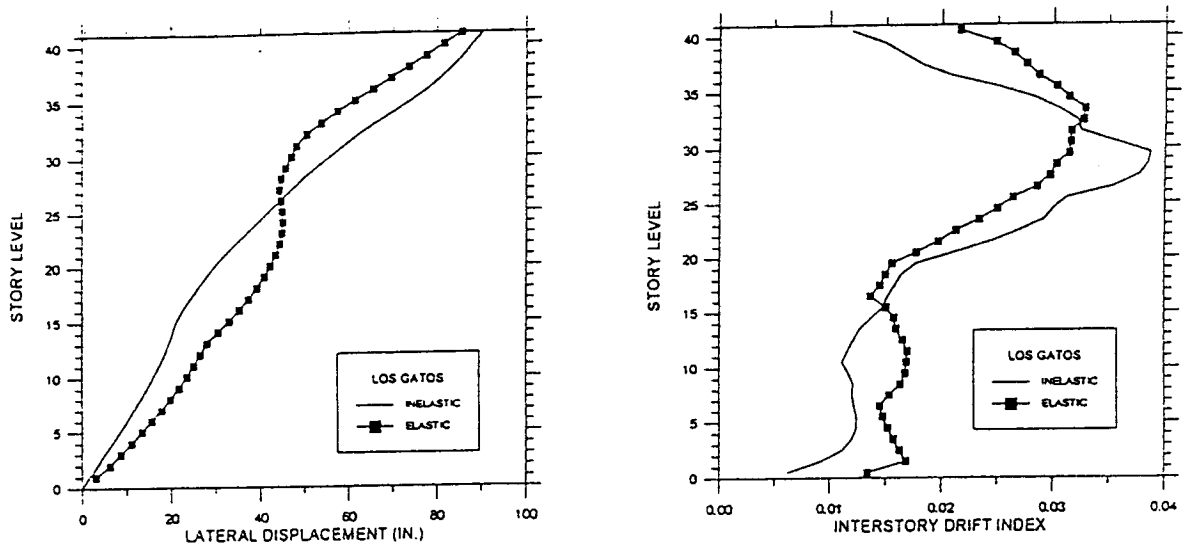

Figure 5.6.2 41 Story Steel, Elastic vs. Inelastic Displacement, Los Gatos

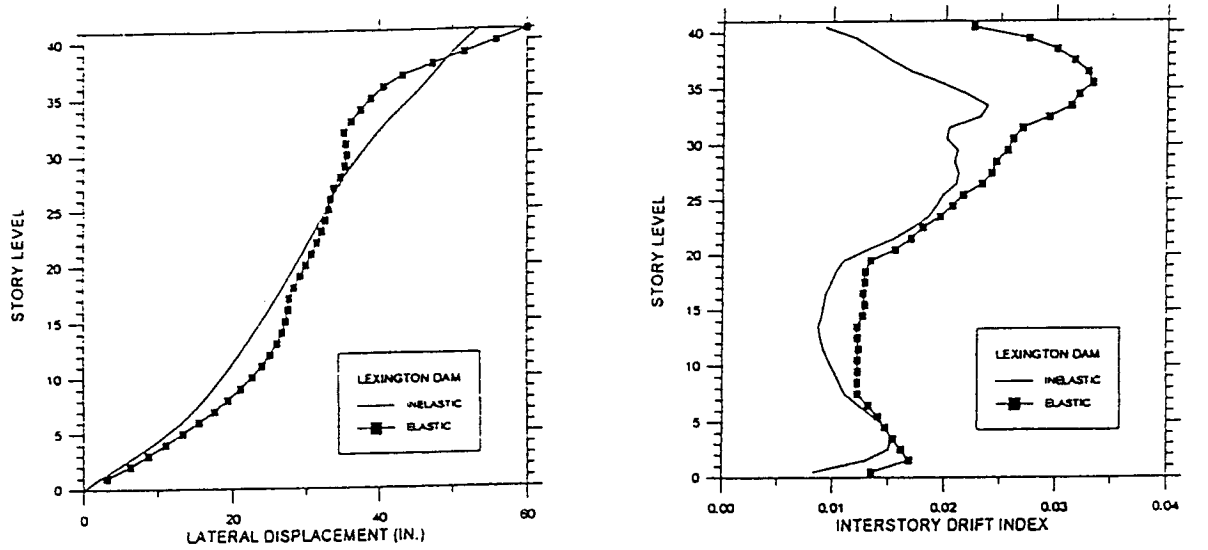

Figure 5.6.3 41 Story Steel, Elastic vs. Inelastic Displacement, Lexington Dam

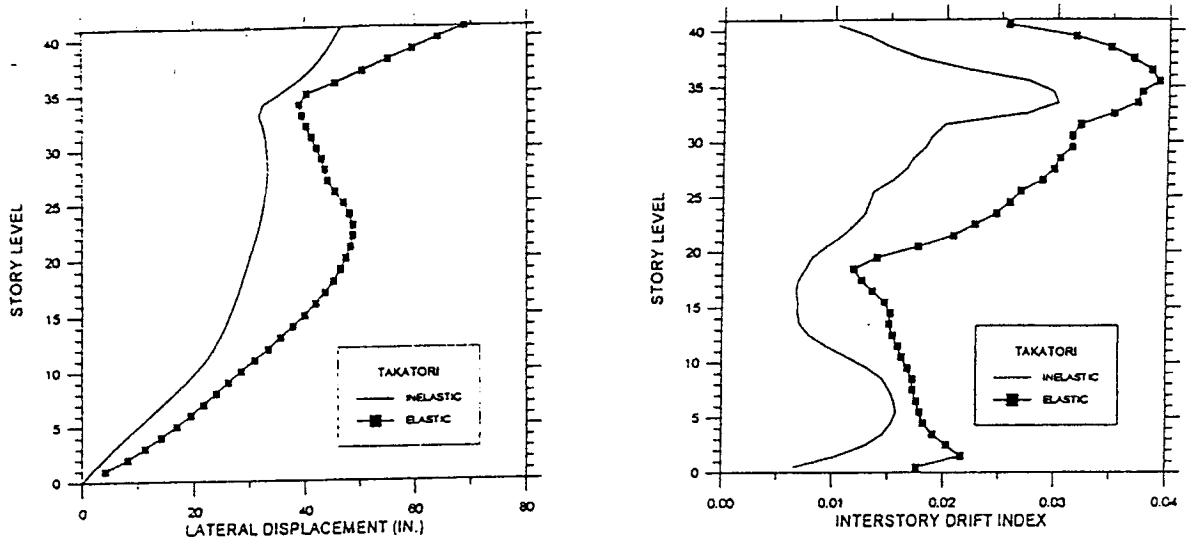

Figure 5.6.4 41 Story Steel, Elastic vs. Inelastic Displacement, Takatori

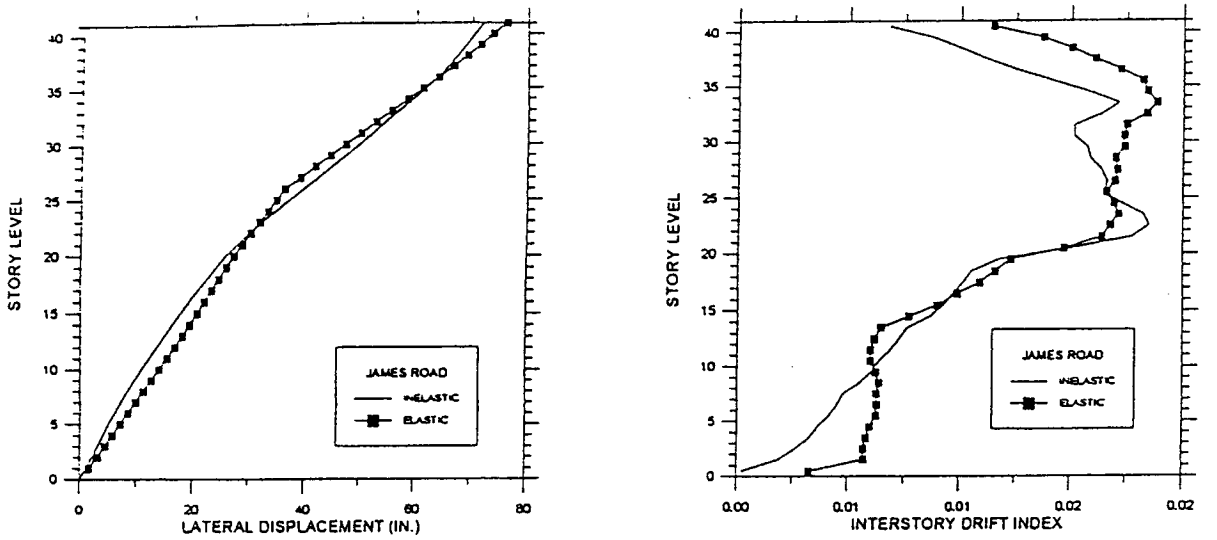

Figure 5.6.5 41 Story Steel, Elastic vs. Inelastic Displacement, James Road

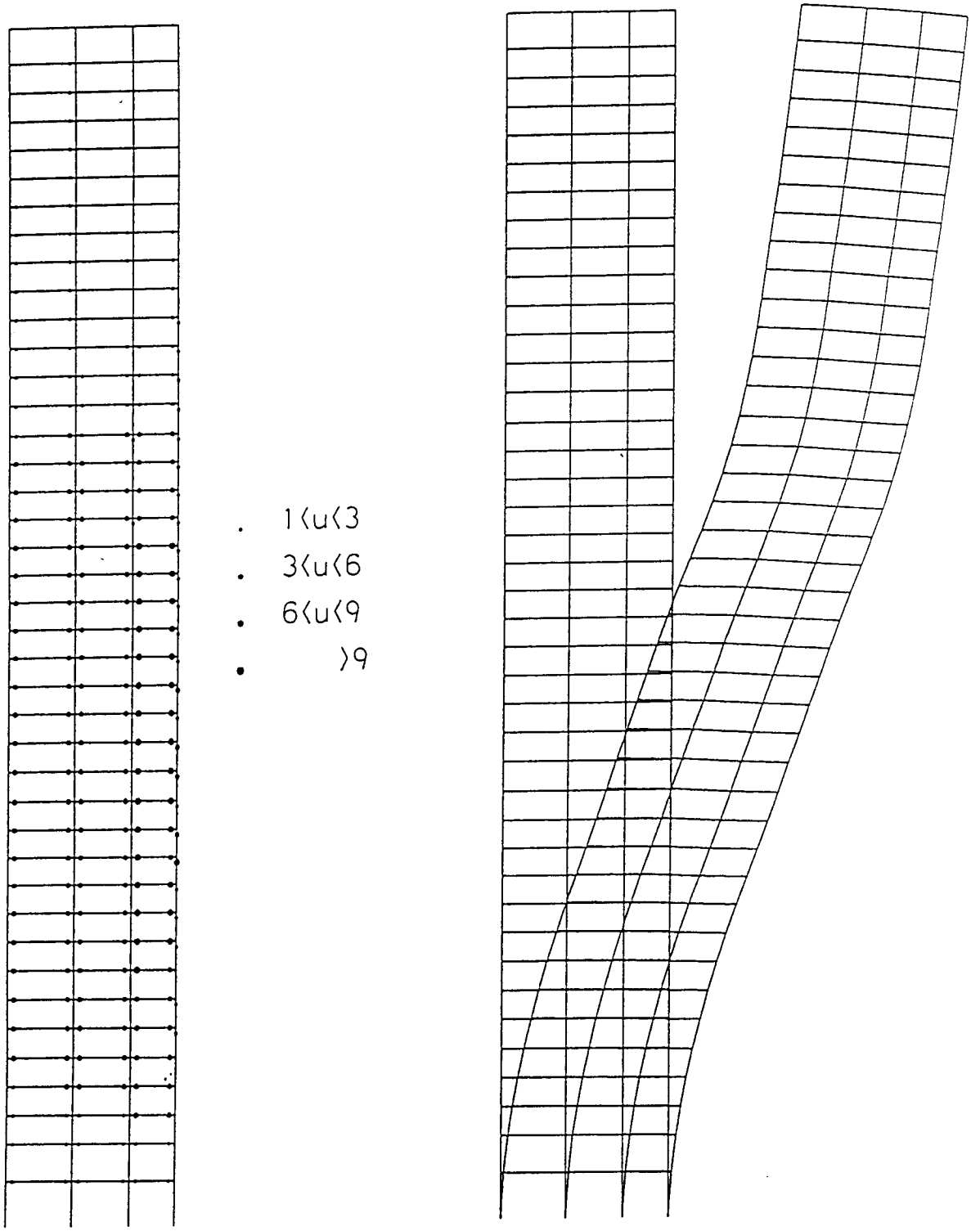

(a) Plastic Hinge Locations

(b) Displaced Shape, Δ_{roof} = 165 inches

Figure 5.6.6 Static Pushover, Plastic Hinges, 41 Story Steel Building

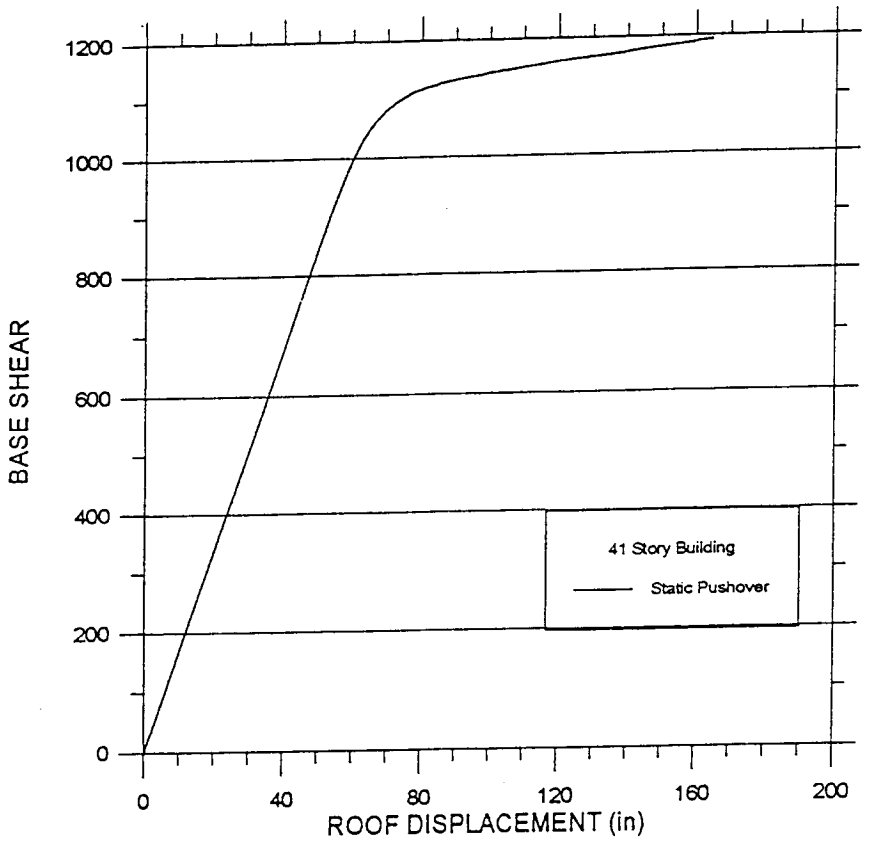

Figure 5.6.7 Static Pushover, Base Shear vs. Roof Displacement, 41-Story Steel Building

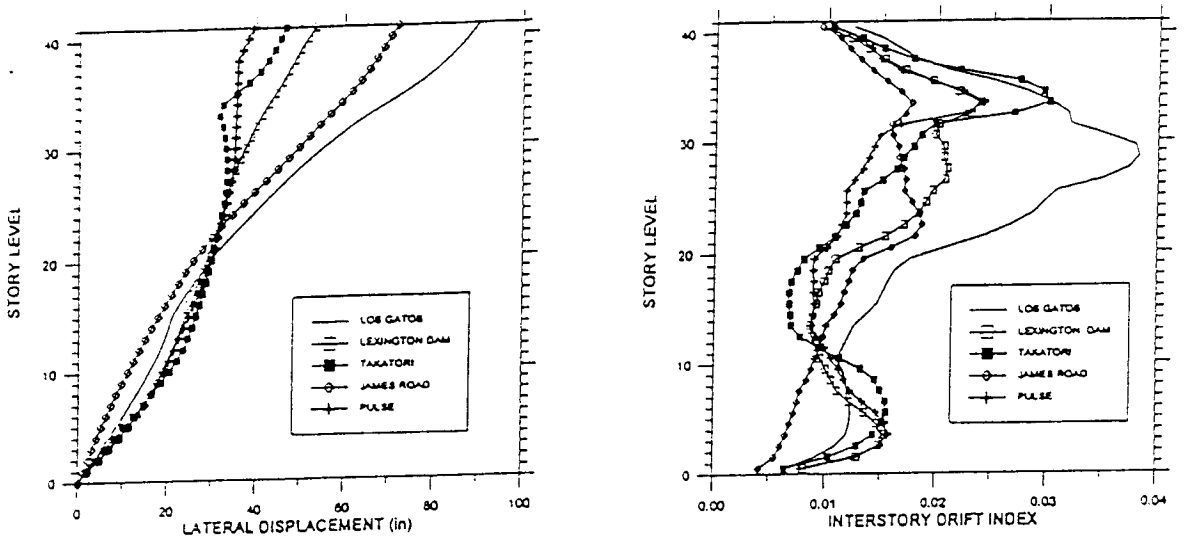

Figure 5.6.8 Displacement and Drift Demands, 41 Story Steel Building

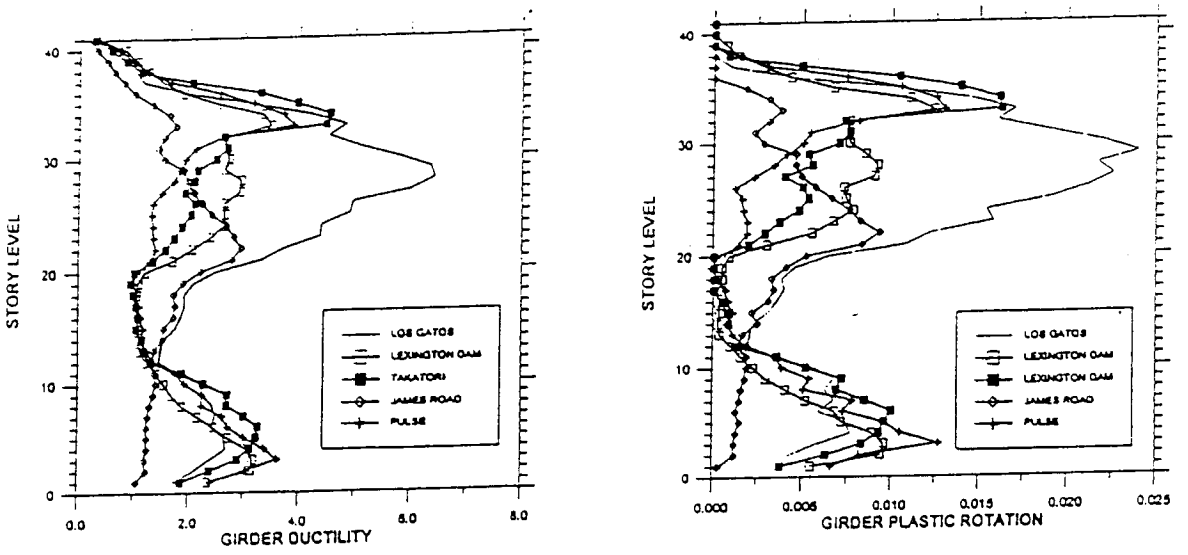

Figure 5.6.9 Ductility and Plastic Rotation Demands, 41 Story Steel Building

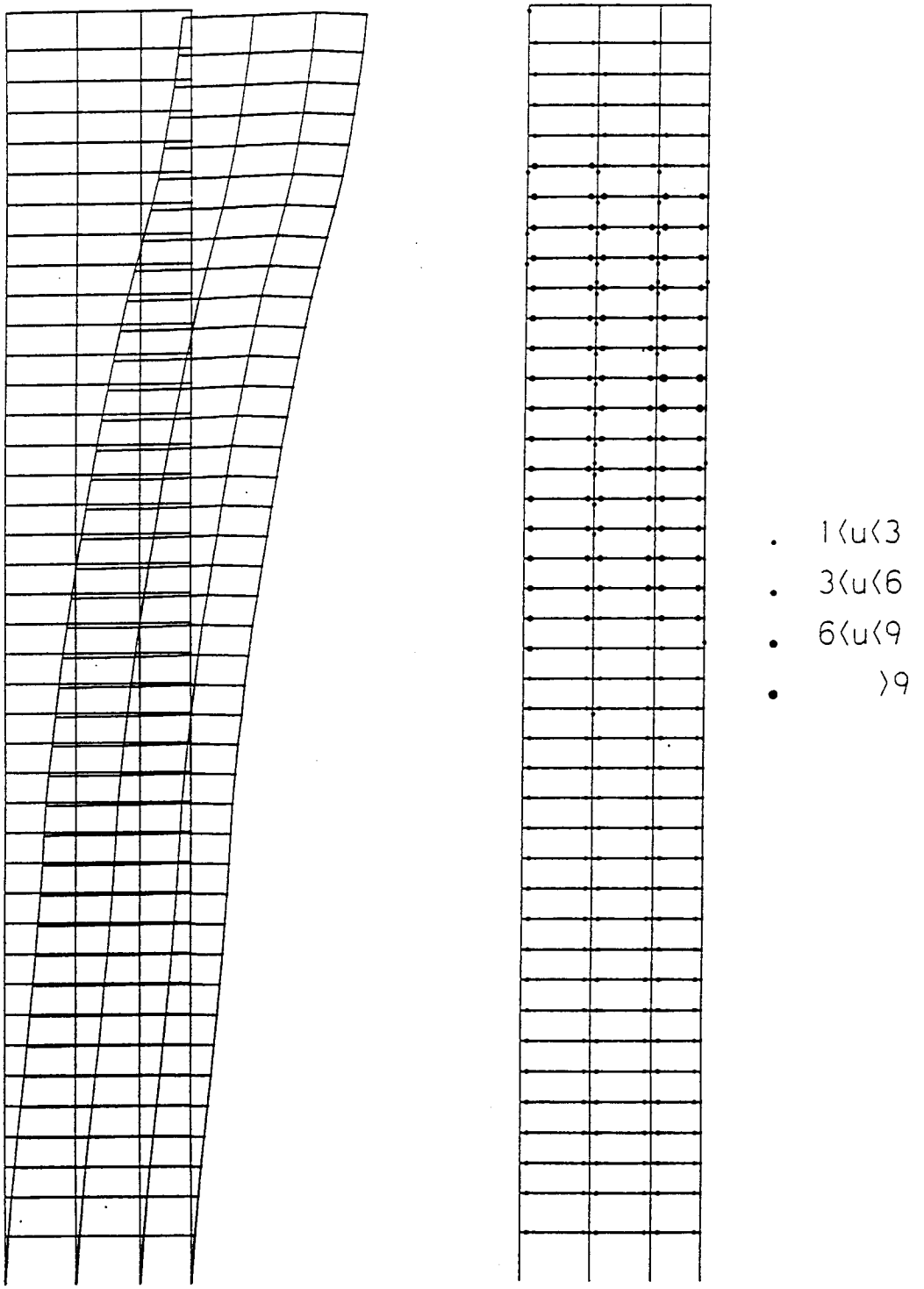

(a) Max. Displaced Shape
Δ_{roof} = 90.2 inches

(b) Plastic Hinge Locations

Figure 5.6.10 41 Story Steel Building Response, Los Gatos

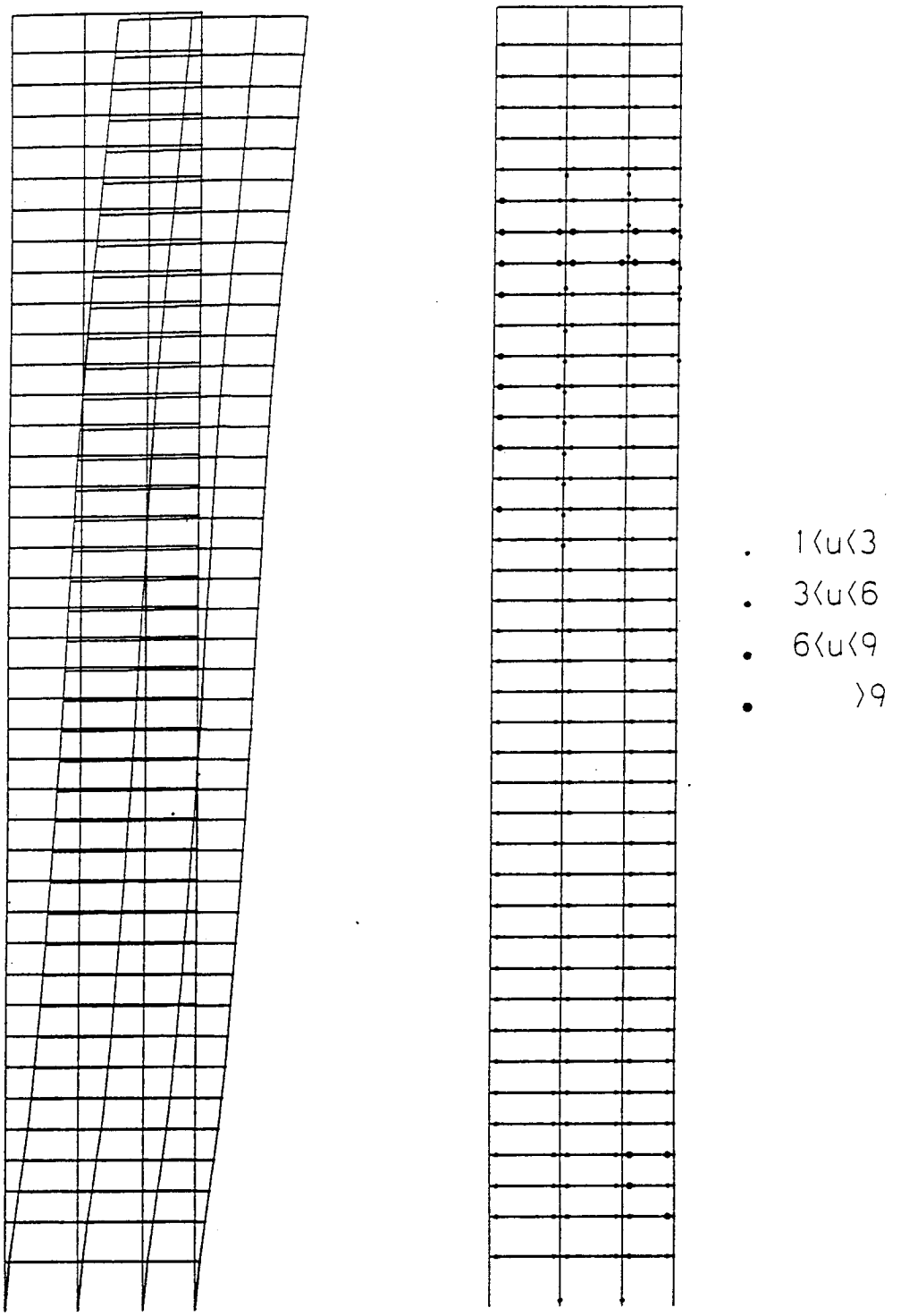

(a) Max. Displaced Shape
Δ_{roof} = 53.3 inches

(b) Plastic Hinge Locations

Figure 5.6.11 41 Story Steel Building Response, Lexington Dam

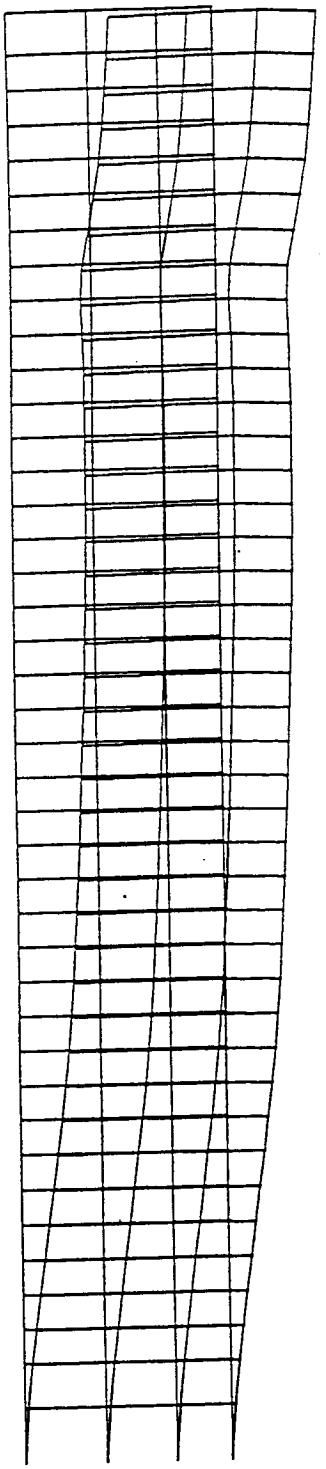

(a) Max. Displaced Shape

Δ_{roof} = 46.5 inches

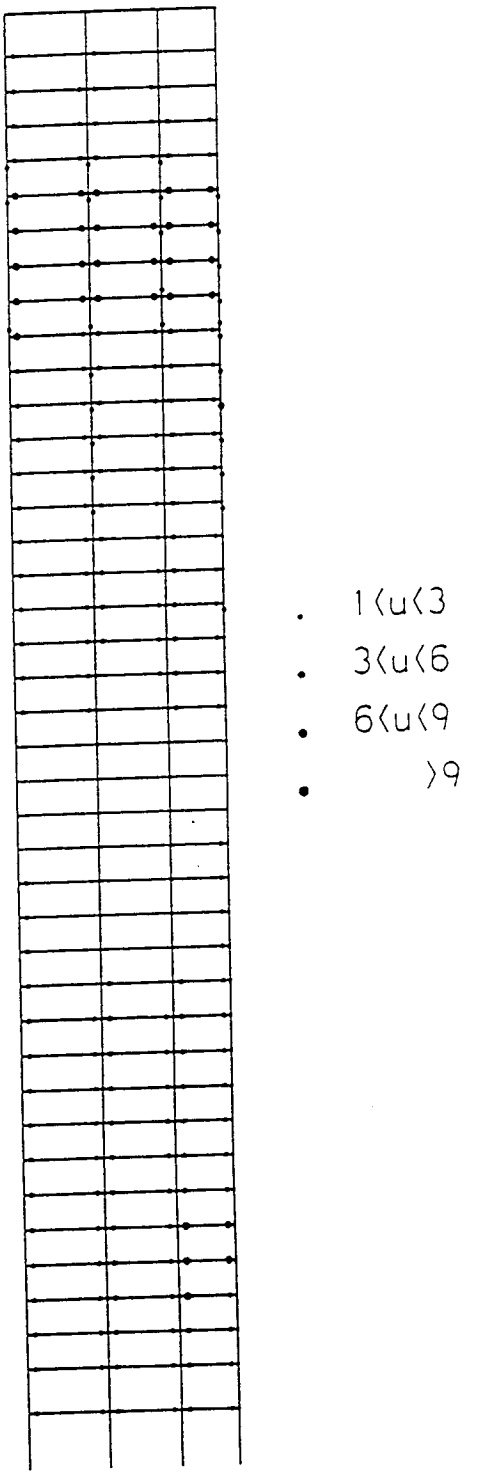

(b) Plastic Hinge Locations

Figure 5.6.12 41 Story Steel Building Response, Takatori

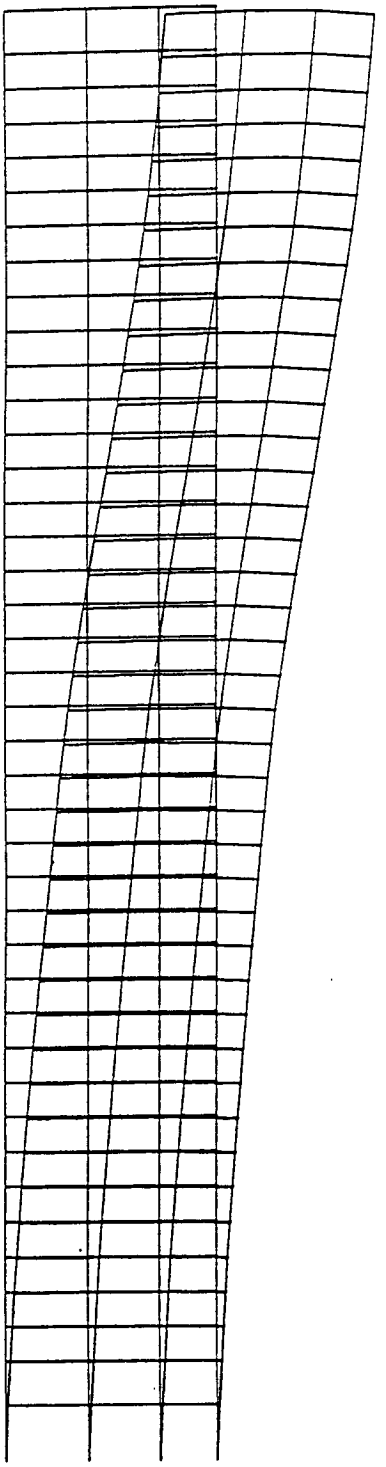

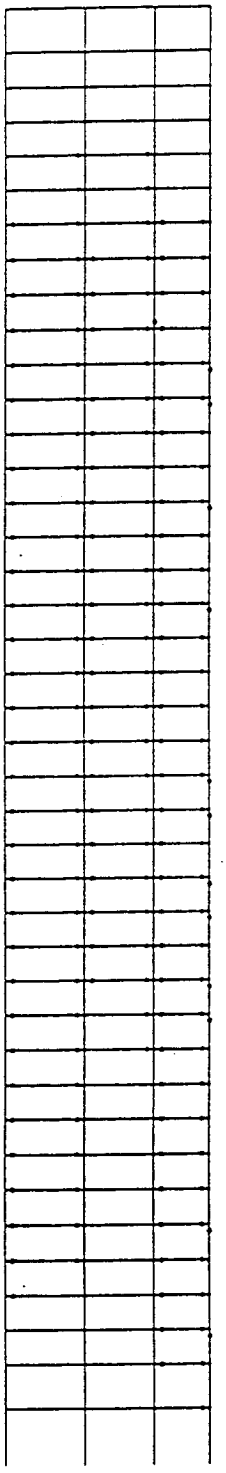

(a) Max. Displaced Shape
Δ_{roof} = 72 inches

(b) Plastic Hinge Locations

Figure 5.6.13 41 Story Steel Building Response, James Road

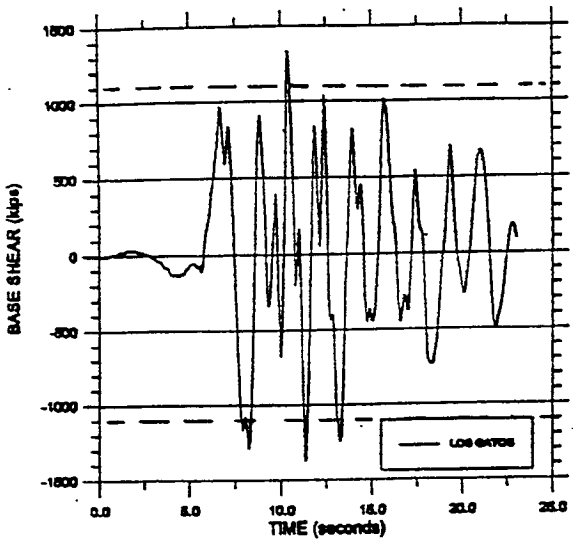

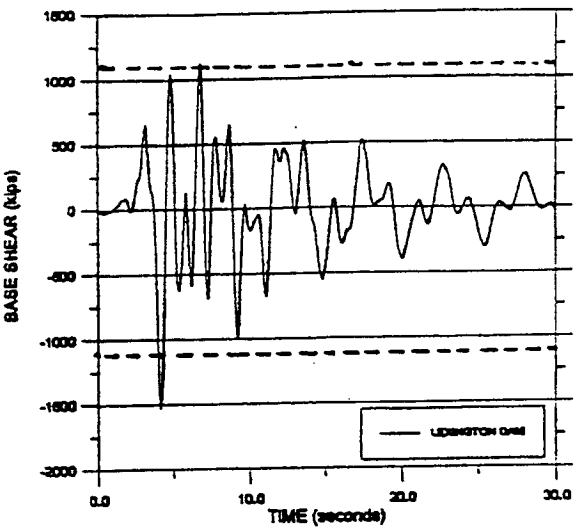

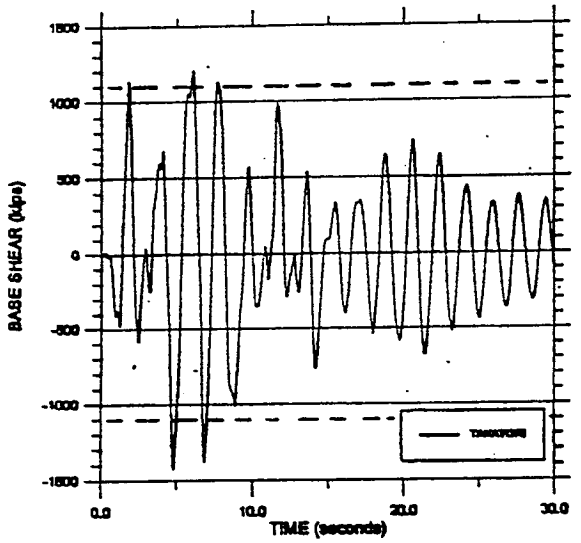

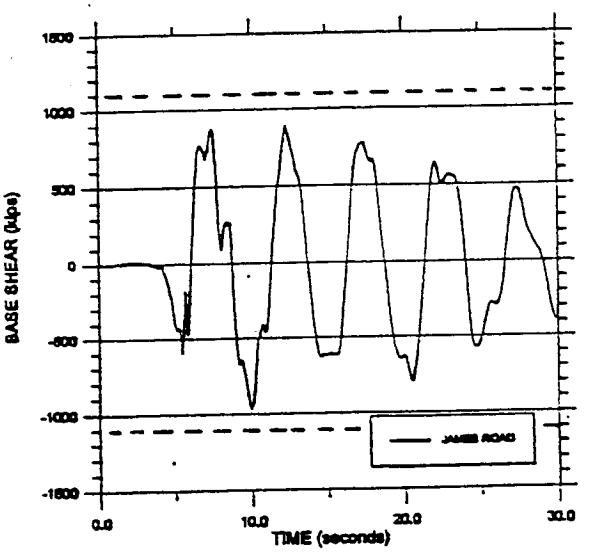

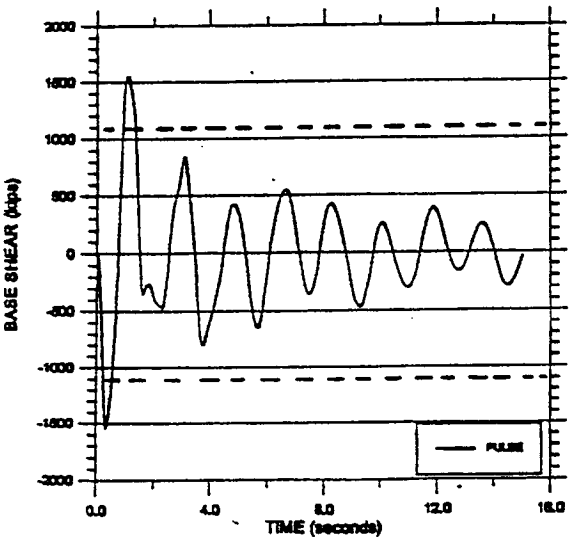

Figure 5.6.14 41 Story Steel Building,
Base Shear Response

5.7 THE 20-STORY STEEL PERIMETER FRAME

The lateral force system for the 20-story steel building is a perimeter moment frame. The building was designed by a Los Angeles structural engineering firm as part of the SAC program of investigation that was conducted following the Northridge earthquake. The lateral force provisions are those specified in the 1994 Uniform Building Code and the framing representative of current building practice in the Los Angeles area. The beams and columns of the perimeter frames are rolled sections with the exception of the corner columns that are welded box sections. The 1994 UBC [ICBO, 1994] static lateral force requirement for this building was defined in terms of the base shear as $V = (ZIC/R_w)W$, where $C=1.25S/(T)^{2/3}$ subject to a minimum value of $C=0.75R_w$. This results in a design seismic resistance coefficient of 0.03 (3.0%) and a base shear of 735 kips (3,271 KN) for the building (368 kips for each SMRF). Note that with a height greater than 240 feet, the 1994 UBC requires a dynamic analysis. The sizes in the perimeter frames are actually based on drift control which is specified to be 0.25% under service load. An isometric view of the ETABS computer model of the building is shown in **Figure 5.7.1,** where shear connections in the interior frames are noted by an open circle. The building has a square plan that is 100 feet by 100 feet as shown in the plan of a typical floor, **Figure 5.7.2**, and a height of 265 feet (81m) as shown in a typical elevation in **Figure 5.7.3**.

5.7.1 Linear and Nonlinear Analyses

The elastic dynamic analyses considered a full three-dimensional model of the building including the gravity load framing as shown in **Figure 5.7.1**. The periods of the first three lateral modes of vibration are 4.06, 1.45 and 0.84 seconds respectively. Results of initial elastic response analyses for an ensemble of recorded ground motions are shown in **Figure 5.7.4**. This data clearly indicates that for this building, Los Gatos is the more severe of these six acceleration records. The Anderson Road and Lucerne ground motions were both recorded in the near-fault region and produce similar responses in the building. The interstory drift demand from Los Gatos is almost 5%, which is more than can be accommodated without significant damage. The drift demands of all of the other records are 2.5% or less. The envelopes of elastic and inelastic dynamic displacement responses for the four recorded pulse-type ground motions are compared in **Figures 5.7.5 – 5.7.8**. For the Los Gatos record, **Figure 5.7.5**, the elastic dynamic response tends to overestimate the displacements in the upper portion of the building. Note that the maximum IDI from both analyses is in excess of 4%. For the Lexington Dam record, **Figure 5.7.6**, the lateral displacement is almost identical for the two methods, however, the elastic analysis overestimates the IDI in the upper portion of the building. For the Takatori ground motion, **Figure 5.7.7**, the elastic analyses tend to overestimate both the lateral displacement and the IDI above the fifth story level. The elastic analysis for the James Road record, **Figure 5.7.8**, overestimates the lateral displacement above the 10^{th} story level and the IDI above the 6^{th} story level.

The results of a pushover analysis for a single perimeter frame, neglecting the effect of axial load, are shown in **Figure 5.7.15.** The locations of plastic hinges are shown in **Figure 5.7.9a,** the envelope of maximum displaced shape is shown in **Figure 5.7.9b** and the base shear versus roof displacement curve is shown in **Figure 5.7.9c**. Envelopes of maximum lateral displacement and

interstory drift index obtained from the nonlinear analyses are compared in **Figure 5.7.10**. It can be seen that the Los Gatos ground motion is clearly the critical motion for this frame. The lateral displacement is just over 71 inches (1.8 m) and the maximum IDI is 4.3%. For this building, the James Road record is the next most severe record. The envelopes of maximum curvature ductility demand and maximum plastic rotation demand in the girders are shown in **Figure 5.7.11**. Curvature ductility values in the lower four floors are higher than would be considered acceptable. The ductility demand of 12 in the third story level under the Los Gatos record is clearly excessive. Both the James Road and Lexington Dam records have ductility demands in excess of 8 in this region. Plastic rotation demands for the Los Gatos record in excess of 4% will be difficult to achieve with standard connection detailing although some more recent connection details using reduced sections have been shown to be capable of developing this amount of plastic rotation with some reduction in moment capacity. The plastic rotation demand for the James Road record exceeds the 3% limit that is currently considered an upper limit for design. The locations of the plastic hinges and the deflected shape envelope of the building for the four recorded pulse-type ground motions are shown in **Figures 5.7.12-5.7.15**. The severely displaced shape of the building under the Los Gatos motion, **Figure 5.7.12**, is clearly cause for concern. Based on the results of the pushover analysis, the seismic yield resistance coefficient, C_y, for this building is estimated to be 0.18 and the yield base shear 2200 kips (9800 kN). Time histories of the base shear for a single frame determined from the nonlinear analyses are shown in **Figure 5.7.16** where the broken line represents the yield base shear of 1100 kips (4,900 kN) obtained from the pushover analysis for a single frame.

5.7.2 Observations Regarding the Results Obtained (20-Story Steel Building)

- The IDI demands of all ground motions are larger than the original limit of 1.5%, which means the structure will have to be modified if it is to meet this requirement under pulse-type motions.

- The large IDI demands in the lower third of the building under the Los Gatos ground motion may lead to serious damage or even collapse.

- Large ductility and displacement demands occurring in the lower third of the building may cause serious second-order effects when combined with the effect of axial load.

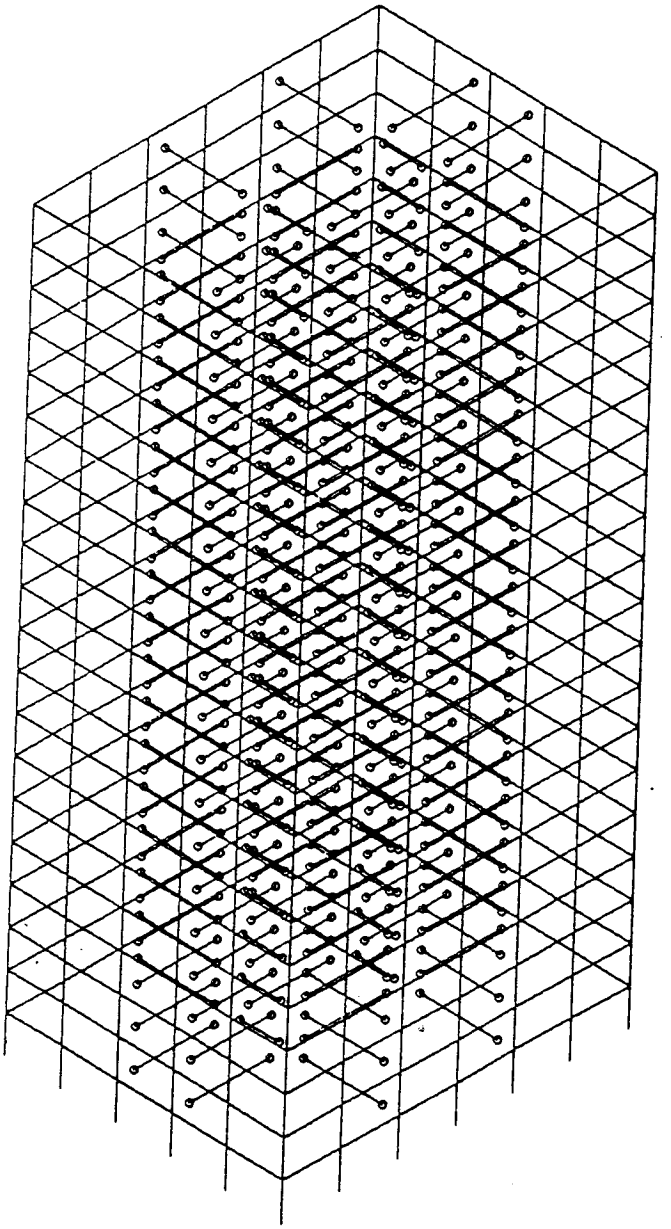

Figure 5.7.1 Steel Perimeter Frame, Computer Model, ETABS

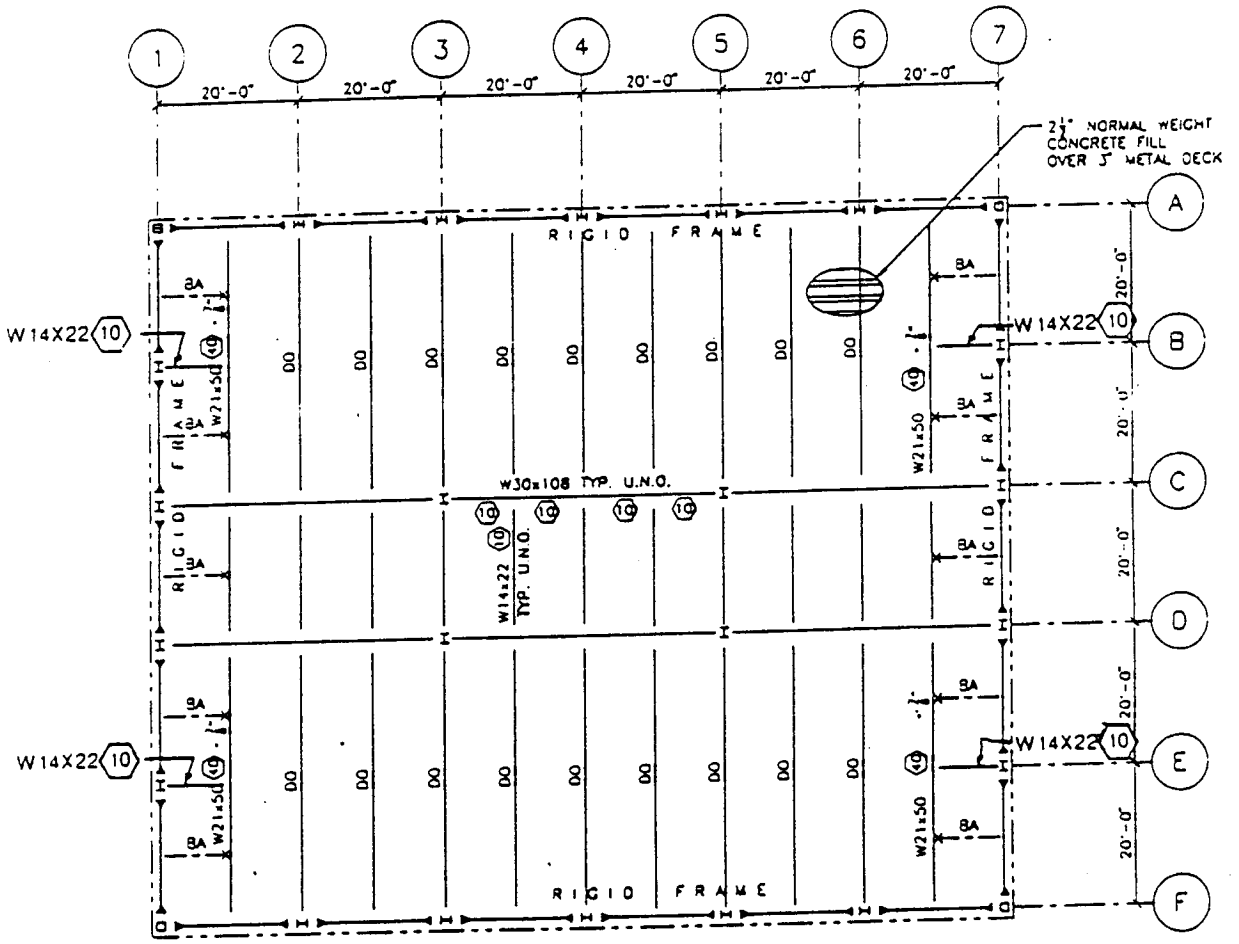

TYPICAL FLOOR PLAN

Figure 5.7.2 Steel Perimeter Frame, Typical Floor Plan

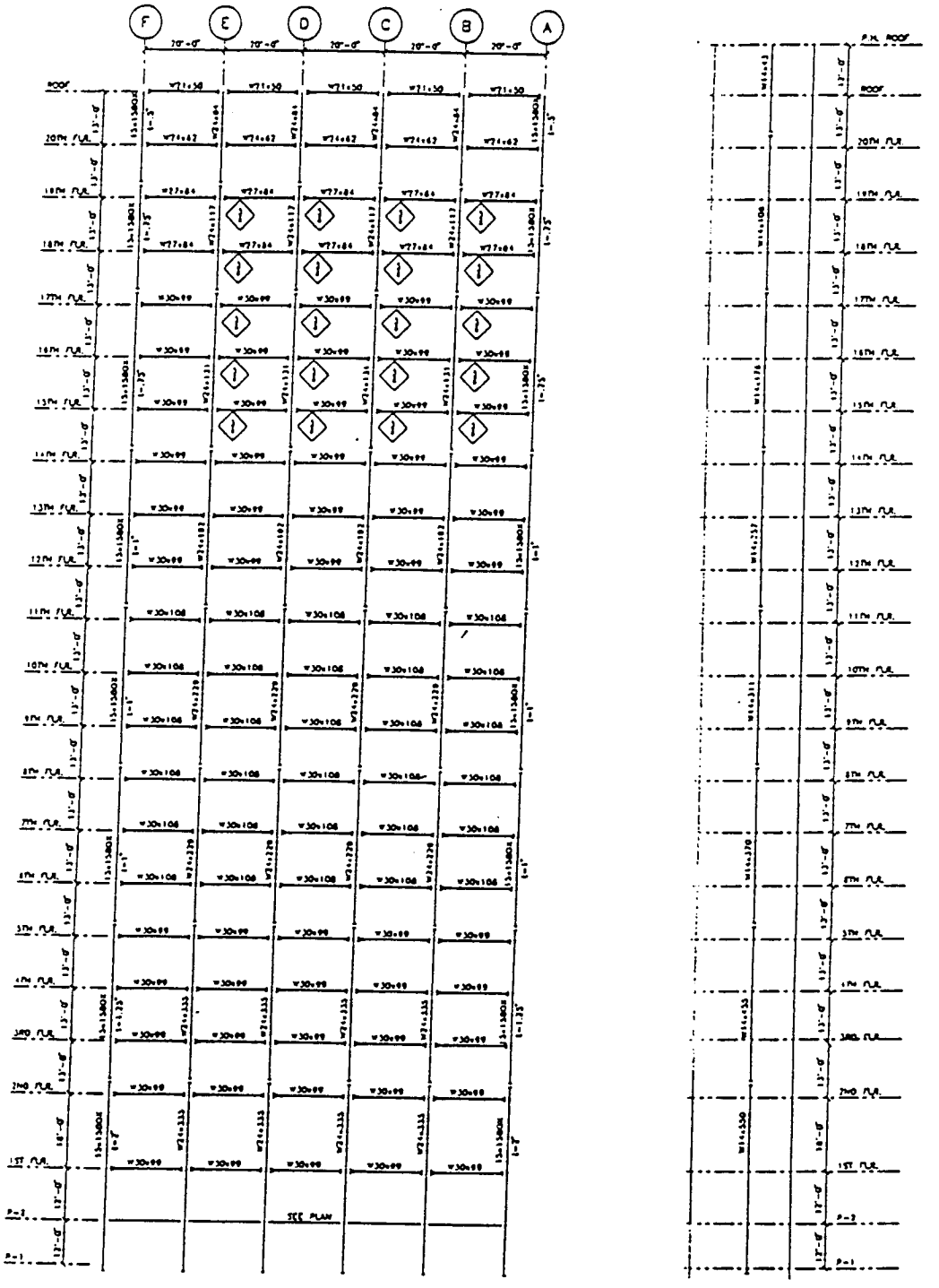

Figure 5.7.3 Steel Perimeter Frame, Elevation

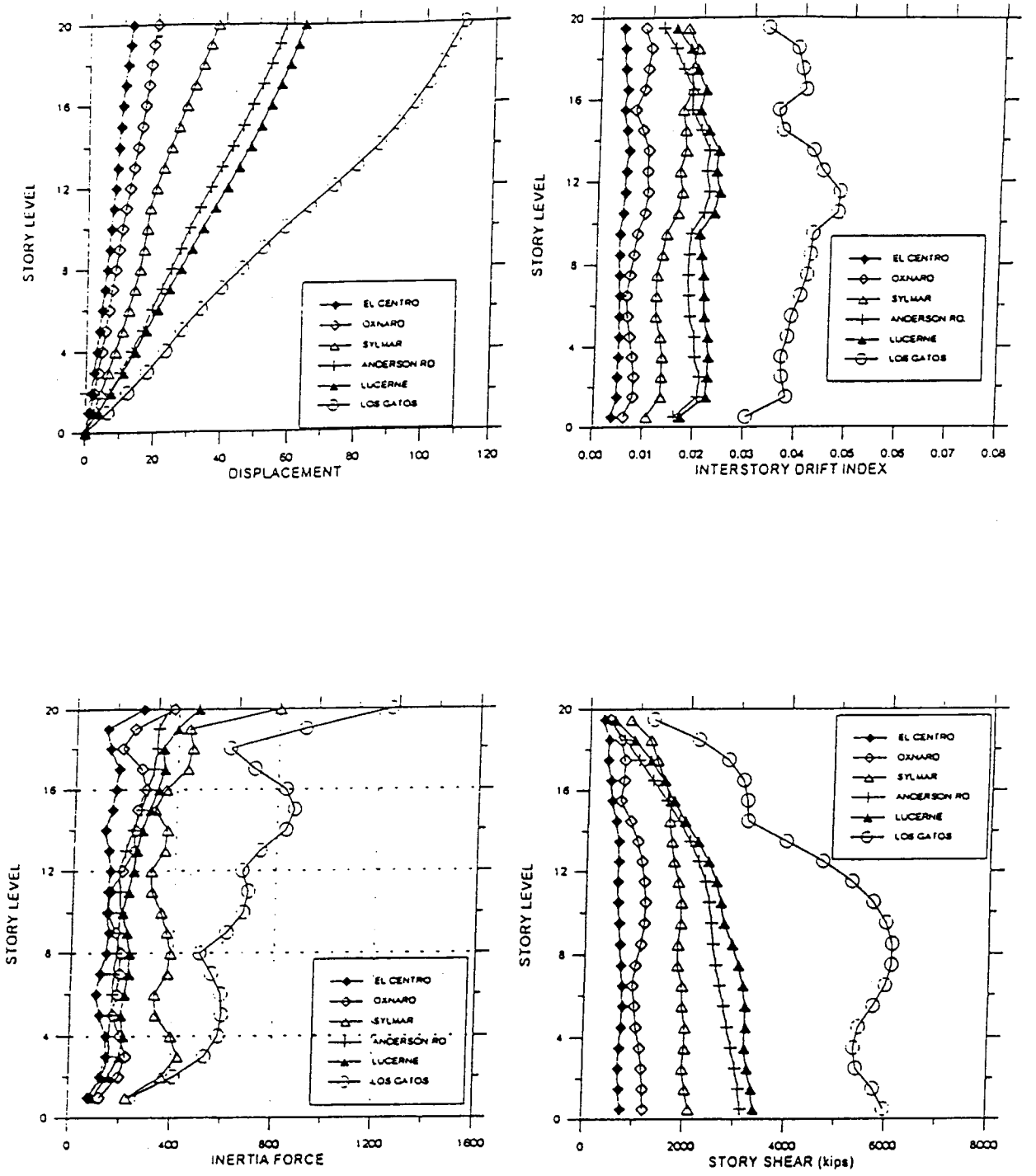

Figure 5.7.4 Steel Perimeter Frame, Elastic Response Comparisons

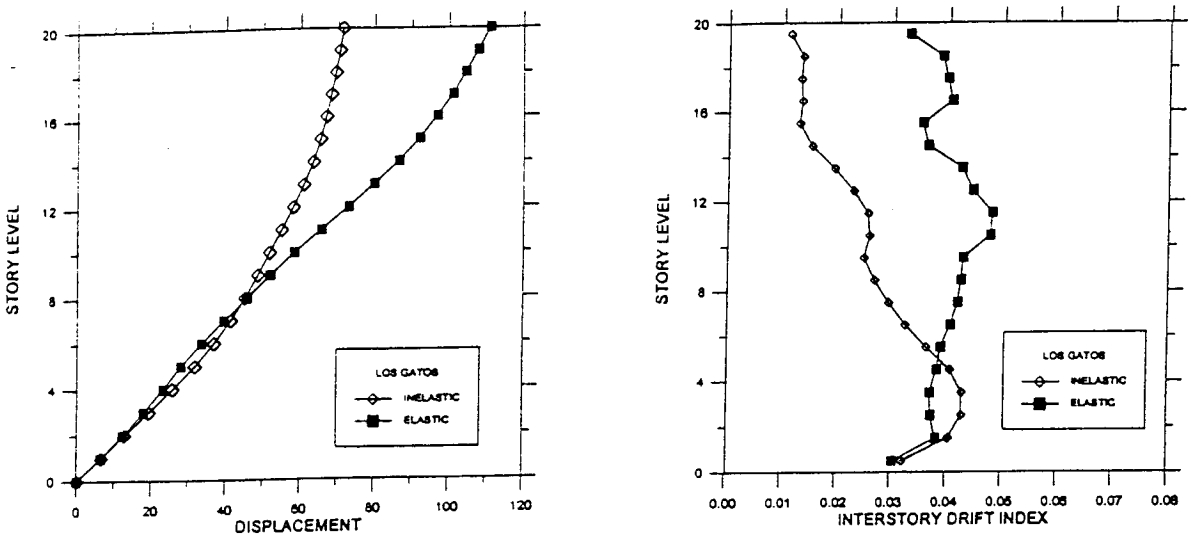

Figure 5.7.5 Steel Perimeter Frame, Elastic vs. Inelastic Displacement, Los Gatos

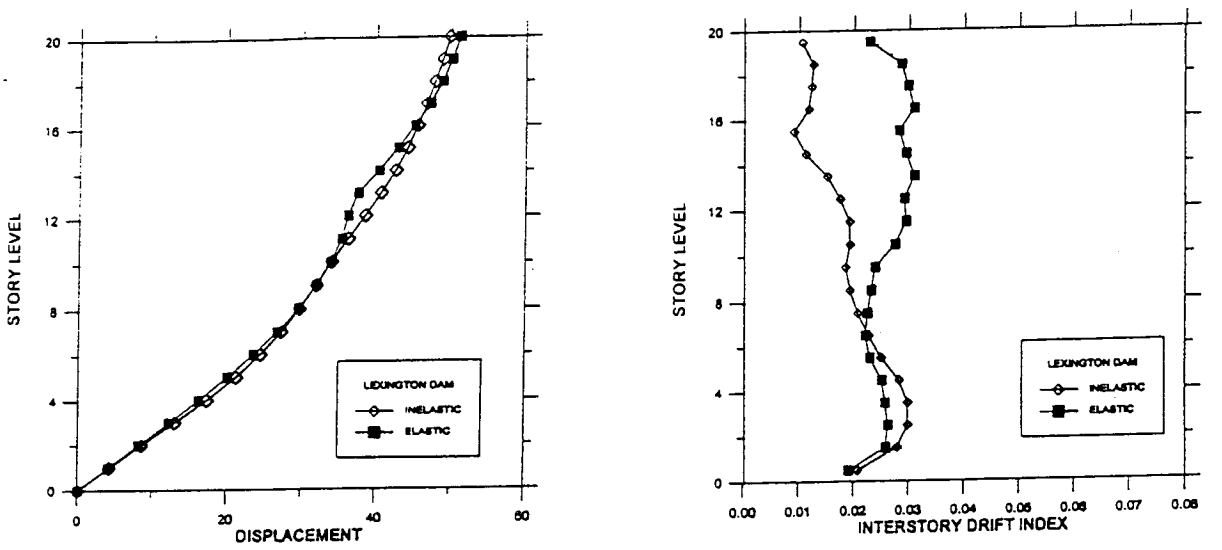

Figure 5.7.6 Steel Perimeter Frame, Elastic vs. Inelastic Displacement, Lexington Dam

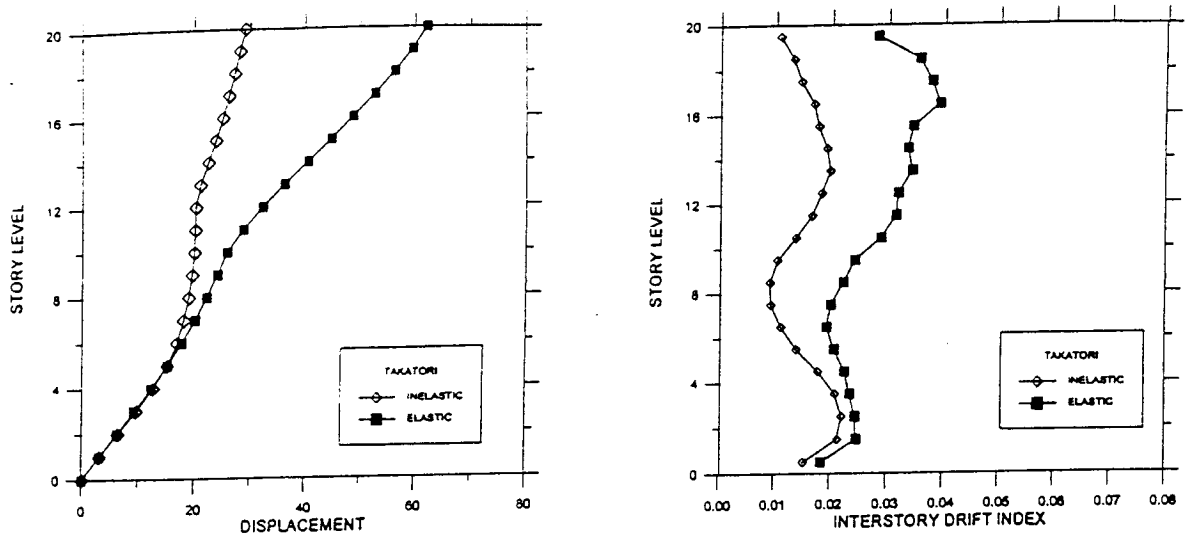

Figure 5.7.7 Steel Perimeter Frame, Elastic vs. Inelastic Displacement, Takatori

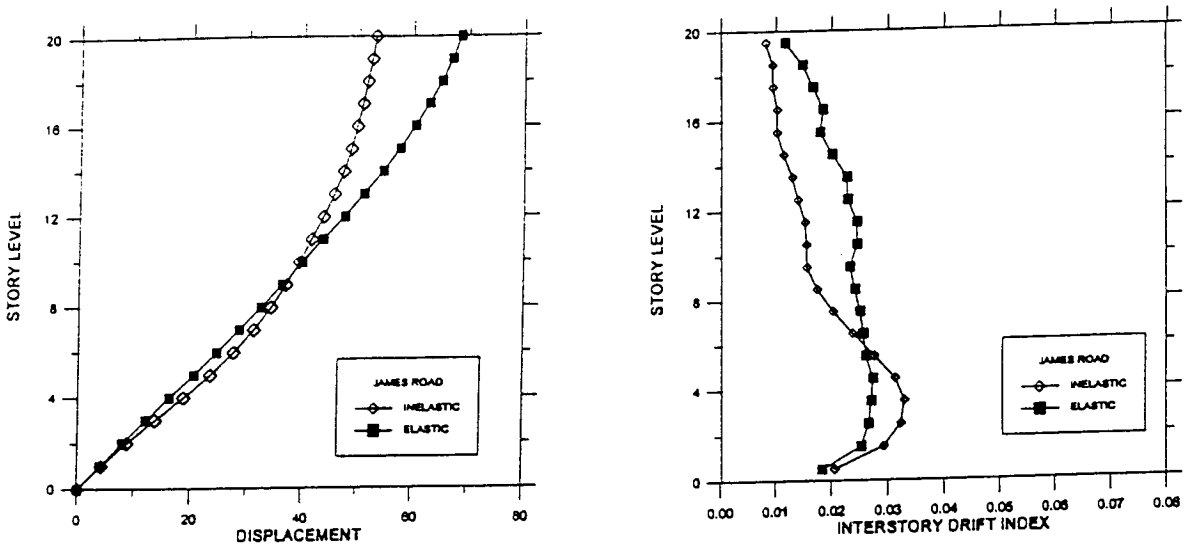

Figure 5.7.8 Steel Perimeter Frame, Elastic vs. Inelastic Displacement, James Road

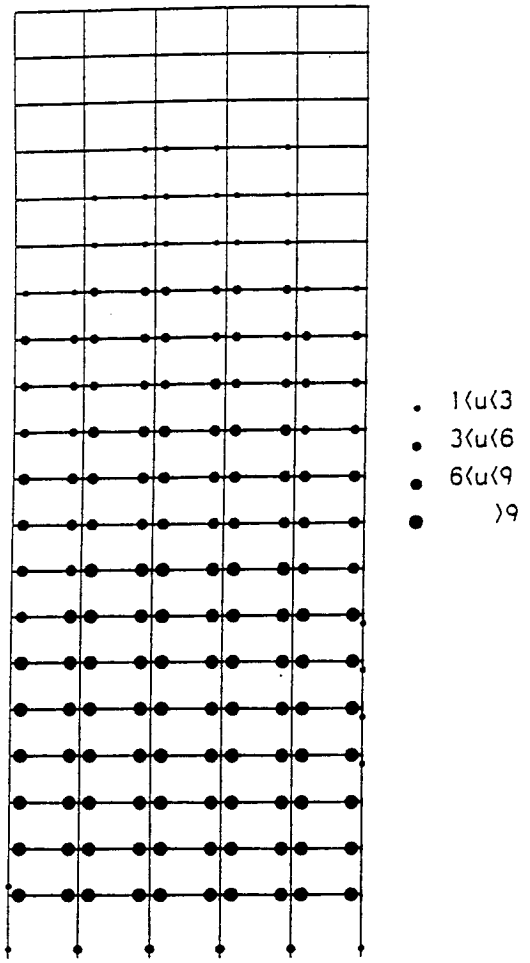

(a) Plastic Hinge Locations

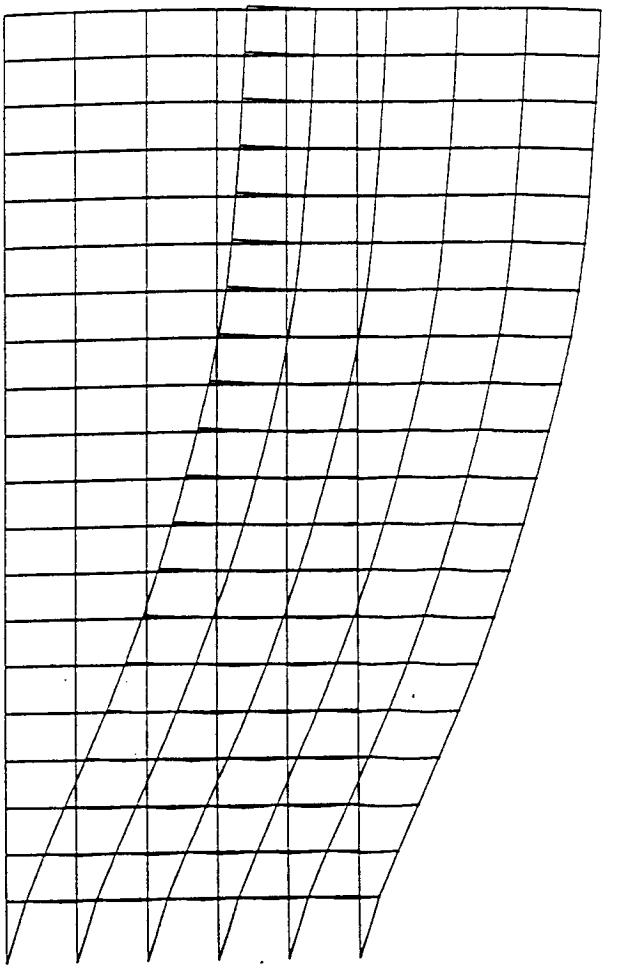

(b) Displaced Shape

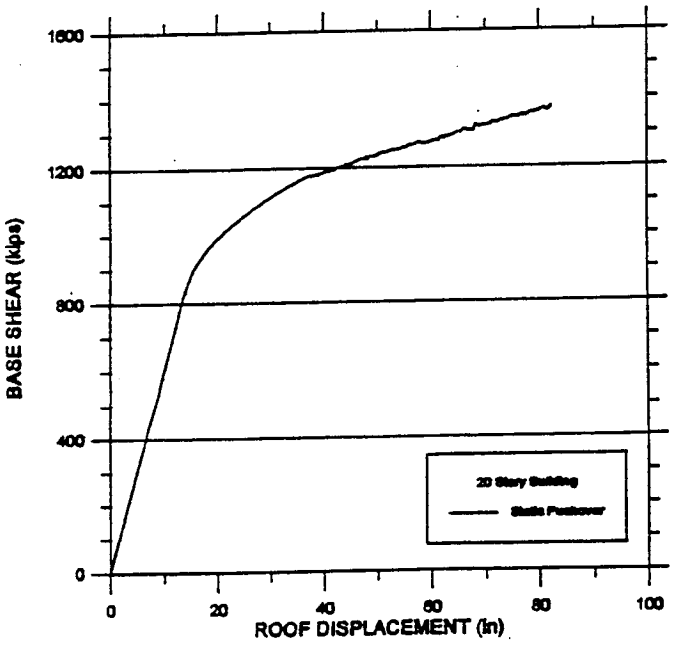

(c) Base Shear vs. Roof Displacement

Figure 5.7.9 Static Pushover, Steel Perimeter Frame Building

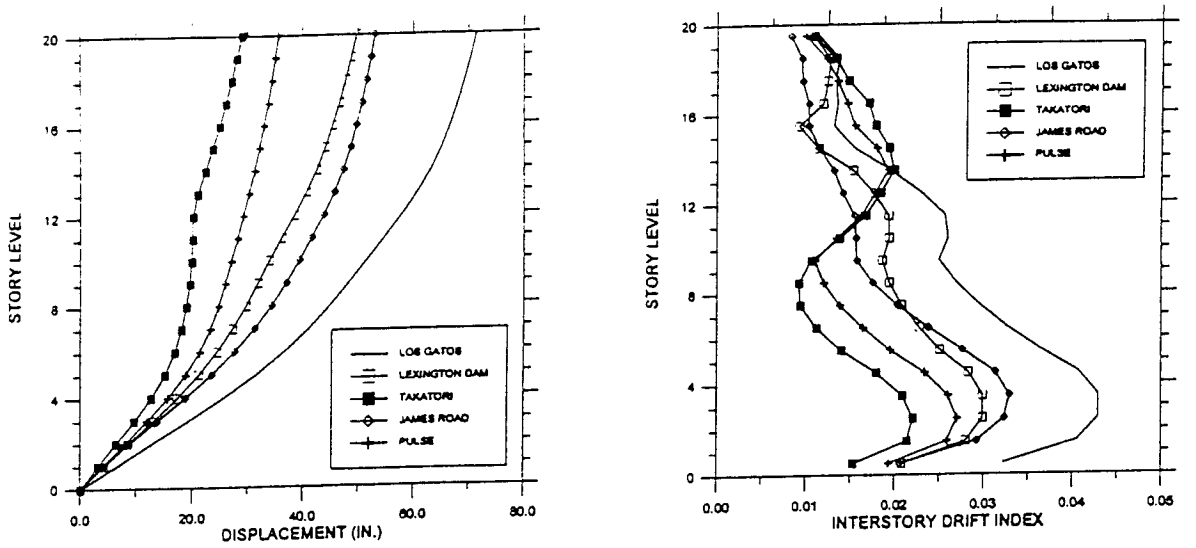

Figure 5.7.10 Displacement and Drift Demands, Steel Perimeter Frame

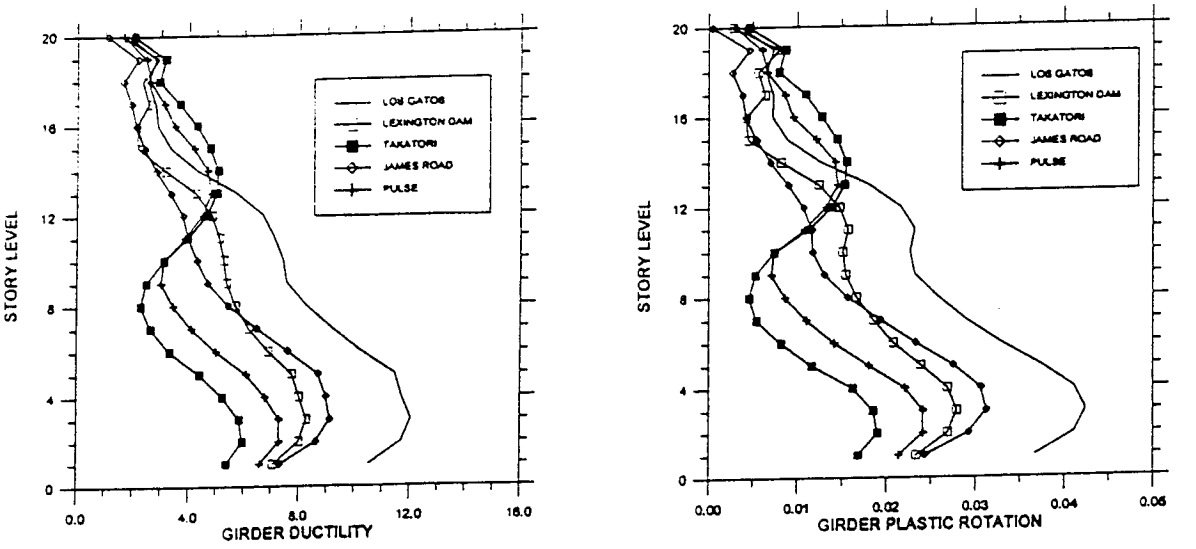

Figure 5.7.11 Ductility and Plastic Rotation Demands, Steel Perimeter Frame

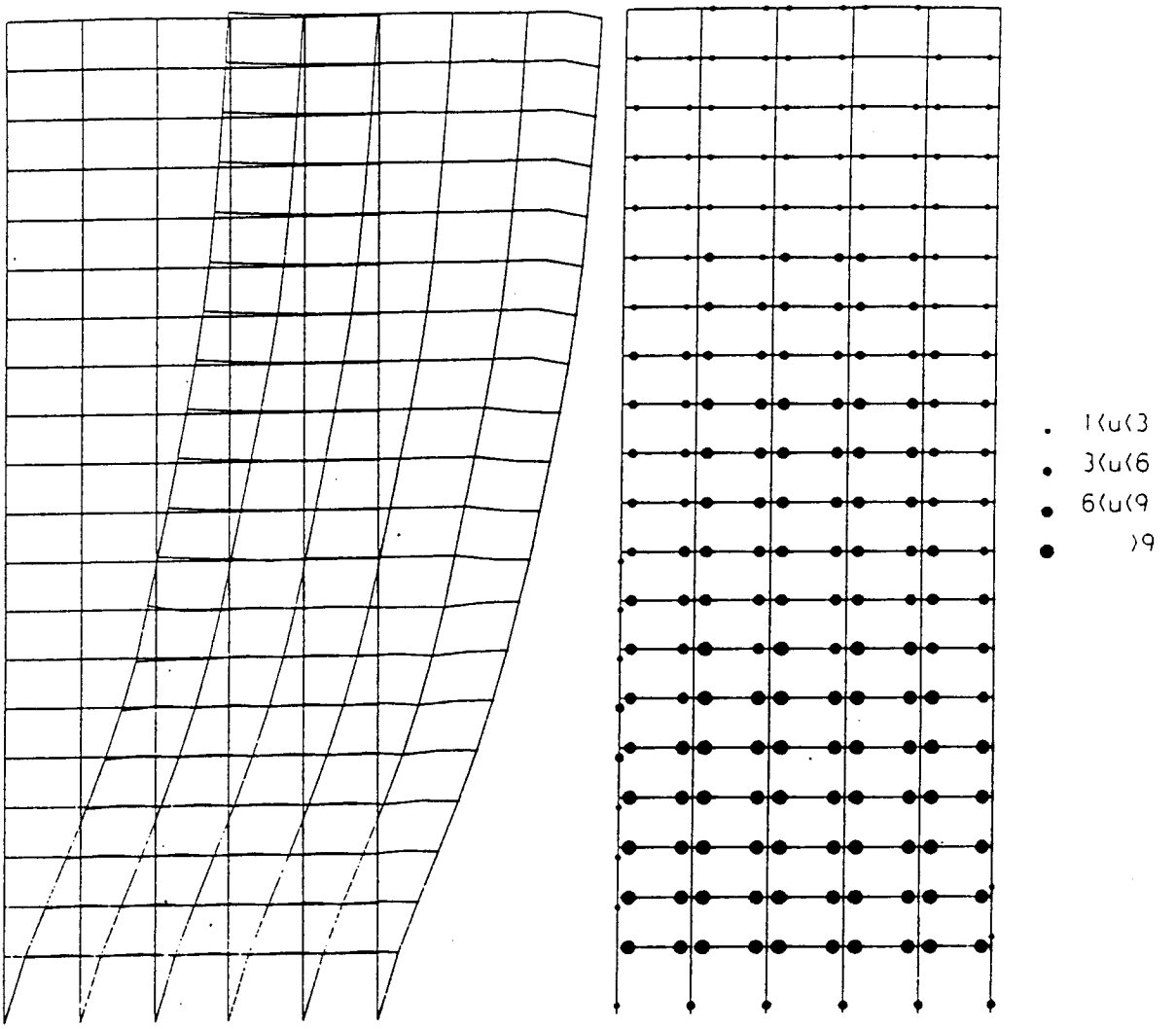

(a) Max. Displaced Shape, $\Delta_{roof} = 71.4$ inches

(b) Plastic Hinge Locations

Figure 5.7.12 Steel Perimeter Frame Building Response, Los Gatos

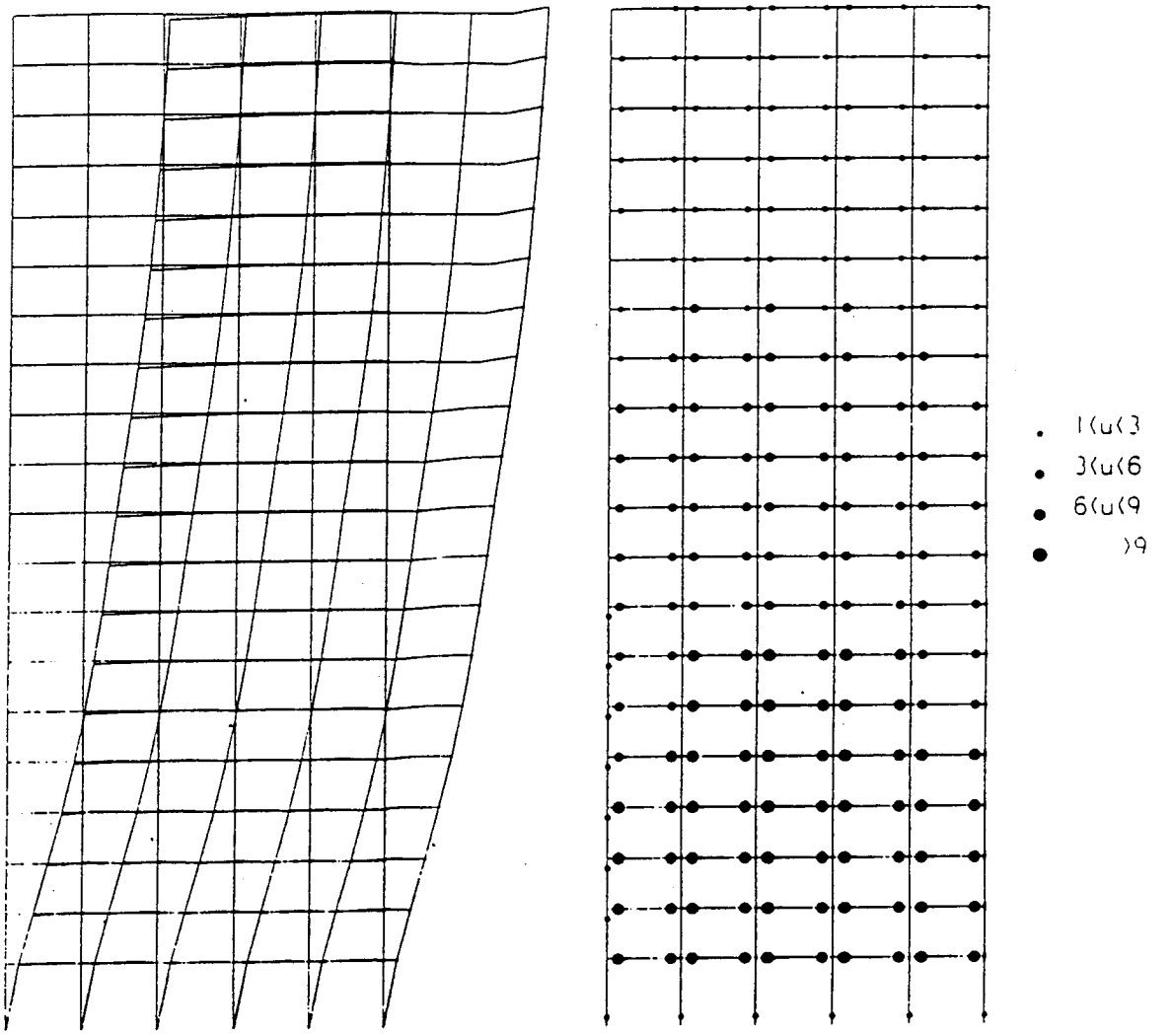

(a) Max. Displaced Shape, $\Delta_{roof} = 49.7$ inches

(b) Plastic Hinge Locations

Figure 5.7.13 Steel Perimeter Frame Building Response, Lexington Dam

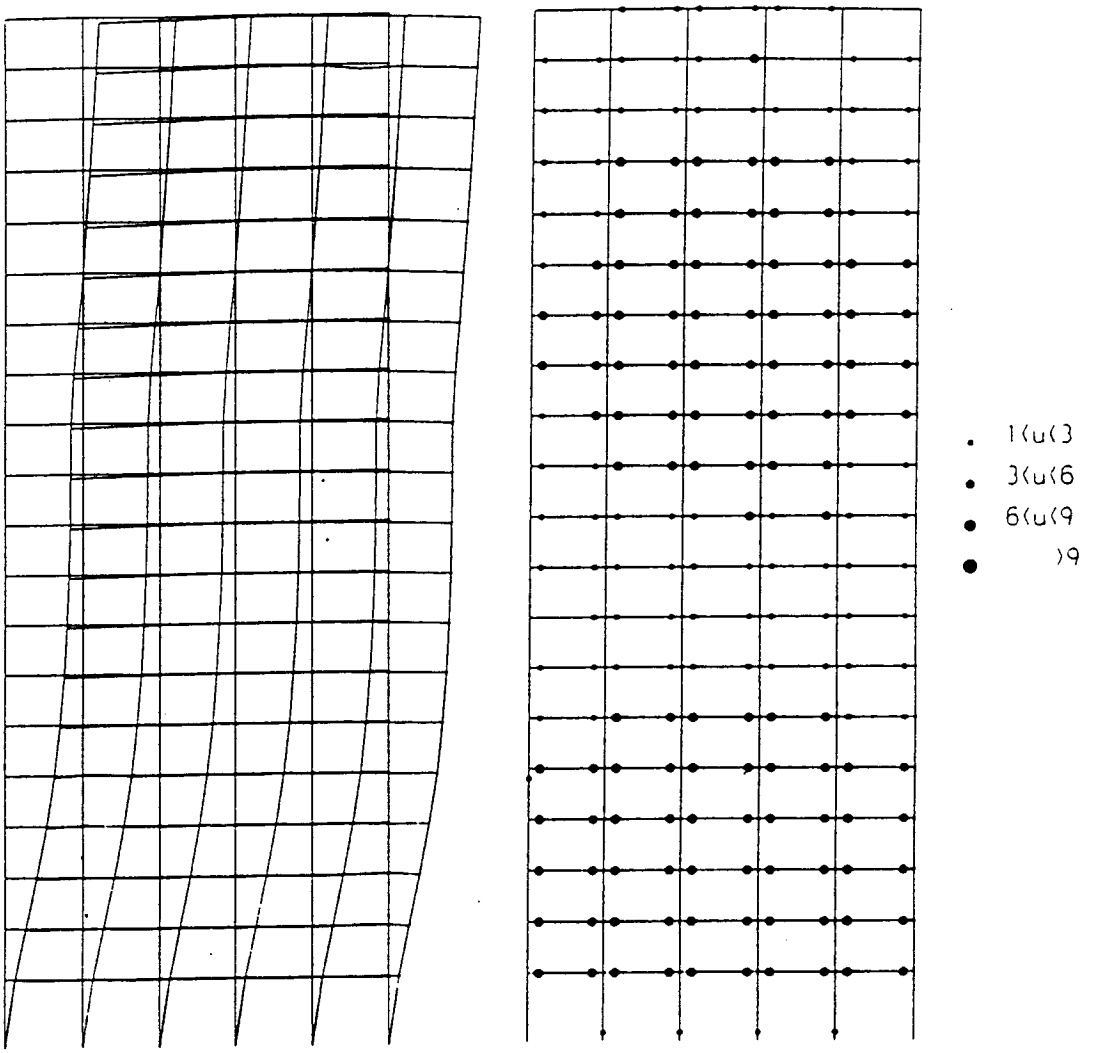

(a) Max. Displaced Shape, $\Delta_{roof} = 29$ inches (b) Plastic Hinge Locations

Figure 5.7.14 Steel Perimeter Frame Building Response, Takatori

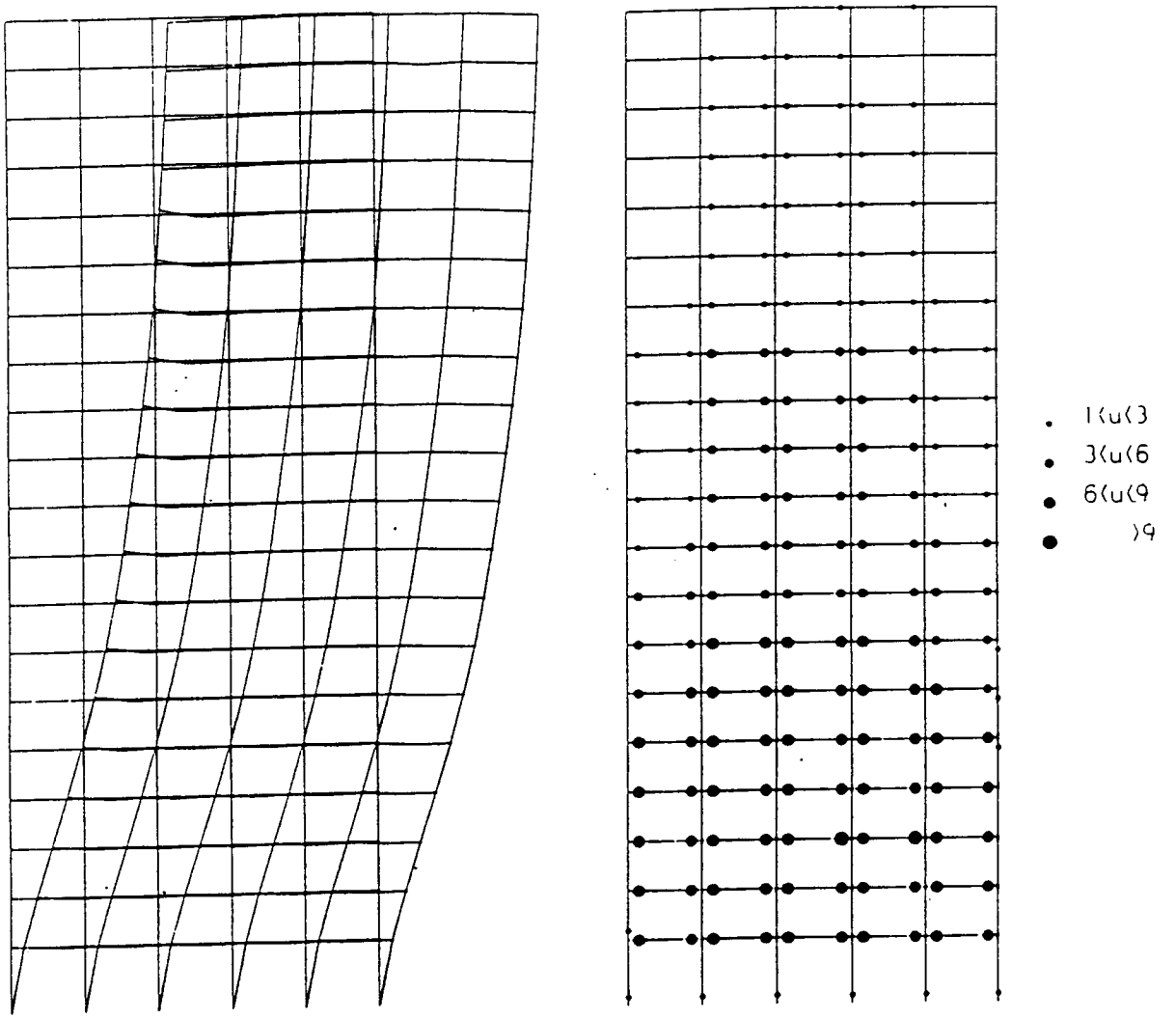

(a) Max. Displaced Shape, $\Delta_{roof} = 53$ inches

(b)Plastic Hinge Locations

Figure 5.7.15 Steel Perimeter Frame Building Response, James Road

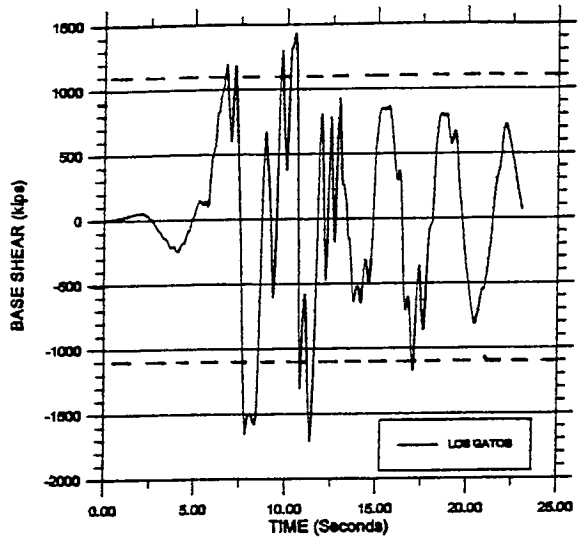

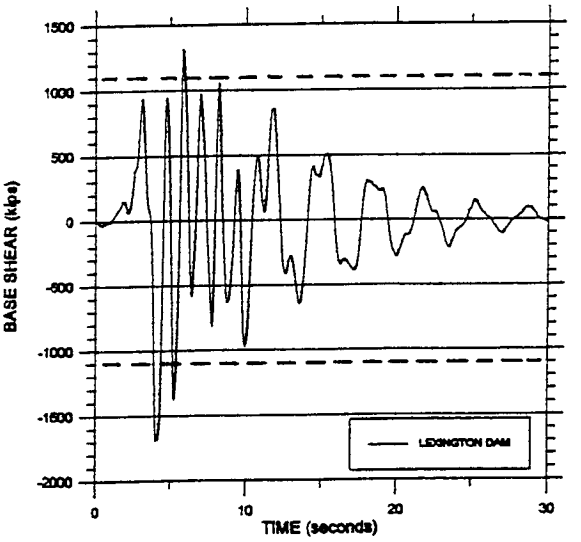

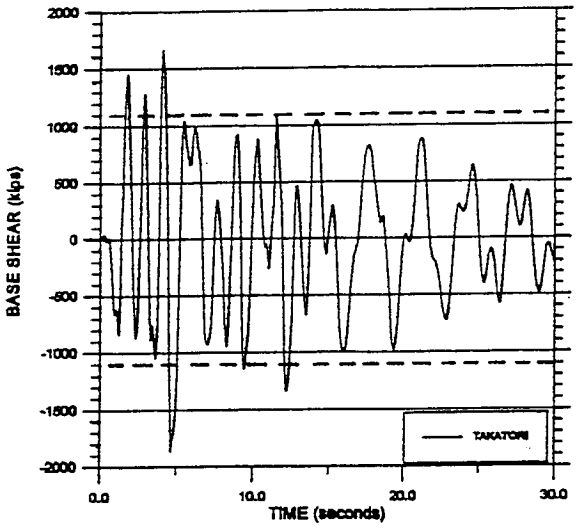

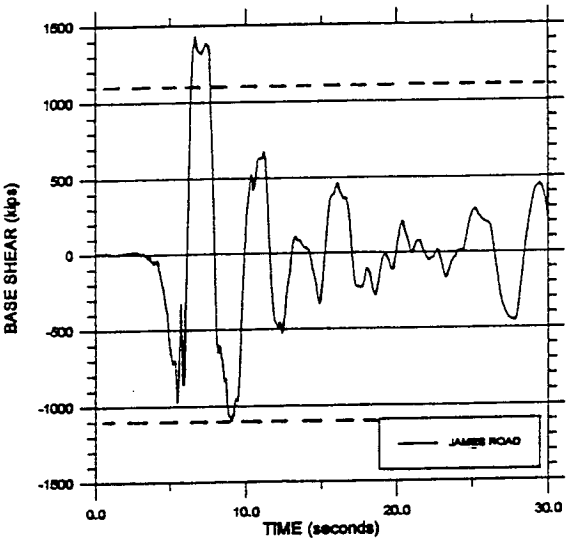

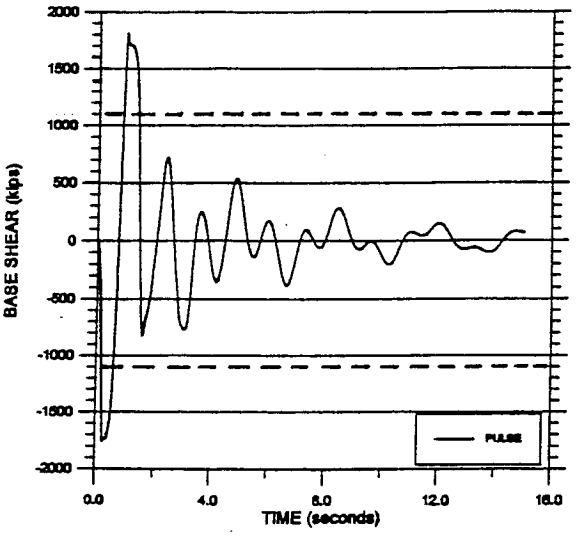

Figure 5.7.16 Steel Perimeter Frame Building,

Base Shear Response

5.8 SUMMARY AND CONCLUSIONS REGARDING THE EFFECTS OF SEVERE PULSE-TYPE EQGMs

From the results presented and the observations made for each of the buildings analyzed, the following preliminary conclusions are formulated:

- Due to the significant variation of the main dynamic characteristics of the recorded pulse-type EQGMs used in this study, the seismic performance (response) of each analyzed building indicates that this performance is very sensitive to the EQGM used.

- Even though the EQGMs used in this study contain only one or a limited number of severe acceleration pulses, studies of SDOFS indicate that the effect of increasing the value of the coefficient of damping ξ is significant and that an increase from 5% to 30% leads to a reduction in the main response parameters of up to 60%.

- Most of the buildings designed for building code requirements established before 1997 will perform poorly when subjected to the severe pulse-type EQGMs considered in this study.

- For structures of midheight (10 to 30 stories), the large ductility and displacement demands tend to be concentrated in the lower third of the building, whereas for taller buildings the largest demands occur in the upper third.

6 Investigation of Possible Efficient Retrofit Procedures for Improved Performance

6.1 GENERAL REMARKS

One of the most pressing problems that needs to be solved in order to mitigate the seismic risks in our urban areas is that of developing a method of efficient seismic retrofitting for the large inventory of vulnerable existing buildings. With the recognition of the large damage potential of severe pulse-type EQGMs, the number of buildings that need to be retrofitted has increased significantly. Thus, there is an urgent need to find efficient (technical and economical) retrofitting procedures for improved seismic performance of existing buildings. Each time a significant earthquake occurs, it is found that the generated EQGMs produce higher damage potentials than those considered in our codes. For this reason, it is necessary to investigate the vulnerability of existing buildings not only for the most critical previously recorded pulse-type EQGMs, but also for EQGMs of this type with higher damage potential which could occur in the future [Bertero, 1977]. Assuming a certain shape of the pulses (in this case, the one illustrated in **Figure 4.1**), there are three recognized ways of increasing the damage potential of severe pulse-type EQGMs:

(1) Increase the magnitude (intensity) of the accelerations;
(2) Increase the duration of the pulses (t_d) or (T_p); and
(3) Increase the magnitude and the duration of the pulses.

In view of time and budget constraints, an investigation was carried out only on the effects of increasing the intensity of the accelerations of the recorded pulse-type EQGMs on the performance of buildings previously designed according to Performance-Based EQRD, such as the **30-story S-K Redesigned Building**. It is highly recommended that the effects of increasing the duration, T_p, of the severe pulse-type EQGMs or the Simplified (idealized) Pulse should be studied in the future as well as the effects of a combined increase of the acceleration intensities and the T_p.

According to the main objectives of 2.1.4 through 2.1.6 and Tasks 5 through 7, attempts have been made to find efficient strategies and techniques for retrofitting some existing buildings, the seismic performance of which has been analyzed in Chapter 5, i.e.:

- **30-Story RC S-K Building Redesigned According to P-B SE in 1992**
- **30-Story RC S-K Building as Built in 1983**
- **15-Story RC Moment-Resistant Frame as Built in 1964**

- **41-Story Steel Space Frame as Built in 1972**

- **20-Story Steel Perimeter Frame as Designed for UBC 1994**

6.2 ANALYSIS OF THE EFFECTS OF INCREASING THE DAMAGE POTENTIAL OF RECORDED SEVERE PULSE-TYPE EQGMs ON THE PERFORMANCE OF THE 30-STORY S-K REDESIGNED BUILDING

To study the effects of increasing the damage potential of recorded severe pulse-type EQGMs, the recorded Los Gatos time history was selected because it was the critical one for the conceptually redesigned S-K building. According to the results presented in Chapter 5, the performance of this building was acceptable except for the IDI which was 2%, i.e., larger than the usually adopted maximum of 1.5%. As its maximum damage index was about 0.5, i.e., significantly below the maximum acceptable values of 0.8 or 1.0, it was decided to investigate how the dynamic (linear and nonlinear) performance of this building will change as the accelerations of the recorded Los Gatos are gradually increased. Although this method has been used previously [Zagajeski and Bertero, 1977] and discussed in detail [Bertero, 1977], more recently it has been denominated as a **"dynamic pushover"** method or procedure. The analytical model used for these analyses is shown in **Figure 6.2.1**. The results obtained by carrying out the nonlinear dynamic time-history analysis under the Los Gatos record are shown in **Figures 6.2.2 to 6.2.4**. When the reference accelerations are magnified by 1.30 and 1.60, the results presented in **Figures 6.2.5 to 6.2.7** and **Figures 6.2.8 to 6.2.10** respectively are obtained. Comparing the results obtained with 1.0 x Los Gatos, 1.3 x Los Gatos, and 1.6 x Los Gatos, it can be seen that there is a relatively small increase in the total base shear from $V_B = \pm 100$ MN ($\pm$ 0.40W) to ± 120 MN ($\pm$0.49W), that the structure would have to resist (about 20%). However, there are significant modifications in (1) the pattern of the IDI and their maximum values, from a +2% at the 20^{th} and 21^{st} stories to a value of -3.1% at the 5^{th} story; (2) the maximum values of plastic rotations of the beams and columns from 0.0207 to 0.0350 (71% increase) in the beams and from 0.0158 to 0.041 (159% increase) in the columns; and (3) in the Damage Index (DI), from 0.51 to 0.84, i.e., a 65% increase. As the values of the maximum IDI and Damage Index (i.e., -3.1% and 0.84) are unacceptable, it can be concluded that the conceptually redesigned S-K building will have to be retrofitted to resist a severe pulse-type EQGM similar to 1.6 x Los Gatos.

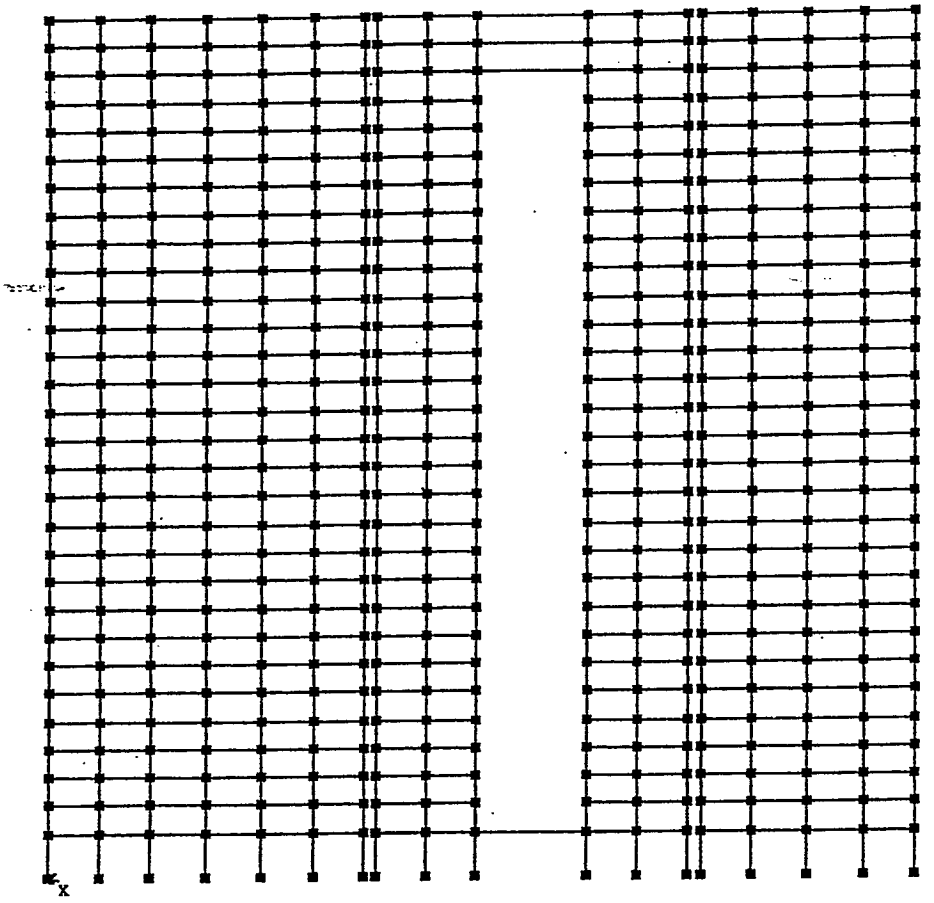

Figure 6.2.1 Model of the S-K Building , Dynamic Pushover

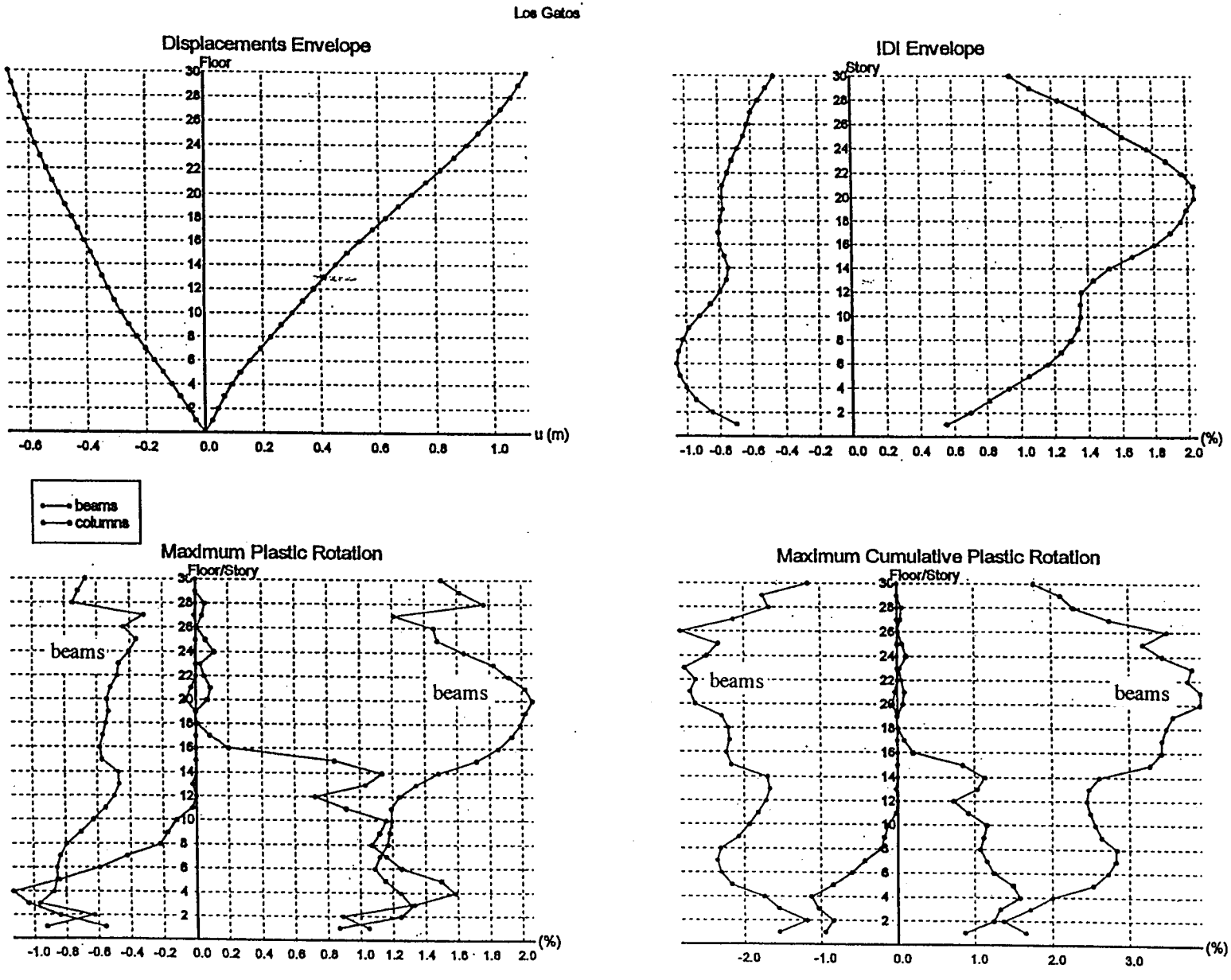

Figure 6.2.2 Building Response Envelopes, 1.0 Los Gatos

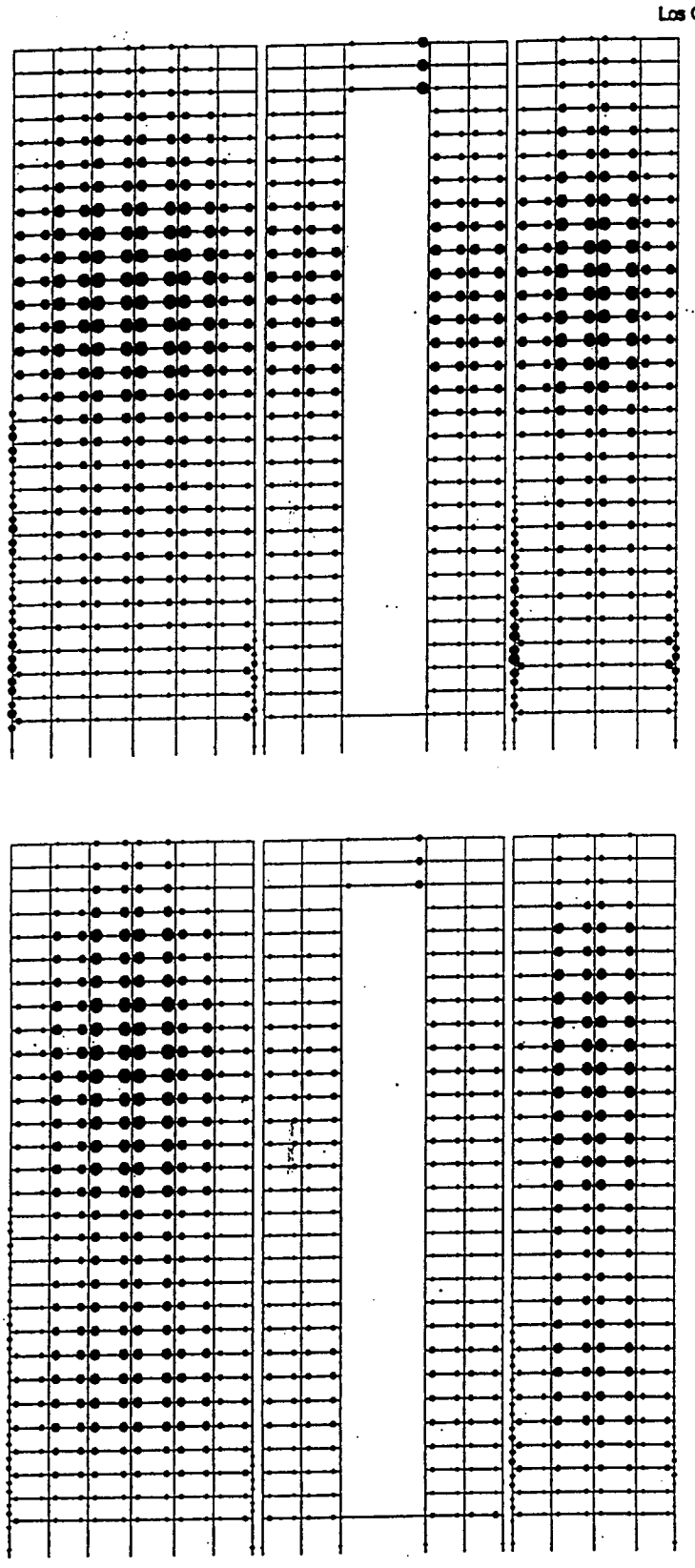

Figure 6.2.3 Plastic Hinge Rotations, 1.0 Los Gatos

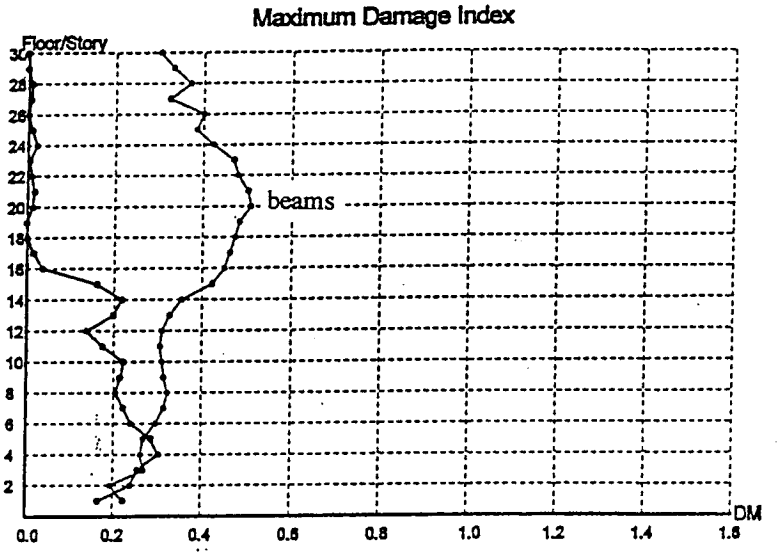

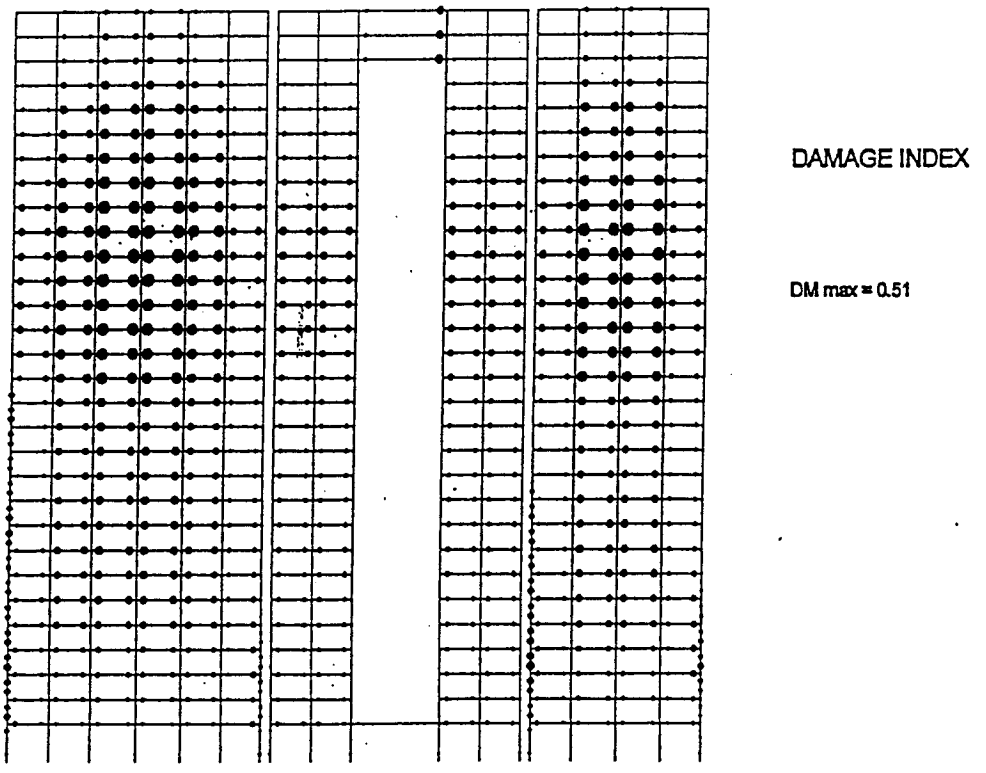

Figure 6.2.4 Damage Index, 1.0 Los Gatos

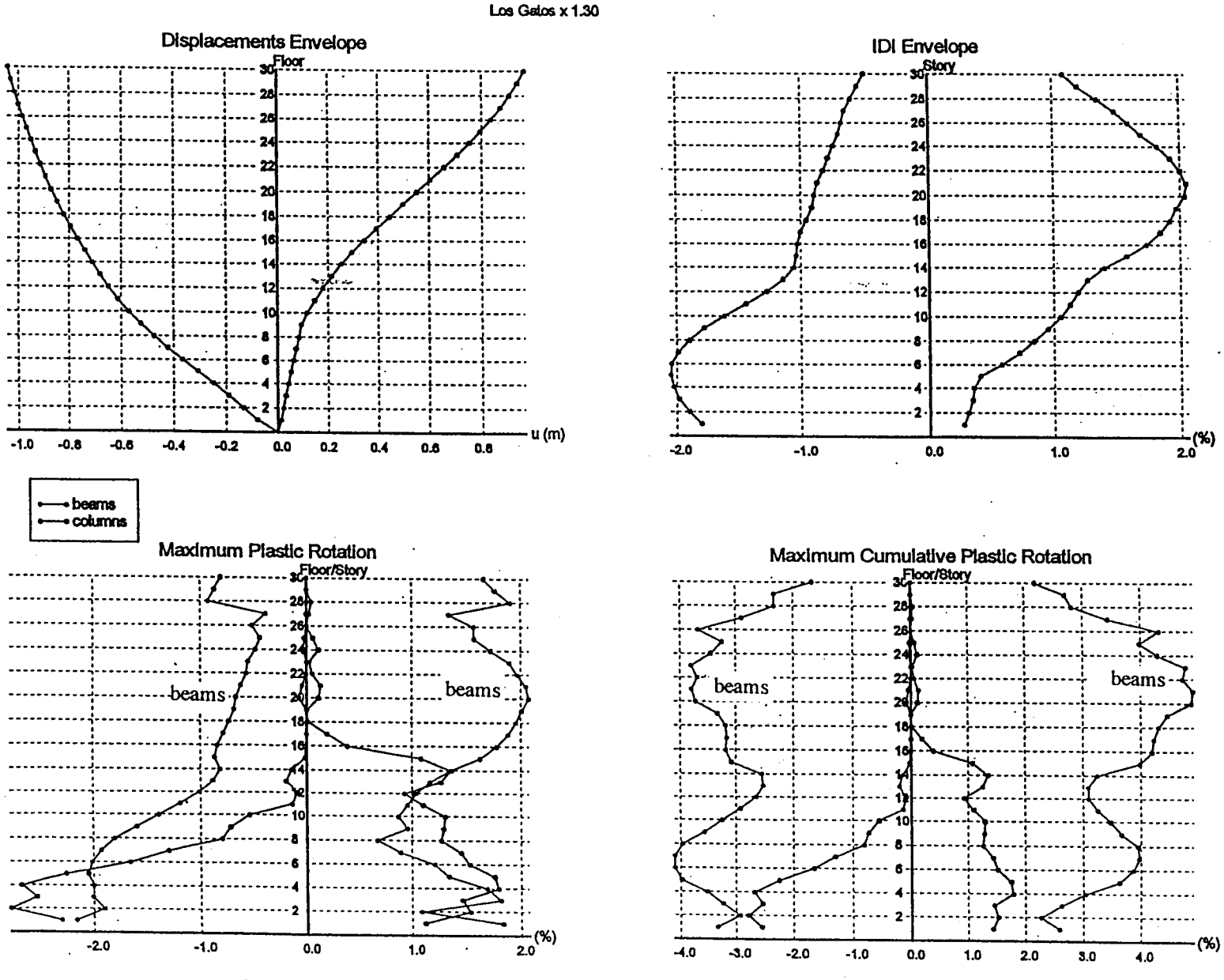

Figure 6.2.5 Building Response Envelopes, 1.3 Los Gatos

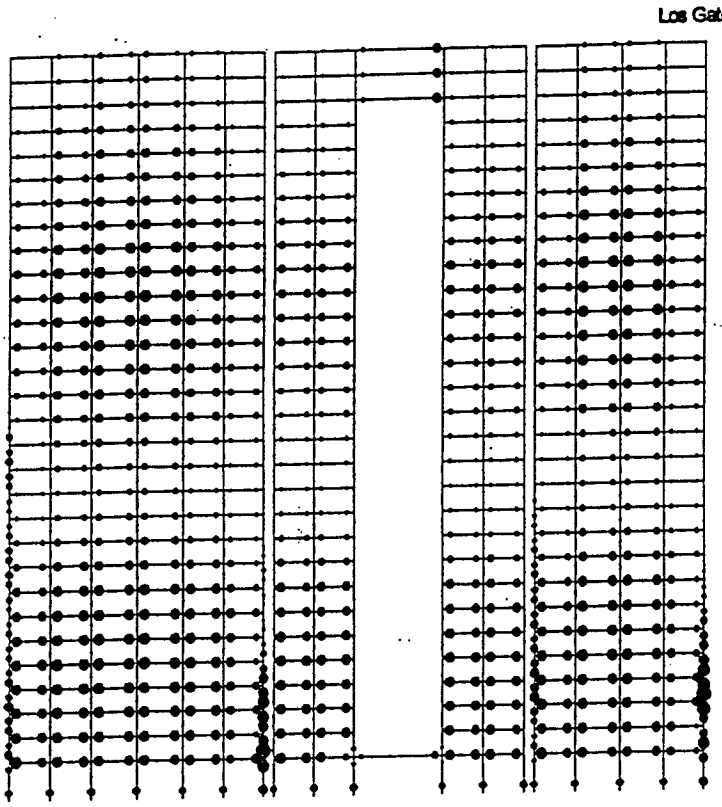

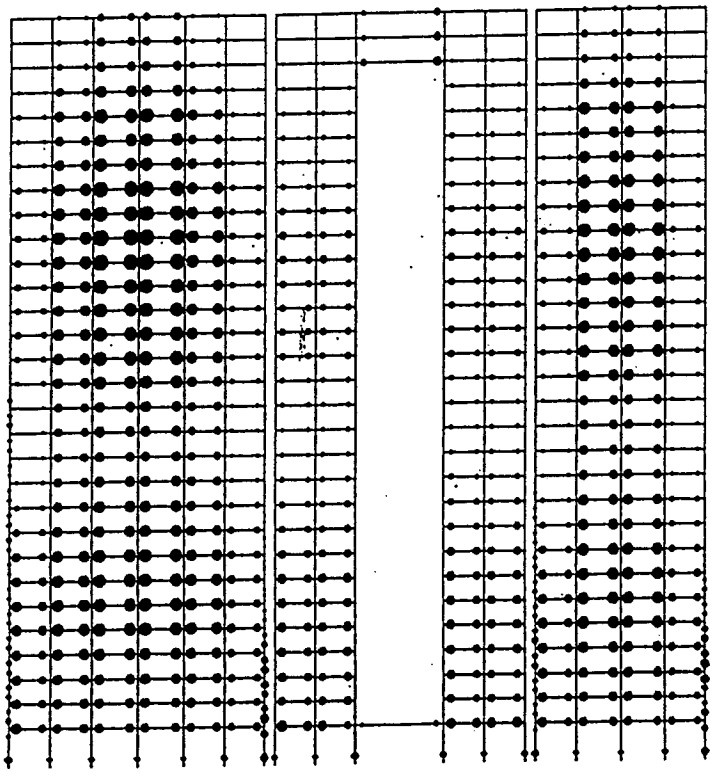

Figure 6.2.6 Plastic Hinge Rotations, 1.3 Los Gatos

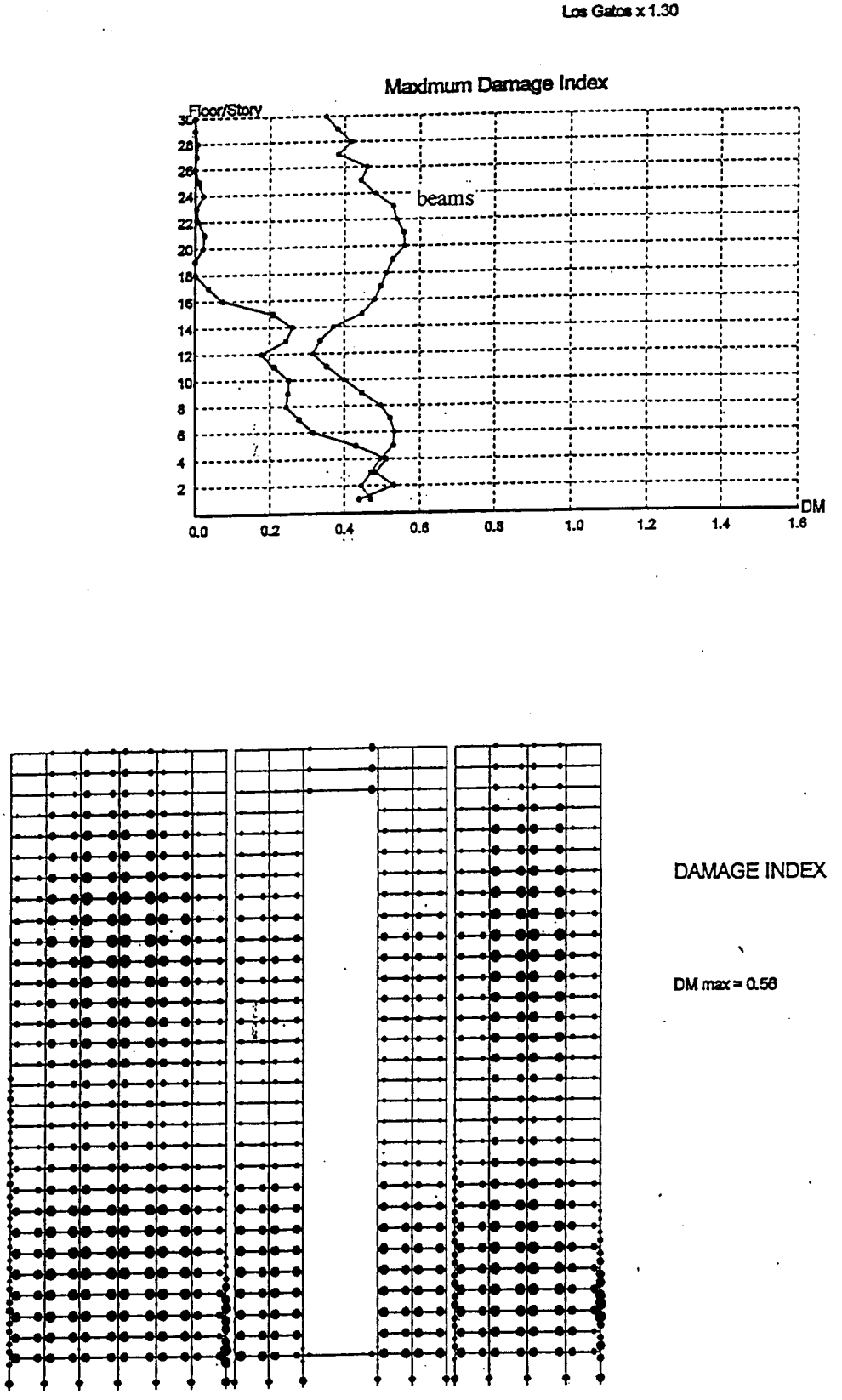

Figure 6.2.7 Damage Index, 1.3 Los Gatos

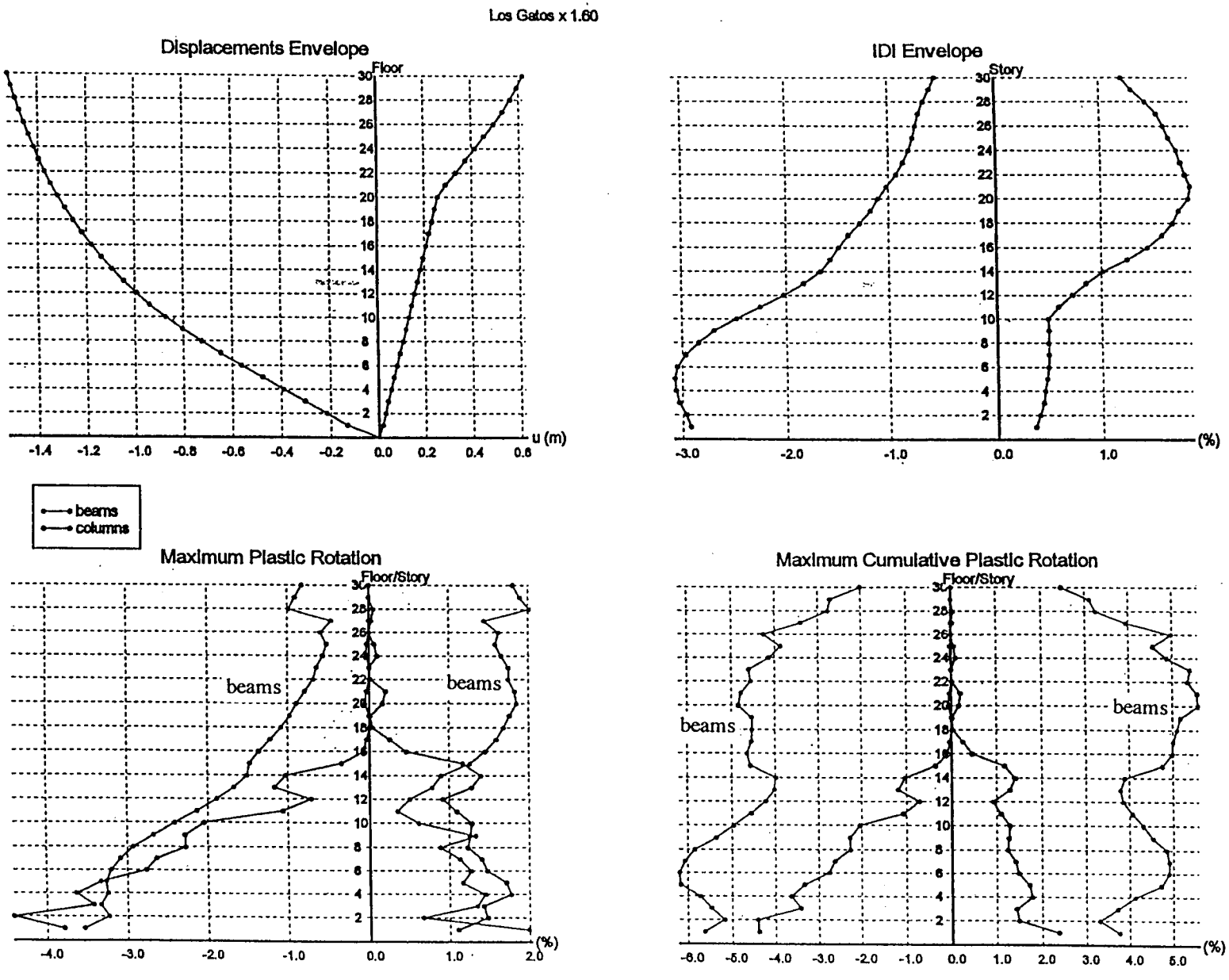

Figure 6.2.8 Building Response Envelopes, 1.6 Los Gatos

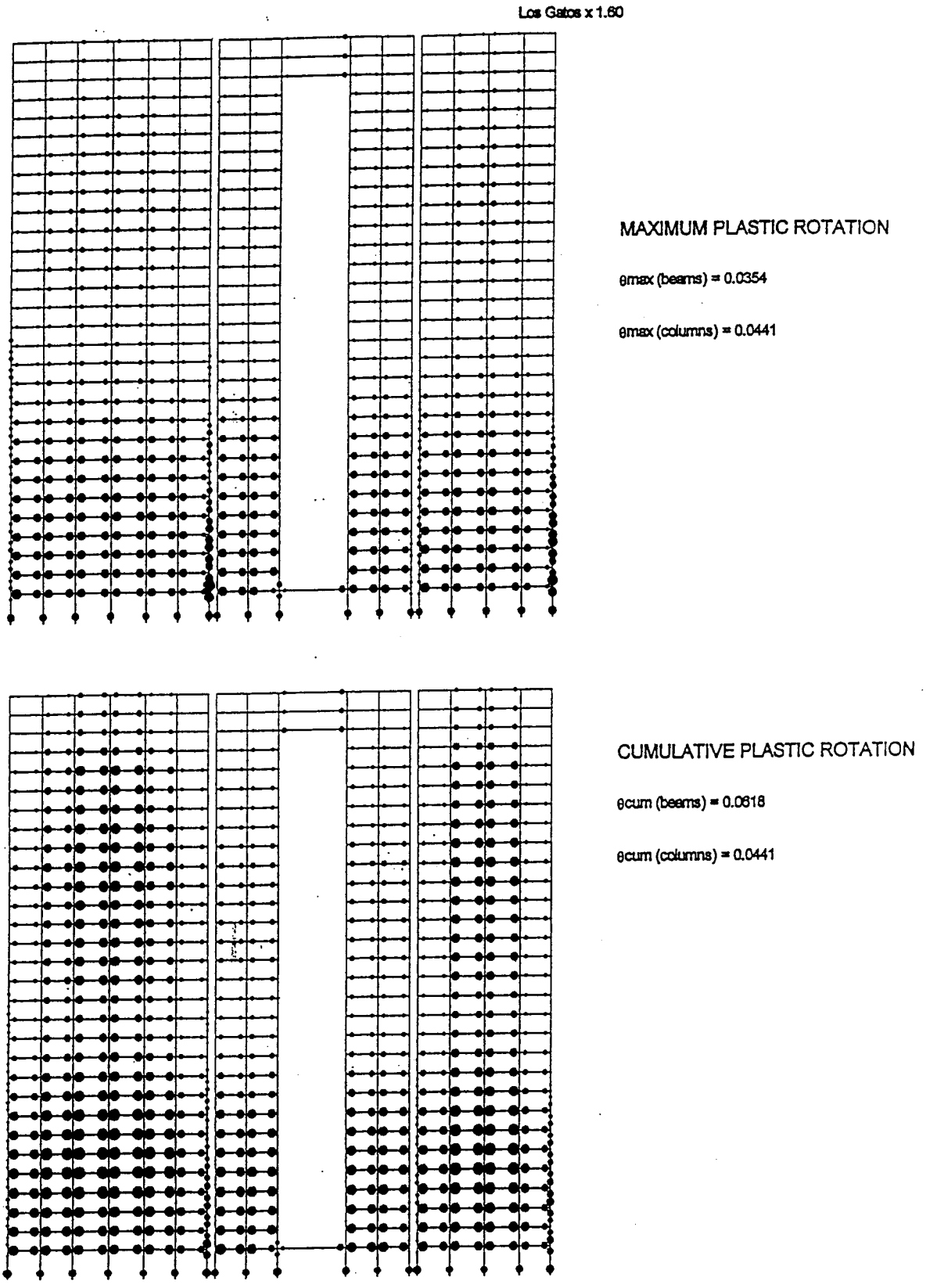

Figure 6.2.9 Plastic Hinge Rotations, 1.6 Los Gatos

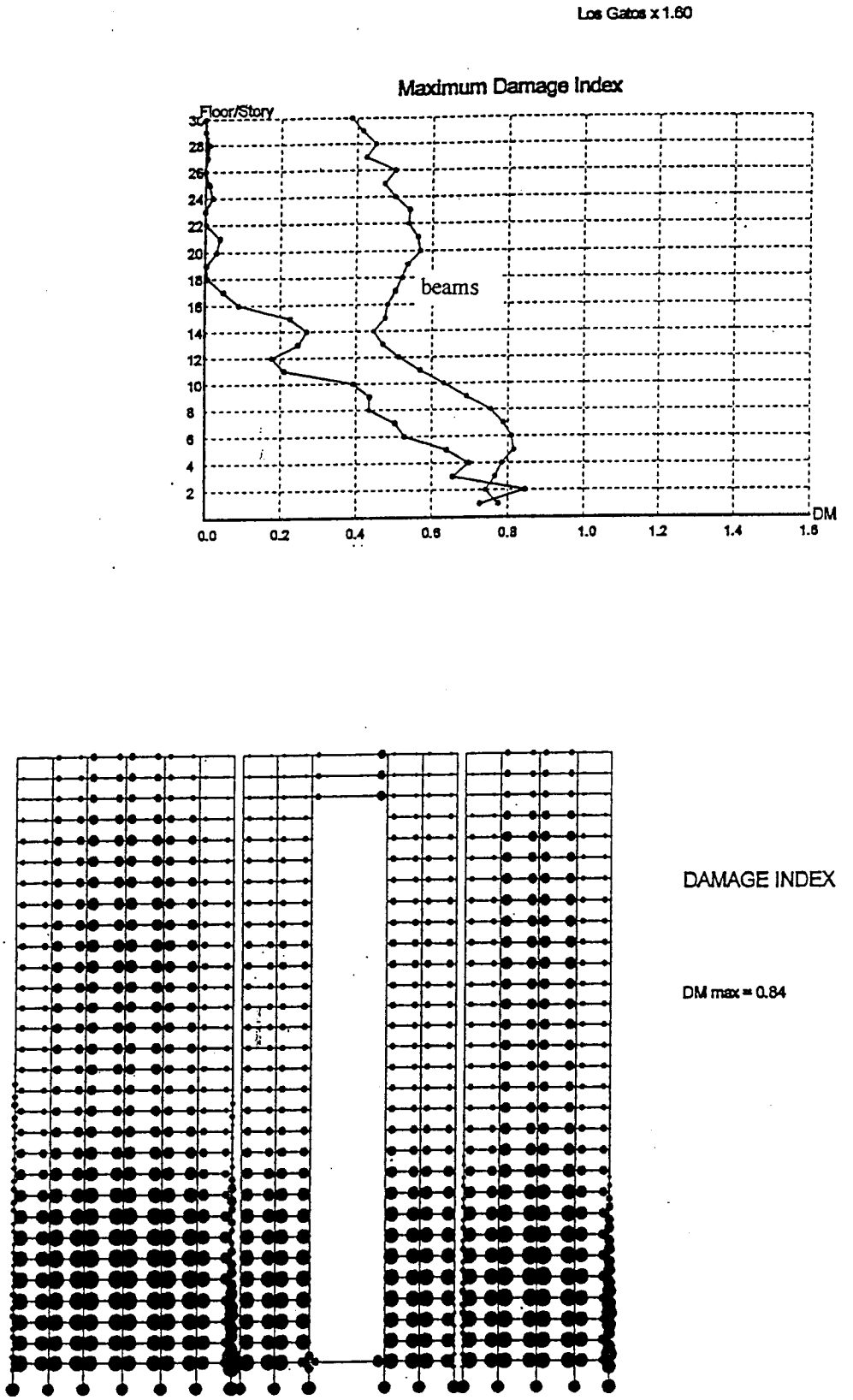

Figure 6.2.10 Damage Index, 1.6 Los Gatos

6.3 RETROFIT OF THE S-K BUILDING (CONCEPTUAL DESIGN)

The initial attempt to retrofit the S-K Building (Conceptual Design) consisted of using conventional procedures of strengthening and stiffening to resist a ***1.60 x Los Gatos*** EQGM.

6.3.1 Shear Walls

As an initial retrofit, the redesigned S-K building was strengthened and stiffened using shear walls as indicated in **Figure 6.3.1.** The results of the analysis of its performance under the 1.60 Los Gatos 1 EQGM are shown in **Figure 6.3.2** through **Figure 6.3.4**. As can be seen in **Figure 6.3.2,** the introduction of the shear walls, while significantly changing the pattern of displacements and IDIs with respect to those obtained for the redesigned building (**Figure 6.2.8**), did not significantly decrease the maximum displacement at the roof (1.42m vs. 1.45m), and decreased the maximum IDI from -3.1%, which occurred at the 5th story, to a value of +2.44%, which occurred at the 27th story. The maximum values of the plastic rotation of the beams and the cumulative plastic rotations increase. The maximum values of the Damage Index increase from a value of 0.84, which occurred at the columns of the 2nd story, to a value of 1.12, which is developed in the beams of the 28th floor.

6.3.2 Coupled Shear Walls

In view of the above results, it was decided to couple the shear walls with strong and stiff coupling beams located at the top of the shear walls as illustrated in **Figure 6.3.5.** The response results obtained when the building, retrofitted with coupled walls, was subjected to 1.60 Los Gatos 1 EQGM are given in **Figure 6.3.6** through **Figure 6.3.8.** Comparing these results with those obtained using shear walls alone, **Figures 6.3.2** through **6.3.4,** it can be seen that while there are significant changes in the distribution pattern of the displacement and IDI over the height of the building, the maximum values for the displacement and IDI do not decrease. Only the maximum plastic rotations of the beams, the cumulative plastic rotations of the beams, and the Damage Index show a small decrease. The damage index of the beams located in the 20th floor is 0.97, which is not acceptable. The maximum IDI is practically the same as that obtained with single shear walls (2.41% vs. 2.44%), but take place at the 17th floor rather than at the 27th floor.

(a) Strong Coupling Girder at Top

In view of the above results, an attempt was made to increase the strength and particularly the stiffness of the coupling girder at the top of the shear walls, as illustrated in **Figure 6.3.9**. The results obtained for the performance of this new retrofit strategy are illustrated in the graphs shown in **Figures 6.3.10 through 6.3.12.** When these results are compared with those obtained in the previous strategy of a more flexible coupling girder, it becomes clear that no improvement has been obtained.

(b) Coupling Girder at Midheight and Top of Shear Walls

This new retrofit attempt is illustrated in **Figure 6.3.13** and the effect of this modification on the response of the structure is illustrated in **Figures 6.3.14 through 6.3.16.** A comparison of these results with those obtained from the previously described retrofit attempts, indicates that while the distribution patterns of the response parameters over the height of the building change significantly (particularly of the IDI, the Plastic Rotation in the critical beams, and the Damage Index), the maximum demanded values do not decrease significantly. For some parameters, such as the Damage Index, an increase occurs (1.08 at the beams located at the 10^{th} floor vs. 0.97 for the beams located at the 20^{th} floor).

(c) Coupling Girders at the 1/3, 2/3, and 1.0 of the Total Height of the Shear Walls

Also considered was an investigation of whether increasing the number of levels at which coupling girders are located will improve the performance. This new retrofit attempt is illustrated in **Figure 6.3.17** and the results of the response to 1.60 Los Gatos 1 EQGM are presented in **Figures 6.3.18 through 6.3.20.** Comparing these results with those obtained previously clearly indicates that although the distribution pattern of the maximum values of the response parameters over the height of the building varies significantly, there is only a very small change in their maximum values. The Damage Index for the beams, which now occurs at the 16^{th} floor with its value being 1.11, is a little larger than the value of 1.08 that occurred in the beams of the 10^{th} floor in the case where coupling girders were used at only two levels **(Figure 6.3.16).**

From the above results, it appears that the use of conventional methods of increasing the strength and/or stiffness for improving the performance of the conceptually redesigned S-K building, subjected to 1.60 Los Gatos 1 EQGM, will not lead to an efficient solution; therefore, the use of innovative strategies and techniques was investigated.

6.3.3 Innovative Retrofit Procedure (Supplemental Damping)

From previously conducted studies [Bertero, 1997], it was decided that the most attractive innovative strategy for this building appears to be the use of supplemental damping. Initially, the authors were reluctant to attempt such a solution due to the characteristics of the critical EQGMs under consideration. As indicated earlier, it is well known that for a single acceleration pulse, damping is not very effective in decreasing the response. However, in view of the following facts (a) that the amplitude of the velocity pulse is very high, (b) that the recorded EQGMs contain at least three severe pulses similar to the idealized pulse-type EQGM illustrated in **Figure 4.1**, and (c) that these severe pulses generally occur after several smaller pulses, it was decided to attempt the use of such a strategy.

The initial study of the use of supplemental damping considered the conceptually redesigned S-K building initially retrofitted with shear walls, **Figure 6.3.21**, with added damping to attain a ξ_{eff} = 30%. The response results shown in **Figures 6.3.22 through 6.3.24,** clearly show that the performance is not only acceptable but that the additional damping could be decreased and still result in acceptable performance. When these results are compared with those obtained with ξ_{eff} = 5%

(Figures 6.3.25 through 6.3.27), it can be seen that the maximum value of the roof displacement has been reduced from a value of 1.32m to 0.65m, a reduction of about 51%. In a similar manner, the maximum value of IDI of 1.98% has been decreased to a value of 0.98%, a reduction of 51%. Similar reductions have been obtained in the maximum Plastic Rotation, Cumulative Plastic Rotation, and the Damage Index of the beams. From the above results, it appears that it might be possible to eliminate the shear walls and retrofit this conceptually redesigned S-K building using only supplemental damping. This possibility should be investigated in future studies.

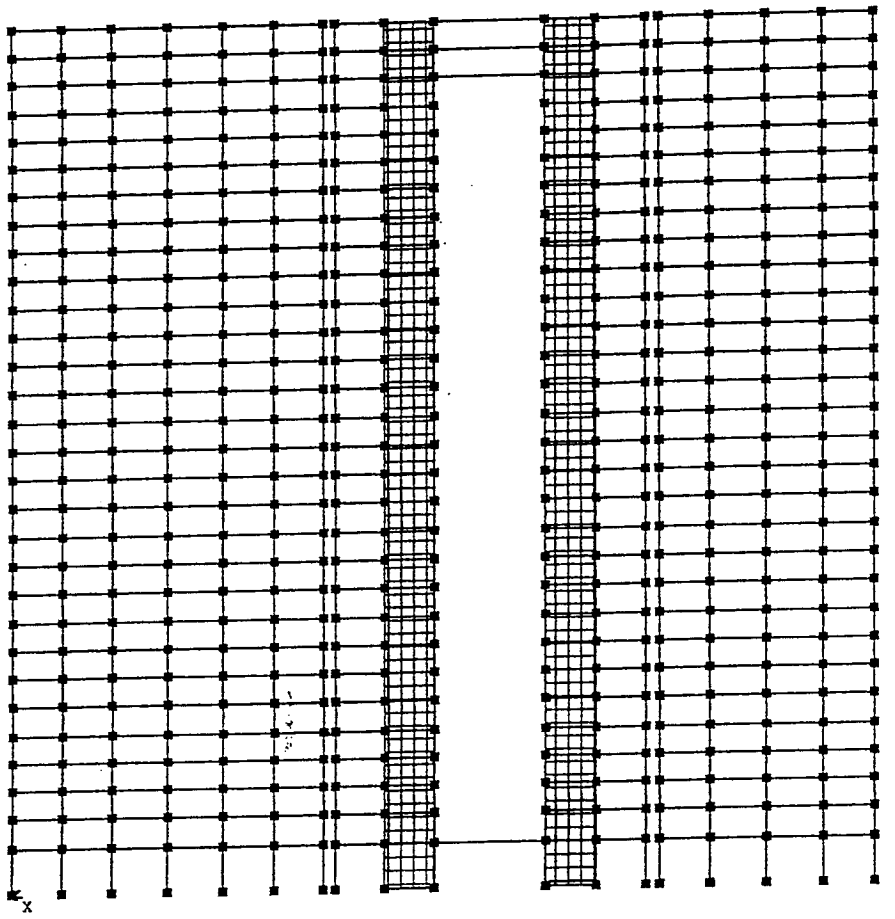

Figure 6.3.1 Model of the S-K Redesigned Building Retrofitted with Single Shear Walls

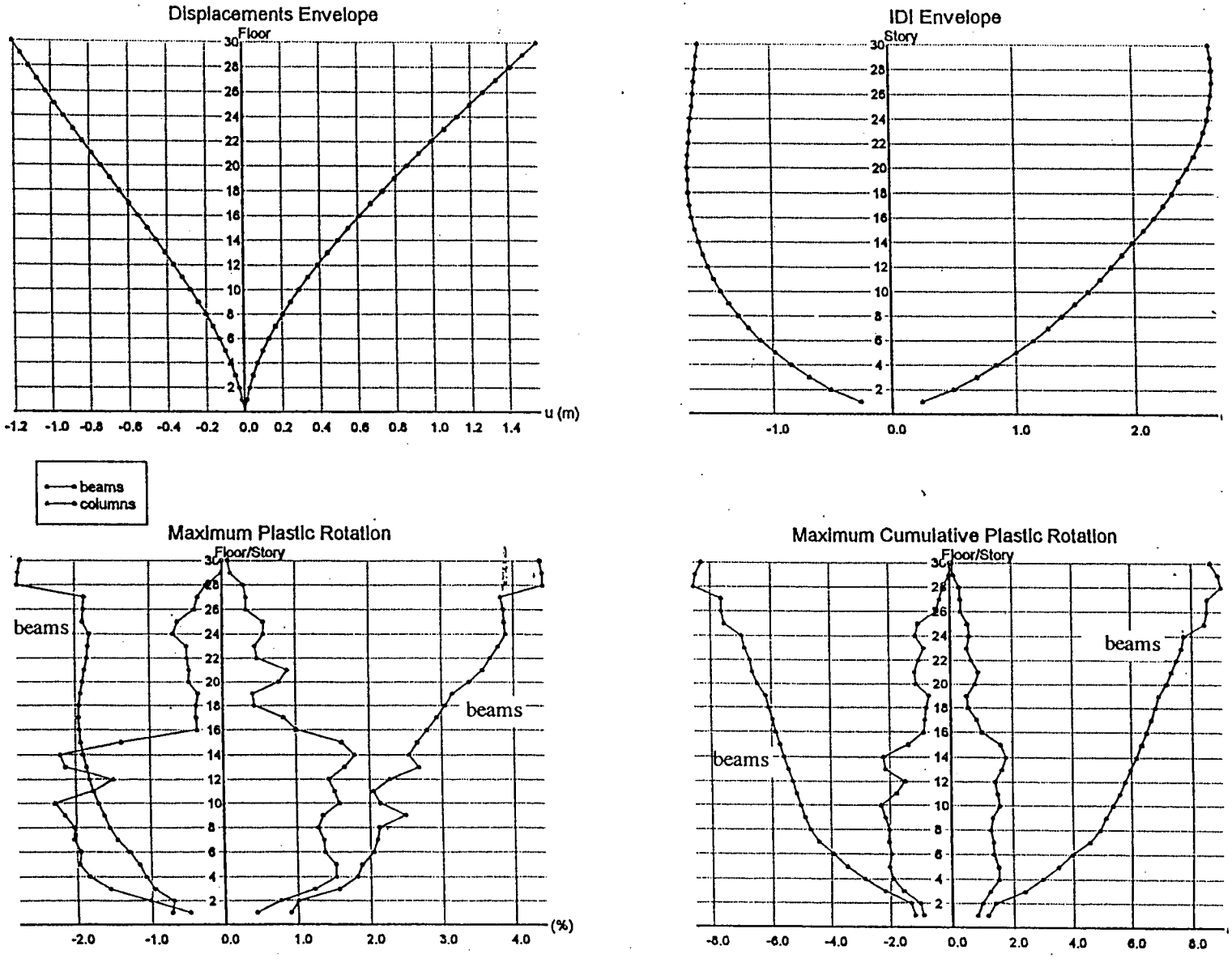

Figure 6.3.2 Response Results, Single Shear Wall

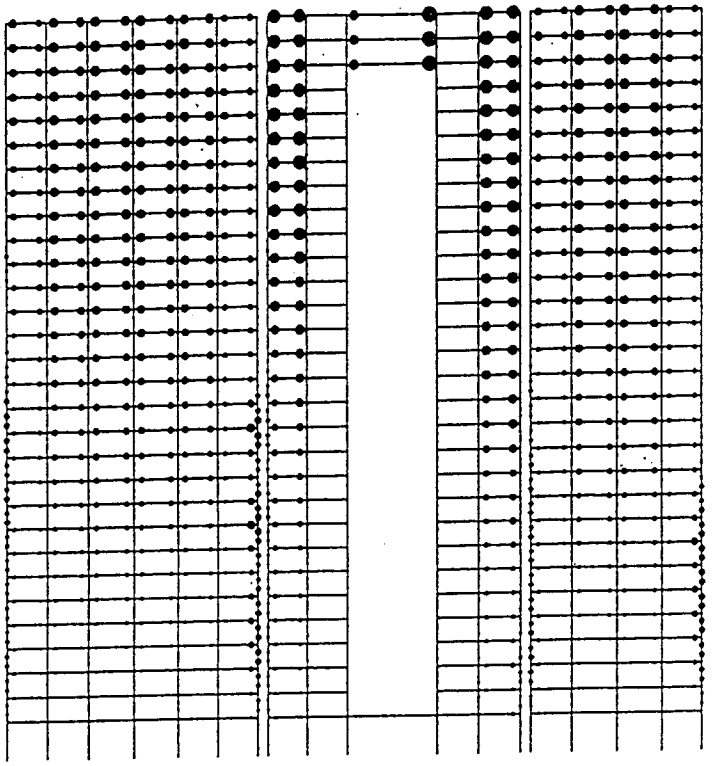

MAXIMUM PLASTIC ROTATION

θmax (beams) = 0.0441

θmax (columns) = 0.0228

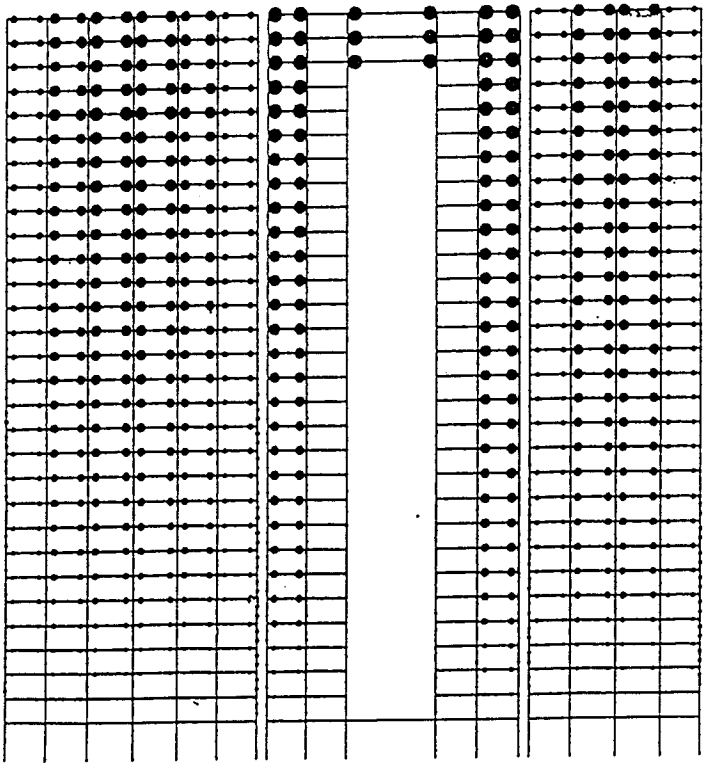

CUMULATIVE PLASTIC ROTATION

θcum (beams) = 0.0897

θcum (columns) = 0.0228

Figure 6.3.3 Plastic Rotation Demands, Single Shear Wall

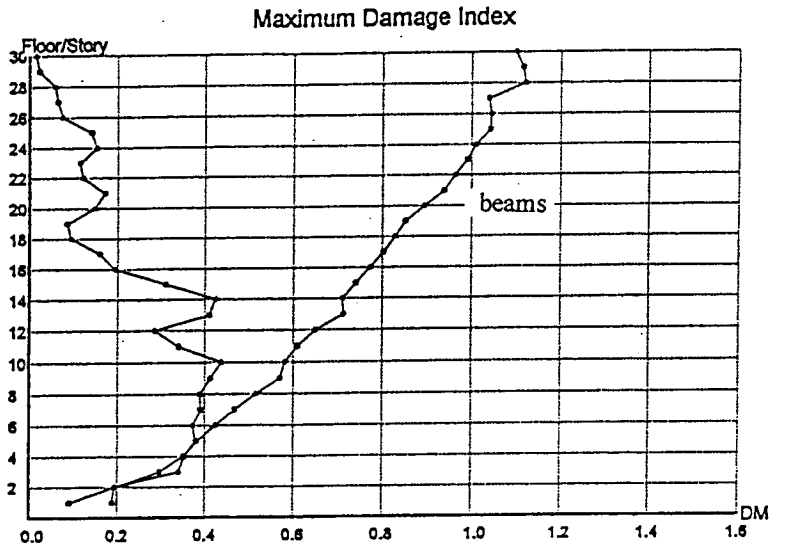

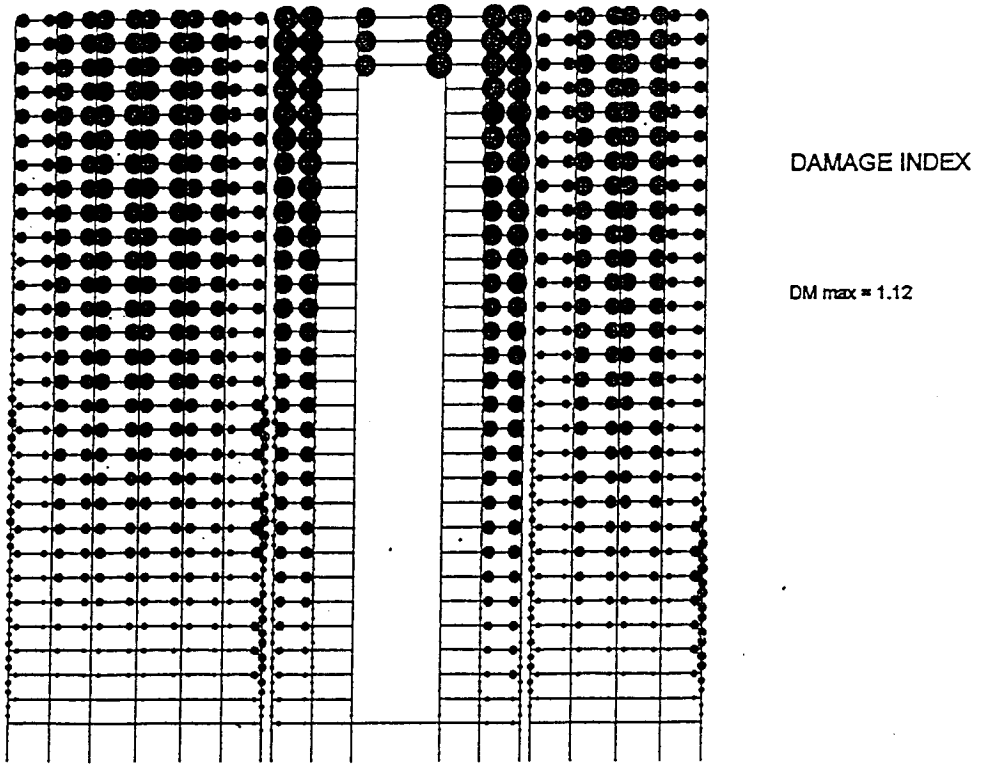

Figure 6.3.4 Damage Index, Single Shear Wall

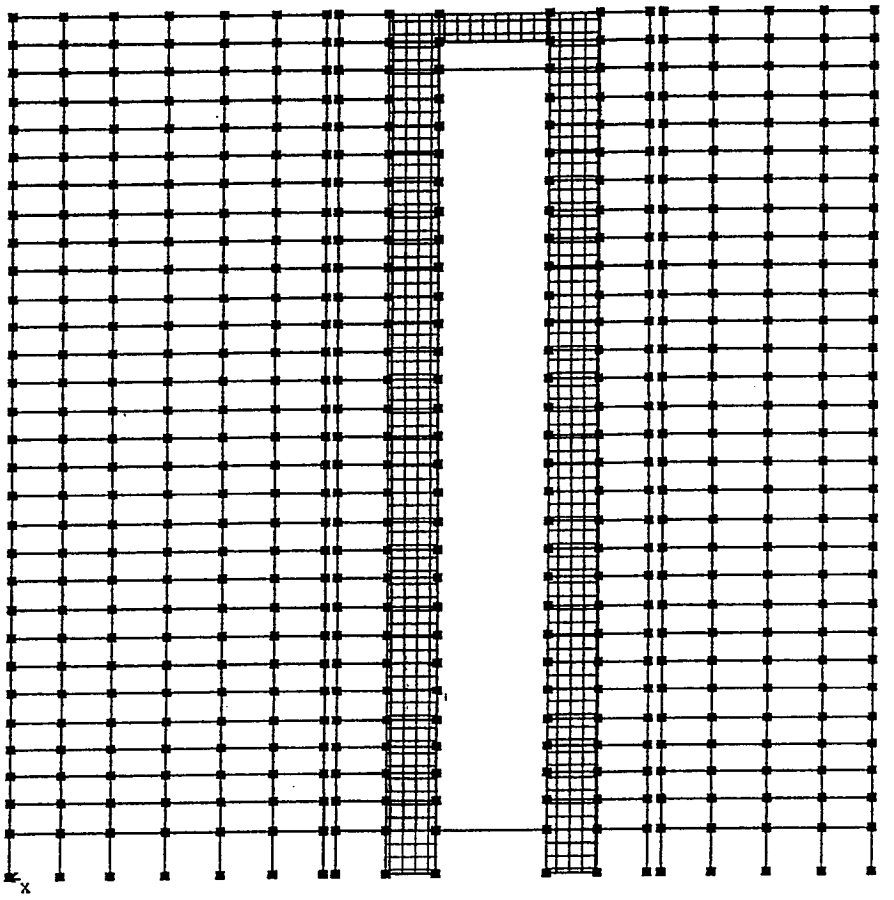

Figure 6.3.5 Retrofitted S-K Redesigned Building, Coupled Shear Walls

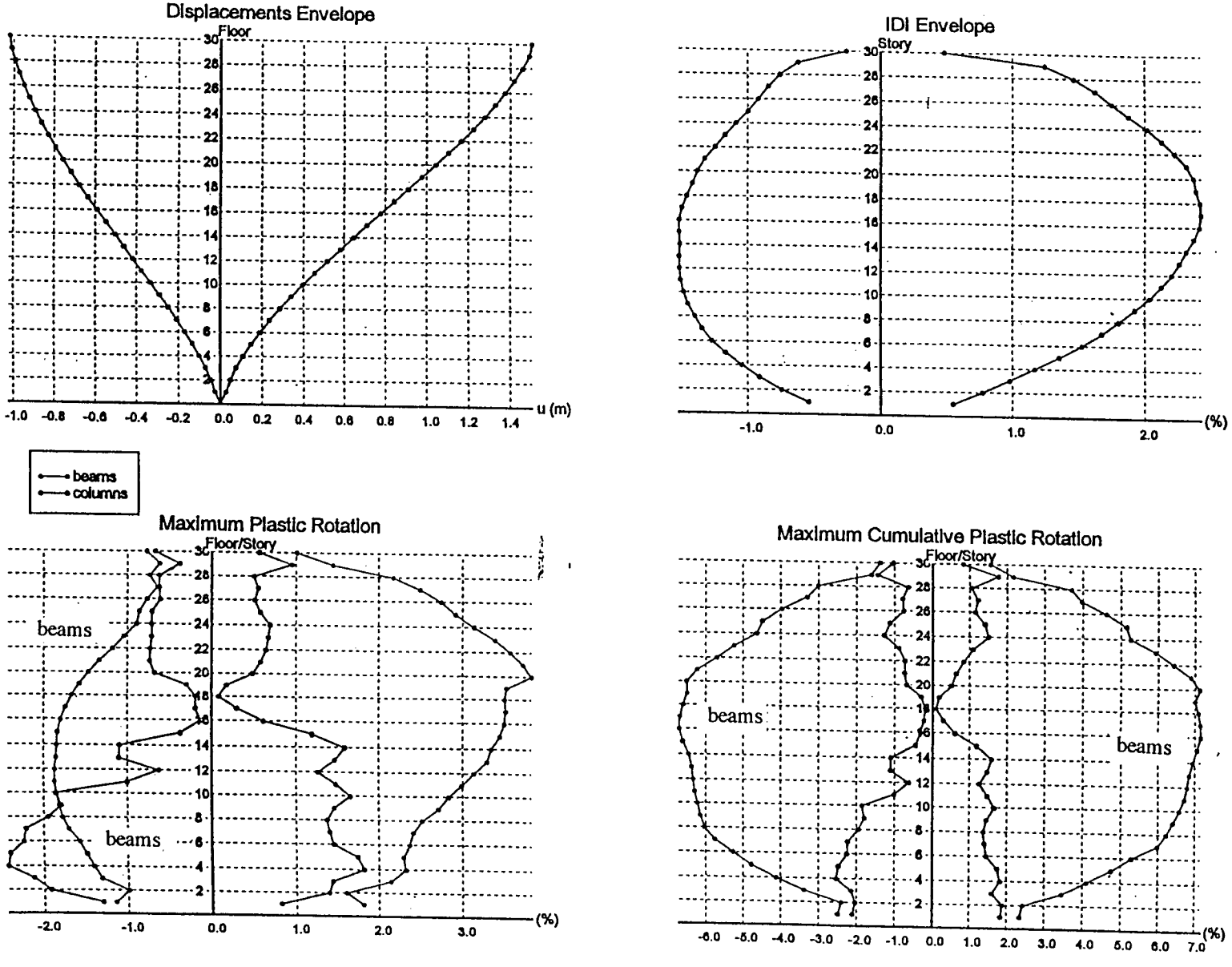

Figure 6.3.6 Response Results, Coupled Shear Wall

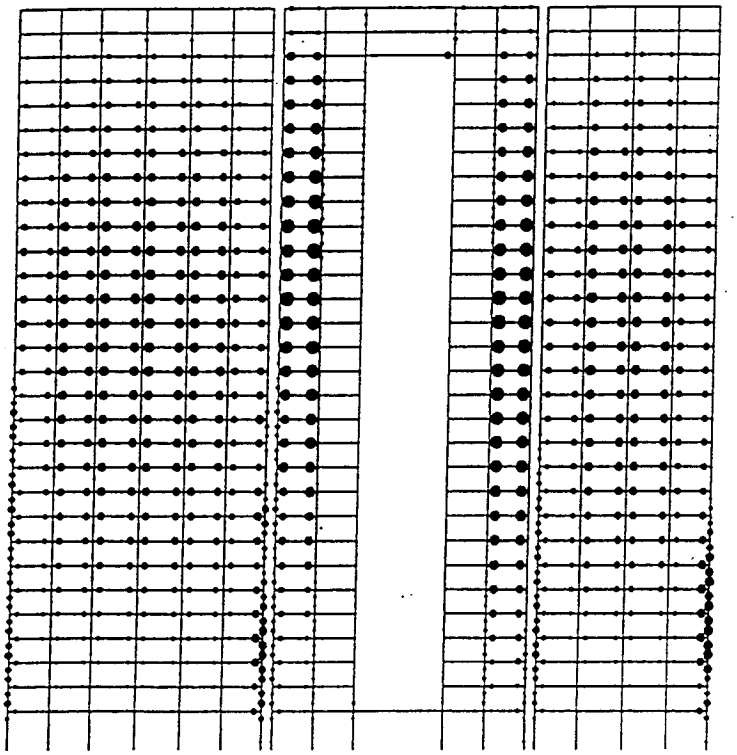

MAXIMUM PLASTIC ROTATION

θmax (beams) = 0.0382

θmax (columns) = 0.0243

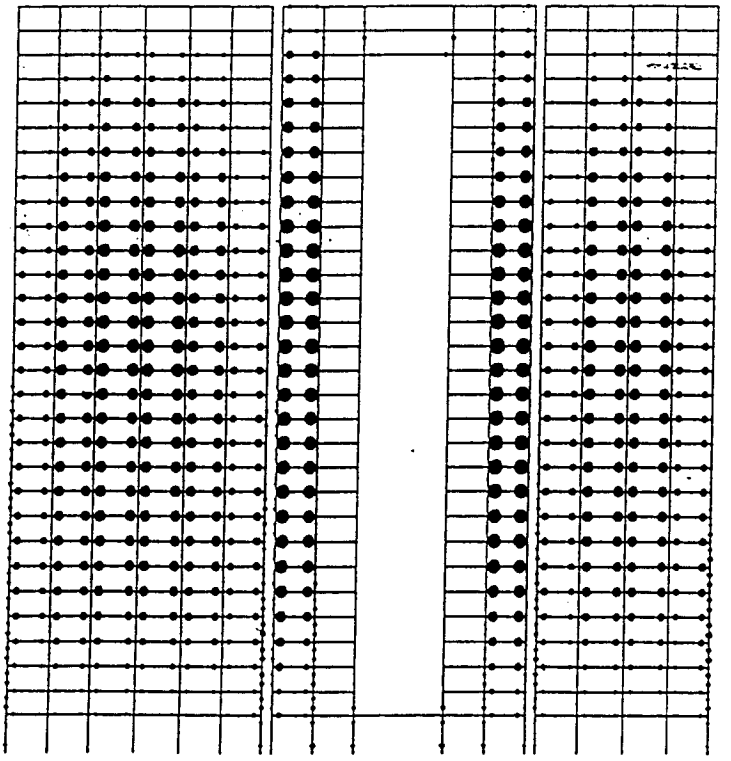

CUMULATIVE PLASTIC ROTATION

θcum (beams) = 0.0716

θcum (columns) = 0.0253

Figure 6.3.7 Plastic Rotation Demands, Coupled Shear Walls

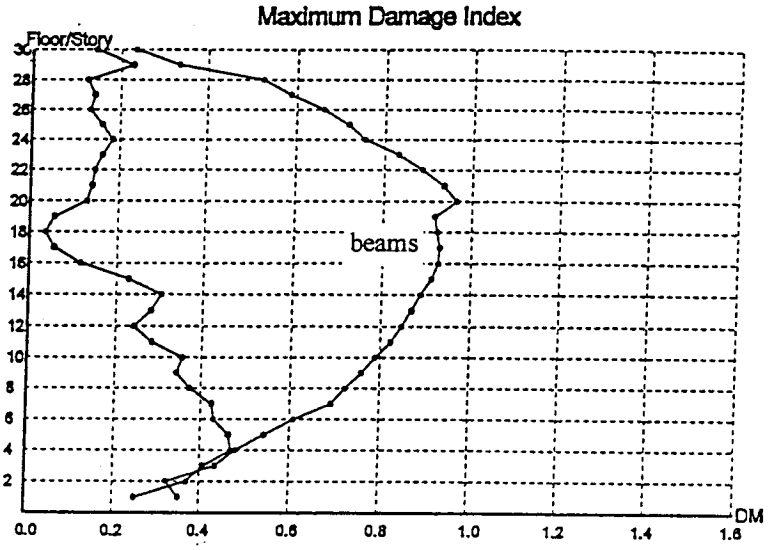

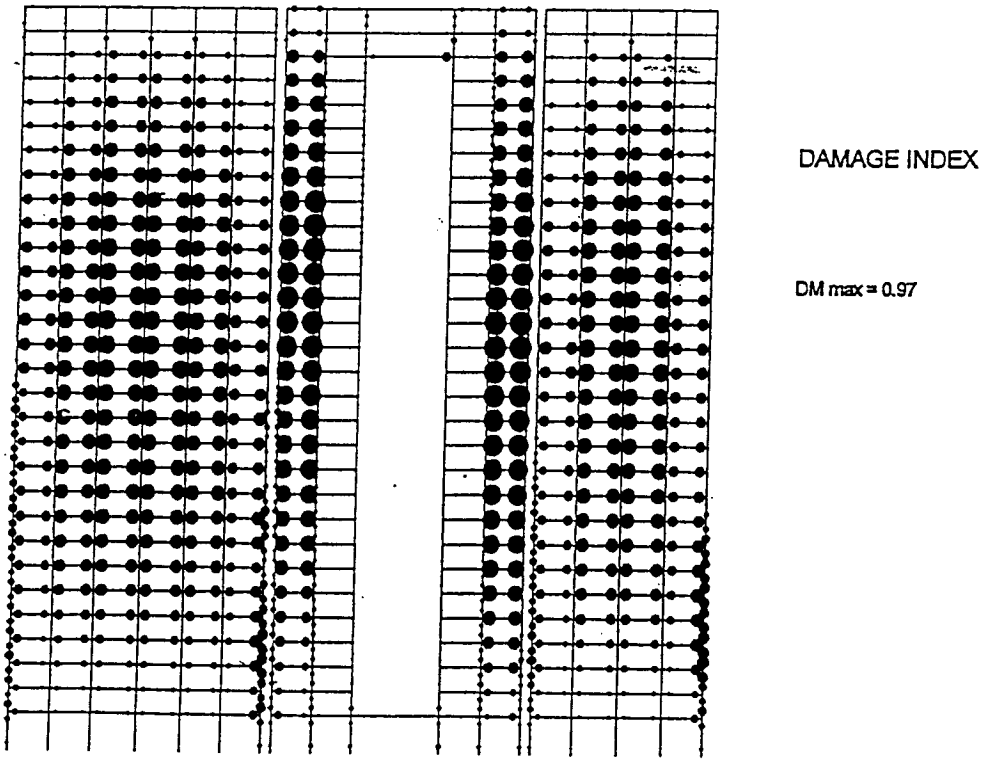

Figure 6.3.8 Damage Index, Coupled Shear Walls

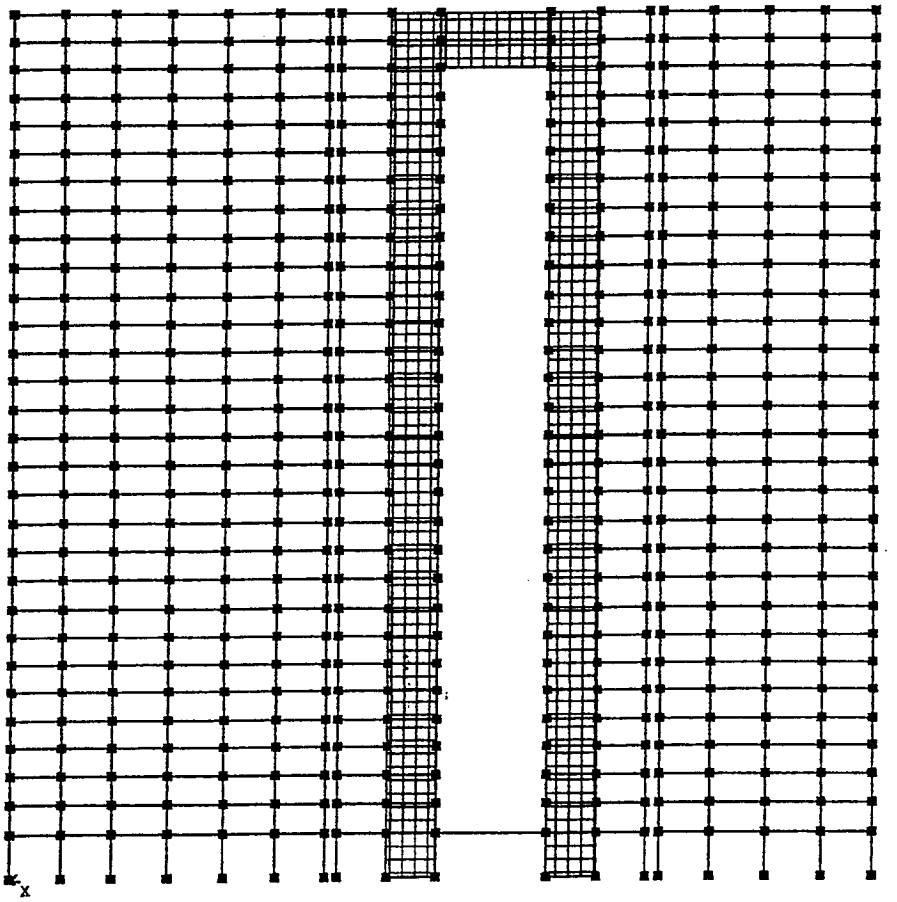

Figure 6.3.9 Retrofitted S-K Redesigned Building, Coupled Shear Walls, Top

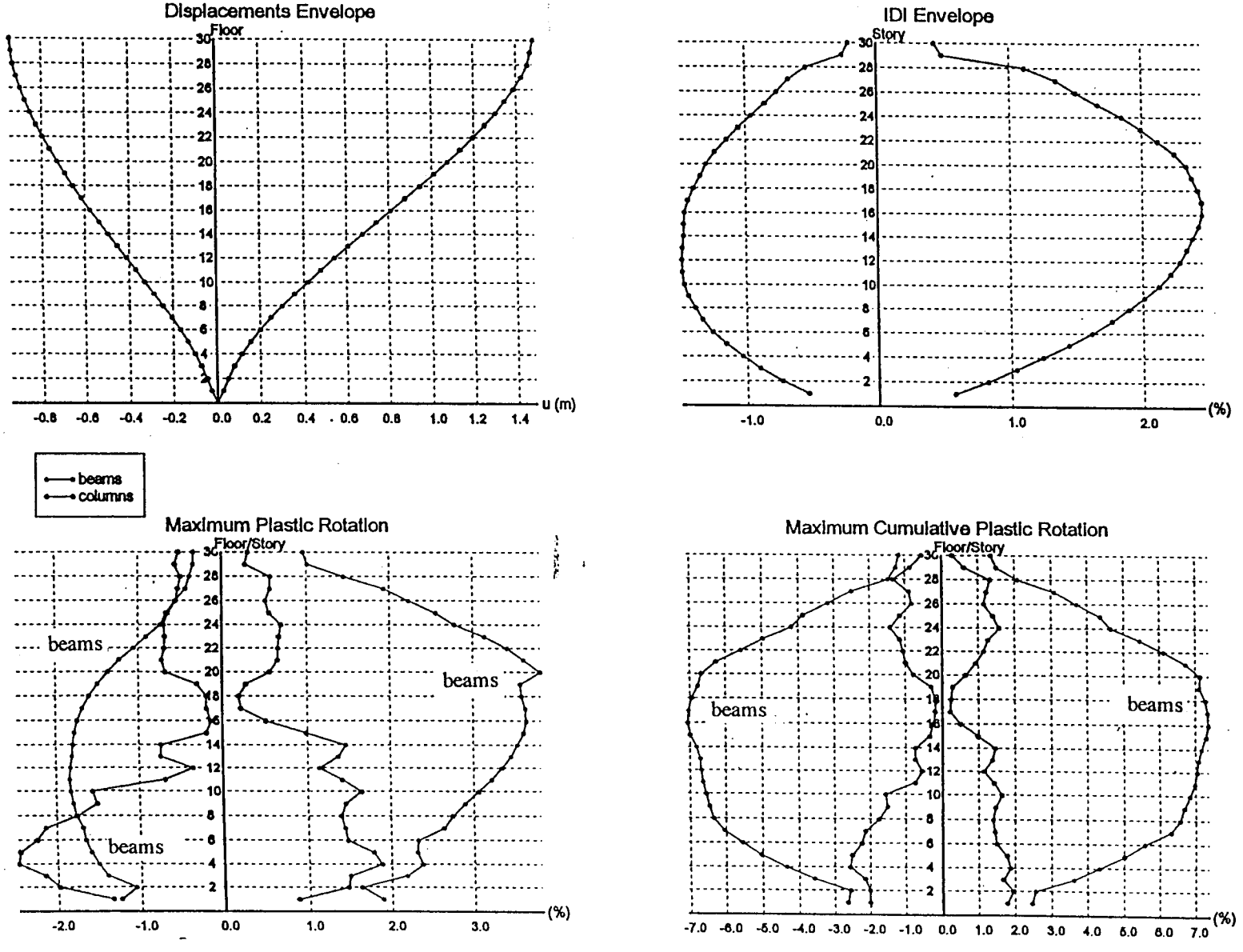

Figure 6.3.10 Response Results, Top Coupled Shear Walls

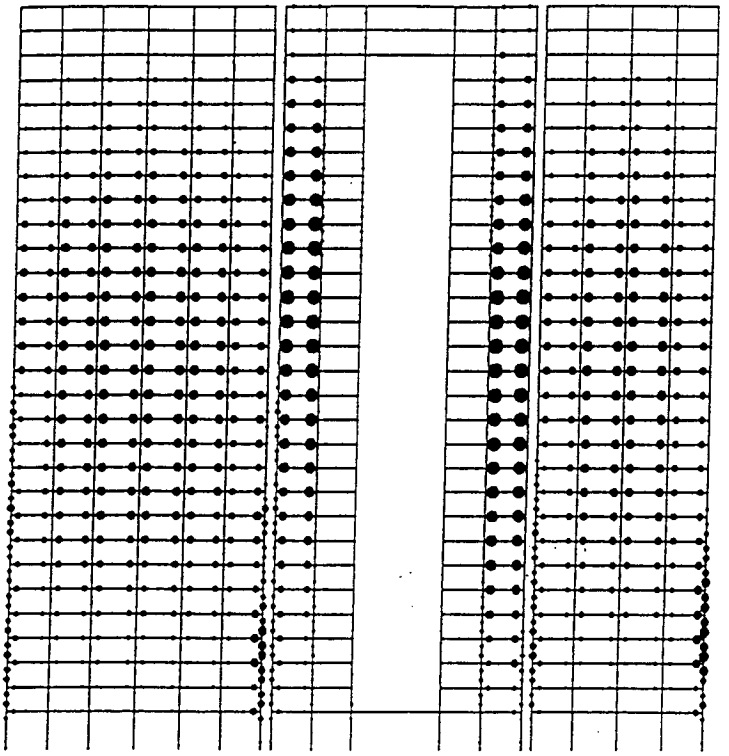

MAXIMUM PLASTIC ROTATION

θmax (beams) = 0.0381

θmax (columns) = 0.0247

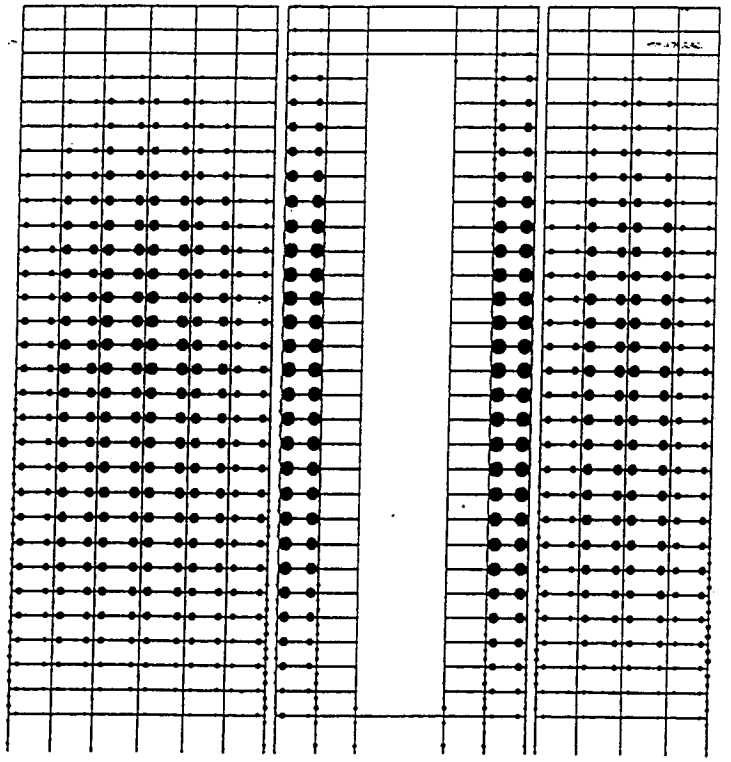

CUMULATIVE PLASTIC ROTATION

θcum (beams) = 0.0737

θcum (columns) = 0.0256

Figure 6.3.11 Plastic Rotation Demands, Top Coupled Shear Walls

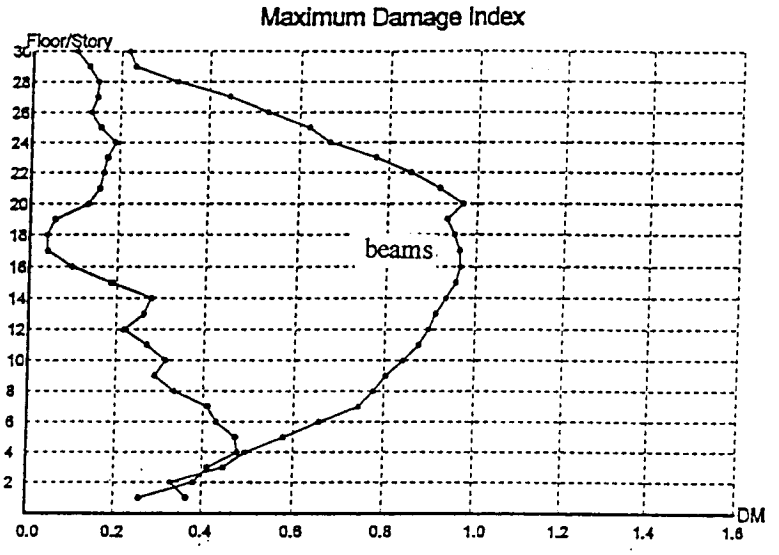

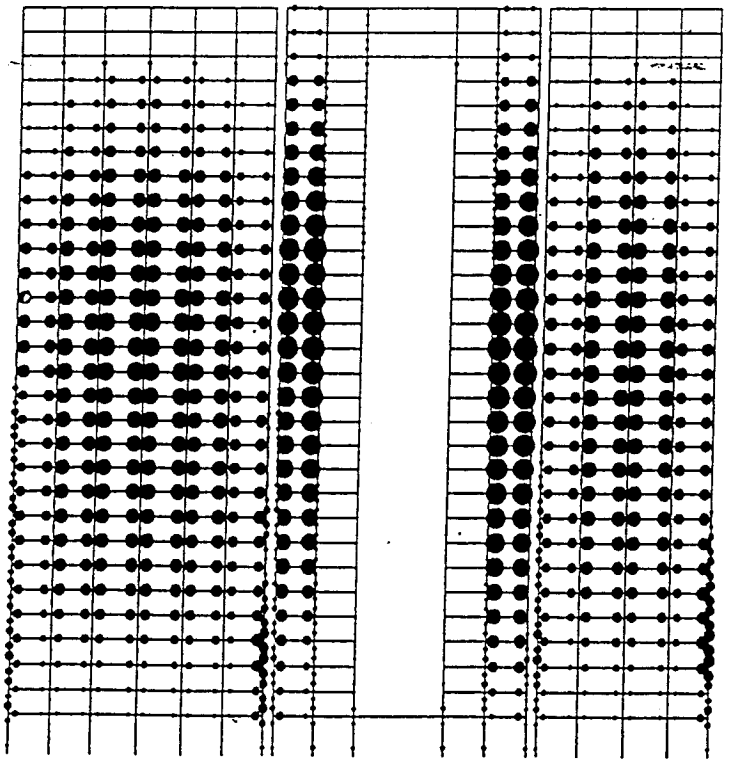

DAMAGE INDEX

DM max = 0.97

Figure 6.3.12 Damage Index, Top Coupled Shear Walls

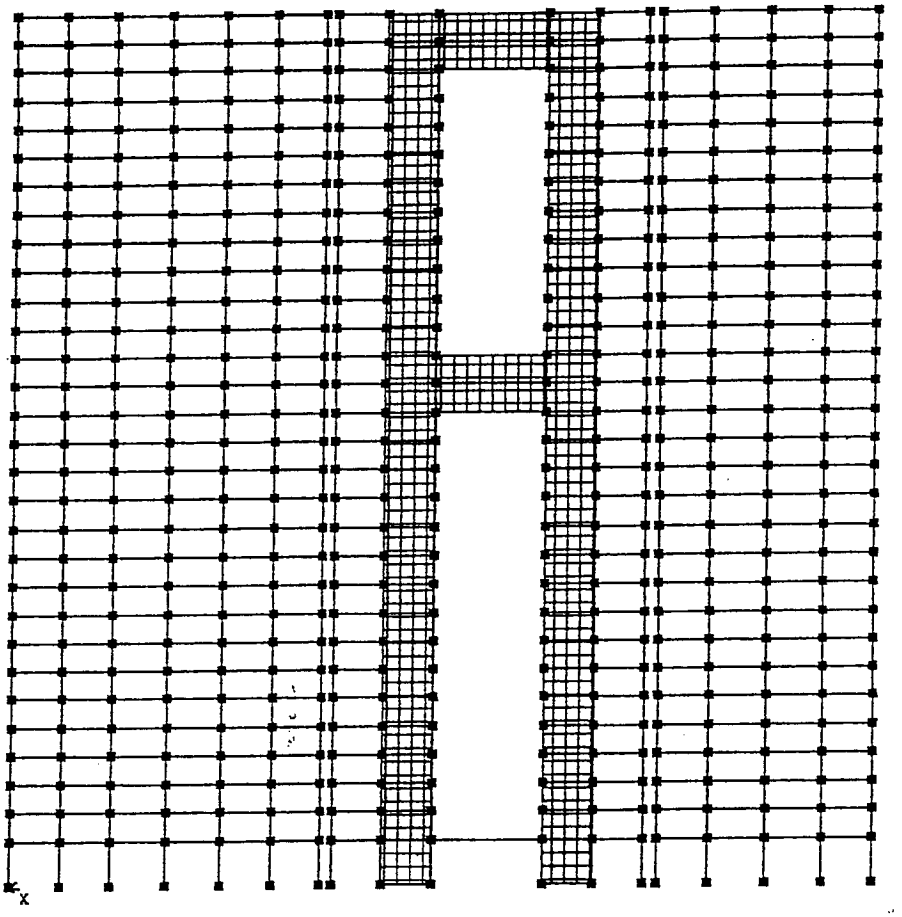

Figure 6.3.13 Retrofitted S-K Redesigned Building, Mid-height and Top Coupled Shear Walls

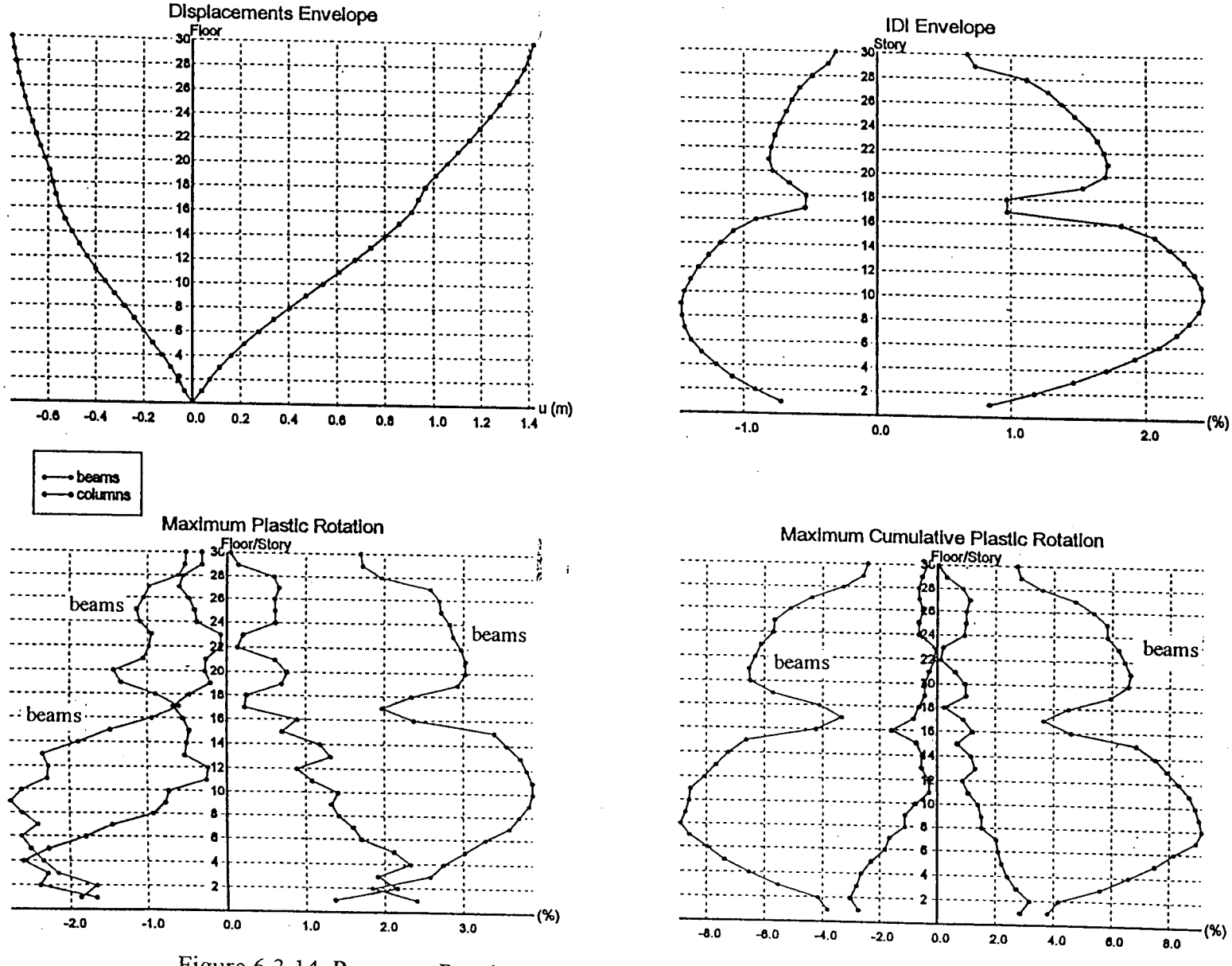

Figure 6.3.14 Response Results, Mid-height and Top Coupled Shear Walls

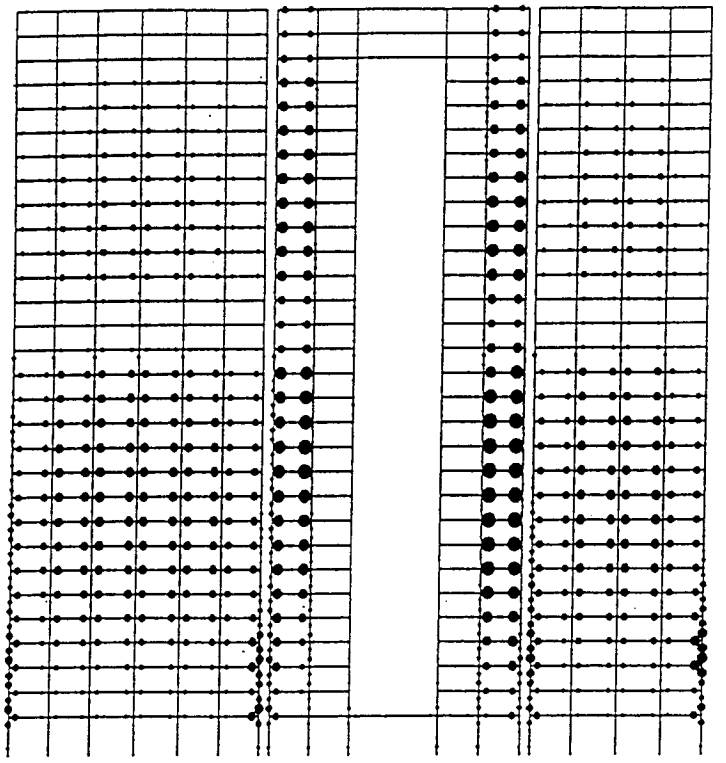

MAXIMUM PLASTIC ROTATION

θmax (beams) = 0.0389

θmax (columns) = 0.0259

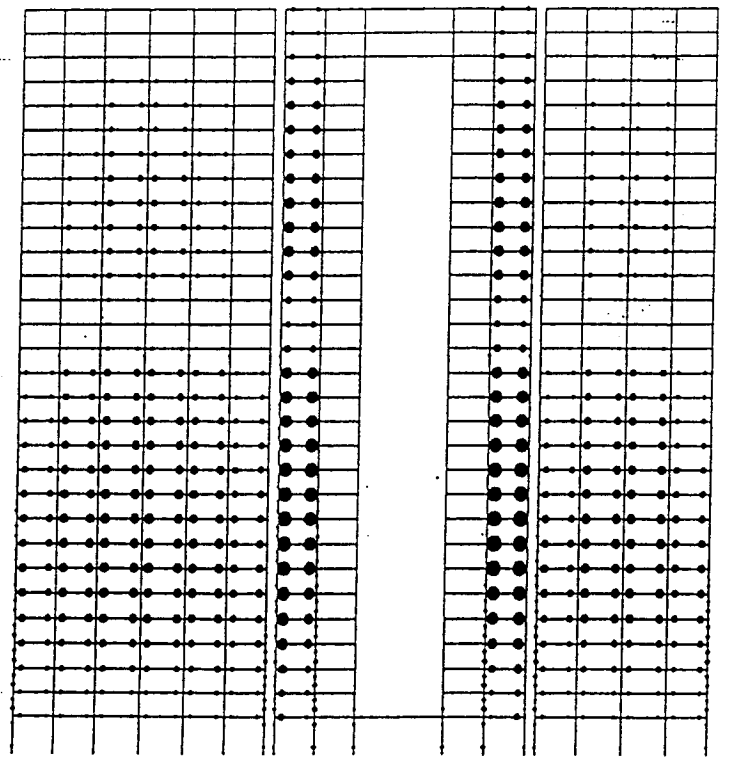

CUMULATIVE PLASTIC ROTATION

θcum (beams) = 0.0912

θcum (columns) = 0.0318

Figure 6.3.15 Plastic Rotation Demands, Mid-height and Top Coupled Walls

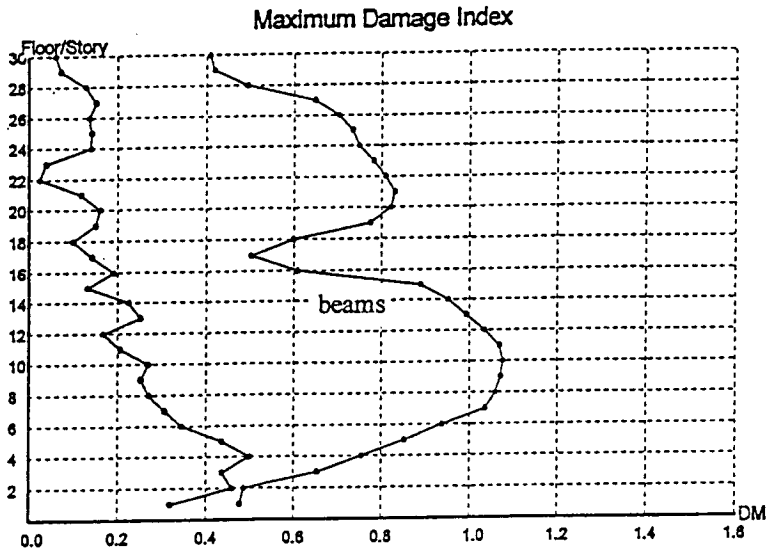

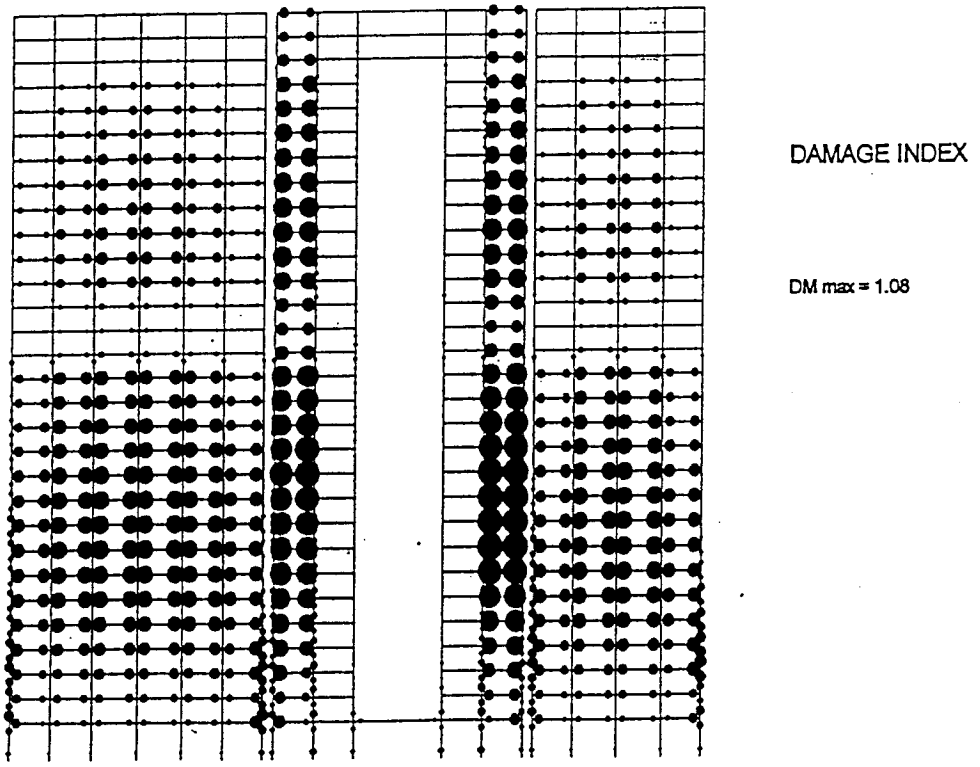

Figure 6.3.16 Damage Index, Mid-height and Top Coupled Shear Walls

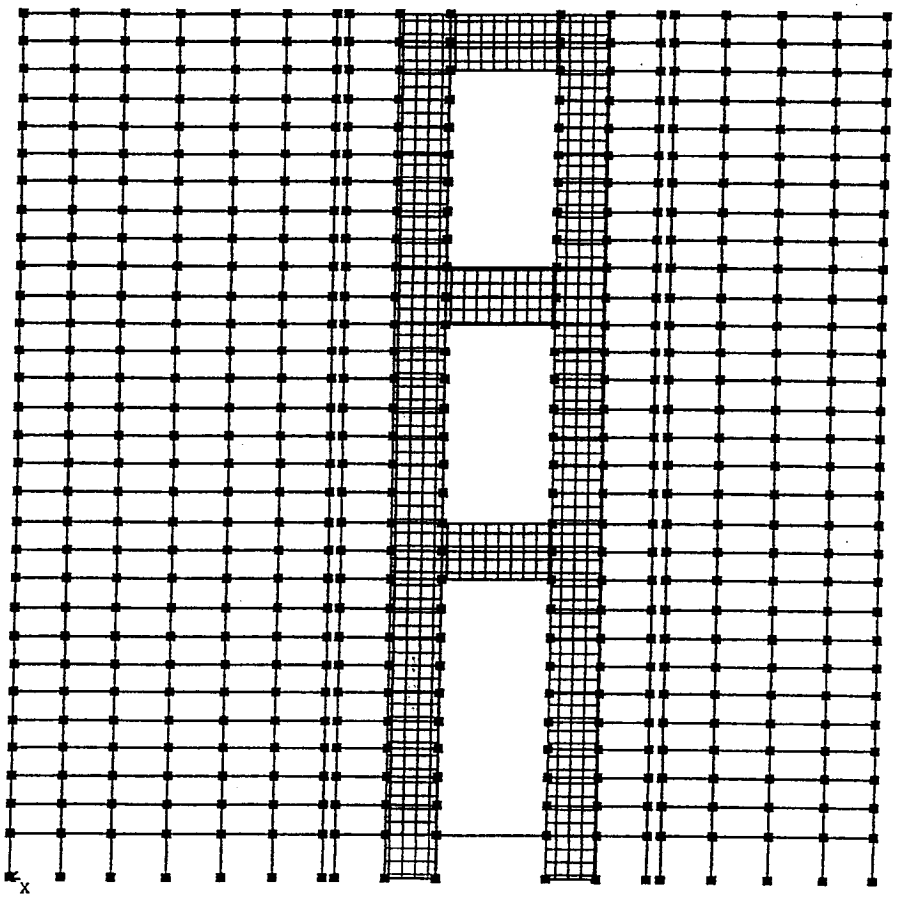

Figure 6.3.17 Retrofitted S-K Redesigned Building, Third Point Coupled Shear Walls

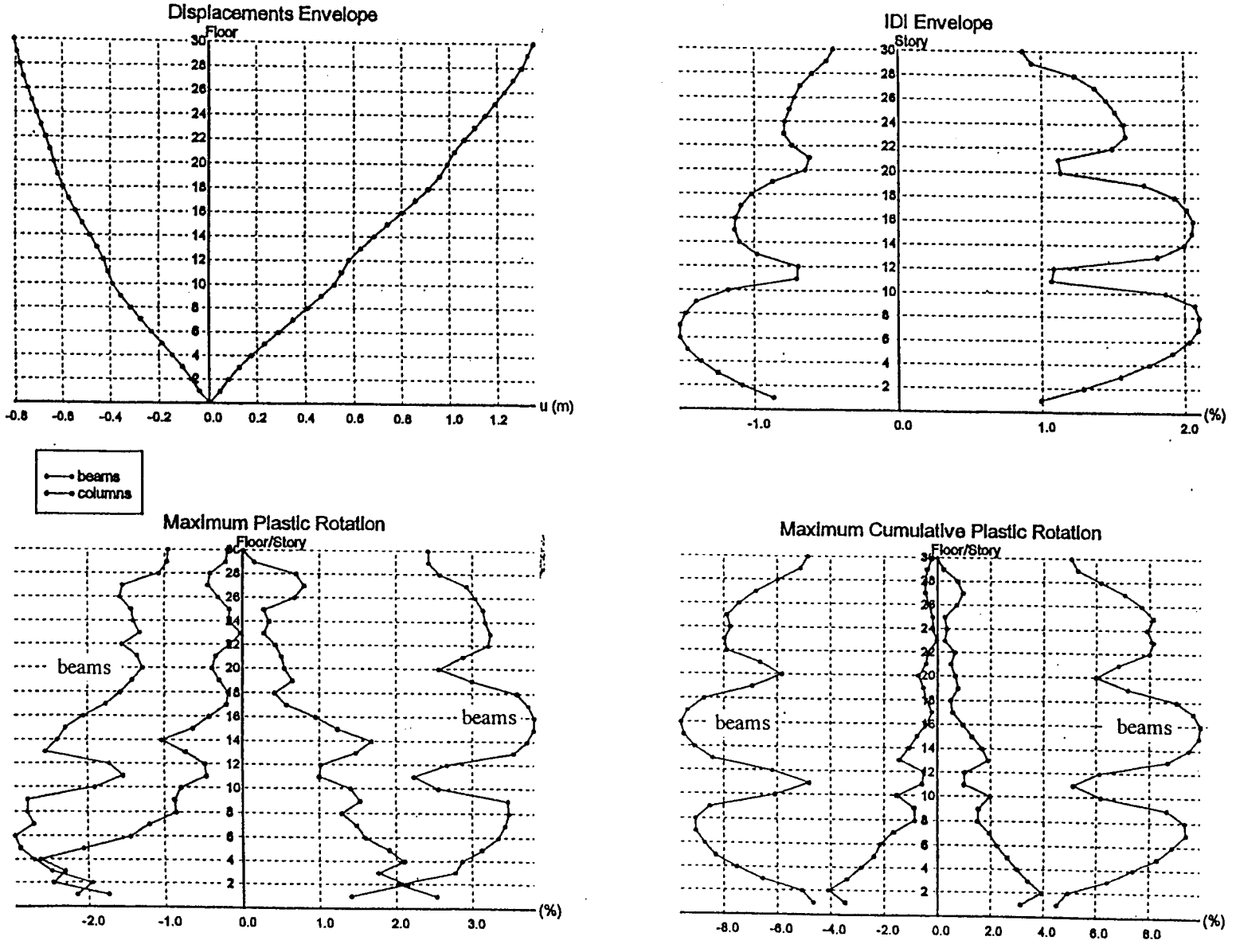

Figure 6.3.18 Response Results, Third Point Coupled Shear Walls

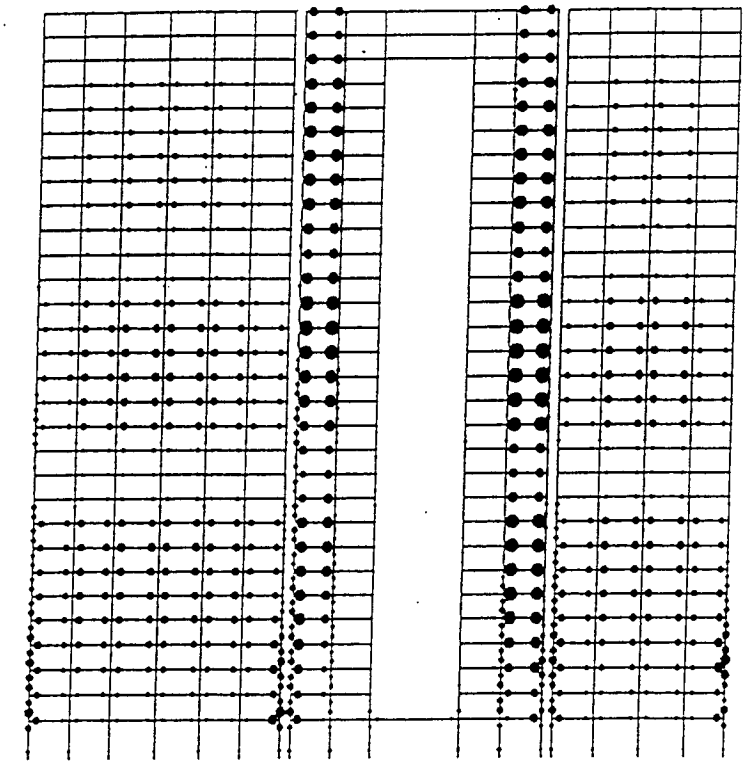

MAXIMUM PLASTIC ROTATION

θmax (beams) = 0.0381

θmax (columns) = 0.0265

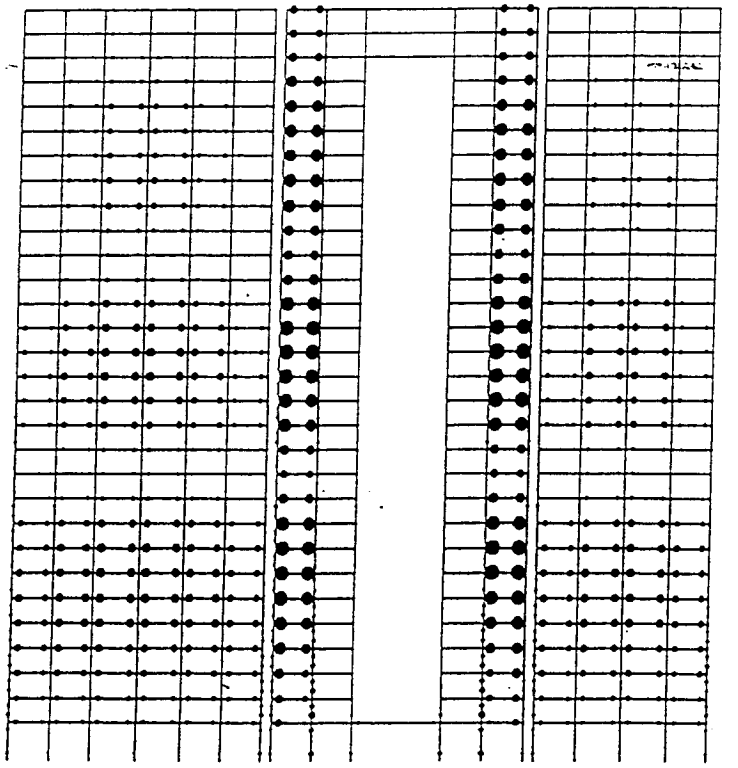

CUMULATIVE PLASTIC ROTATION

θcum (beams) = 0.0991

θcum (columns) = 0.0407

Figure 6.3.19 Plastic Rotation Demands, Third Point Coupled Shear Walls

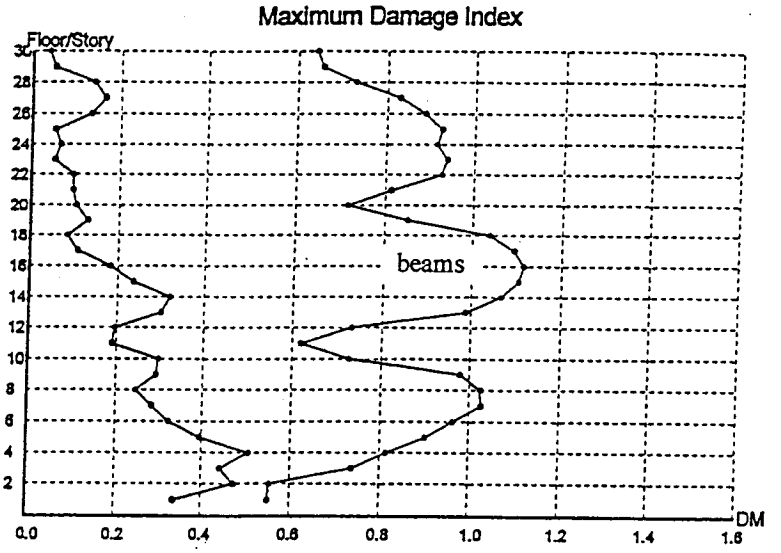

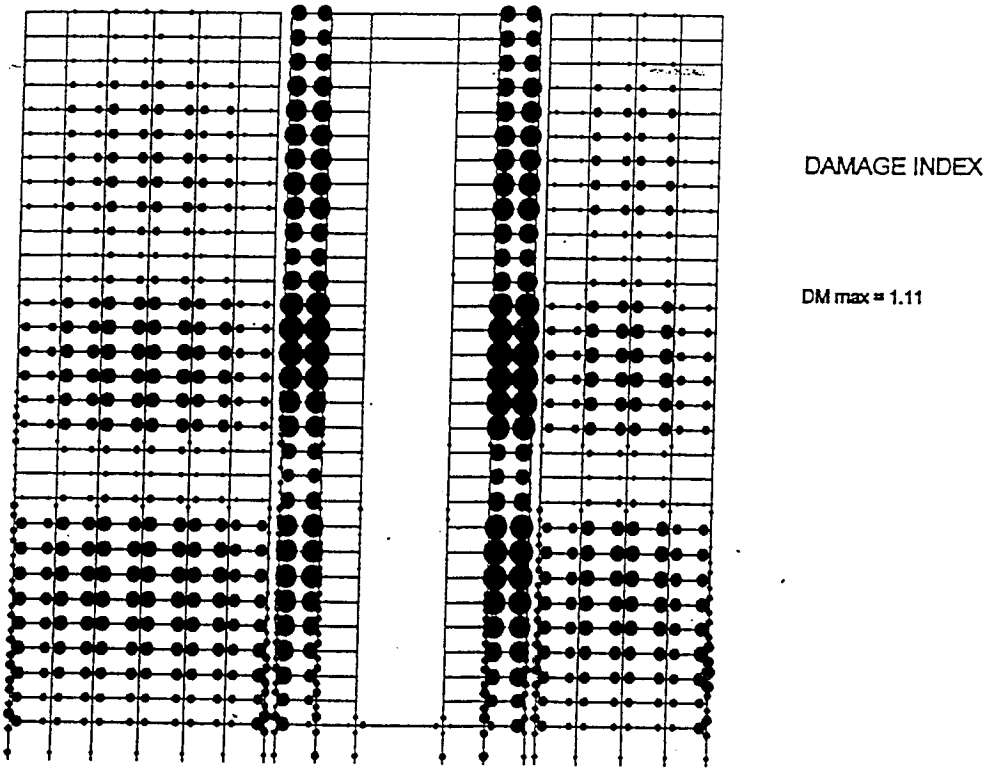

Figure 6.3.20 Damage Index, Third Point Coupled Shear Walls

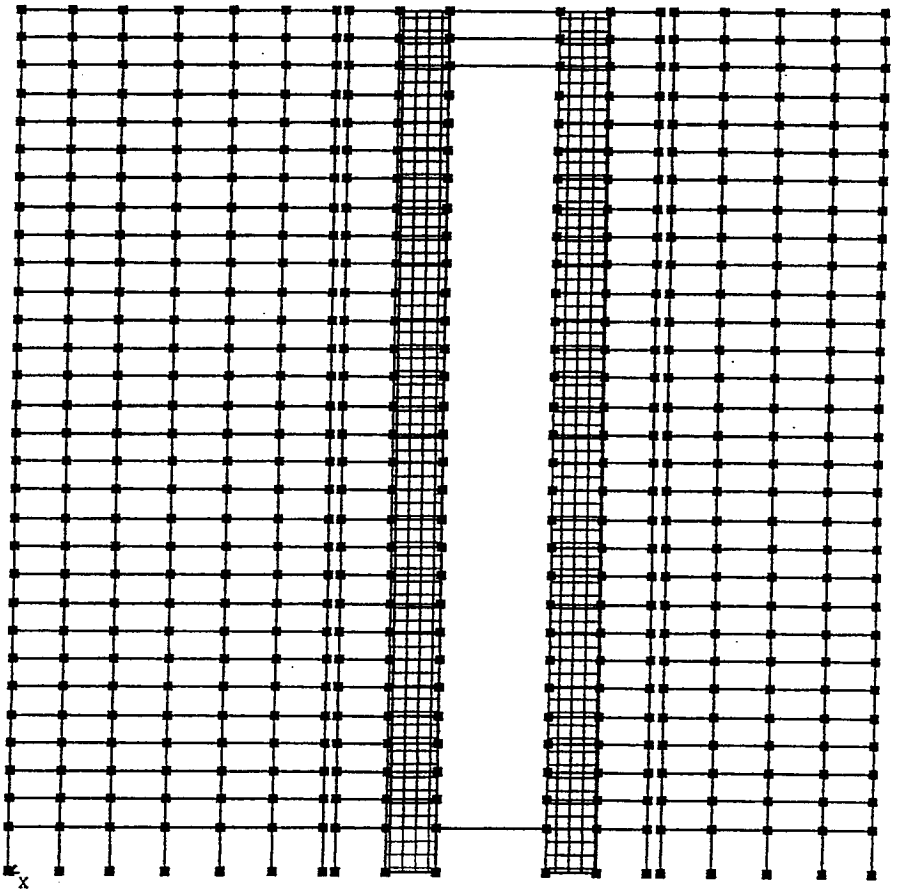

Figure 6.3.21 Retrofitted S-K Redesigned Building, Single Shear Walls, ξ=30%

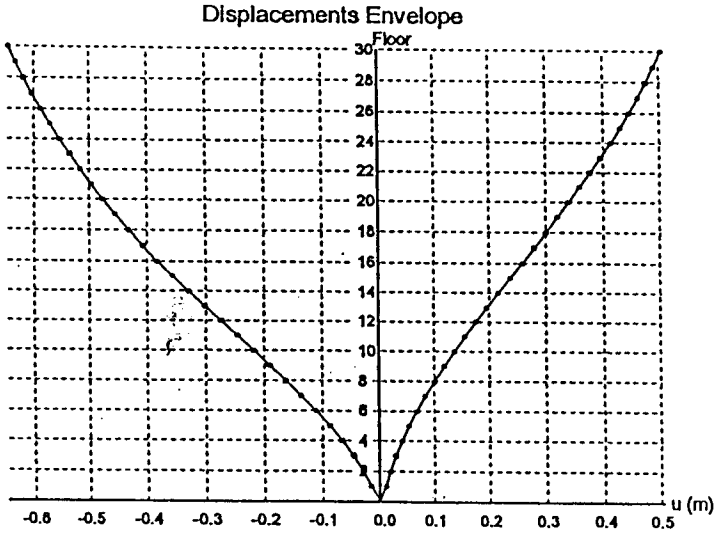

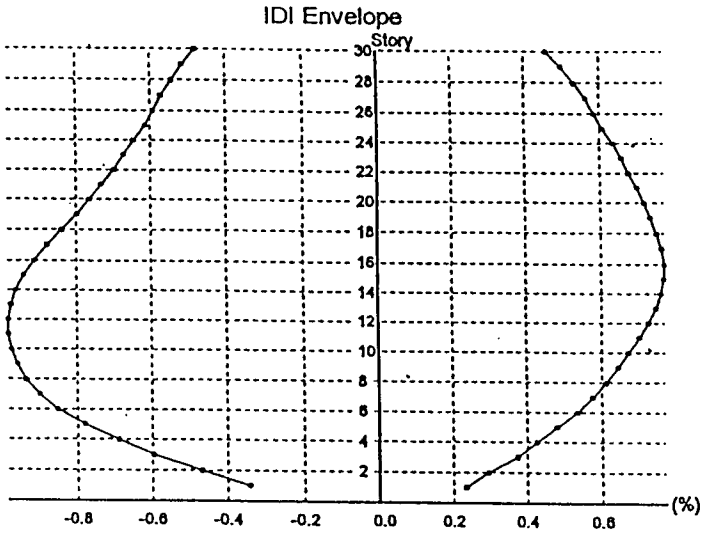

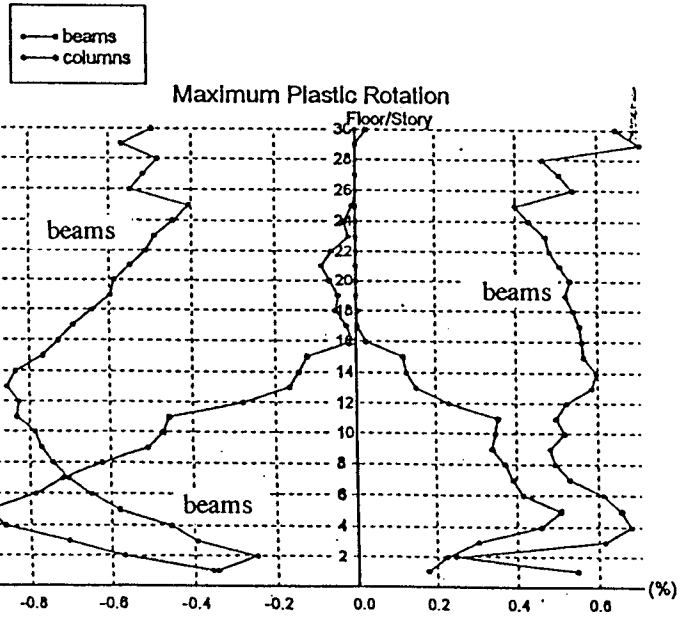

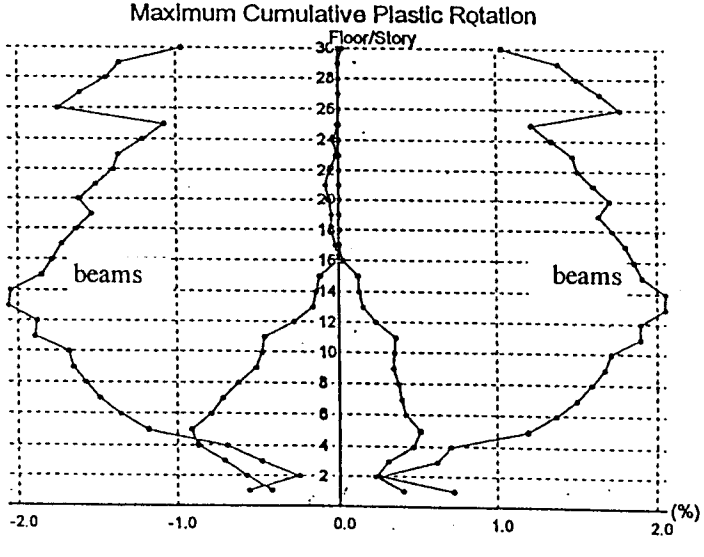

Figure 6.3.22 Response Results, Single Shear Walls, ξ=30%

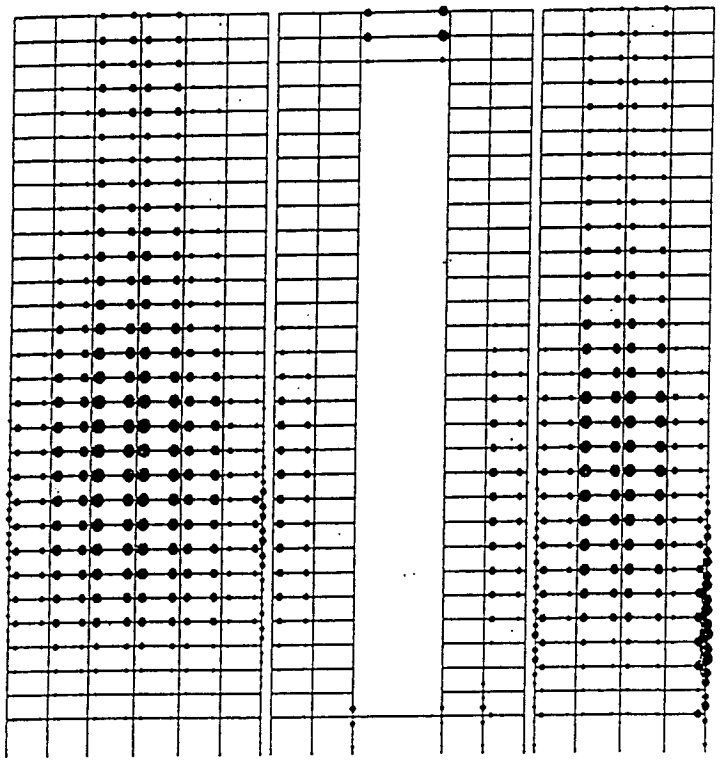

MAXIMUM PLASTIC ROTATION

θmax (beams) = 0.0086

θmax (columns) = 0.0091

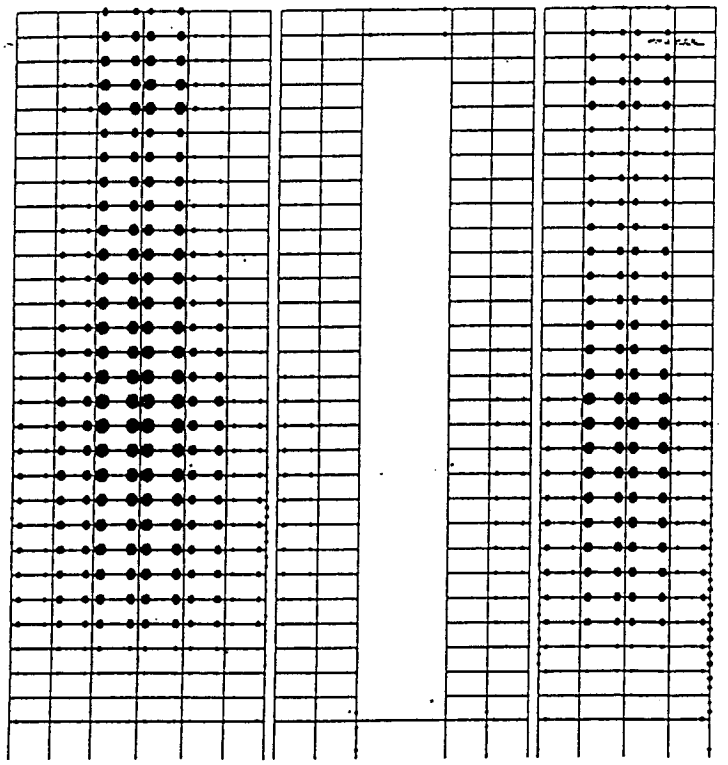

CUMULATIVE PLASTIC ROTATION

θcum (beams) = 0.0206

θcum (columns) = 0.0091

Figure 6.3.23 Plastic Rotation Demands, Single Shear Walls, ξ=30%

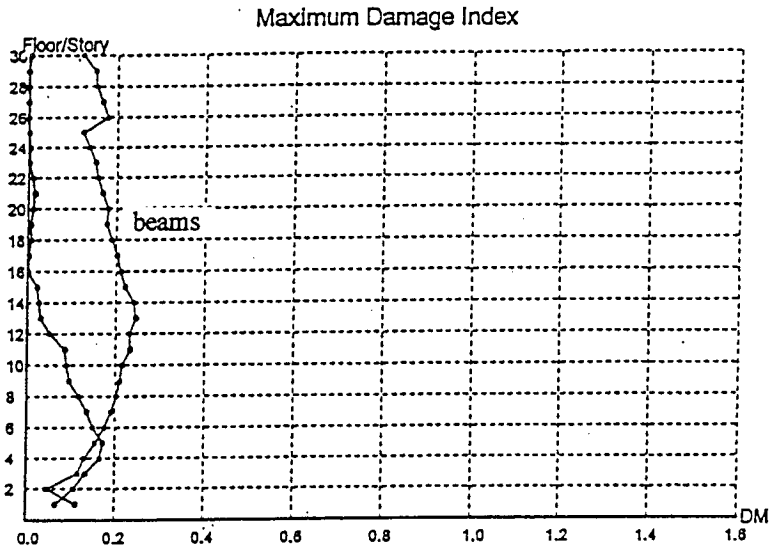

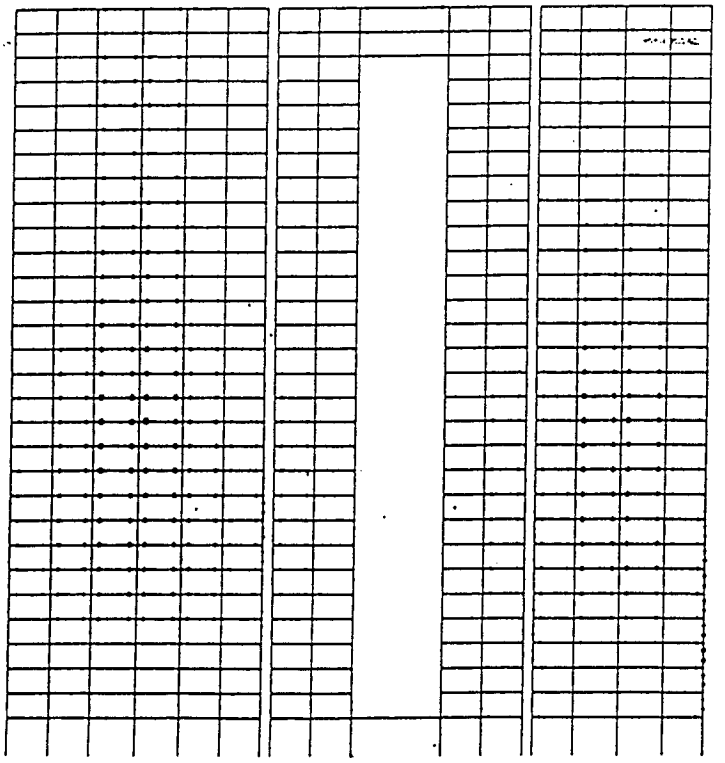

DAMAGE INDEX

DM max = 0.25

Figure 6.3.24 Damage Index, Single Shear Walls, ξ=30%

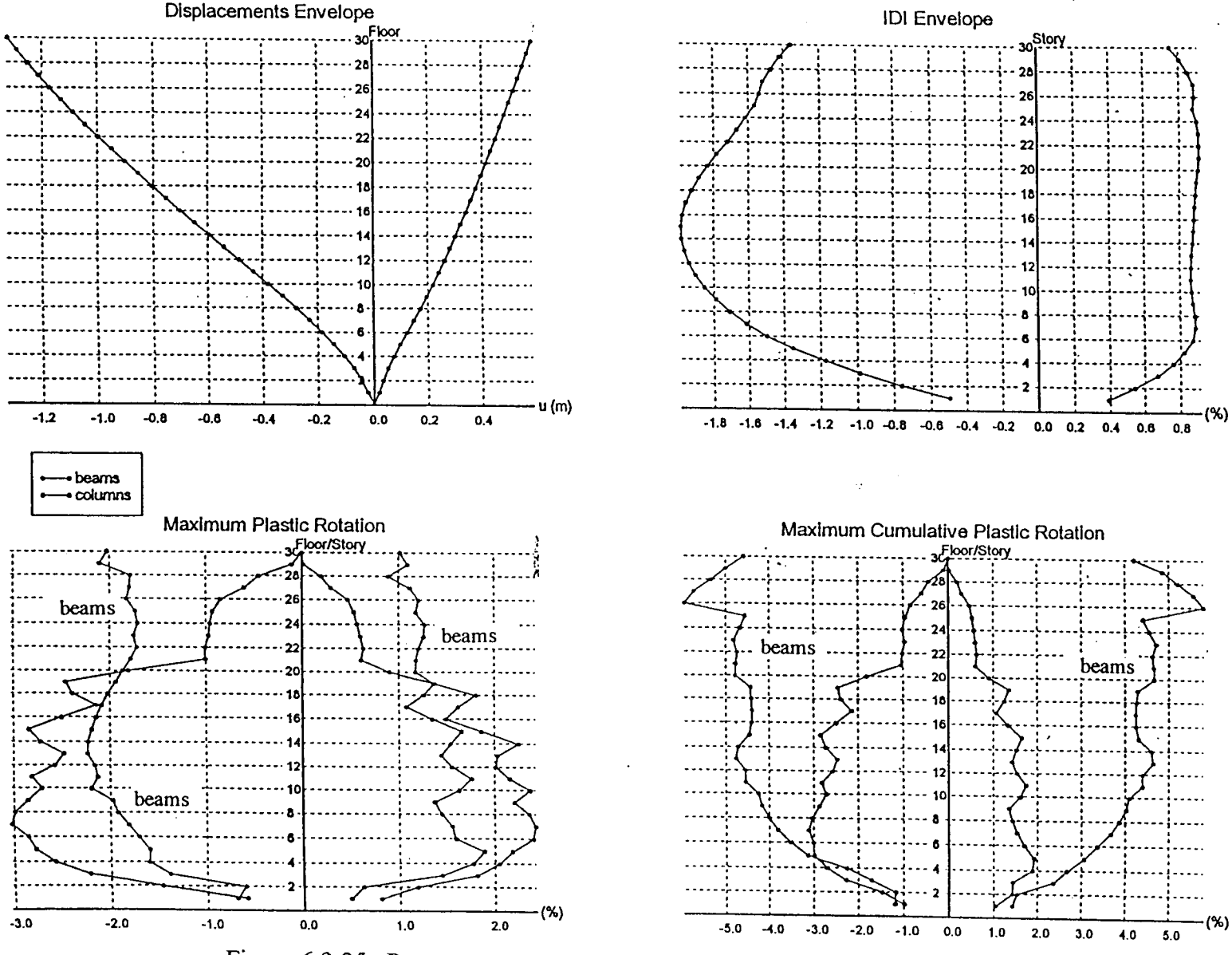

Figure 6.3.25 Response Results, Single Shear Walls, ξ=5%

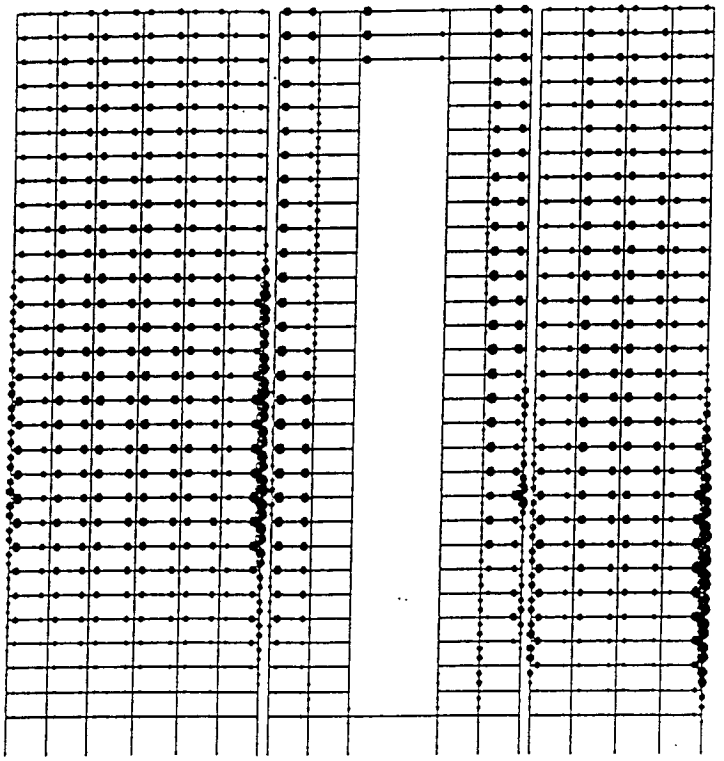

MAXIMUM PLASTIC ROTATION

θmax (beams) = 0.0244

θmax (columns) = 0.0302

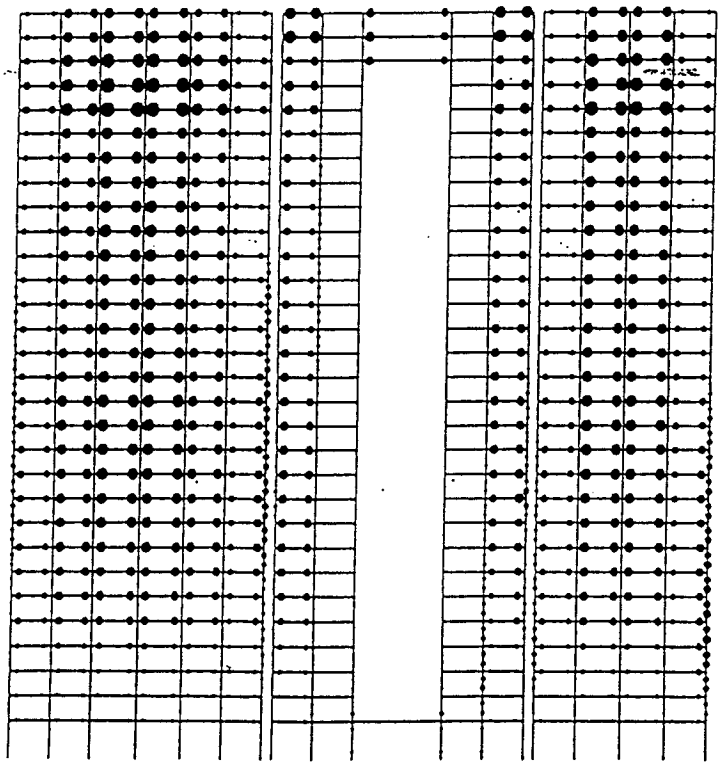

CUMULATIVE PLASTIC ROTATION

θcum (beams) = 0.0594

θcum (columns) = 0.0311

Figure 6.3.26 Plastic Rotation Demands, Single Shear Walls, ξ=5%

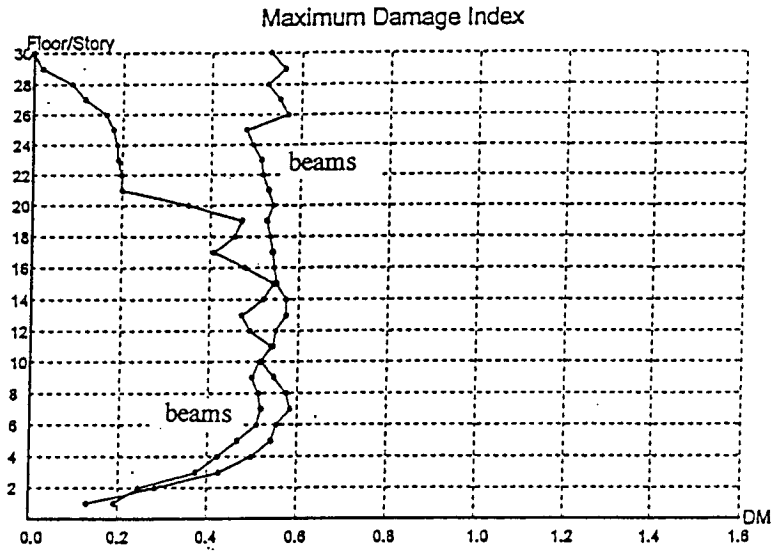

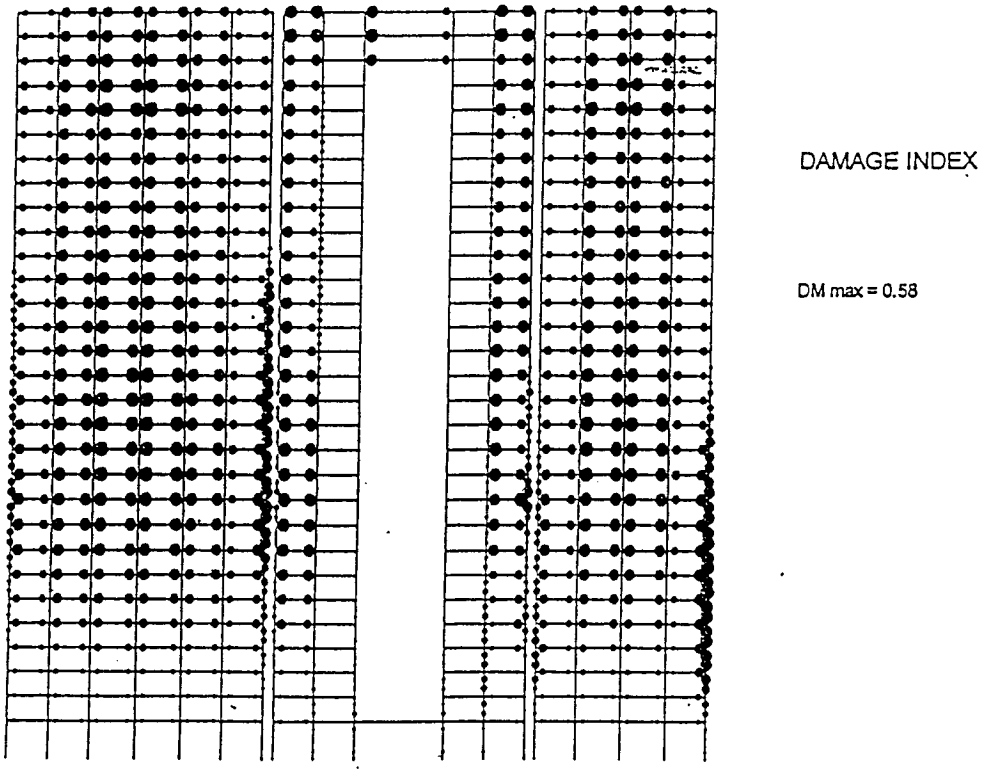

Figure 6.3.27 Damage Index, Single Shear Walls, ξ=5%

6.4 RETROFIT OF THE S-K BUILDING (AS BUILT)

Due to the results obtained for the S-K Building (Conceptual Design) it was decided to abandon the conventional retrofit procedure and go directly to investigating the innovative procedure using supplemental damping to obtain ξ_{eff} = 30%. The analytical model for this building is shown in **Figure 6.4.1.** As described in Section 5.3, and illustrated in **Figures 5.3.2 through 5.3.4**, when this building is subjected to the recorded ***Los Gatos EQGM*** (ξ_{eff} = 5%), the performance is unacceptable because this EQGM demands an IDI of about 3.3% (**Figure 6.4.2**) and a Damage Index of 1.03 in the columns located at the 7th story (**Figure 6.4.4**). Using additional damping for a total ξ_{eff} = 30%, improves the performance of this retrofitted building significantly, as can be seen by comparing the results shown in **Figures 6.4.2 through 6.4.4** with those shown in **Figures 6.4.5 through 6.4.7.** Changes in the maximum values are as follows: (1) the displacement at the roof has been reduced from 1.41m to 0.7m (a reduction of more than 50%); (2) the IDI has been reduced from 3.3% to 1.4% (a reduction of more than 57%); (3) the Plastic Hinge Rotation in the beam has been decreased from 3.8% to 1.3% (a reduction of about 66%); (4) the Cumulative Plastic Rotation in the beams has been reduced by about 62% (from 0.060 to 0.023); and (5) the Damage Index of the beams has been reduced from 1.03 to 0.31 (a reduction of about 70%). An analysis of the maximum demanded values for this retrofitted building (ξ_{eff} = 30%) indicates that considering the maximum value for the IDI as 1.5%, its seismic performance under the most critical recorded pulse-type EQGM (Los Gatos 1) is acceptable.

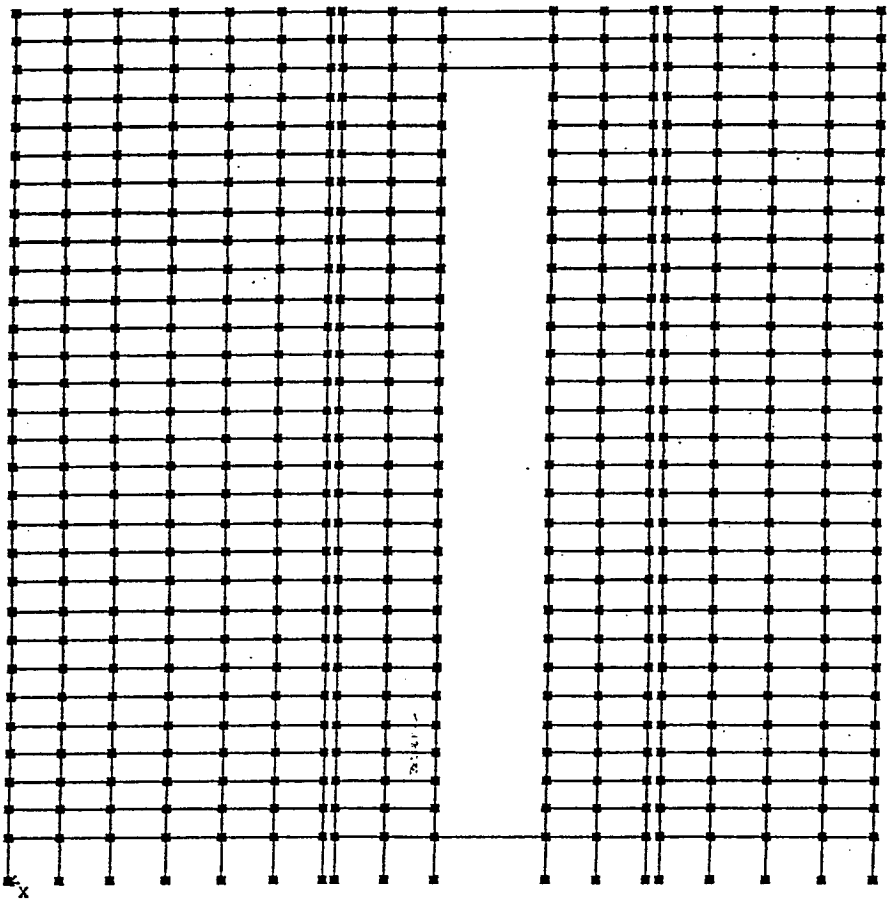

Figure 6.4.1 Model of S-K Building As Built

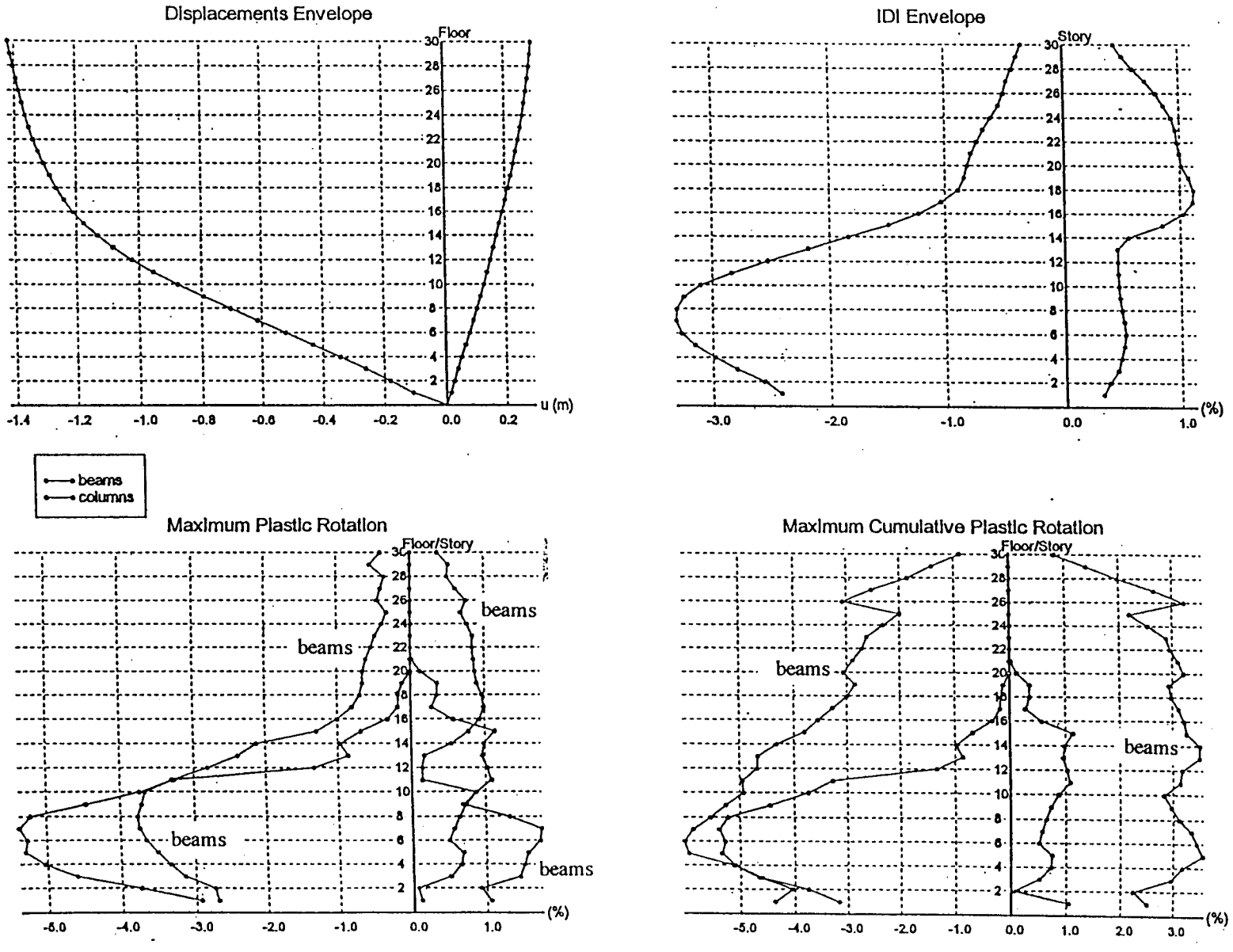

Figure 6.4.2 Response Results, S-K As Built, ξ=5%

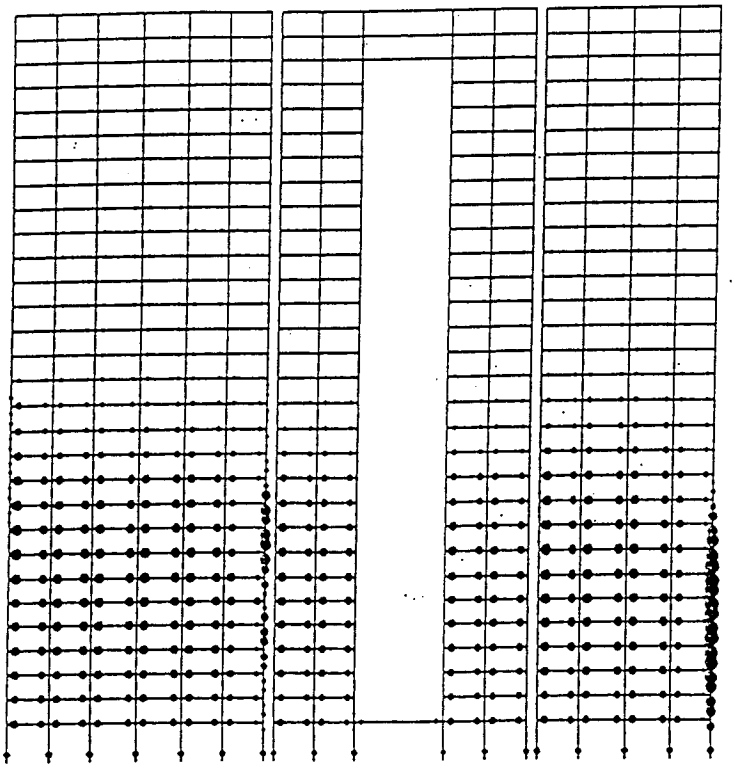

MAXIMUM PLASTIC ROTATION

θmax (beams) = 0.0377

θmax (columns) = 0.0538

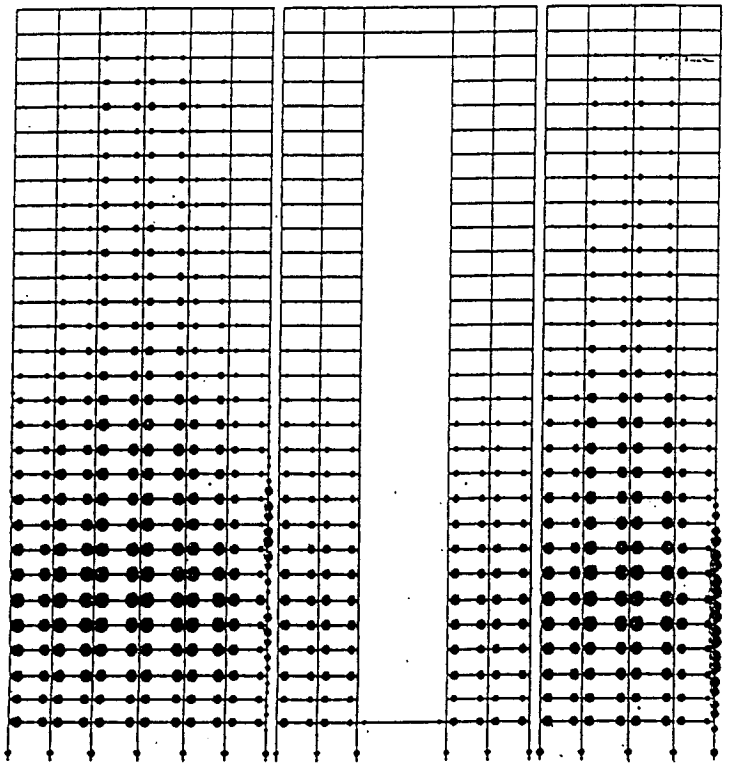

CUMULATIVE PLASTIC ROTATION

θcum (beams) = 0.0599

θcum (columns) = 0.0538

Figure 6.4.3 Plastic Rotation Demands, S-K As Built, ξ=5%

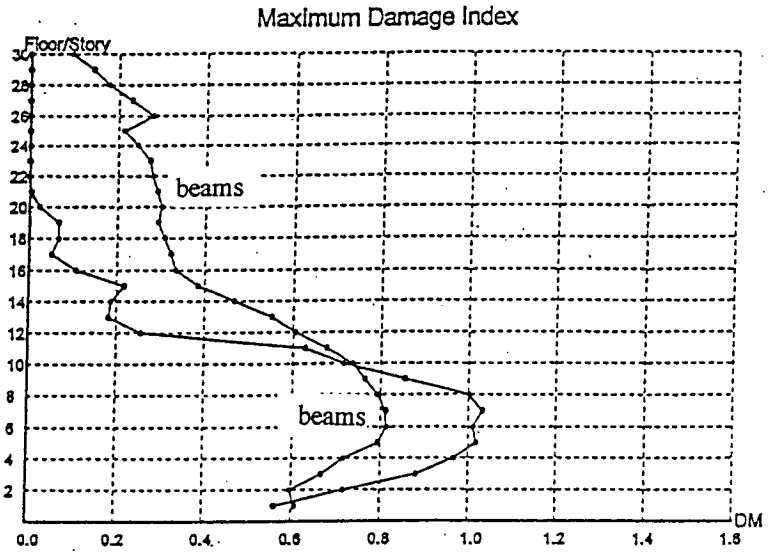

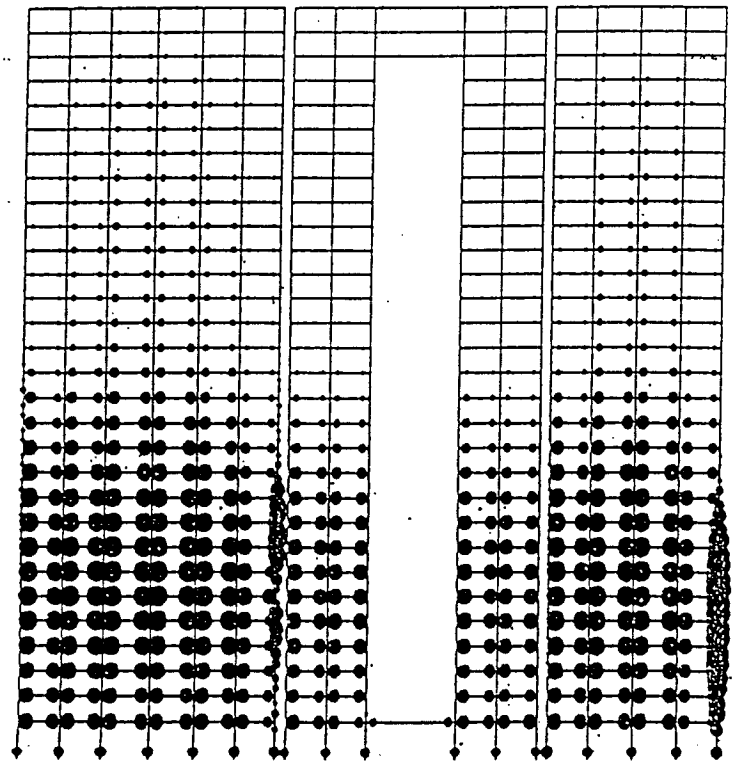

DAMAGE INDEX

DM max = 1.03

Figure 6.4.4 Damage Index, S-K As Built, ξ=5%

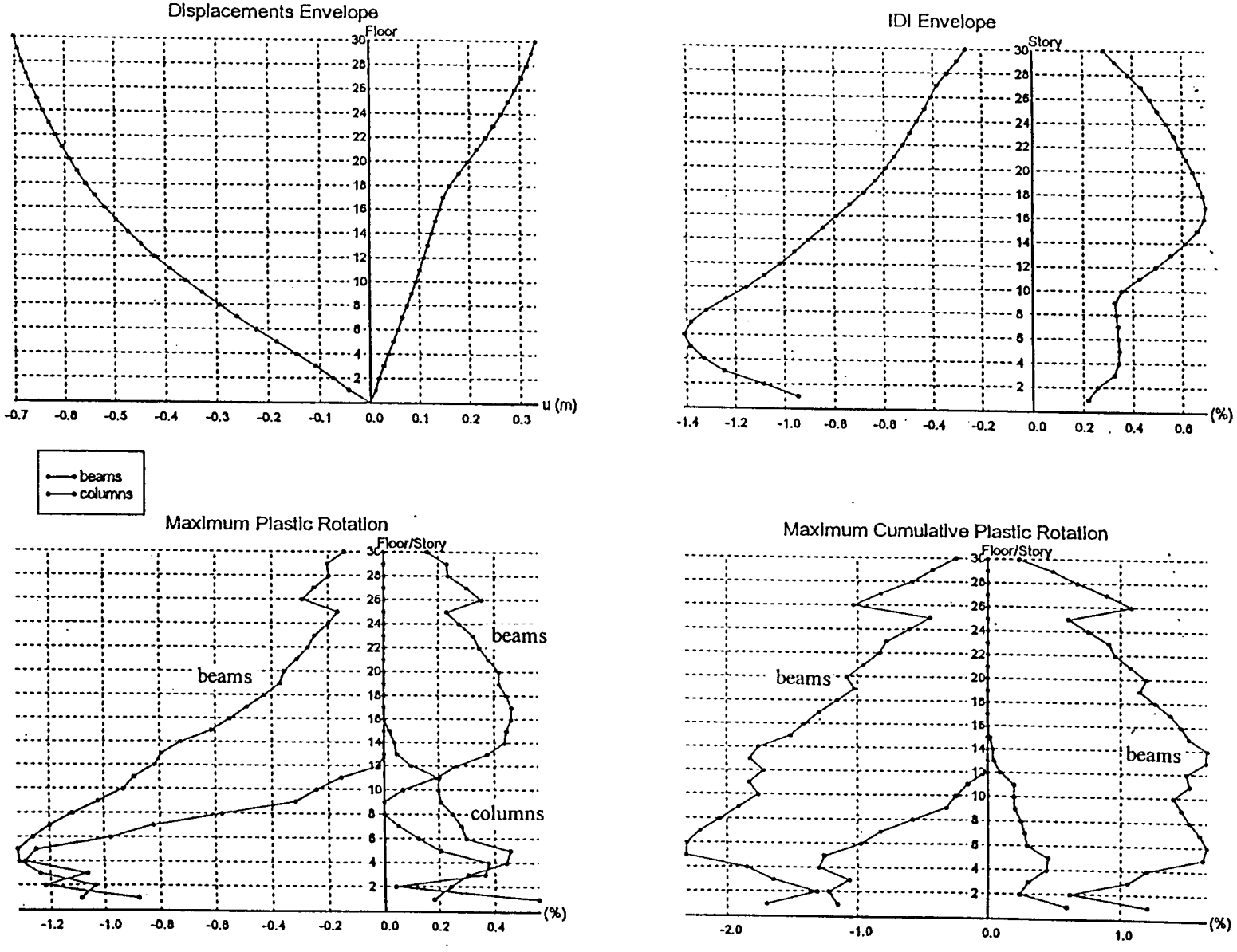

Figure 6.4.5 Response Results, S-K As Built, ξ=30%

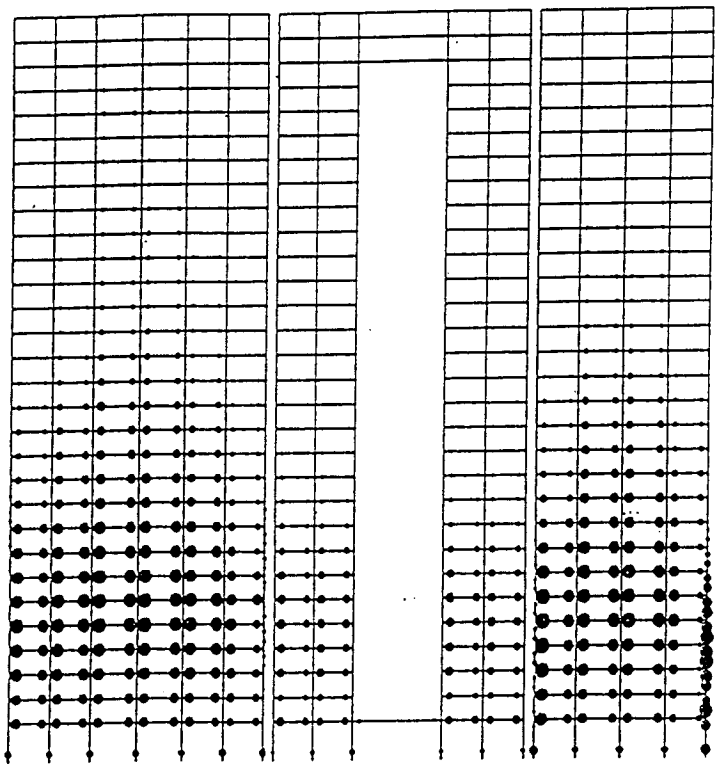

MAXIMUM PLASTIC ROTATION

θmax (beams) = 0.0132

θmax (columns) = 0.0129

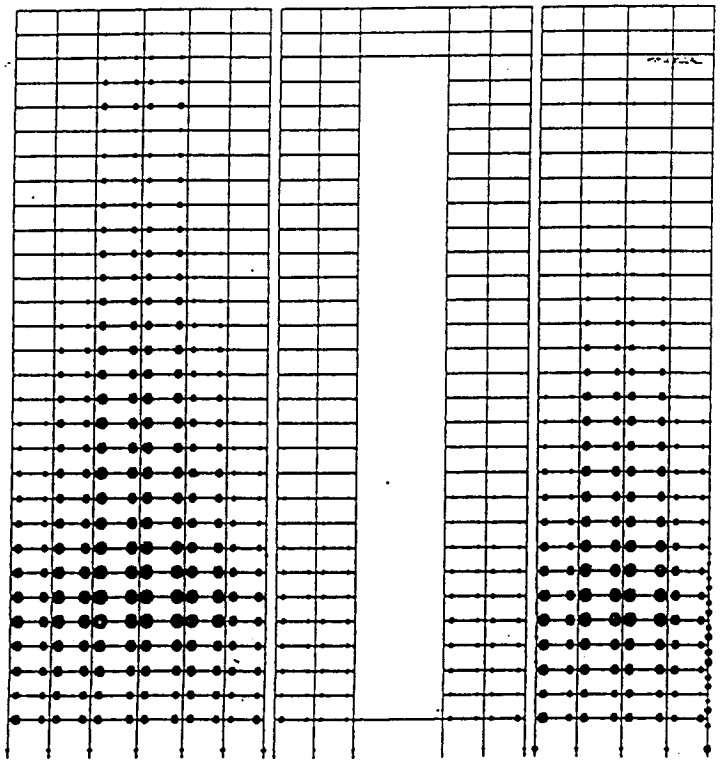

CUMULATIVE PLASTIC ROTATION

θcum (beams) = 0.0232

θcum (columns) = 0.0129

Figure 6.4.6 Plastic Rotation Demands, S-K As Built, ξ=30%

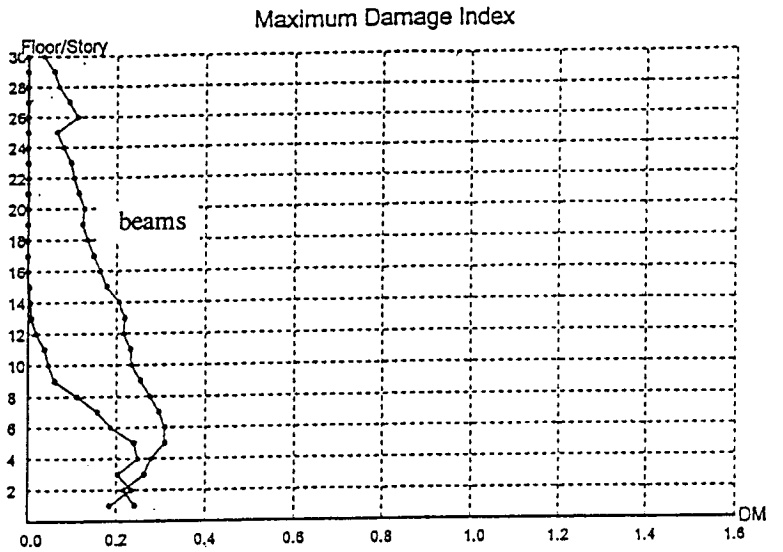

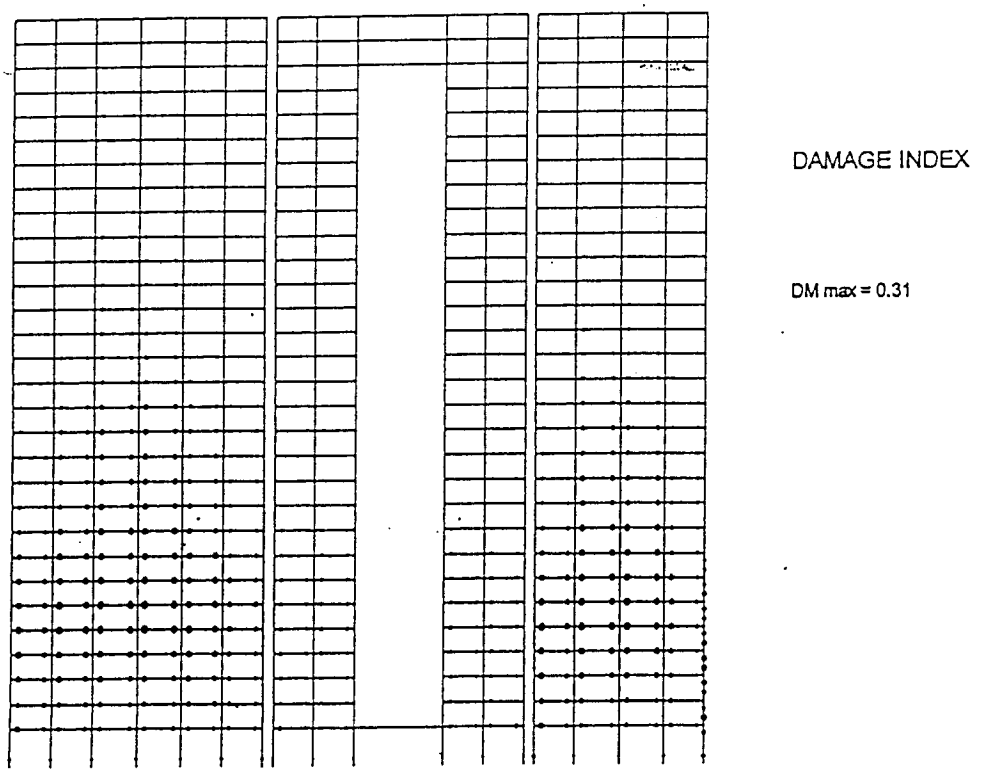

Figure 6.4.7 Damage Index, S-K As Built, ξ=30%

6.5 RETROFIT OF THE 15-STORY RC MOMENT-RESISTANT FRAME BUILDING (1965)

As shown in **Figure 5.5.2** and described in Section 5.5, this building has 13 stories above grade and a 2-story basement. Under the Los Gatos 1 EQGM, the maximum top displacement at the roof is about 69 inches and the maximum IDI is about 5.4%, which occurred at the third and fourth stories (**Figure 5.5.4**). As this value of IDI is unacceptable, an attempt was made to retrofit it trying first to use the conventional approaches of increasing its stiffness, or its strength, or both.

6.5.1 Retrofit Using Conventional Procedures

Because of the large number of significant weaknesses detected in this building as built (as described in Section 5.5), it was decided that a promising retrofit strategy would be to place steel jackets on the beam-column joints and to encase the beams and columns with steel plates. As discussed in detail by Sasani, et al. [1999], different thicknesses of steel plates were used without success. Even the use of what was considered to be the largest thickness steel plate that can be used efficiently (½" plates for beams at the 2nd floor, 7/16" plates for the 3rd to 5th floors, 3/8" plates for the 6th to 8th floors, ¼" plates for the 9th to 11th floors, 3/16" plates for the 12th to 14th floors, and ½" plates for all columns) did not prove to be effective.. With these reinforcements, the fundamental period of the retrofitted structure was estimated to be about 2.4 seconds.

The main results obtained from the nonlinear dynamic analysis of the building under the Los Gatos 1 recorded ground motion are shown by the graphs in **Figure 6.5.1.** As illustrated in the figure, a maximum IDI of about 4.5% is demanded in the first story as a consequence of the formation of a soft story mechanism at this location. To avoid this weak column-strong beam behavior, the thickness of the steel plates on the columns of the first story was increased to 1.0 inch (0.4cm). The main results from the nonlinear dynamic analysis are summarized in **Table 6.1** and shown in **Figure 6.5.2.** Although the maximum displacement at the roof has been decreased from 69 inches (**Figure 5.5.4 and Table 5.4**) to 61 inches, and the IDI has been reduced from 5.4% to 3.8% which now occurs at the 4th and 5th stories, it is still unacceptable in spite of the fact that the estimated C_y is about 0.58. In view of these unacceptable results, it was concluded that it would not be efficient to try to retrofit this building by stiffening, strengthening, and increasing its toughness through the use of thicker steel plates. Thus, a new approach based on using energy dissipation devices was attempted.

6.5.2 Retrofit Using Innovative Procedure

Because of the significant weakness in this building, particularly in the detailing of the longitudinal and transverse reinforcement, it was concluded that there is a need for steel jacketing to improve its deformation capacity including anchorage of main bars, shear resistance, and ductility (toughness) of the members. Since the use of steel jacketing with even very thick steel plates did not help to sufficiently decrease the IDI, it was decided to use the practical minimum steel plate thickness and add energy dissipation devices to effectively reduce deformation. In view of the results obtained

previously, it was decided to use 1/8" thick steel plates and to increase the damping from 5% to 30%. Results from the analysis of the structure retrofitted in this manner are summarized in **Table 6.2**. As shown in **Figure 6.5.3**, the results obtained in the analysis of the response indicate that the maximum IDI is reduced to 2.1% of which 0.70% is due to the rotation of the ground floor due to deformations of the two-story basement and rotation of the foundation.

Table 6.1 Summary for Retrofitted Structure (W=28,000 Kips and H=167 feet)

Type of Supports	Response Parameters	Pushover Analysis[1]	Los Gatos Ground Motion (1989 Loma Prieta Earthquake)			Takatori Ground Motion (1995 Kobe Earthquake)		
			Spectral Response[2] (ξ=5%)	Dynamic Analysis[1] (ξ=5%)	Dynamic Analysis[1] (ξ=30%)	Spectral Response[2] (ξ=5%)	Dynamic Analysis[1] (ξ=5%)	Dynamic Analysis[1] (ξ=30%)
Basement & Foundation Flexibility Included (T=2.3 sec) ($\Delta_y \approx 44$ in)	Δ_{top} (in)	100(μ=2.3)		61 (μ=1.4)	31		60 (μ=1.4)	33
	$\Delta_{2/3H}$ (in)	78	50	44	21	55	43	22
	IDI_{ave}	5.0%		3.1%	1.6%		3.1%	1.7%
	IDI_{max}	7.0%		3.8%	1.7%		3.7%	1.8%
	IDI_{ratio}	1.4		1.2	1.1		1.2	1.1
	$max\theta_{found}$	2.0%		1.9%	1.0%		1.8%	1.0%
	IDI_{tang}	5.0%		1.9%	0.7%		1.9%	0.8%
	V_{base} (W%)	64%	66%[3]	58%[4]	35%[4]	68%[3]	58%[4]	35%[4]
Fixed-Base (T=1.3 sec) ($\Delta_y \approx 15$ in)	Δ_{top} (in)	100(μ=6.7)		23 (μ=1.5)	15		37 (μ=2.5)	21
	$\Delta_{2/3H}$ (in)	89	18	19	10	31	32	16
	IDI_{ave}	5.0%		1.2%	0.75%		1.9%	1.1%
	IDI_{max}	7.6%		1.7%	1.0%		2.8%	1.5%
	IDI_{ratio}	1.5		1.4	1.3		1.5	1.4
	V_{base} (W%)	71%	73%[3]	60%[4]	56%[4]	76%[3]	66%[4]	71%[4]

(1) P-Δ effects are included.
(2) Single Degree of Freedom system is elastic-perfectly plastic and P-Δ effect is not included (response for corresponding ductility).
(3) Viscous damping forces not included.
(4) Viscous damping forces included.

Table 6.2 Summary for Lightly Retrofitted Structure (W=26,000 kips & H=167 feet)

Type of Supports	Response Parameters	Pushover Analysis[1]	Los Gatos Ground Motion (1989 Loma Prieta Earthquake)			Takatori Ground Motion (1995 Kobe Earthquake)		
			Spectral Response[2] (ξ=5%)	Dynamic Analysis[1] (ξ=5%)	Dynamic Analysis[1] (ξ=30%)	Spectral Response[2] (ξ=5%)	Dynamic Analysis[1] (ξ=5%)	Dynamic Analysis[1] (ξ=30%)
Basement & Foundation Flexibility Included (T=2.6 sec) ($\Delta_y \approx 29$ in)	Δ_{top} (in)	100(μ=3.4)		52 (μ=1.8)	31		38 (μ=1.3)	31
	$\Delta_{2/3H}$ (in)	92	59	44	25	31	32	22
	IDI_{ave}	5.0%		2.6%	1.6%		1.9%	1.6%
	IDI_{max}	8.7%		4.0%	2.1%		2.7%	2.0%
	IDI(ratio)	1.7		1.5	1.3		1.4	1.3
	$max\theta_{found}$	1.0%		0.7%	0.7%		0.7%	0.7%
	IDI_{tang}	7.7%		3.3%	1.4%		2.0%	1.3%
	V_{base} (W%)	30%	50%[3]	34%[4]	34%[4]	33%[3]	30%[4]	29%[4]

(1) P-Δ effects are included.
(2) Single Degree of Freedom system is elastic-perfectly plastic and P-Δ effect is not included (response for corresponding ductility).
(3) Viscous damping forces not included.
(4) Viscous damping forces included.

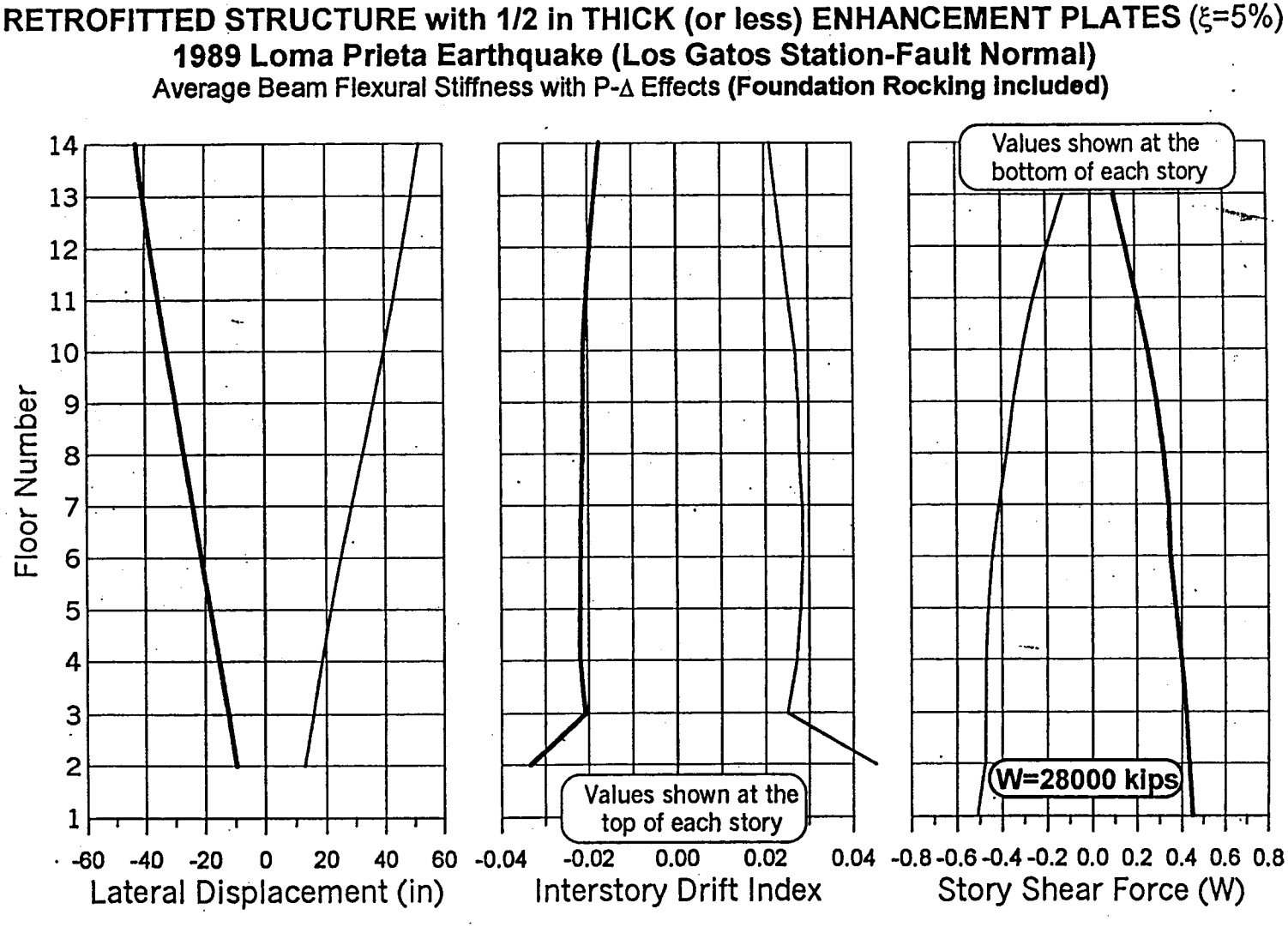

Figure 6.5.1 Retrofitted Structure with ½ in. Thick (or less) Enhancement Plates (ξ=5%)

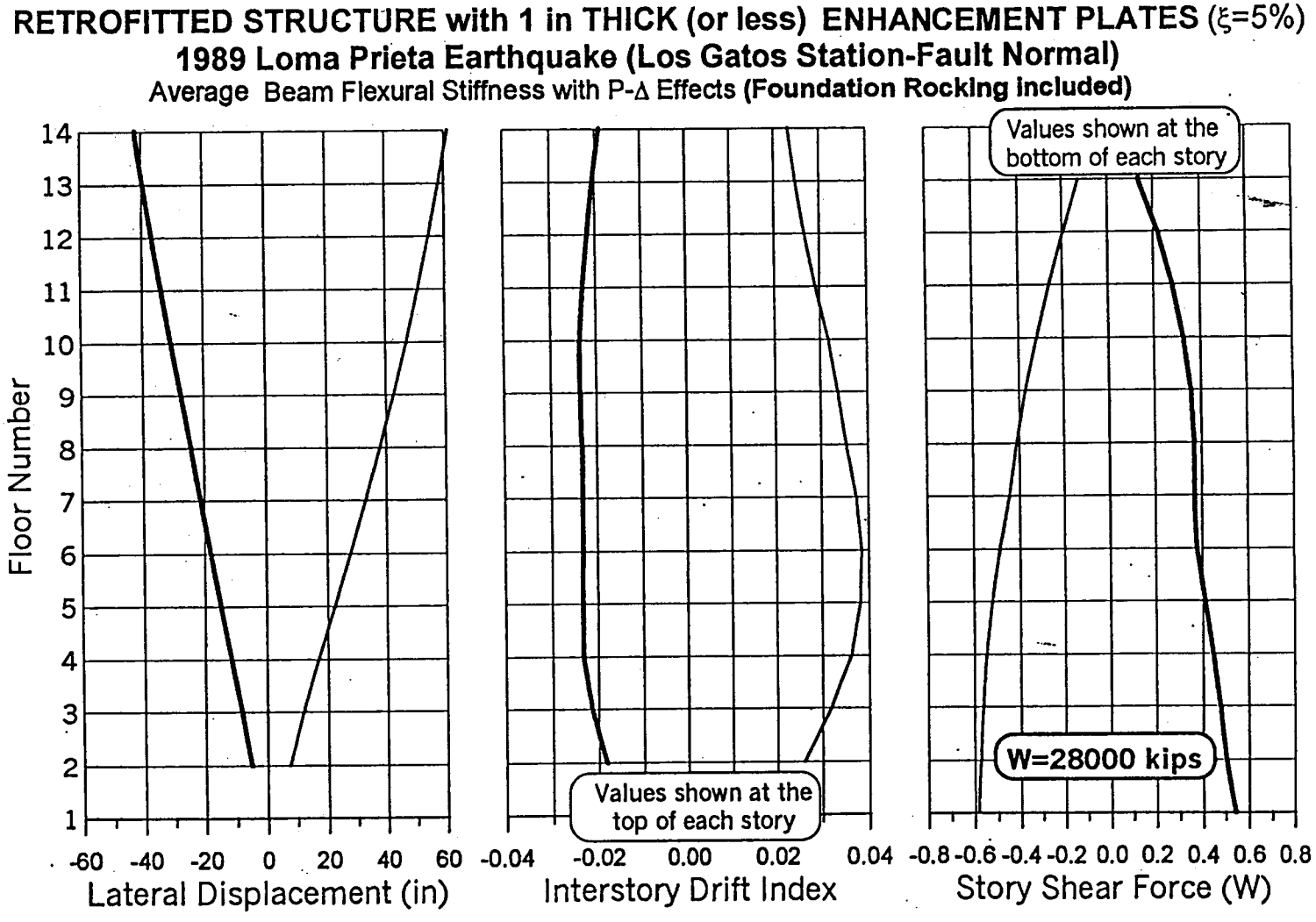

Figure 6.5.2 Retrofitted Structure with 1 in. Thick (or less) Enhancement Plates (ξ=5%)

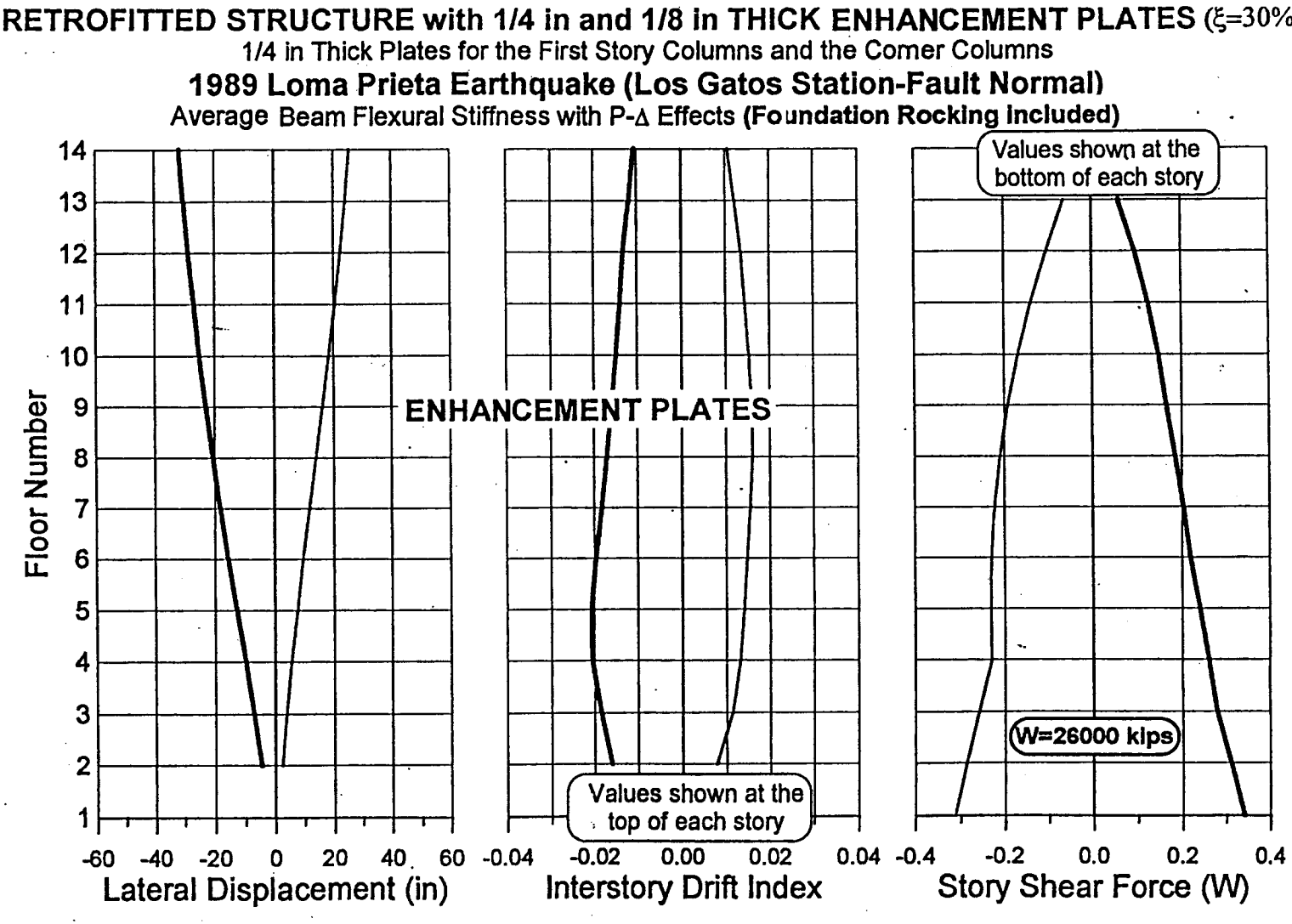

Figure 6.5.3 Retrofitted Structure with ¼ in. and 1/8 in. Thick Enhancement Plates (ξ=30%)

6.6 RETROFIT OF THE 41-STORY STEEL SPACE FRAME

As discussed previously, the largest demands on the response parameters occur in the upper third of the building. Initially the use of conventional strengthening and stiffening procedures was investigated.

6.6.1 Conventional Procedure

The conventional means of reducing the displacements in a steel moment frame is to brace one or more of the bays. Considering the transverse direction, cross-bracing was added to bays B5, B11 and B18 (**Figure 5.6.1b**). An isometric view of the braced frame is shown in **Figure 6.6.1a**. The application of the cross-bracing reduced the periods of the first three translational modes of vibration to 4.95, 1.49 and 0.76 seconds. The deflected shapes for these three modes are shown in **Figures 6.6.1b to 6.6.1d**. In an effort to further stiffen the structure, the use of a braced core was considered by adding cross-bracing to bays B8, B11 and B15 in the transverse direction and bays B32, B33, B38 and B39 in the longitudinal direction (**Figure 5.6.1b**). An isometric view of the framing for this system is shown in **Figure 6.6.2a**. The deflected shapes of the first three vibration modes in the transverse direction are shown in **Figures 6.6.2b to 6.6.2d**. The undeformed shape in the longitudinal direction is shown in **Figure 6.6.3a** along with the deflected shapes of the first three translation modes of vibration in **Figures 6.6.3b to 6.6.3d**. It was surprising to find that the addition of the braced core system had almost no effect on the vibration periods of the transverse modes relative to the initial cross-bracing system discussed previously. For this reason, it was not given further consideration.

6.6.2 Innovative Procedure (Supplemental Damping)

An alternative to the purely braced frame systems is the use of supplemental damping which is often used in conjunction with bracing elements as shown in **Figure 6.6.4a**. The manufacturer of the supplemental damping device (fluid viscous damper) claims that the structural damping can be increased to 20% to 50% of critical damping. For the purposes of this study a damping of 30% of critical was used.

(a) Elastic Response Analyses

The elastic dynamic response of the unbraced frame with 5% damping, the cross-braced frame with 5% damping and the unbraced frame with 30% damping are compared in **Figure 6.6.5** for the Los Gatos ground motion. The envelope of maximum lateral displacement is shown in **Figure 6.6.5a**. The supplemental damping is shown to be very effective in reducing the peak displacement at the roof level from 90 inches (2.3m) to 53 inches (1.3m). It can also be seen that the supplemental damping eliminates much of the response from the higher modes and makes the displacement envelope almost linear. The displacement envelope for the braced frame is very similar to that for the unbraced frame for the first twenty-two stories. Beyond that level, the envelope for the braced frame exceeds that of the unbraced frame. This may well be an effect of the interaction of the

dynamic characteristics of the building and those of the input ground motion. With a period of 5.75 seconds, the unbraced frame is beyond the peak response region of the response spectrum. As the period of the frame is reduced to 5.0 seconds by the addition of the cross-bracing, the structure moves closer to the peak response region and develops higher lateral inertia forces.

The effect of bracing and supplemental damping on the interstory drift index is shown in Figure **6.6.5b** which also indicates that the damping has a very positive effect. The IDI becomes almost uniform over the height of the building and does not exceed 1.5%. The bracing results in a small reduction in the IDI of the lower floors but the IDI of the upper eleven stories is actually increased by the addition of bracing. The envelopes of maximum inertia forces are shown in **Figure 6.6.5c**. This figure indicates that the supplemental damping is very effective in reducing the inertia forces, whereas the addition of bracing actually increases these forces. A similar effect is shown very clearly in **Figure 6.6.5d** in which the maximum story shear envelopes are compared. The supplemental damping reduces the story shears by approximately 50% compared to the unbraced frame and the addition of bracing increases the story shears relative to the unbraced frame over the entire height of the building.

(b) Nonlinear Dynamic Analyses

The effect of increased energy dissipation through supplemental damping is investigated for the four pulse-type ground motions. In these analyses, the nonlinear response of the unbraced frame with 5% damping is compared to that of the unbraced frame with 30% damping.

Maximum response envelopes for the Los Gatos ground motion are shown in **Figure 6.6.6**. The lateral displacement envelope, shown in **Figure 6.6.6a** indicates that the peak displacement at the roof level is reduced from 90 inches (2.29m) to 60 inches (1.52m) for a reduction of 33%. The reduction in peak IDI, shown in **Figure 6.6.6b**, is even more dramatic dropping from 3.8% to 1.5% at the critical 29th story level, a reduction of 69%. The curvature ductility demands in the critical girders at the 28th floor are reduced a similar amount as shown in **Figure 6.6.6c**. It can be noted that the curvature ductility demands of all girders are less than 2.0 with the supplemental damping. The displaced shape of a typical frame with 30% damping and a displacement of 60 inches at the roof is shown in **Figure 6.6.7** along with the distribution of plastic hinges.

Maximum response envelopes for the Lexington Dam ground motion are shown in **Figure 6.6.8**. The reduction in lateral displacement, shown in **Figure 6.6.8a** is not as dramatic as in the previous case, reaching a maximum reduction at the roof level of approximately 30%. However, the reduction in IDI, shown in **Figure 6.6.8b** is very significant, particularly in the floor levels which have the higher IDI demands. With supplemental damping the maximum IDI demand is 1.3% compared to 2.4% without. The girder curvature ductility demands are compared in **Figure 6.6.8c,** which indicates that the curvature ductility demands are all less than 2.0. The deflected shape of the 30% damped building with a peak displacement of 38 inches is shown in **Figure 6.6.9** along with the distribution and magnitude of the plastic hinging.

Envelopes of maximum response under the Takatori ground motion are shown in **Figure 6.6.10**. As in the previous case, the main reduction in lateral displacement occurs in the upper six

floors where the displacements in the 5% damped condition are the largest (**Figure 6.6.10a**). The maximum IDI demand at the 34th floor level is reduced significantly (60%) as shown in **Figure 6.6.10b**. In a similar manner, the maximum girder ductility demand at the 34th floor level is reduced from 4.6 to 1.5 as indicated in **Figure 6.6.10c**. The reduced amount of lateral displacement and the reduced plastic hinging can be seen in **Figure 6.6.11**.

Similar data for the James Road ground motion is shown in **Figures 6.6.12** and **6.6.13**. The lateral displacement, shown in **Figure 6.6.12a**, is reduced from 72 inches (1.8m) to 48 inches (1.2m) at the roof level. The maximum IDI demand, shown in **Figure 6.6.12b**, is reduced by approximately 50% and the maximum curvature ductility demand in the girders, shown in **Figure 6.6.12c**, is reduced to almost unity, indicating that the behavior of the girders will be predominately elastic. The deflected shape of the structure with supplemental damping is shown in **Figure 6.6.13a** and the location of the plastic hinging is shown in **Figure 6.6.13b**. It can be seen that only three hinges occur in the exterior girders at the 22nd, 23rd, and 24th story level.

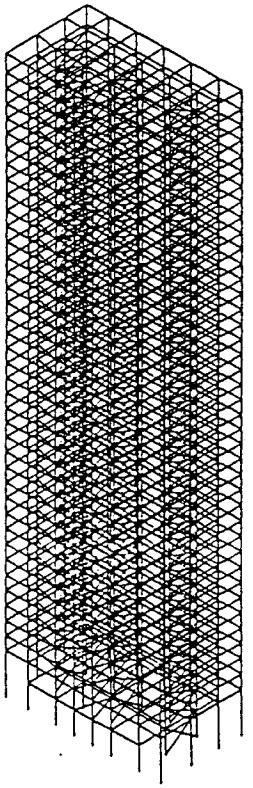

(a) Computer Model

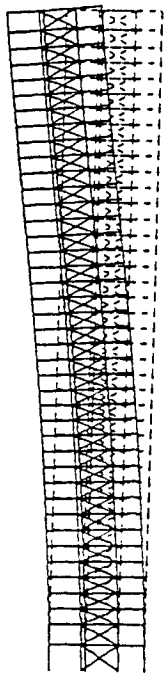

(b) Transverse Mode 1

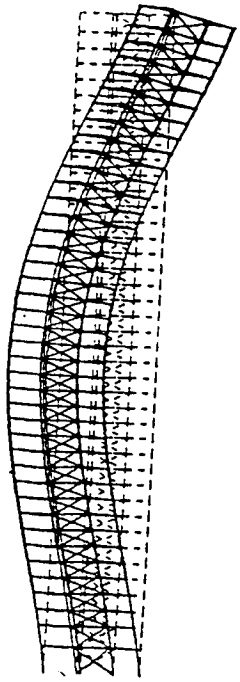

(c) Transverse Mode 2

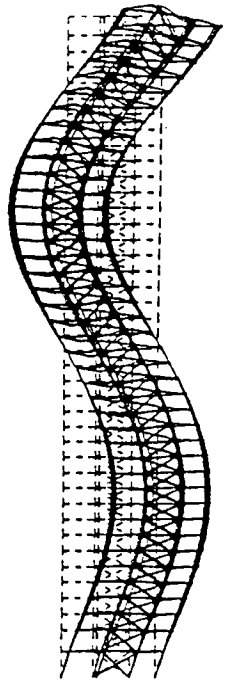

(d) Transverse Mode 3

Figure 6.6.1 Retrofitted Steel Space Frame, Single Braced Bay

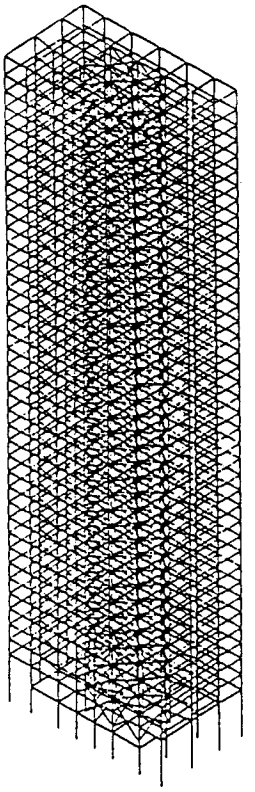

(a) Computer Model

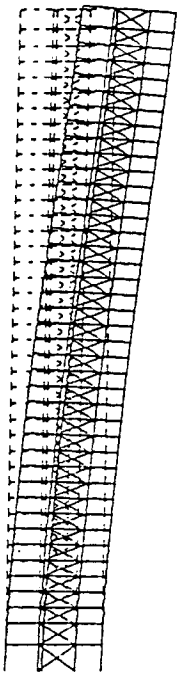

(b) Transverse Mode 1

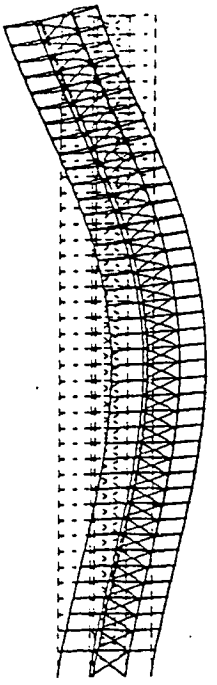

(c) Transverse Mode 2

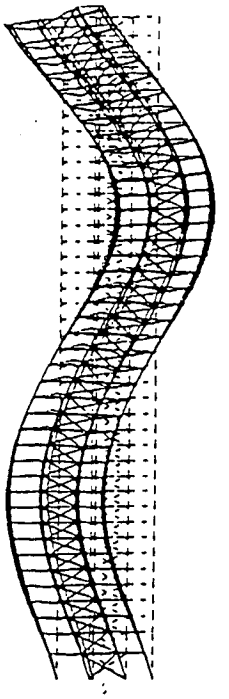

(d) Transverse Mode 3

Figure 6.6.2 Retrofitted Steel Space Frame, Braced Core, Transverse

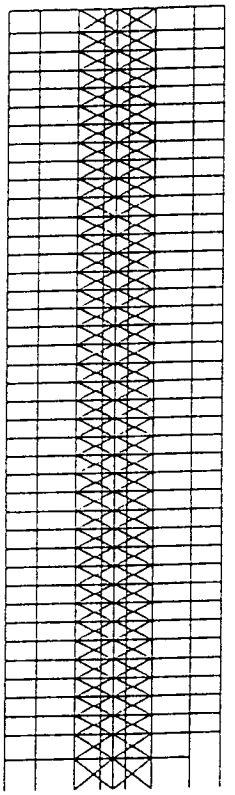

(a) Longitudinal Elevation

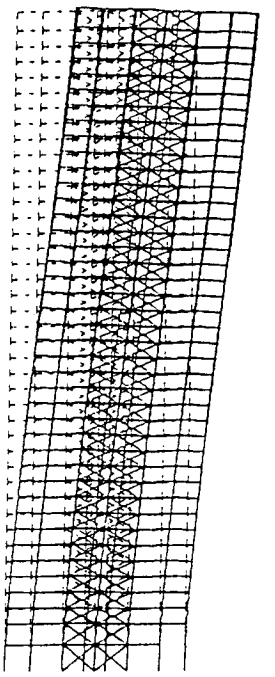

(b) Longitudinal Mode 1

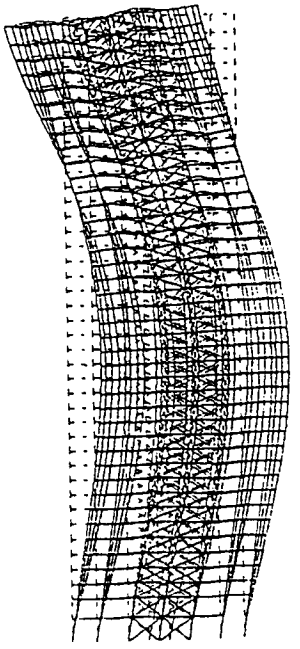

(c) Longitudinal Mode 2

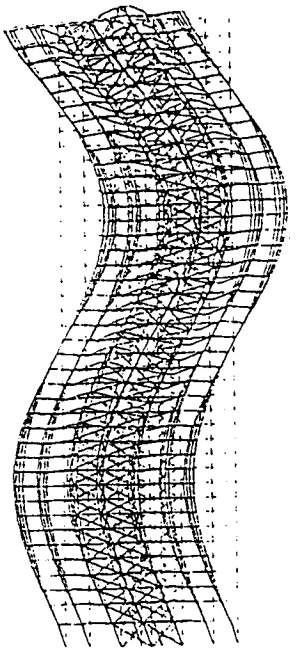

(e) Longitudinal Mode 3

Figure 6.6.3 Retrofitted Steel Space Frame, Braced Core, Longitudinal

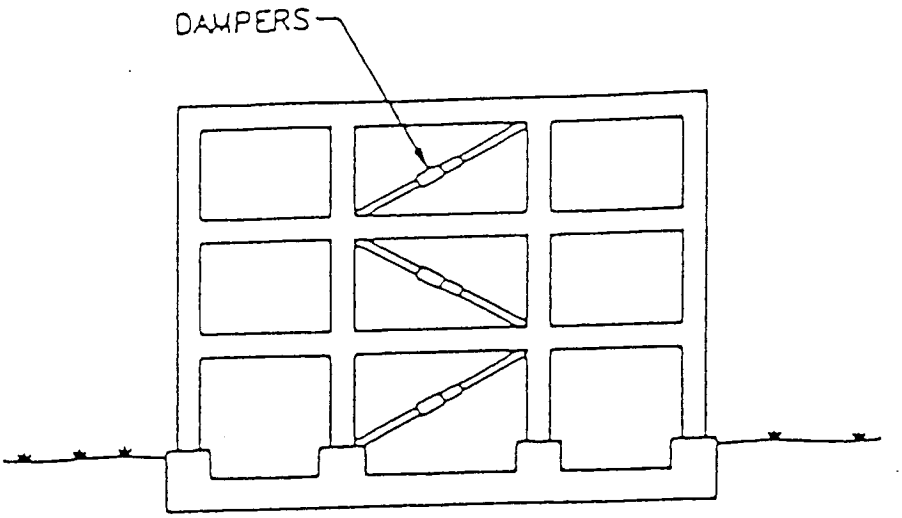

DIAGONAL BRACING WITH DAMPERS

(a) Diagonal Cross Bracing

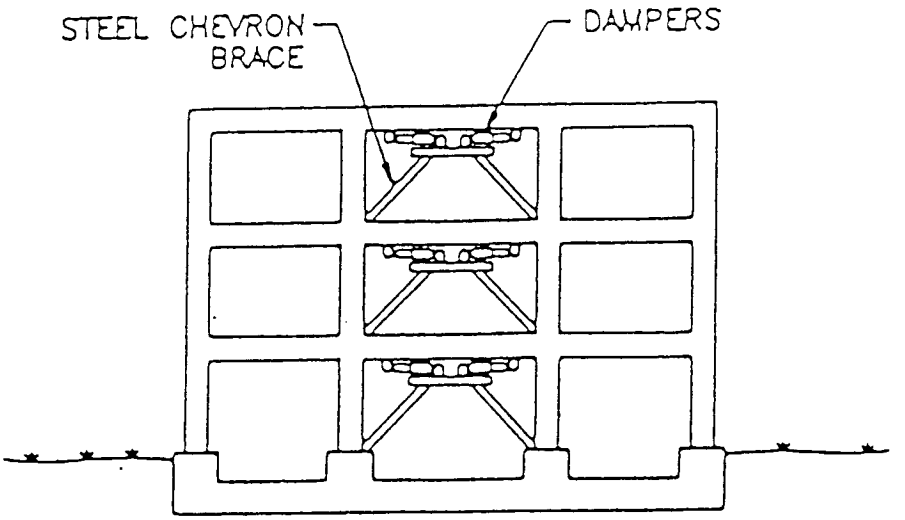

DAMPERS IN CHEVRON BRACES

(b) Chevron Bracing

Figure 6.6.4 Bracing With Supplemental Dampers

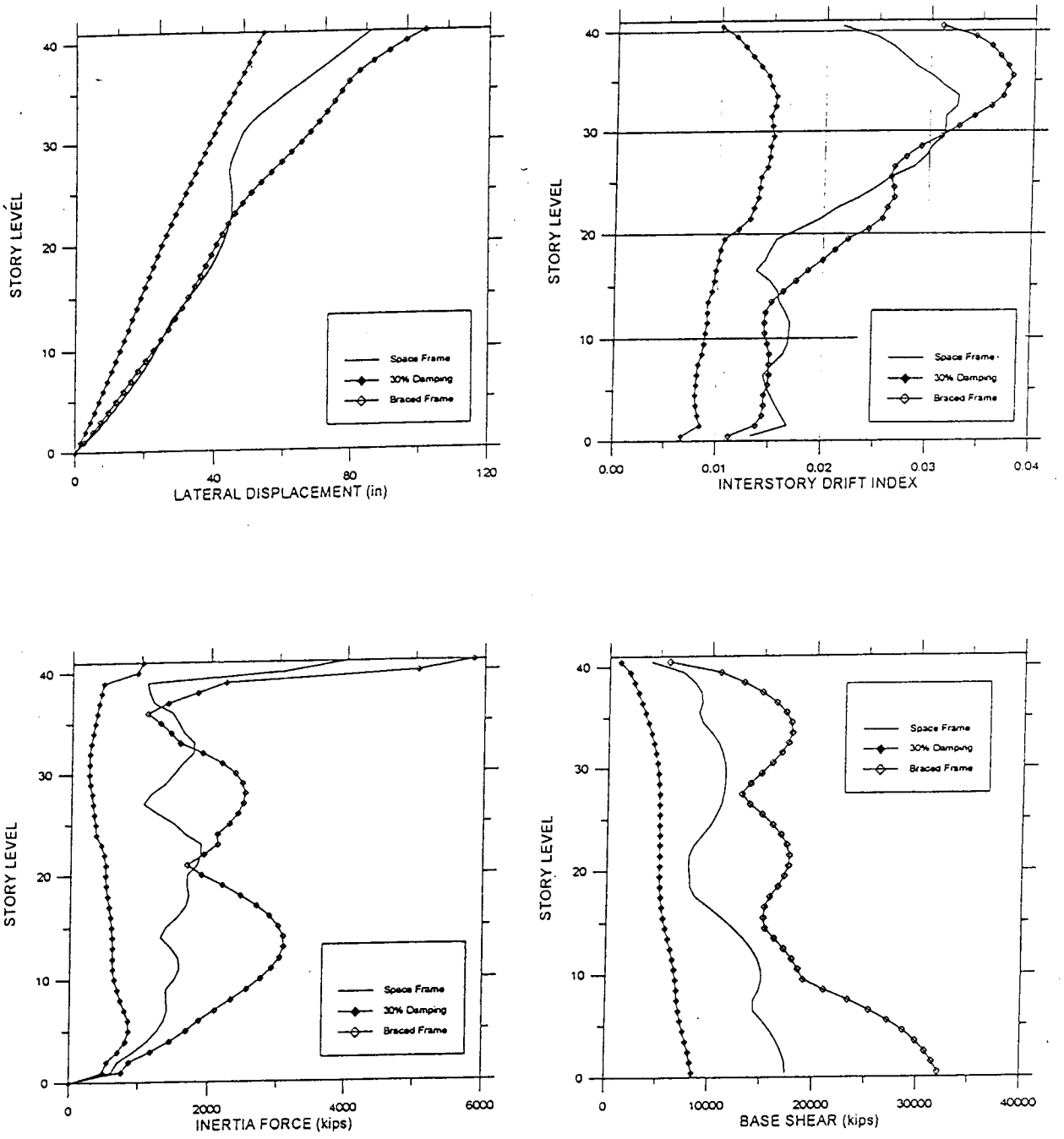

Figure 6.6.5 Elastic Response Results, Retrofitted Steel Space Frame

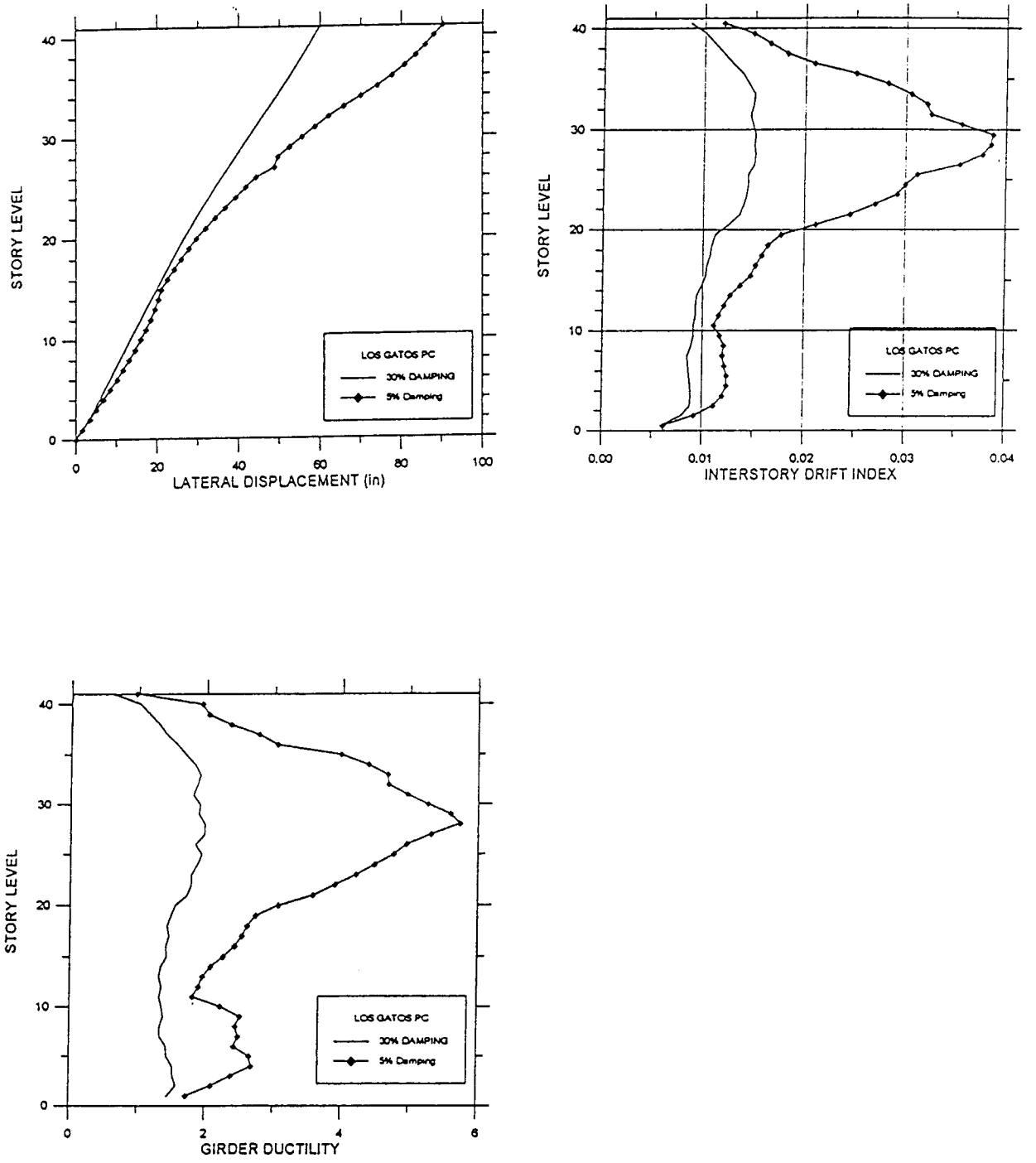

Figure 6.6.6 Effect of Supplemental Damping on Nonlinear Response; Steel Space Frame, Los Gatos

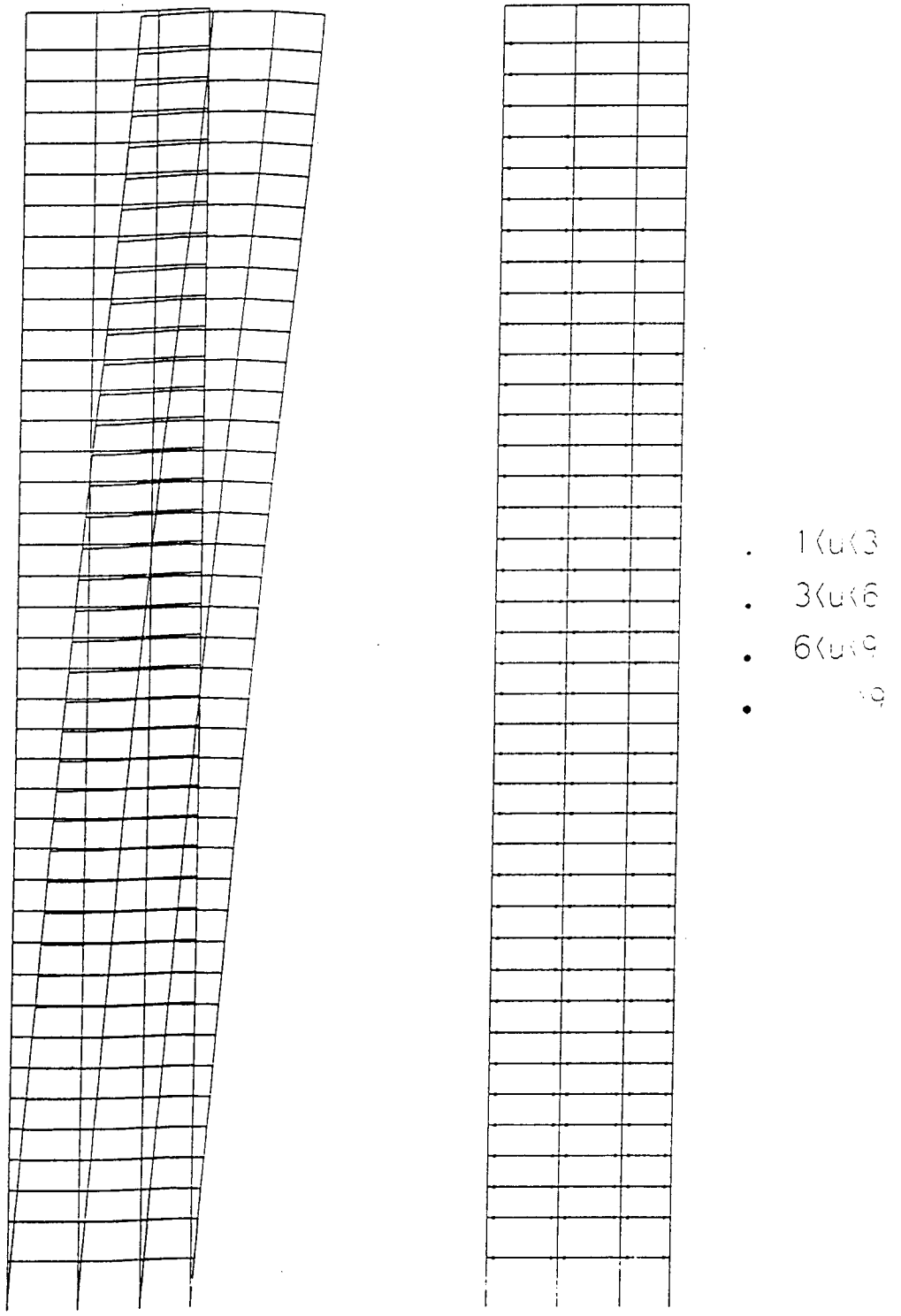

(a) Max. Displaced Shape
Δ_{roof} = 59.9 inches

(b) Plastic Hinge Locations

Figure 6.6.7 Steel Space Frame Response, Los Gatos, ξ=30%

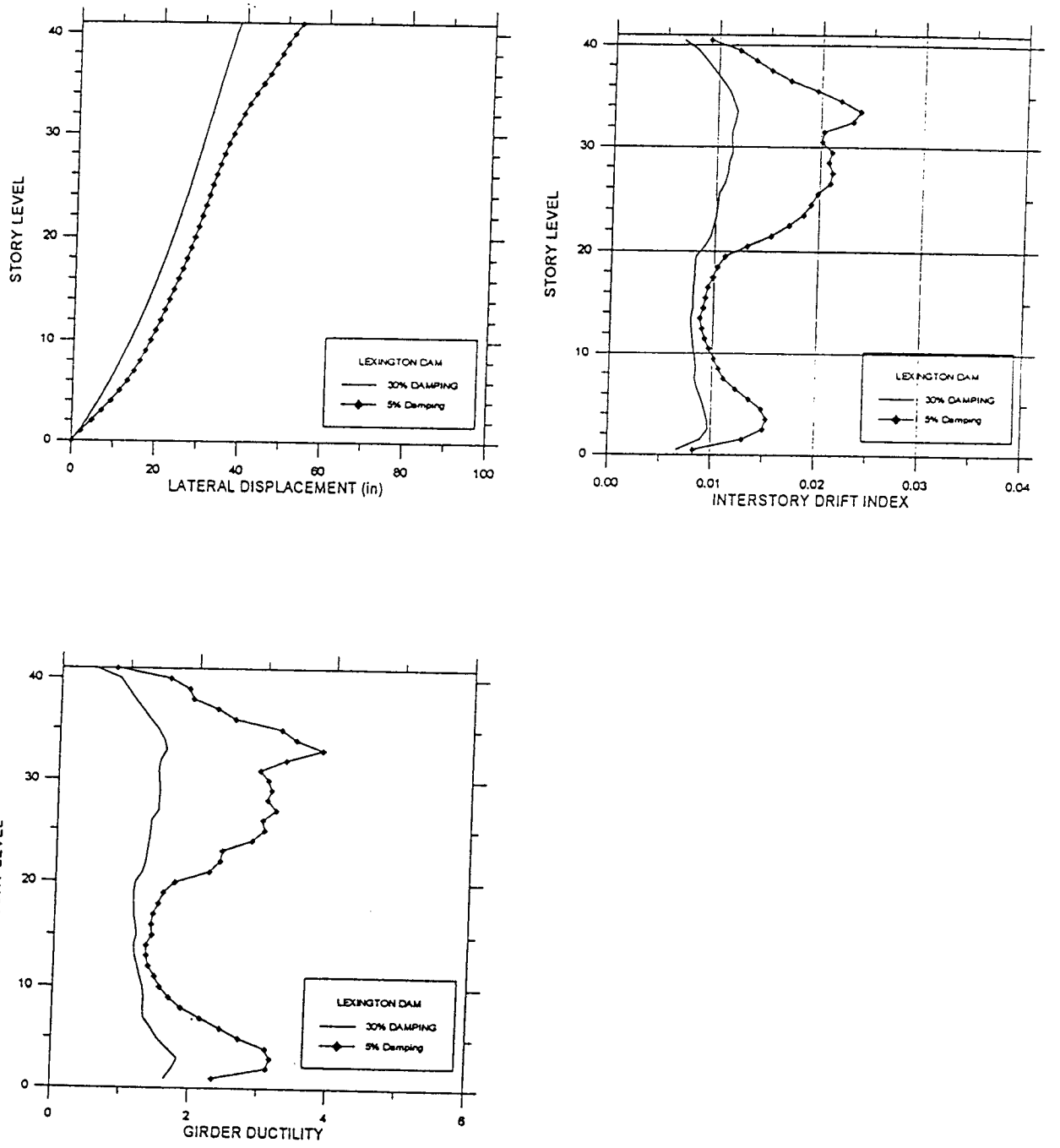

Figure 6.6.8 Effect of Supplemental Damping on Nonlinear Response, Steel Space Frame, Lexington Dam

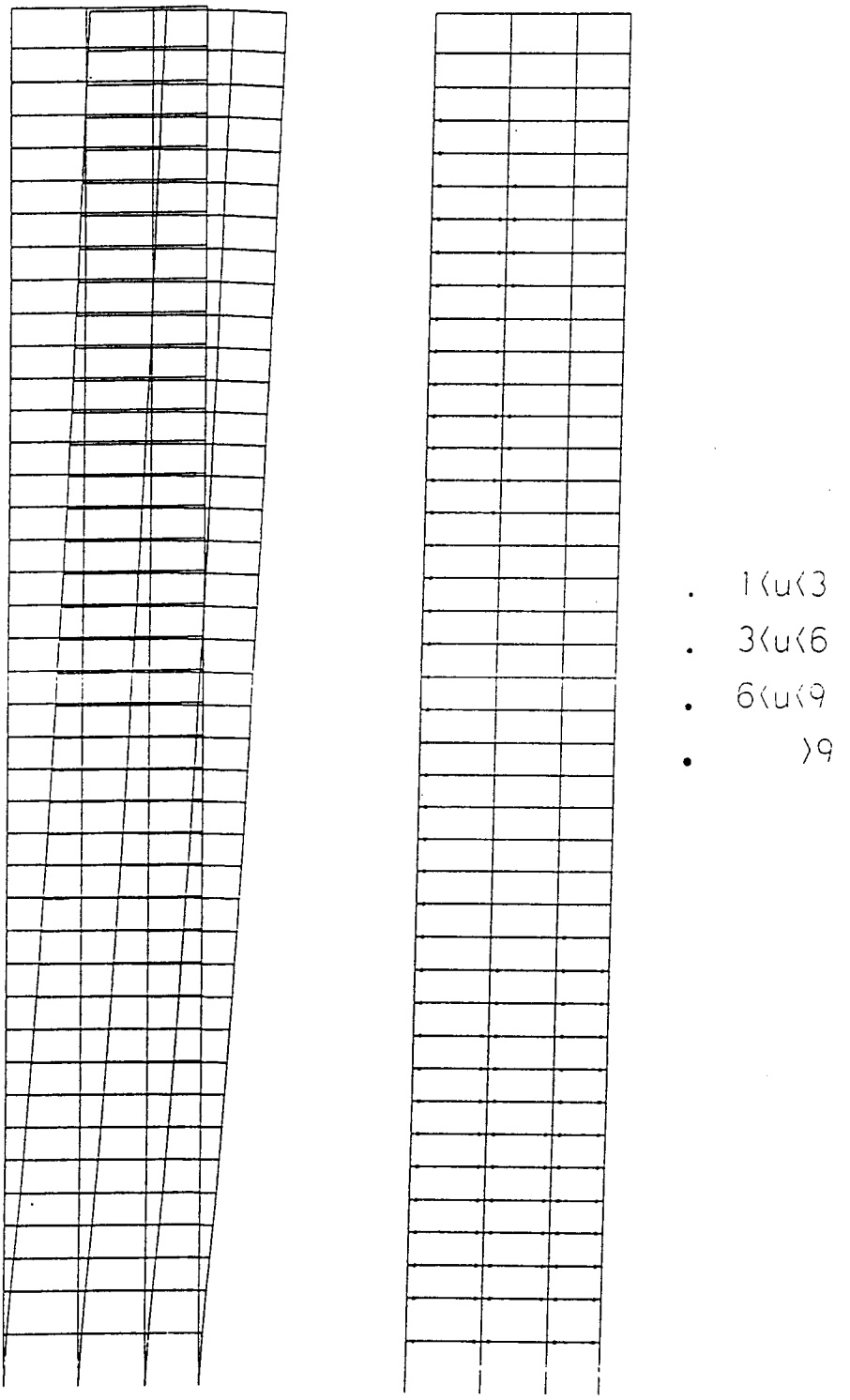

(a) Max. Displaced Shape
Δ_{roof} = 38.4 inches

(b) Plastic Hinge Locations

Figure 6.6.9 Steel Space Frame Response, Lexington Dam, ξ=30%

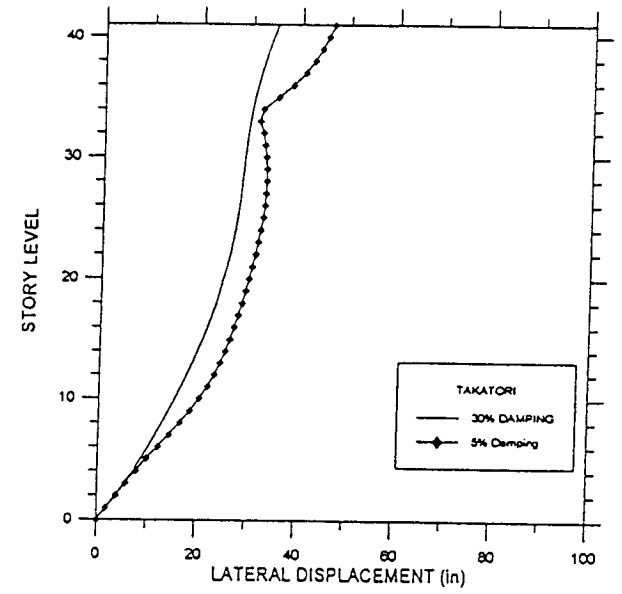

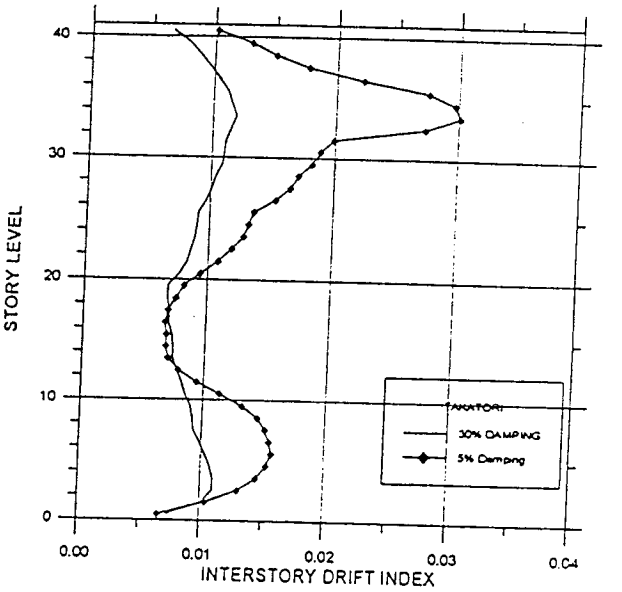

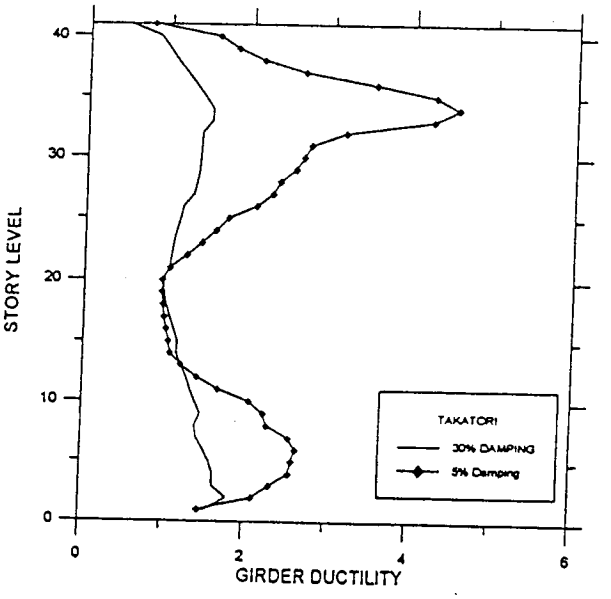

Figure 6.6.10 Effect of Supplemental Damping on Nonlinear Response; Steel Space Frame, Takatori

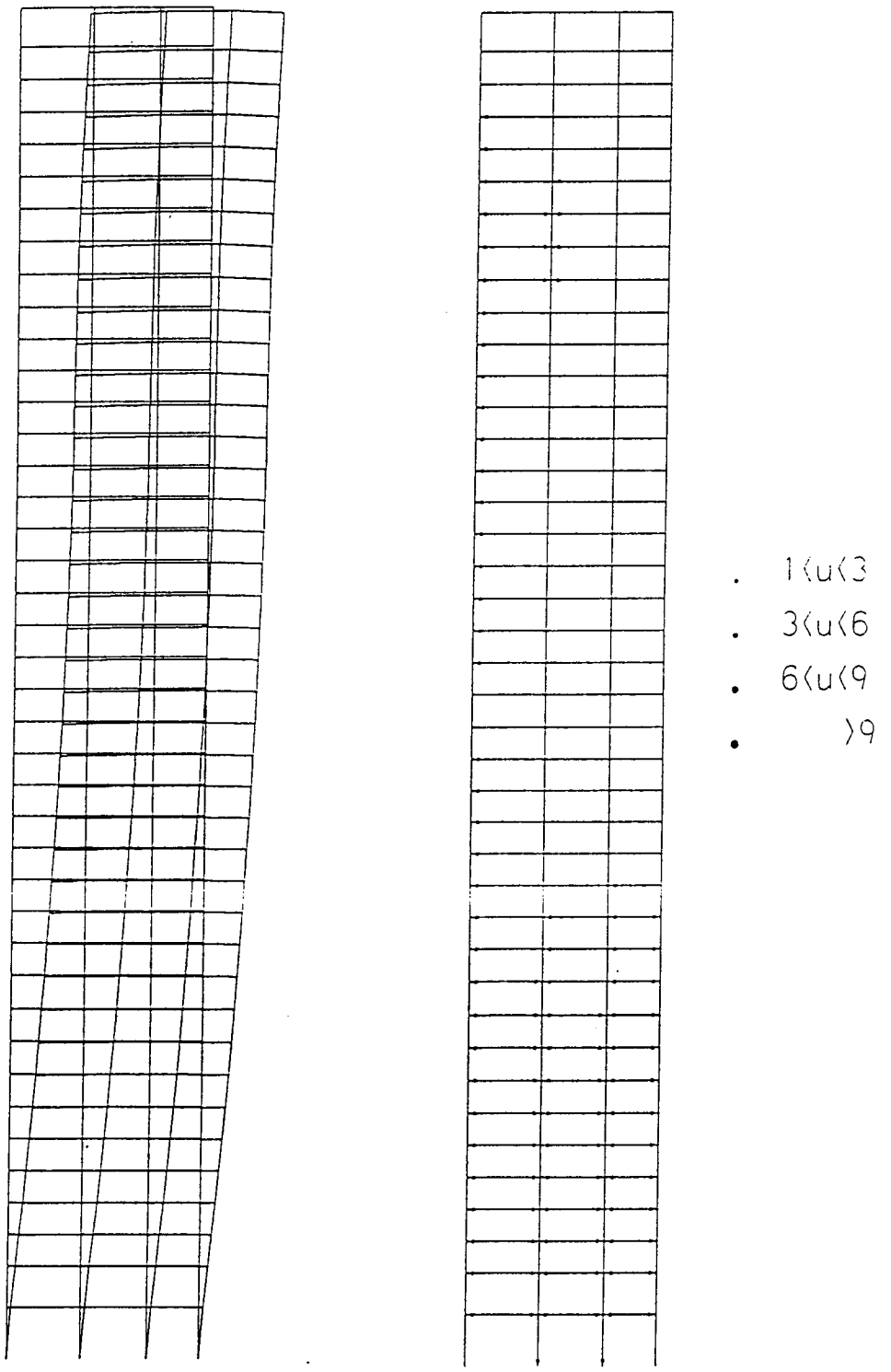

(a) Max. Displaced Shape
Δ_{roof} = 35 inches

(b) Plastic Hinge Locations

Figure 6.6.11 Steel Space Frame Response, Takatori, ξ=30%

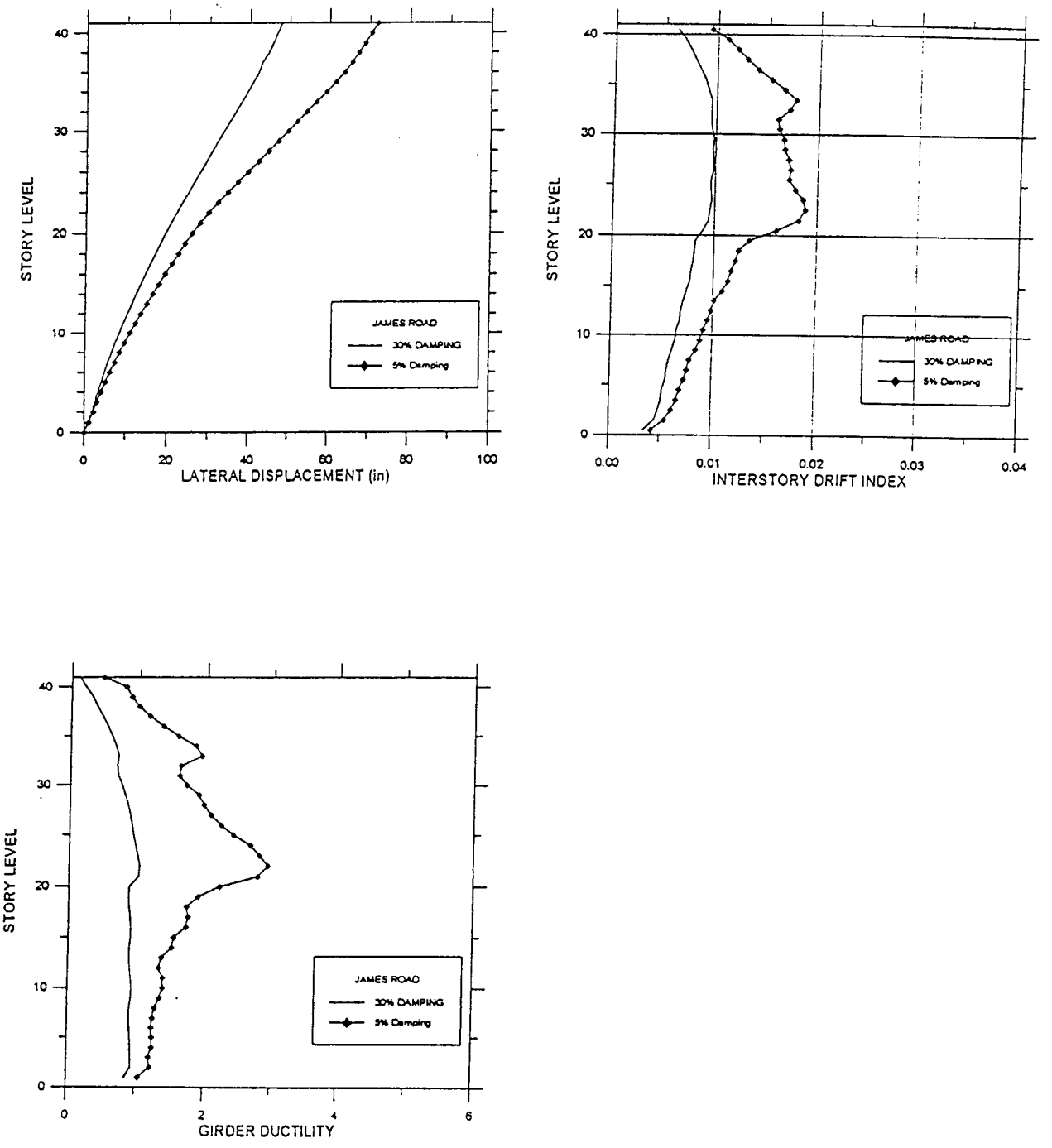

Figure 6.6.12 Effect of Supplemental Damping on Nonlinear Response, Steel Space Frame, James Road

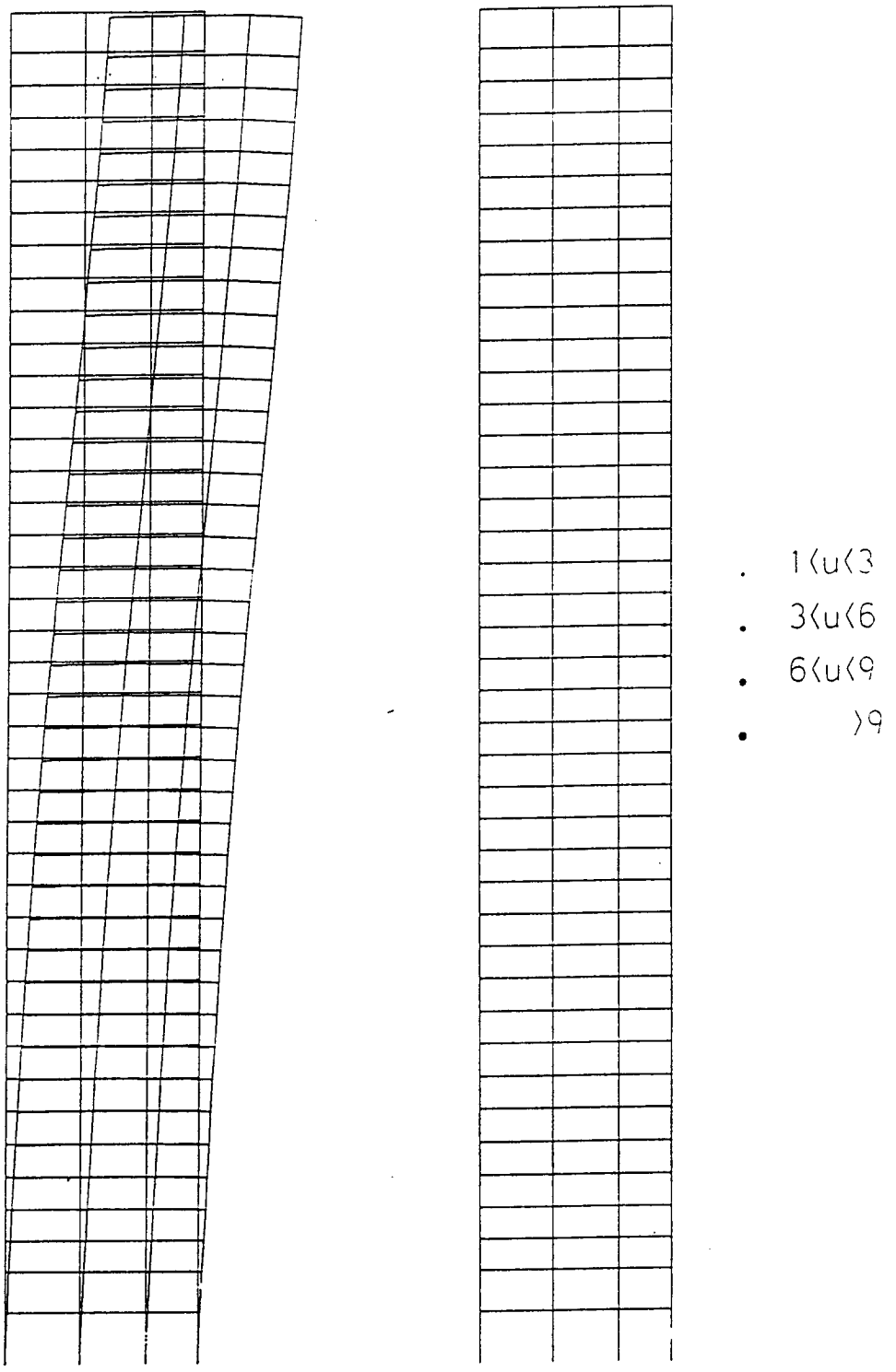

(a) Max. Displaced Shape
Δ_{roof} = 48 inches

(b) Plastic Hinge Locations

Figure 6.6.13 Steel Space Frame Response, James Road, ξ=30%

6.7 RETROFIT OF THE 20-STORY STEEL PERIMETER FRAME

As mentioned previously, the conventional means of reducing the displacements in a steel moment frame is to brace one or more of the bays. This is sometimes supplemented by the insertion of an outrigger (belt) truss at selected levels. The application of these procedures to improve the seismic performance of the 20-story perimeter frame will be investigated. As a basis of comparison, the first three translational modes of vibration of the initial, unbraced frame were calculated to be 4.04, 1.45, and 0.84.

6.7.1 Conventional Procedure (Chevron Bracing)

An initial braced configuration considered only a single bay of chevron bracing over the height of the frame as shown in **Figure 6.7.1a**. The deflected shape of the first three modes of vibration, having periods of 2.86, 0.954 and 0.519 seconds, which are significantly lower than those for the unbraced frame (Section 5.7.1) are shown in **Figures 6.7.1b to 6.7.1d**. In order to investigate the effect of the addition of outrigger trusses (sometimes referred to as a belt trusses), outrigger trusses were inserted at the 10^{th} and 20^{th} story levels as shown in **Figure 6.7.2**. Also shown in the figure are the deflected mode shapes of the first three modes of vibration which were determined to have vibration periods of 2.73, 0.928 and 0.478 seconds. Comparing this with the previous result indicates that the addition of the outrigger has minimal effect on the dynamic properties. A third configuration considered the use of two bays of chevron bracing over the height of the building as shown in **Figure 6.7.3**. Also shown are the deflected shapes of the first three translational modes of vibration which have calculated periods of 2.49, 0.797 and 0.425 seconds. A final configuration considered the addition of the outrigger trusses at the 10^{th} and 20^{th} story levels as shown in **Figure 6.7.4**. Periods of vibration were calculated to be 2.369, 0.775 and 0.394 for this configuration. As in the previous case, the addition of the outrigger has minimal effect on the dynamic properties.

The effects of these modifications on the elastic displacement response of the building to the pulse-type motion recorded at Anderson Road during the Imperial Valley earthquake (1979) are summarized in **Figure 6.7.5**. This figure indicates that the use of a single bay of chevron bracing has a significant effect in reducing both the lateral displacement and the IDI. The inclusion of outrigger (belt) trusses reduces the lateral displacement further but the amount of additional reduction is not significant. It can be seen that the outrigger (belt) truss has the negative effect of introducing a sharp discontinuity in the IDI curve at the story levels where it is inserted. For this reason, the outrigger truss is not considered a viable option. However, regarding displacement, either the single bay of bracing or the two bays of bracing appear capable of reducing the IDI to within acceptable limits.

The effects of the braced bays on the elastic forces generated in the perimeter frame are also illustrated in **Figure 6.7.5**. It is indicated that the unbraced frame has the lowest inertia forces and corresponding story shears. The addition of the bracing increases both the inertia and story shear forces although the increase is not dramatic. The reason for this increase can be seen from the elastic response spectra for the pulse-type ground motions. With a fundamental period of 4 seconds, the unbraced frame is on the long period side of the peak response. Increasing the stiffness by the

addition of the bracing members reduces the period and moves the structure into a stronger response region of the spectra. Hence while the bracing is effective in reducing the displacements, it tends to increase the force levels in the structure.

6.7.2 Innovative Procedure (Supplemental Damping)

Supplemental damping devices can readily be inserted into chevron bracing as shown in **Figure 6.6.4b**. As for the 40-story building, a modal damping of 30% is considered in evaluating the effect of supplemental damping on the response of the retrofitted structure and the as-built structure to pulse-type ground motions. Initial studies considered the effect on the elastic dynamic response.

(a) Elastic Dynamic Analyses

The effect of the supplemental damping on the maximum elastic dynamic response due to the Los Gatos ground motion is shown in **Figure 6.7.6**. The envelopes of maximum displacement, **Figure 6.7.6a**, indicate that the maximum lateral displacement is reduced to 52 inches (1.3m) from 110 inches (2.8m) for the unbraced frame which is also significantly smaller than the 75 inches (1.9 m) for the braced configuration. In a similar manner, **Figure 6.7.6b** indicates the IDI is reduced such that it varies from 1% to 2% over the entire height of the frame. The maximum inertia forces and story shears developed in the frame are summarized in **Figure 6.7.6c and 6.7.6d**. The effect of the supplemental damping is even more dramatic with regard to these forces. Forces generated by higher modes of vibration are eliminated and the inertia force is almost constant at 200 kips (890 kN) over the height of the building. The base shear is reduced from 11,500 kips (51,152 knN) to 2,500 kips (11,200 kN).

(b) Nonlinear Dynamic Analyses

The effect of the higher damping on the nonlinear dynamic response of the space frame was also investigated. The envelopes of the maximum response parameters under the Los Gatos ground motion are shown in **Figure 6.7.7**. The maximum lateral displacement, shown in **Figure 6.7.7a** is reduced from 71 inches to 48 inches at the roof level, a reduction of 32%. It can be seen that similar reductions occur in the other parameters. The maximum IDI at the third story, shown in **Figure 6.7.7b**, is reduced from 4.3% to 2.6%, a reduction of 39%. The girder curvature ductility demands that reached a maximum value of 12 are reduced to a more manageable 7 as shown in **Figure 6.7.7c**. The important plastic rotation demand, shown in **Figure 6.7.7d**, is reduced from 4.3% to 2.2%, a reduction of almost 50%. These results indicate that supplemental damping has a very beneficial effect on the dynamic response of this type of framing system under pulse-type excitation. The displaced shape of the frame and distribution of plastic hinges are shown in **Figure 6.7.8**.

Data for the Lexington Dam ground motion is shown in **Figure 6.7.9**. The maximum lateral displacement at the roof level, **Figure 6.7.9a**, is reduced from 50 inches to 36 inches for a reduction of 28%. The IDI, shown in **Figure 6.7.9b** is reduced from 3% to 2.1% for a reduction of 30%. Similar reductions occur in the curvature ductility demands (**Figure 6.7.9c**) and the plastic rotation demands (**Figure 6.7.9d**). The maximum displaced shape of the frame is shown in **Figure 6.7.10**

along with the distribution of the plastic hinges.

The response data for the Takatori ground motion, shown in **Figure 6.7.11**, indicates only a small reduction in the lateral displacement envelope as shown in **Figure 6.7.11a**. However, reductions in the other three response parameters are much more significant. The maximum IDI demand at the second story level (**Figure 6.7.11b**) is reduced from 2.2% to 1.3% for a reduction of 41%. It can also be seen that the Takatori ground motion tends to excite a strong response from the higher modes of vibration in the frame with 5% damping, whereas, in the frame with supplemental damping the IDI demand is almost uniform over the height of the building. This higher mode response is also evident in the maximum curvature ductility demand as shown in **Figure 6.7.11c**. The peak demand of almost 6 is reduced to 3.3 for a reduction of 45%. A similar pattern is shown in **Figure 6.7.11d** for the envelope of maximum plastic hinge rotation. The demand on this important parameter is reduced from almost 2% to less than 1% for a reduction of approximately 50%. The deformed shape of the frame is shown in **Figure 6.7.12** along with the distribution of the plastic hinging.

Response data for the James Road ground motion is shown in **Figure 6.7.13**. This figure indicates that the reductions due to supplemental damping for this record are the largest of the group considered. The peak displacement at the roof level, **Figure 6.7.13a**, is reduced from 51 inches to 29 inches for a reduction of 43%. The peak IDI demand which occurs at the fourth story level is reduced from 3.3% to 1.7% for a reduction of 48% as shown in **Figure 6.7.13b**. The girder curvature ductility demand, shown in **Figure 6.7.13c**, is reduced from just over 9 to 4.5 for a reduction of approximately 50%. The envelope of maximum plastic rotation demand (**Figure 6.7.13d**) indicates a reduction from 3.2% to 1.3% (59%). The displaced shape of the frame and the distribution of the plastic hinging is shown in **Figure 6.7.14**.

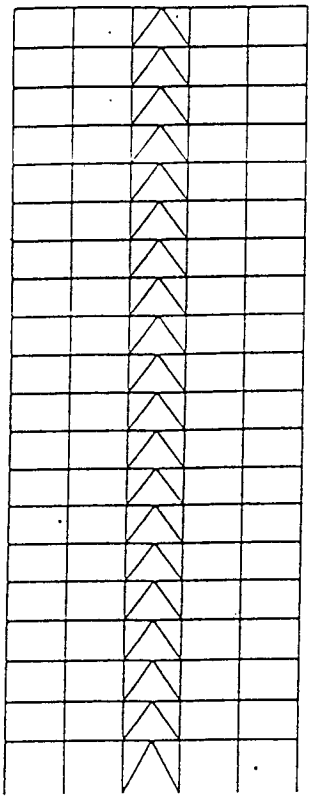

(a) Typical Elevation

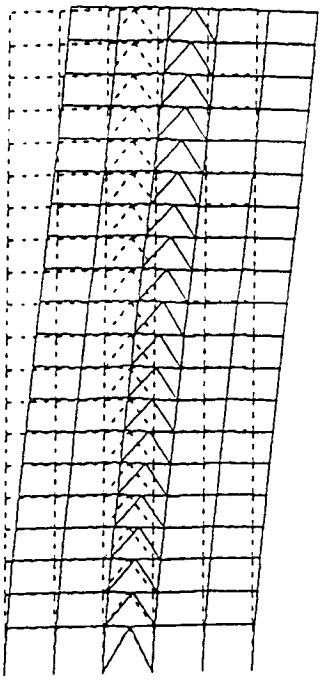

(b) Mode 1

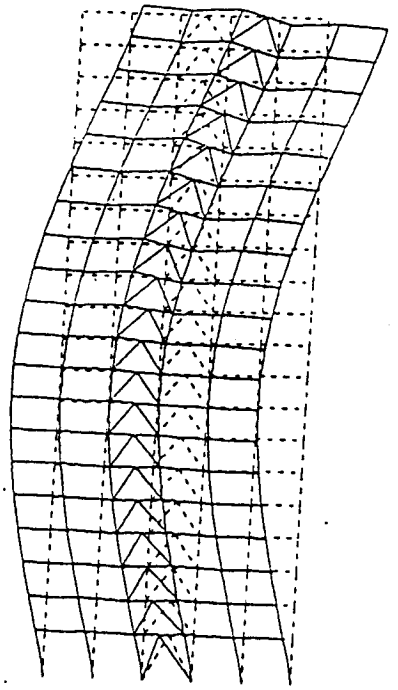

(c) Mode 2

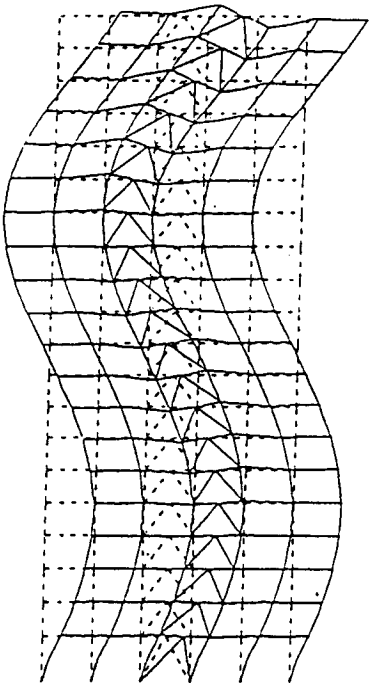

(d) Mode 3

Figure 6.7.1 Retrofitted Steel Perimeter Frame, Single Braced Bay

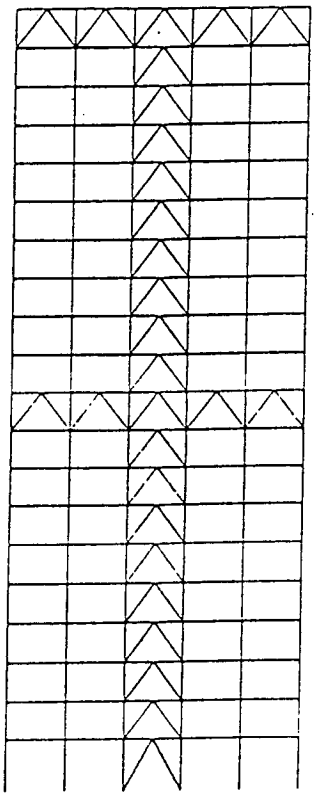

(a) Typical Elevation

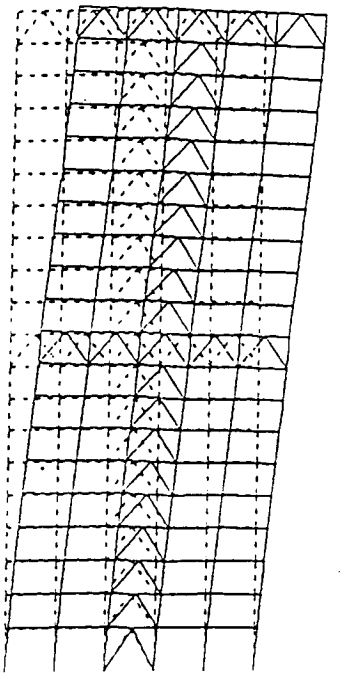

(b) Mode 1

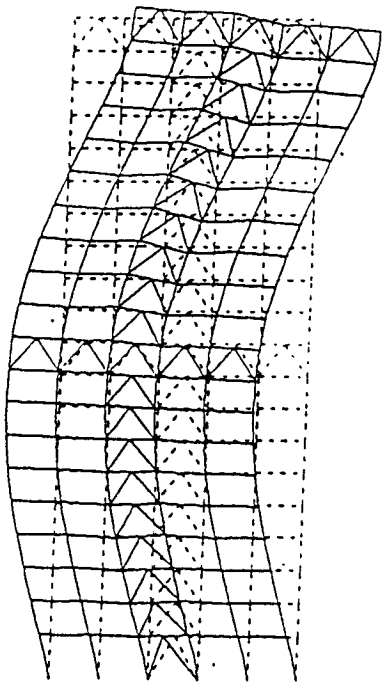

(c) Mode 2

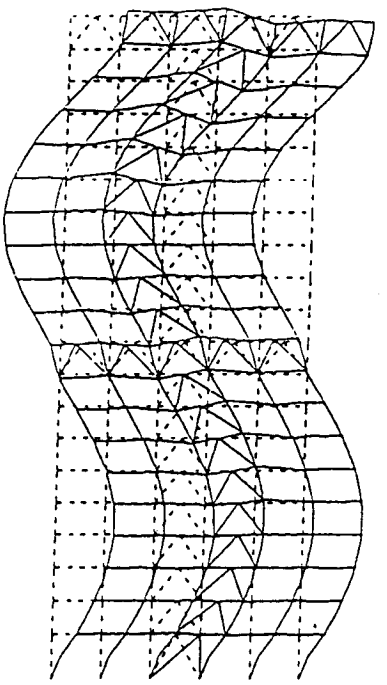

(d) Mode 3

Figure 6.7.2 Retrofitted Steel Perimeter Frame, Single Braced Bay with Belt Trusses

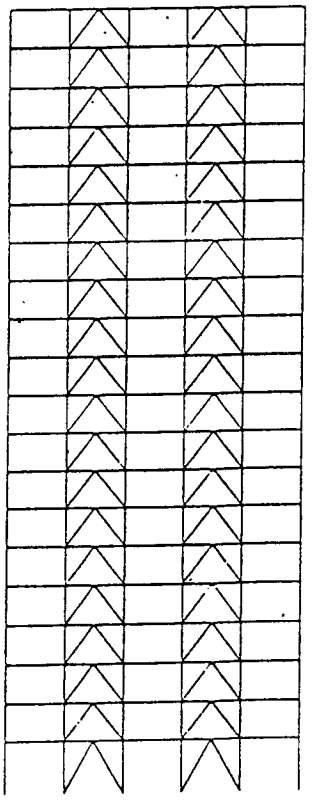

(a) Typical Elevation

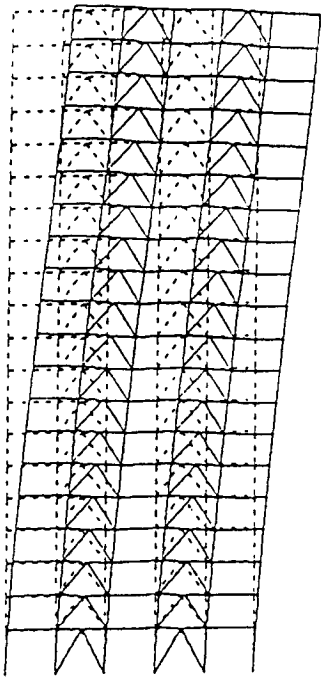

(b) Mode 1

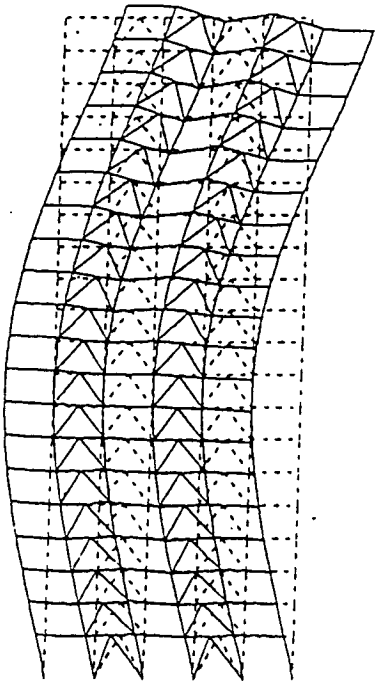

(c) Mode 2

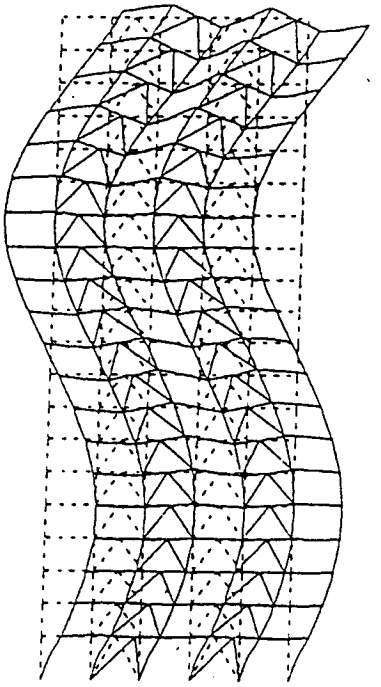

(d) Mode 3

Figure 6.7.3 Retrofitted Steel Perimeter Frame, Two Braced Bays

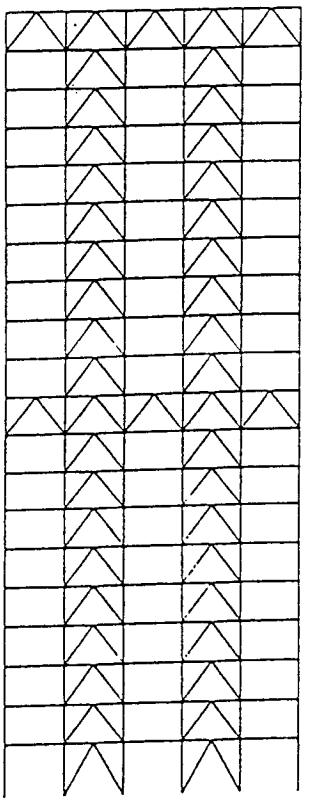

(a) Typical Elevation

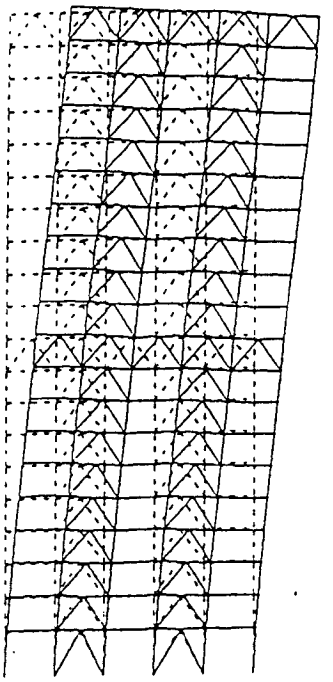

(b) Mode 1

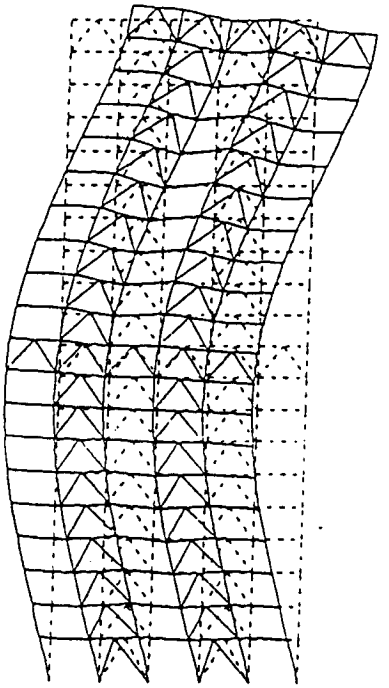

(c) Mode 2

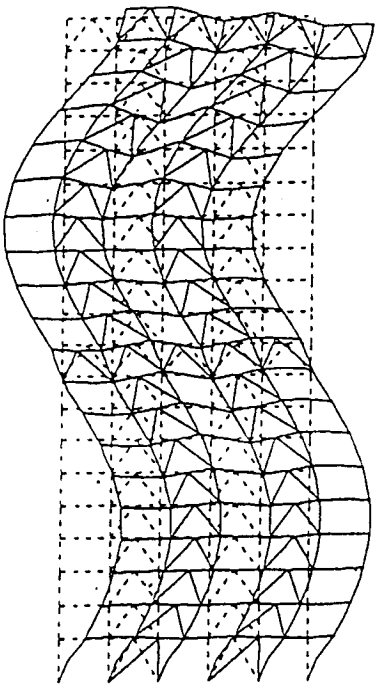

(d) Mode 3

Figure 6.7.4 Retrofitted Steel Perimeter Frame, Two Braced Bays with Belt Trusses

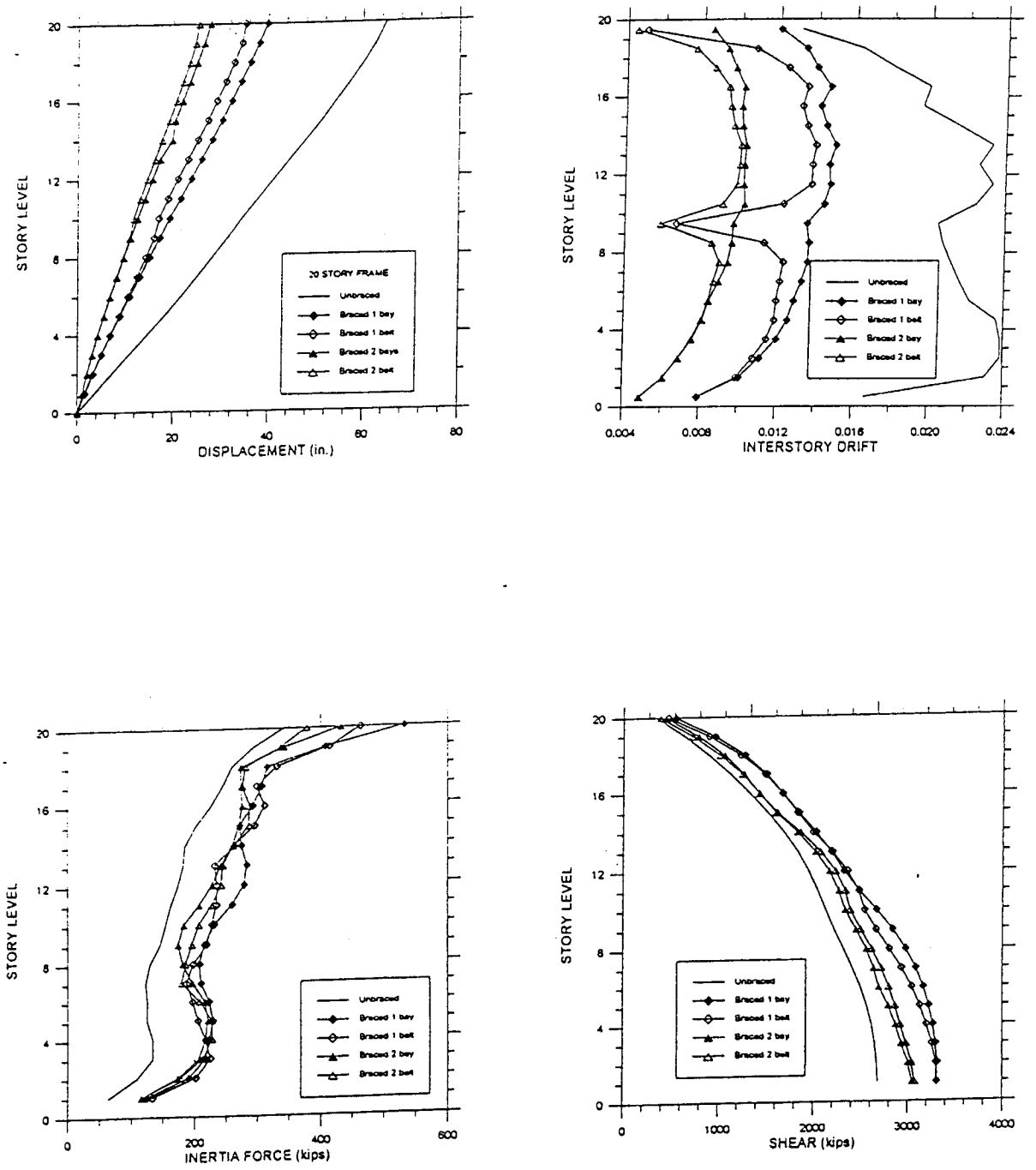

Figure 6.7.5 Elastic Response Results, Retrofitted Steel Perimeter Frame, Los Gatos

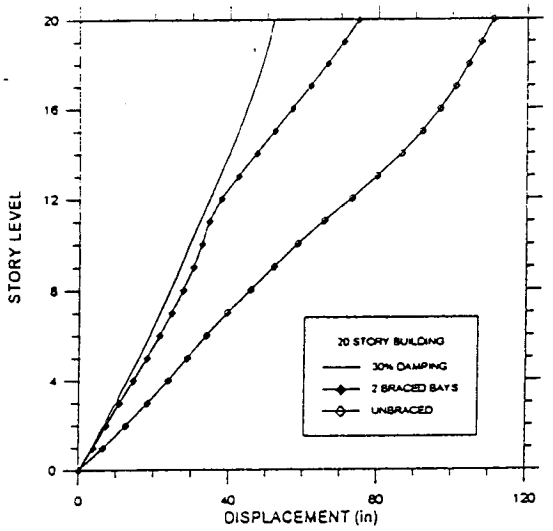

(a) Lateral Displacement

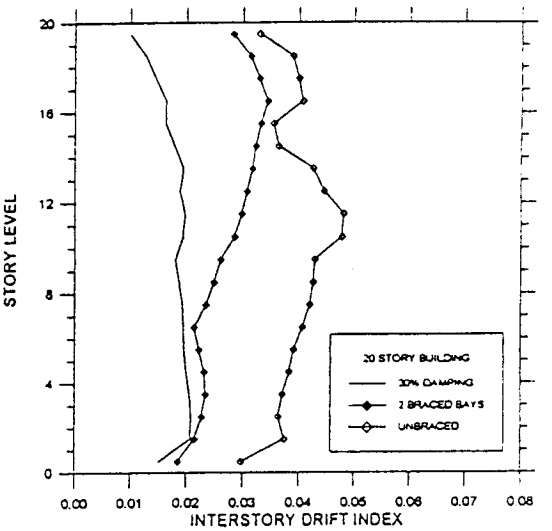

(b) Interstory Drift Index

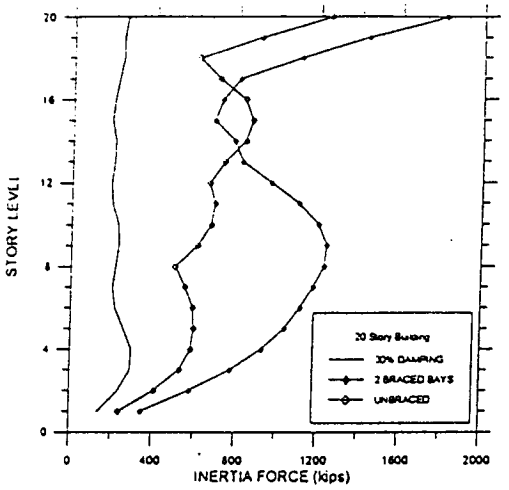

(c) Inertia Force

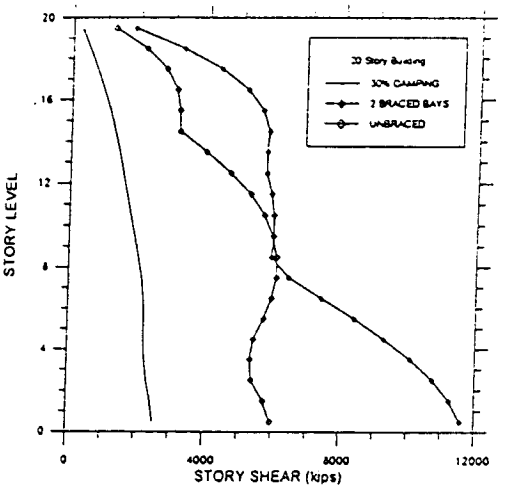

(d) Story Shear Force

Figure 6.7.6 Elastic Response of Retrofit Schemes, Los Gatos

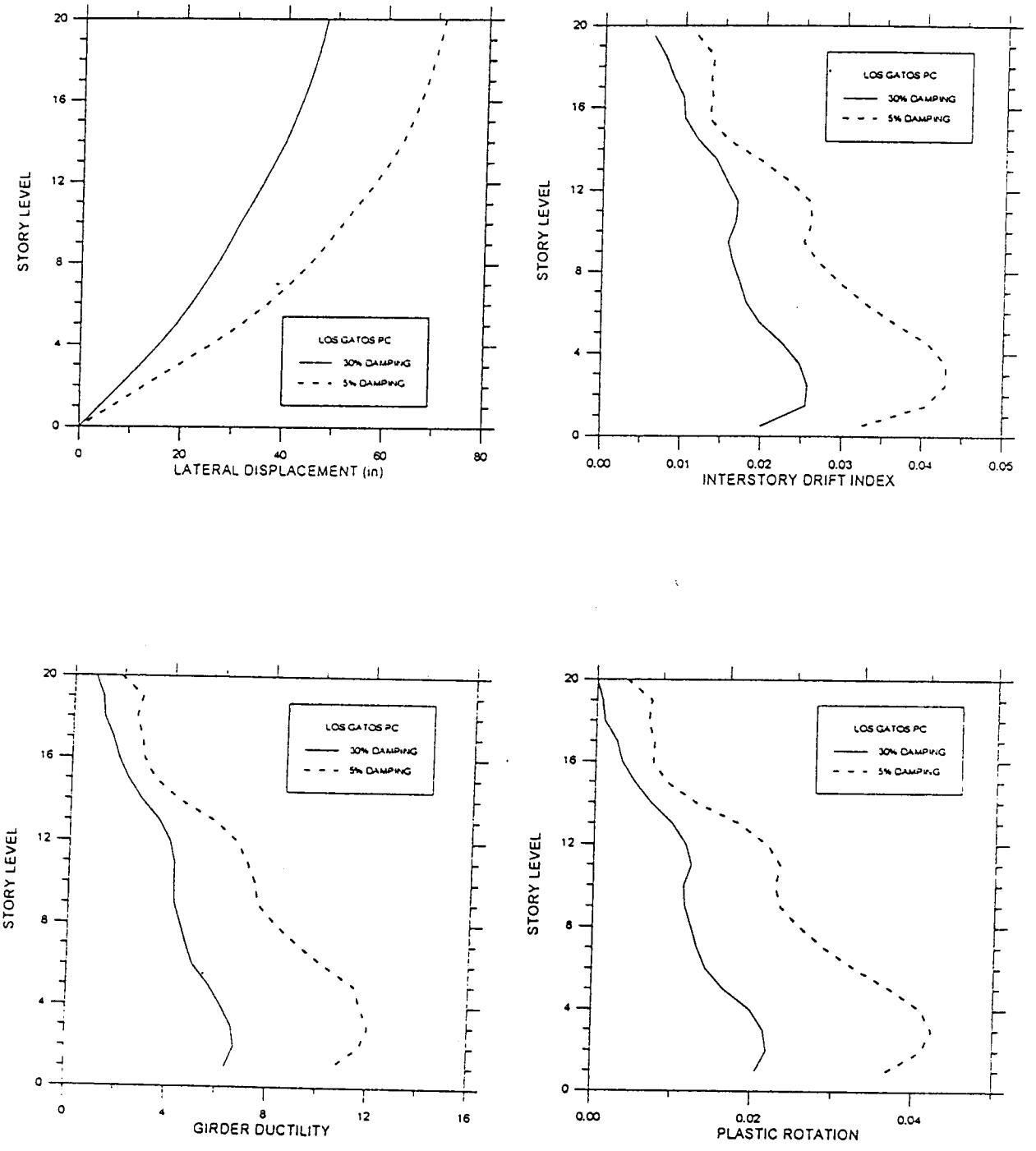

Figure 6.7.7 Influence of Supplemental Damping on Nonlinear Response, Steel Perimeter Frame, Los Gatos

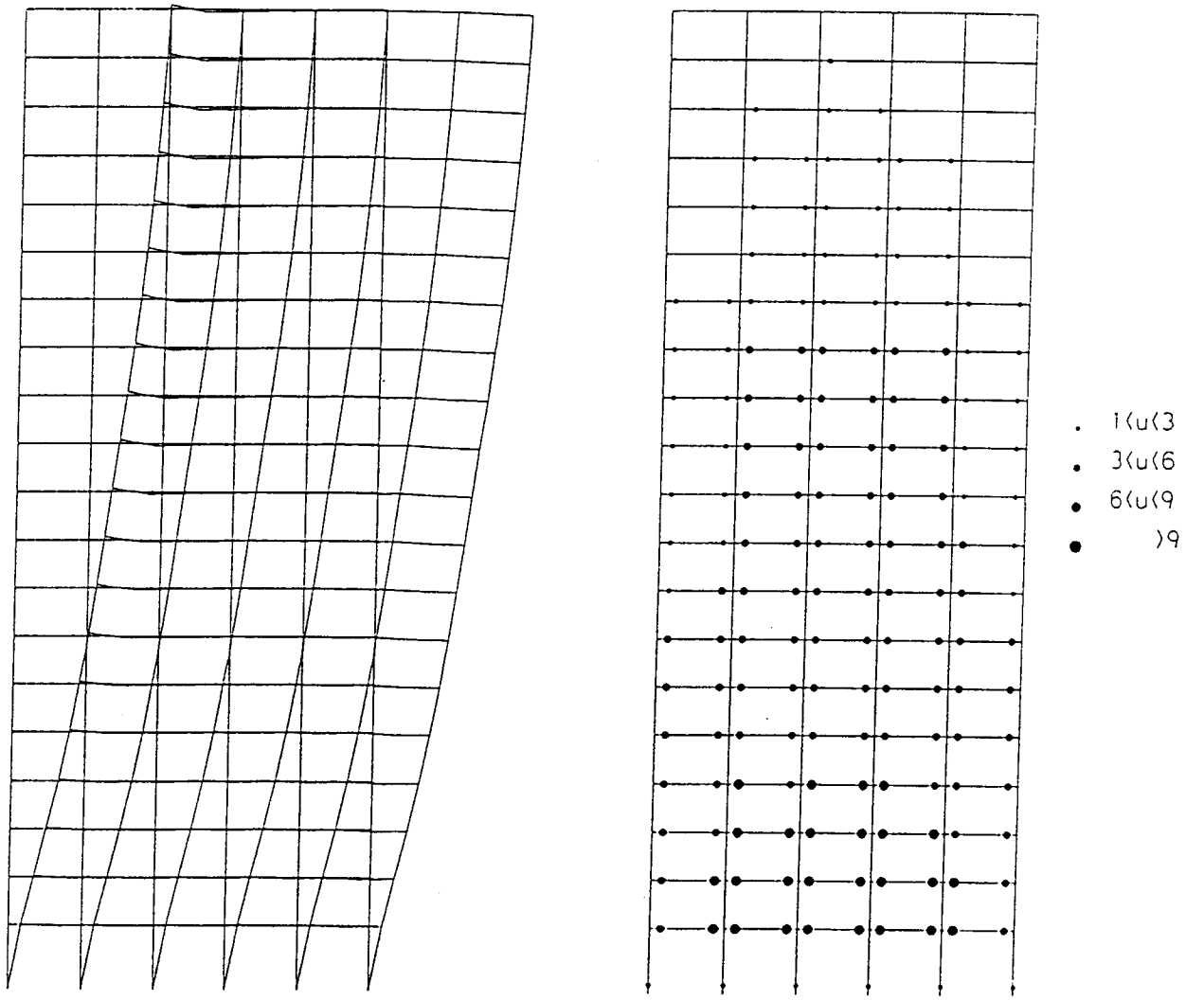

(a) Max. Displaced Shape, Δ_{roof} = 47.9 inches

(b) Plastic Hinge Locations

Figure 6.7.8 Steel Perimeter Frame Response, Los Gatos, ξ=5.0%

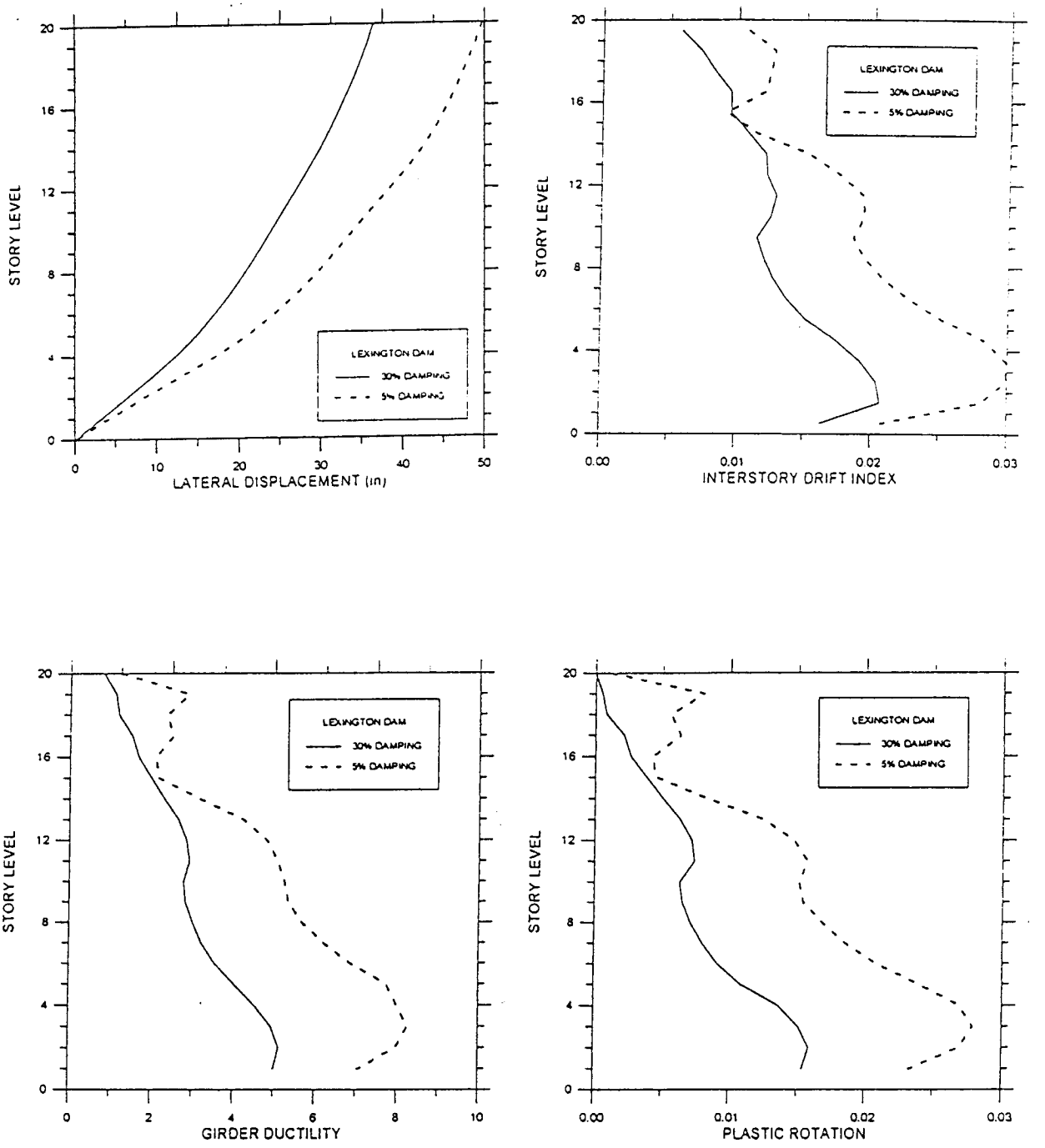

Figure 6.7.9 Influence of Supplemental Damping on Nonlinear Response; Steel Perimeter Frame, Lexington Dam

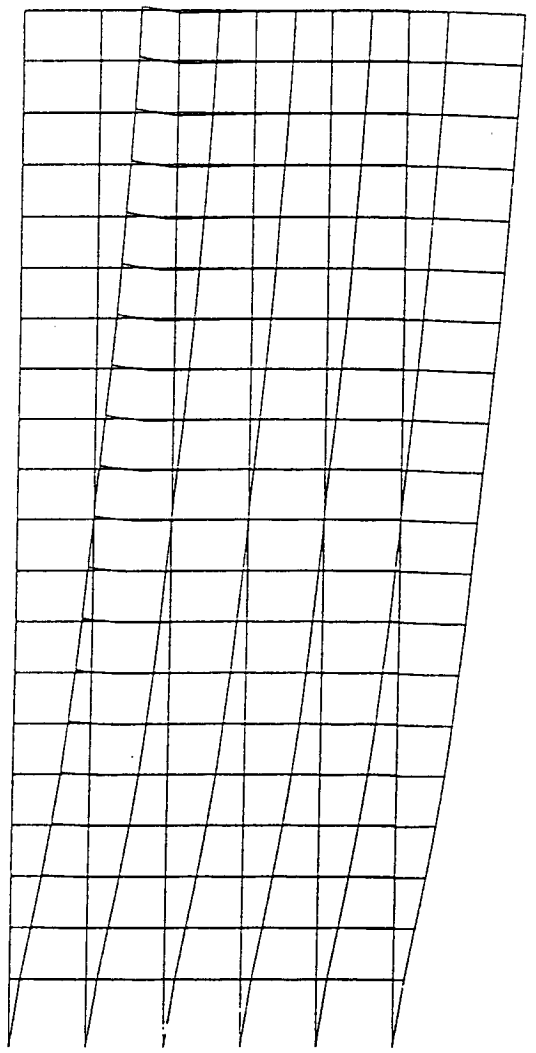

(a) Max. Displaced Shape, Δ_{roof} = 36.4 inches

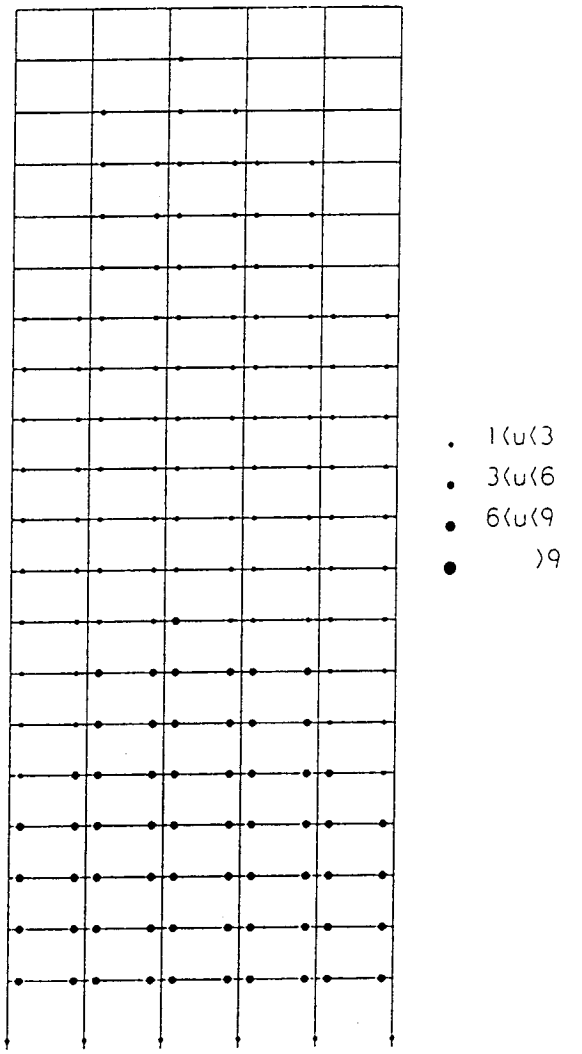

(b) Plastic Hinge Locations

Figure 6.7.10 Steel Perimeter Frame Response, Lexington Dam, ξ=30%

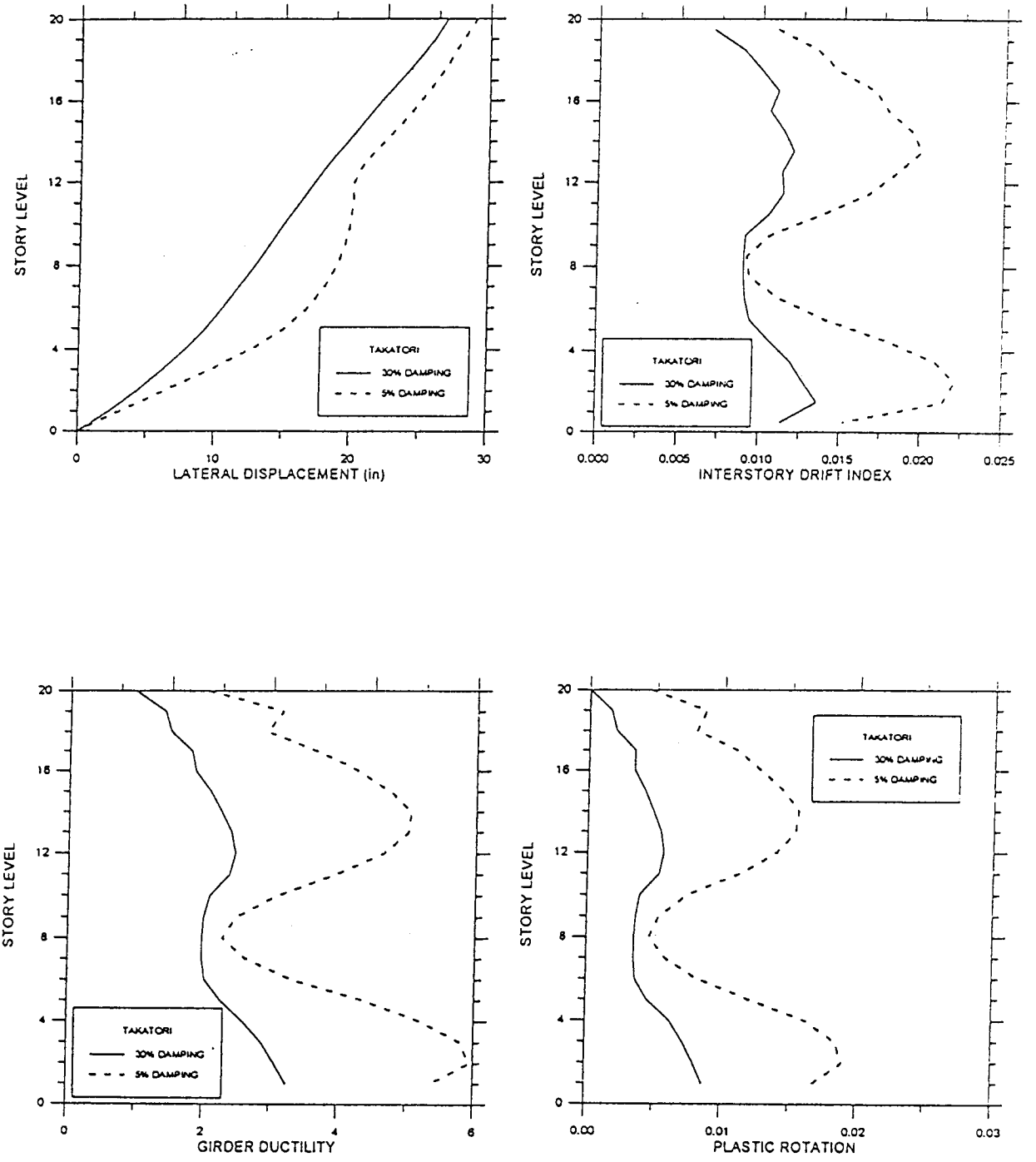

Figure 6.7.11 Influence of Supplemental Damping on Nonlinear Response, Steel Perimeter Frame, Takatori

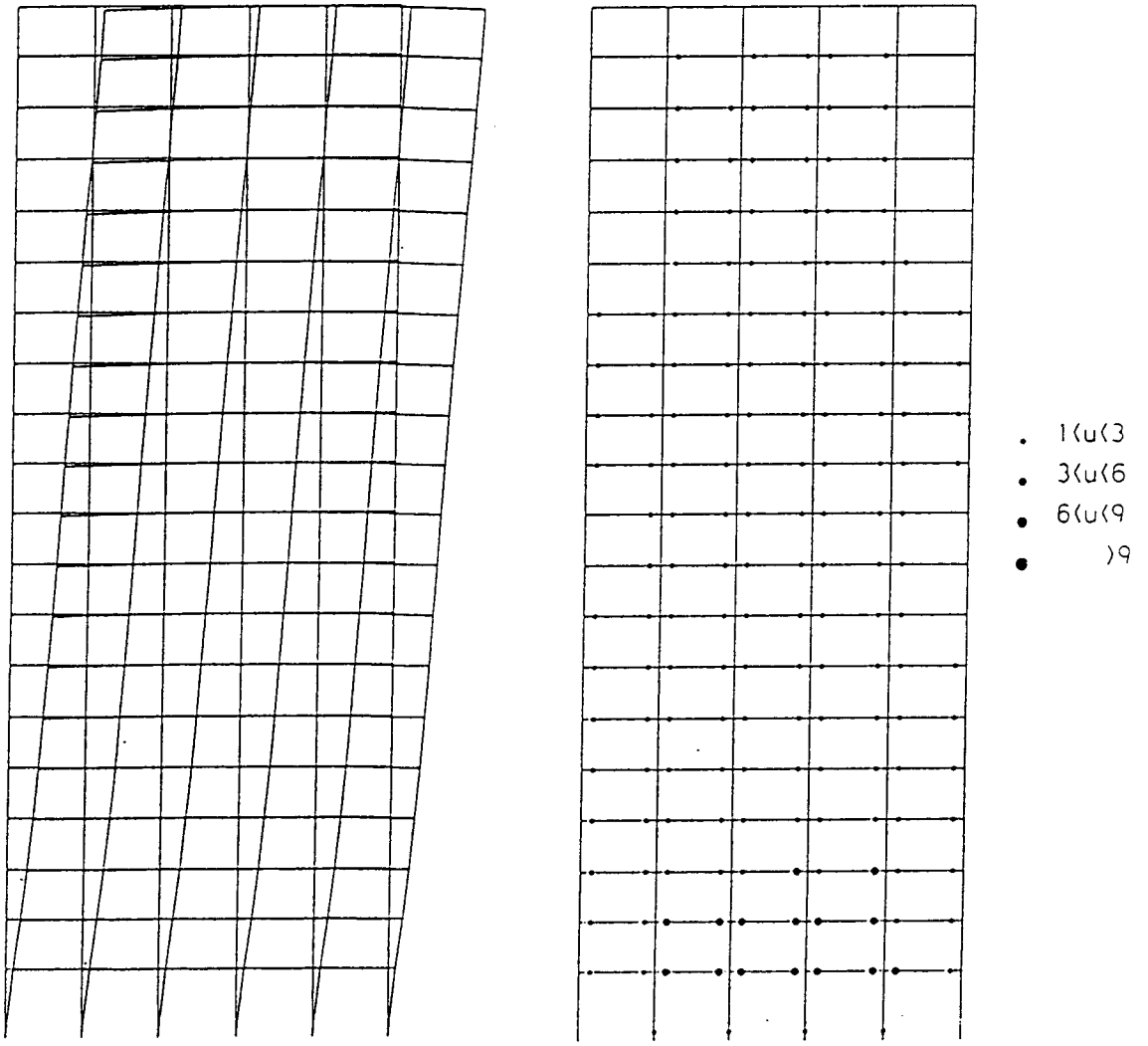

(a) Max. Displaced Shape, Δ_{roof} = 26.9 inches (b) Plastic Hinge Locations

Figure 6.7.12 Steel Perimeter Frame Response, Takatori, ξ=30%

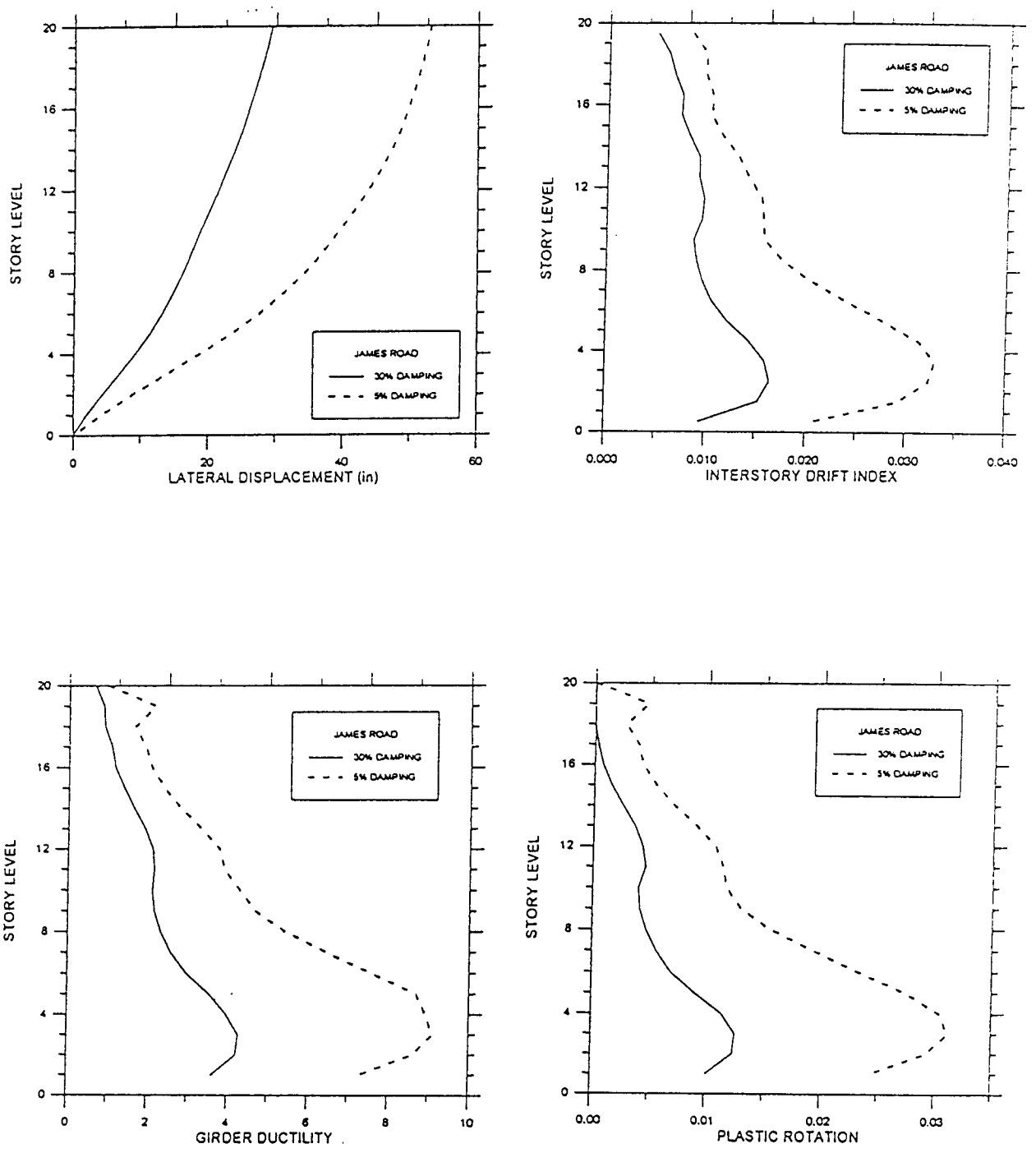

Figure 6.7.13 Influence of Supplemental Damping on Nonlinear Response, Steel Perimeter Frame, James Road

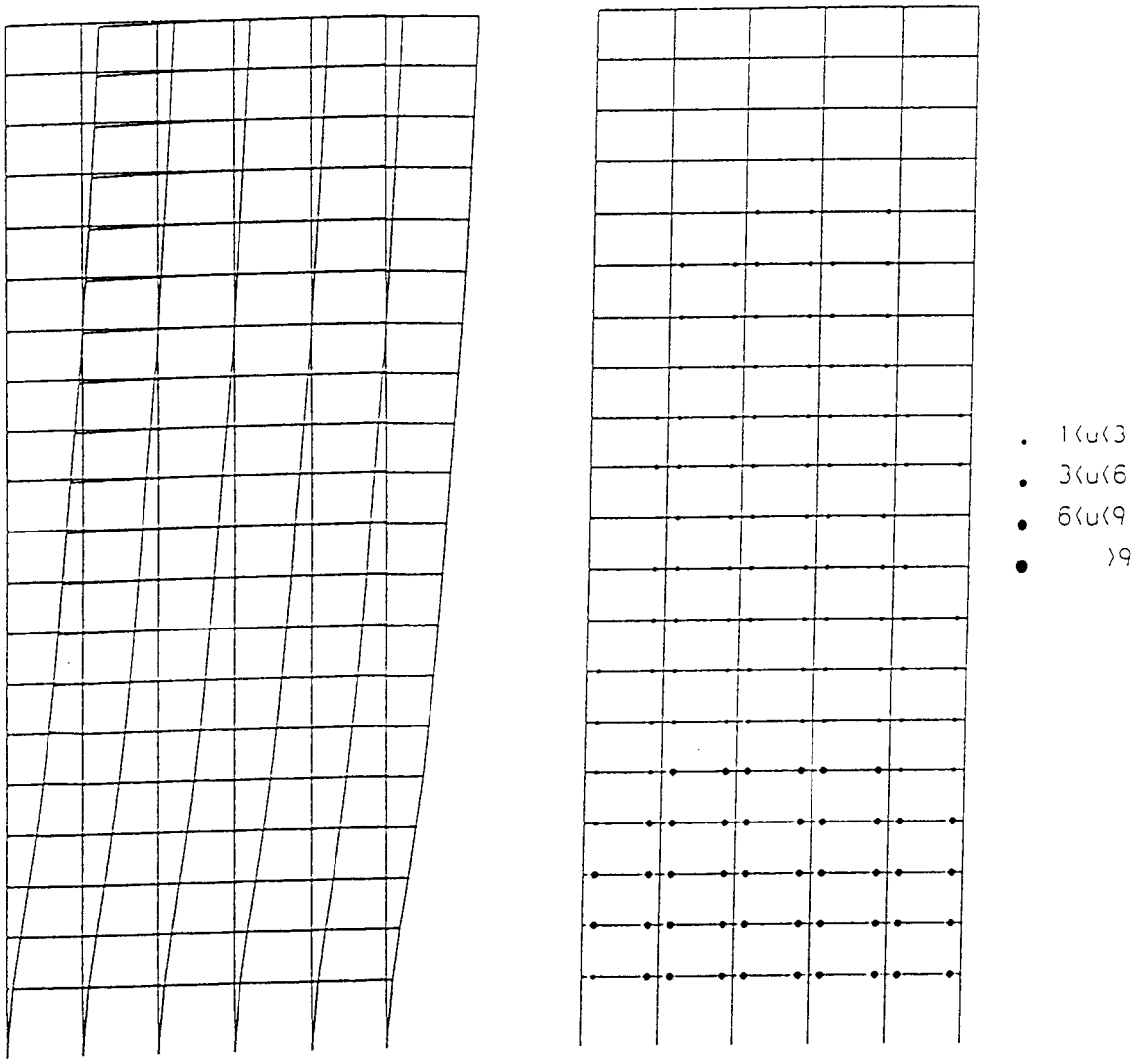

(a) Max. Displaced Shape, Δ_{roof} = 53 inches (b) Plastic Hinge Locations

Figure 6.7.14 Steel Perimeter Frame Response, James Road, ξ = 30%

6.8 OBSERVATIONS REGARDING THE RESULTS OBTAINED IN THE STUDIES CONDUCTED TO INVESTIGATE EFFICIENT STRATEGIES AND TECHNIQUES FOR RETROFITTING (PERFORMANCE IMPROVEMENT) OF EXISTING BUILDINGS

From an analysis of the results obtained in the attempt to attain efficient ways for retrofitting existing buildings of long fundamental periods which are located in sites where severe pulse-type EQGMs can occur, the following observations can be made:

- It will be very difficult to attain efficient (technical and economical) solutions using the conventional strategies and techniques of increasing the stiffness, the strength, or both.

- The use of innovative strategies based on energy dissipation devices, particularly those based on dissipating the input energy through the use of supplemental damping, seems to be very promising, but the required additional damping is high because an effective ξ_{eff} of about 30% is necessary for most of the buildings investigated in this study.

- To efficiently use the innovative strategy, the following problems need to be investigated: (1) what are the most promising techniques for achieving the required supplemental damping and what are the most efficient dampers that should be used; (2) how should these dampers be designed and at what locations should they be placed; (3) how many dampers are necessary, and how should they be installed, supported and interconnected with the existing structure; (4) what is the effect of the velocity-related force generated by the dampers on the structure and (5) what are the design procedures and design criteria to use for the proposed innovative strategy. Regarding the first problem, it appears that the most promising dampers are the viscoelastic or fluid viscous dampers. As far as the second problem, the solution is the use of a very stiff additional structural system to attain what recently has been denominated as ***The Mixed Flexible-Stiff Structure for Controlling Building Performance***, ***Damage Tolerant Structures*** or ***Damage Control Structures*** [Wada, et al., 1999].

7 Selection of Additional Stiff Structure to Support the Dampers to Attain an Efficient Retrofitted Mixed Flexible-Stiff Structure

7.1 GENERAL COMMENTS

The proposed innovative strategy uses supplemental damping to dissipate a significant portion of the input energy and thereby decrease the demanded strength and deformation capacities of the buildings when subjected to severe pulse-type EQGMs. For efficient implementation it is necessary to select what is considered to be the most promising supplemental damping device and then to analyze their location, their design and their support and interconnection with the existing structure. A brief discussion of the type of dampers that could be used and how to locate, support, and interconnect them with the existing structure follows.

7.2 TYPE OF DAMPERS

Although different types of supplemental damping devices have already been used in several countries to control the seismic response of buildings, it appears that in order to obtain a total ξ_{eff} of approximately 30%, the most promising type is the fluid viscous dampers. For certain of the buildings considered in this study, the combined use of viscoelastic and fluid viscous dampers may have application. The selection and design of these devices should be investigated in the next phase of the overall research program.

7.3 SUPPORT AND INTERCONNECTION OF THE DAMPERS WITH EXISTING STRUCTURE: USE OF A MIXED FLEXIBLE-STIFF STRUCTURE SYSTEM

A very preliminary conceptual design of the stiff structural system that could be added to the existing or redesigned S-K building was sketched in **Figure 6.6.4b**. The stiff system consists of steel braces connected to the bottom beam-column joints of the existing structure (which in the bottom stories might need to be reinforced) and the top of these supports the fluid viscous dampers (and layers of viscoelastic material, if necessary) which are connected to the top beam-column joints of the existing

structure. The relative movement at each story between the relatively flexible structure and the very stiff braced system permits the development of the needed damping. The steel braces have to be designed to remain in their elastic range of response under the maximum expected response of the entire mixed structural system.

8 Summary of Results, Conclusions, Recommendations, and Guidelines for Solutions to Control the Seismic Effects of Severe Pulse-Type EQGMs

8.1 SUMMARY OF RESULTS

After reviewing the main characteristics of ground motions recorded at stations close to fault rupture, the following records were selected for consideration in the detailed analyses:

- 8 records obtained before the 1994 Northridge EQ
- 13 records obtained during the 1994 Northridge EQ
- 10 records obtained during the 1995 Kobe EQ

The damage potential of most of these recorded ground motions that are critical for the case study buildings was analyzed. This analysis shows that for buildings with fundamental period, $T \geq 1.0$ sec, the Los Gatos 1 and Takatori 1 recorded EQGMs give the largest demands on velocity and displacement of SDOF systems.

To study the effects of severe pulse-type EQGMs on tall multi-degree-of-freedom structures, the response of the following existing and redesigned buildings were considered:

- **30-Story RC S-K Building** redesigned using performance-based engineering through the Comprehensive Conceptual Approach [Bertero, R.D., and Bertero, V.V. [1992].
- **30-Story RC S-K Building** as built in 1983.
- **30-Story RC S-K Building** redesigned for UBC 1991 [Anderson and Chen, 1992].
- **15-Story RC Building** (13 stories above grade and 2-story basement) as built in 1965.
- **40-Story Steel Space Frame** as built [Anderson and Bertero, 1998].
- **20-Story Steel Perimeter Frame** as designed for 1994 UBC.

Earthquake records used for the analyses of the case study buildings included Loma Prieta (2), Kobe (2), Imperial Valley (1) and Idealized Pulse (1).

8.2 CONCLUSIONS

From the results of the studies conducted, the following preliminary conclusions can be drawn:

8.2.1 Conclusions Regarding the Damage Potential of Recorded Severe Pulse-Type EQGMs

- The spectral values for the main response parameters [(Yielding Seismic Coefficient (C_y), Maximum Displacement (u), Interstory Drift Index (IDI), Maximum Curvature Ductility, Maximum Plastic Rotation, Maximum Cumulative Plastic Rotation, Input Energy (E_I), Hysteretic Dissipated Energy (E_H), and Damage Potential] of the recorded severe pulse-type ground motions are significantly larger than those obtained from standard design EQGMs considered in the Seismic Provisions of the Building Codes, particularly for buildings with long periods.

- Similar demands (damage potential) to those of the recorded pulse-type EQGMs can be obtained by idealizing these recorded ground motions by three successive acceleration pulses that lead to a full-cycle of reversal sine velocity pulse and a half-cycle of sine displacement pulse.

- The response of SDOFSs and MDOFSs to the idealized pulses (and consequently to the recorded severe pulse-type EQGMs) are very sensitive to the intensity and period (duration) of the severe pulse. Furthermore, in the case of MDOFSs for a given pulse intensity, the distribution of the IDI, the story ductility, local ductility, and damage index demands along the height of the buildings vary significantly with the supplied yielding strength (C_y) to the building. There is a migration of the maximum demand values from the lower stories of the building toward the upper stories with an increase in the supplied C_y values.

- For buildings with a $\xi = 5\%$, 1.00 sec $\leq T \leq$ 2.5 sec, the Los Gatos and Takatori recorded EQGMs (which are the normal components to the causative fault) give the largest demands on velocity and displacement. For 2.5 sec $\leq T \leq$ 4.0 sec, the Los Gatos is the most critical recorded EQGM. For this last range of the values of T, while the elastic response spectra for most of the recorded severe pulse-type EQGMs demand displacements that are about twice those demanded by the "standard design EQGMs." The Los Gatos spectra demands are 3.00 to 4.75 times these "standard demands."

- For buildings with $\xi = 5\%$ and T = 1.5 sec, the Takatori record requires an elastic Seismic Coefficient, C, that is about 3.8 times that required by the 1997 UBC for sites having soil profile S_d and located at a distance greater than 15 km from the causative fault. For sites that are less than 2 km from a Seismic Source Type A, this value drops to about 1.9 times. For buildings with a T = 2.5 sec, the Los Gatos record requires an elastic C that is about 3.1 times or nearly 1.55 times the value required by the code depending on whether the sites are at distances greater than 15 km or less than 2 km from the fault, respectively. For buildings with

T = 4.0 sec, the above ratios for the Los Gatos record are about 2.7 and 1.35, respectively.

- The ultimate strengths required by the 1997 Code for standard occupancy buildings having a period between 1.5 sec and 3.5 sec and a $\xi = 5\%$ are significantly less than the demanded strength of recorded pulse-type EQGMs, even if the buildings can develop a global ductility of 6 which allows the use of an R value of 8.5. For the Los Gatos 1 record and T = 2.5 sec, the ultimate strength demand is about 4 times greater than the Code required strength for buildings located at distances greater than 15 km from the fault. The ultimate strength demand is about 2.7 times greater if the sites are less than 2 km from the seismic source. Therefore if buildings designed according to the 1997 UBC are subjected to EQGMs like those recorded at the Los Gatos PC, these buildings will be required to develop very high ductilities (global, story, and local) which cannot be economically supplied. Even if this could be accomplished, they could not be used because limitations in the acceptable IDI values will control the maximum ductility that can be used.

- The IDI spectra for the recorded pulse-type EQGMs indicate that for buildings with a total height greater than 60 m (15 or 20 stories), it will be necessary for their fundamental period to be smaller than about 1.2 sec if the acceptable IDI is 1.5%, and 0.9 sec if the acceptable IDI is 1.0%. The design for these low values of the IDI could lead to the use of uneconomical structural systems, thus larger acceptable IDI should be allowed; however, this will require changing the way of designing and detailing the so-called nonstructural components.

- The velocity response spectra (S_v) vary significantly in shape and intensity (peak values) with the different recorded severe pulse-type EQGMs. They also differ significantly from those corresponding to the "standard design EQGMs" which show a flat top with a value of about 143 cm/sec. For the range of T between 1 .5 sec and 4 sec, the S_v for the severe pulse-type EQGMs show peak values up to 4.5 times that of the "standard design EQGMs."

8.2.2 Conclusions Regarding the Expected Seismic Performance of Existing and Redesigned Long Period Buildings under Severe Pulse-Type EQGMs

The performance of three existing, one designed and two redesigned, buildings was investigated. From this investigation, the following preliminary conclusions can be formulated:

- The results obtained in the nonlinear static (pushover) and dynamic (time-history) analyses reveal that the seismic performance of each of the six analyzed buildings is unacceptable if they can be subjected to the critical pulse-type EQGM that has been recorded. The main reason for unacceptable performance is that the IDI exceeds what is at present considered an acceptable value for the life safety performance level. The best performance has been obtained with the conceptually performance-based designed building. The only weakness in the response of this building is that the demanded maximum IDI is a little above 2% which may be acceptable in the United States.

- The resulting poor performance could have been anticipated in the light of the results obtained from the studies on the damage potential of the recorded pulse-type EQGMs. Their comparison with the Pseudo Acceleration (ultimate strength) design spectra adopted by the US Building Codes and the Velocity Spectra recommended in the Japanese Building Code (200 cm/sec for soft soils) clearly indicate this behavior.

- The performance of the buildings that have been studied has been shown to be very sensitive to variations in the dynamic characteristics (shape, intensity, and T_p) of pulse-type EQGMs.

- A very welcome surprise has been the significant effects of increasing the damping coefficient ξ_{eff} on the demanded performance of the buildings. An increase from $\xi_{eff} = 5\%$ to $\xi_{eff} = 30\%$ leads to reductions of up to 60% on the demanded values for the different main response parameters.

- Most of the medium-rise and highrise buildings in the US which are built on sites located in regions where severe pulse-type EQGMs can occur and that have been designed and constructed according to just the minimum seismic requirements of the building codes prior to 1997 will perform poorly. Even the application of the 1997 UBC seismic design provisions may result in buildings with poor performance.

- For a selected pulse-type EQGM, the location of the maximum demanded values for the deformation and damage response parameter of a given tall structural system is very sensitive to any variation in its global stiffness and yielding strength. In making the structure stiffer, there is a migration of the maximum deformation demands from the upper to the lower stories. In making the structure stronger, the demanded maximum values migrate from the lower stories toward the upper stories.

8.2.3 Conclusions Regarding the Seismic Upgrading (Retrofitting) of Existing Long Period Structures Subjected to Pulse-Type EQGMs

From the results of the studies conducted to seismically upgrade (retrofit) three existing buildings, one that has been designed according to the conceptual approach of performance-based seismic design, and one that has been designed according to the 1994 UBC, the following preliminary conclusions can be formulated:

- The most significant weakness of all the buildings that have been studied seems to be the unacceptably high IDI.

- While in two of the three RC buildings (the as-built and the conceptually redesigned S-K building), the critical regions of the members have been supplied with adequate usable toughness. In the case of the 15-story as-built building, most of its critical regions lack not only adequate toughness but also required strength because of the small amount and poor detailing of its longitudinal and transverse reinforcements. These weaknesses seem to be

present in most of the RC moment-resistant buildings designed and built in the United States before 1960. A promising strategy for removing such weakness appears to be the use of steel jacketing of the beam-column joints and encasing the columns and beams (with part of their adjacent slab) with steel plates. However, the use of this seismic upgrading strategy alone to remove the main weakness (which is the large interstory drift indices (IDI)) does not seem to work.

- The use of a traditional or conventional approach for improving the performance of existing structures by the strategy of increasing the stiffness and/or strength does not seem to lead to an efficient seismic upgrading solution when the structures have long periods and can be subjected to severe pulse-type EQGMs. The stiffening of the structure will reduce the IDI, however, it will also shorten the period of the structure and consequently move it toward a region of higher spectral acceleration response. Hence, it results in higher lateral forces which make it necessary to increase the strength (seismic coefficient C_y) to such high values that it becomes uneconomical.

- Innovative strategies and techniques are needed to control the seismic response at the life-safety performance level of these long period structures if they can be subject to severe pulse-type EQGMs. The most promising strategy seems to be the use of energy dissipation devices; among the many different types of these devices the most efficient seems to be the viscoelastic and/or fluid viscous dampers.

- The performance of the two 30-story S-K buildings and the 40-story steel building can be improved to acceptable levels for life-safety by additional damping that will result in a total effective damping (ξ_{eff}) of about 30% of critical.

- For the 15-story RC building, a combined retrofit (upgrading) procedure of strengthening and increasing the energy dissipation is necessary to accomplish the following: (1) strengthen all the members with the minimum practical thickness of steel plates that can be used for jacketing the beam-column joints and columns and for encasing the beams and portion of the adjacent slabs; and (2) add supplemental damping to increase the ξ_{eff} to a value of 30%.

- The addition of supplemental damping to the 40 Story Steel Building will reduce the IDI to less than 1.5%, thereby meeting the current acceptable value for life safety. Girder curvature ductility demands for all four of the recorded pulse-type motions are reduced to less than 2.0.

- Supplemental damping reduces the IDI demand for the 20 Story Steel Frame to a maximum of 2.5%. Since this is still above the acceptable level, it will be necessary to combine an increase in stiffness (chevron bracing) with supplemental damping in order to meet the 1.5% IDI criteria. Girder ductility demands of 5-6 are within possible bounds and the maximum plastic rotation demands are approximately 2% which should be attainable.

8.3 RECOMMENDATIONS AND GUIDELINES TO CONTROL THE SEISMIC EFFECTS OF SEVERE PULSE-TYPE EQGMs ON NEW AND EXISTING BUILDINGS

From the results obtained in the studies conducted herein and the above preliminary conclusions, the following preliminary recommendations and guidelines are suggested to control the effects of severe pulse-type ground motions on new buildings and existing buildings designed and constructed in the United States.

8.3.1 New Buildings

- Avoid constructing long period, slender buildings on or near active faults and particularly on sites with soft soils.

- Select a structural layout that is as regular as possible and which allows the use of a structural system having a relatively large number of bays with short spans to facilitate the design and construction of stiff and strong buildings.

- Increase the damping that is inherent in the structural system by the addition of supplemental damping devices that will increase the effective damping to more than 25% of critical.

- For short period buildings less than ten stories in height, consider the use of base isolation to decrease the required strength and stiffness that would be required using a more conventional fixed base structural system.

- For long period, medium to tall buildings, the innovative system based on the use of passive energy dissipation devices which in Japan has been called the "***Mixed Flexible-Stiff Structural System***" or the "***Damage Control Structural System***" appears to be very promising.

8.3.2 Existing Buildings

(a) Reinforced Concrete (RC) Frame Buildings

- Most of the existing R/C frame buildings designed and constructed in the U.S. before 1972 offer many weaknesses in practically all their structural members (beams, columns, beam-column joints, slabs and foundations). A technique which can be used to remove these weaknesses is to jacket the beam-column joints and columns and to encase the beams and a portion of the adjacent slabs with thin steel plates which will increase the building global ductility and strength. The upgrading is then completed as follows:

- For short period, low-rise buildings up to ten stories in height, use base isolators either alone or in combination with passive energy dissipation devices.

- For long period buildings with fifteen or more stories, use energy dissipation devices by adding a stiff secondary structure to support these devices according to the innovative strategy known in Japan as "***Mixed Flexible-Stiff Structural System***" or the "***Damage Control Structural System.***"

*(b) **Steel Frame Buildings***

- Most of the existing steel frame buildings in the U.S. are too flexible. The application of passive energy dissipation devices supported by either diagonal cross bracing or chevron bracing offers an attractive means of reducing the deformation demands on the members and joints in these buildings.

- The performance of steel buildings during the Northridge earthquake has clearly indicated that welded moment connections used in steel building construction during the 1970s and 1980s are susceptible to severe damage. In order to retrofit these buildings it will be necessary to upgrade the connections and to reduce the seismic demand, particularly the plastic rotation at the welded connections, through the use of passive energy devices in the buildings.

9 References

Alavi, B., and H. Krawinkler. H. 1997. *Effects of Near-Field Ground Motion on Long Period Building Structures.* Progress Report. Stanford, California: Dept. of Civil and Environmental Engineering, Stanford University.

Anderson, J. C., and V. V. Bertero. 1998. *Seismic Response of a 41-Story Steel Building.* U.S. Geological Survey Professional Paper 1552C. Washington, D.C.: U.S. Government Printing Office.

Anderson, J.C., and W. Chen. 1992. *Aseismic Design of the Thirty Story S-K Building.* Report No. CE93-05. Los Angeles: Dept. of Civil Engineering, University of Southern California.

Bertero, R. D., and V. V. Bertero. 1992. *Tall R/C Buildings: Conceptual Earthquake-Resistant Design Methodology.* Report No. UCB/EERC-92/16. Berkeley, California: Earthquake Engineering Research Center, University of California.

Bertero, V. V. 1997. *State-of-the-Art-Report on the Use of Innovative Strategies and Techniques to Reduce Seismic Risks.* (In-House Report). Berkeley, California: Earthquake Engineering Research Center, University of California.

Bertero, V. V. 1977. "Strength and Deformation Capacities of Buildings under Extreme Environments," in *Structural Engineering and Structural Mechanics,* Karl Pister, ed., pp.188–237. Englewood Cliffs, N.J.: Prentice Hall.

Bertero, V. V., et al. 1999. "Impulse Earthquake Ground Motions: A Historical and Critical Review," in *Proceedings, 1999 SES Structures Congress,* pp. 91–94. Reston, Va.: ASCE.

Bertero, V. V., et al. 1976. "Establishment of Design Earthquakes —— Evaluation of Present Methods," in *Proceedings, International Symposium on Earthquake Structural Engineering, St. Louis, Missouri,* vol 1, pp. 551–80. University of Missouri-Rolla.

CSI. 1992. *ETABS, Three Dimensional Analysis of Building Systems.* Berkeley, California: Computers and Structures, Inc.

Prakash, V., G. H. Powell, and S. Campbell. 1993. *DRAIN 2DX Base Program Description and User Guide. Version 1.1.* Report No. UCB/SEMM-93/17. Berkeley, California: University of California.

International Conference of Building Officials. 1991, 1994, 1997. *Uniform Building Code (UBC).* Whittier, California.

Paulay, T. 1977. "Seismic Design of Ductile Moment-Resisting Reinforced Concrete Frames, Columns: Evaluation of Actions." Bulletin, New Zealand National Society for Earthquake Engineering 10(2).

Sasani, M., and V. V. Bertero. 1997. *Effects of Severe-Pulse-Type of Earthquake Ground Motions.* (In House Report). Berkeley, California: Earthquake Engineering Research Center, University of California.

Sasani, M., et al. 1999. *Seismic Assessment of an Old Instrumented Reinforced Concrete Frame Structure.* PEER Report (forthcoming). Berkeley, California: Pacific Earthquake Engineering Research Center, University of California.

SEAOC.1996. "Recommended Lateral Force Requirements and Commentary." *Blue Book,* 6th ed. Sacramento, California: Structural Engineers Association of California.

SEAOC Vision 2000 Committee. 1995. *Performance-Based Seismic Engineering.* Report. Sacramento, California: Structural Engineers Association of California.

Wada, A., et al. 1999. "Passive Damping Technology for Buildings in Japan," in *Progress in Structural Engineering and Materials* 2(3):1–15. London: Construction Research Communications, Ltd.

Zagajeski, S. W., and V. V. Bertero. 1977. *Computer Aided Optimum Seismic Design of Ductile Reinforced Concrete Moment-Resisting Frames.* Report UCB/EERC-77-16. Berkeley, California: Earthquake Engineering Research Center, University of California.

APPENDIX A

IMPULSE EQGMs: AN HISTORICAL AND CRITICAL REVIEW

IMPULSE EQGMs: A HISTORICAL AND CRITICAL REVIEW

Vitelmo V. Bertero (FM)[1], James C. Anderson (M)[2], and Mehrdad Sasani[3]

Abstract

This paper presents a historical and critical review of recorded earthquake ground motions (EQGMs) that contain severe acceleration pulses and the effects of these motions on the performance of buildings in order to identify the major issues and directions for their solution. The results of some previous studies are summarized.

Introduction

Earthquake ground motions generally consist of random vibrations; however, their possible effect on structures has been visualized and analyzed by assuming that they are periodic or harmonic motions. In spite of the fact that analyses of accelerograms recorded during earthquakes that have occurred since the 1950s show that EQGMs can also be of impulse type, only recently has the possible occurrence of EQGMs with one or more severe acceleration pulses and their importance for the earthquake-resistant design of civil engineering structures been recognized and introduced into the seismic provisions of building codes through the introduction of the near-source factor (UBC 1991, 1977). The main objective of this paper is to present a historical and critical review of recorded EQGMs that contain severe acceleration pulses, and of the studies regarding the effects of these pulses on the seismic performance of buildings. The critical review focuses on identifying the following: the main results obtained from the studies conducted; the reasons for the delay in recognizing the importance of these results and incorporating them into the building code seismic provisions; the reasons for limiting the possible occurrence of EQGMs having severe acceleration pulses to building sites located less than 15 km from the seismic source when recorded data have indicated that severe acceleration pulses can occur at sites located at epicentral distances larger than 150 km; the reliability of applying the recommended near source factor to only the required strength (i.e., the seismic base shear).

Historical and Critical Review

The record obtained during the Port Hueneme earthquake of March 18, 1957, was shown to be essentially a single pulse of energy (Housner and Hudson, 1958). In spite of the small Richter magnitude (M) of 4.7 and low peak ground acceleration of 0.08g, the earthquake caused exceptional damage. Destructive single-shock EQGMs associated with moderate M (5.4 to 6.2) and shallow foci (<30 km) occurred in Agadir in 1960 (Despeyroux, 1960), Libya in 1963 (Minami, 1965), Skopje in 1963 (Ambraseys, 1964), and San Salvador in 1965 (Rosenblueth and Prince, 1965).

A relatively small M=5.6 shallow earthquake occurred on the San Andreas fault at Parkfield on June 27, 1966. An EQGM record obtained at a distance of 200 feet from the fault shows that the strong phase of shaking was very short, about 1.5 seconds, and

[1] Nishkian Emeritus Professor and Research Engineer, Earthquake Engineering Research Center, University of California, Berkeley
[2] Professor, Department of Civil Engineering, University of Southern California, Los Angeles
[3] Graduate Student, University of California, Berkeley

consisted of four successive acceleration pulses, one of triangular shape and a very high PGA of 0.5g but a short duration of only 0.3 seconds. The four acceleration pulses resulted in one displacement pulse of about 23 cm and a duration of 1.3 seconds. This EQGM did relatively little damage because of the very short duration of the pulses and of the total phase of the strong ground motions (Cloud, 1967). For this reason it did not receive much attention in the engineering community.

Perhaps the first destructive earthquake in the United States with recorded accelerograms that contained acceleration pulses with very severe damage potential was the February 9, 1971, San Fernando earthquake with M=6.2. The derived records from the recorded accelerations at the top of the Pacoima Dam and at the Van Norman Dam have acceleration pulses that resulted in very large incremental velocities of 158 cm/sec at Pacoima and 172 cm/sec for Van Norman. The senior author and his researchers carried out several studies on the effects of these recorded and derived EQGMs on buildings and compared the effects with those that can be expected from the design earthquake specified in the seismic codes. In one paper (Bertero, et al., 1976), they offered a series of conclusions and recommendations among which the following are considered relevant for this review: (1) When safety rather than serviceability controls the design, large but controllable inelastic deformations can be tolerated; (2) The use of inelastic design response spectra (IDRS) derived directly from recommended linear elastic design response spectra (LEDRS) through displacement ductility factors as suggested by present methods does not appear to be conservative for buildings located in the immediate area of causative faults; (3) The main drawback of present methods is that direct derivation of IDRS from LEDRS has been shown to be basically untenable due to the fact that the dynamic characteristics of the critical ground excitations for elastic and inelastic responses are completely different. While periodic pulses having frequencies equal to those of the predominant modes of vibration of the building constitute the critical ground motions for linear-elastic systems, a critical inelastic response can be induced by accelerations of equal to or greater value than the effective seismic resistance coefficient of the structure; (4) Near-fault records of the San Fernando earthquake, such as those for Pacoima and Van Norman dams contain severe long acceleration pulses which resulted in large velocity increments. These have been found to be characteristic of near-fault motions. Results of an analytical study of a building near the fault zone using the Pacoima record correlated well with the observed damage. This damage appears to have been the result of only a few large displacement excursions rather than of numerous oscillations; (5) Unusually large ground velocities may be developed at near fault sites. Methods for constructing elastic and inelastic design response spectra should reflect the larger values recorded at such sites. Additional research is needed to establish bounds on the different parameters that define the characteristics of severe long pulses, i.e., the largest incremental velocity and associated effective acceleration that can be developed according to the mechanical (dynamic) characteristics of the soil present at a site. These values will enable the design engineer to determine an upper bound on the energy that can be transmitted to the foundation of the structure so that the structure can be designed accordingly. It is also necessary to know the number of long severe pulses that can occur at the site since repeated pulses can lead to an incremental (crawling) type of collapse. Furthermore, the above authors describe a procedure that could be implemented for

establishing design earthquakes for near-fault sites. In 1975, in discussing the magnitudes, aftershocks and fault dynamics of the 1971 San Fernando earthquake, Bolt gave a detailed explanation for the resultant large horizontal displacement pulse obtained from the recorded EQGMs on the abutment of Pacoima Dam. He called the ground velocity and displacement pulses the source "fling." Bolt also emphasized that this pulse-like ground displacement seemed likely to be the normal condition because it had a theoretical justification in the elastic rebound mechanics of a rupturing fault.

In 1979 the Imperial Valley earthquake produced several records of EQGMs which contained severe acceleration pulses resulting in severe velocity and displacement pulses. The record obtained at the James Road station (approximately 2.5 miles from the fault trace) had a long duration acceleration pulse having a PGA of 0.36g which resulted in an incremental velocity of 160 cm/sec. As reported by Singh in 1981 and in more detail in 1985, the presence of these severe pulses had a theoretical justification which was that given by Bolt in 1975. Anderson and Bertero investigated the effects of several of these recorded EQGMs on flexible steel frame buildings. The results of this study are summarized in an ASCE paper (Anderson and Bertero, 1987) which contained the following observations that are relevant to this critical review: (1) In certain geological regions, such as the near-fault region, structures may be subjected to impulse-type EQGMs that can be particularly damaging to the lower floors of buildings. This part of a structure is more critical than the upper floors due to the high axial loads carried by the columns. Under an impulse-type load, the deformation tends to be concentrated in the lower floors, thereby increasing the interaction effects between lateral displacement and axial load (P-delta); (2) The peak ground acceleration is not a very accurate means of classifying the severity of strong ground motion with regard to structural damage potential. In order to obtain a more meaningful classification, the use of other parameters such as incremental velocity and peak ground displacement may be required; (3) Current design response spectra do not recognize two important factors that are the result of impulse-type ground motions: (a) the increase in spectral response in the long-period region (1-4 seconds) that results in significantly higher accelerations, velocities and displacements that should be included in spectra used to design structures in close proximity to active faults, and (b) the increase in the ductility requirement for more rigid structures which is due to the increase in the ratio of the pulse duration to the period of the structure; (4) This study has shown that EQGMs resulting from the same earthquake may have significant variations in dynamic characteristics due to such factors as local geological conditions, directionality of fault propagation and distance from the fault plane. In addition, the nonlinear structural response is sensitive to the duration of the acceleration pulse relative to the fundamental period of the structure and to the yield resistance seismic coefficient of the designed structure. These factors combine to create a large uncertainty in the establishment of a design EQGM which must be taken into account in the design process; (5) These studies have shown that a structure in the near-fault region may experience a dynamic response that is twice that of a similar structure located at some distance from a fault even though the peak ground accelerations are about the same; (6) The El Centro record used for evaluating the response of structures has very little damage potential when compared with the more recent Imperial Valley (1979)

records. This illustrates the importance of directionality effects associated with the direction of fault rupture propagation.

Although the presence of severe pulses creating impulsive types of EQGMs might be mainly a characteristic of near-source records, they have also been recorded at sites far from the earthquake source, such as the Bucharest accelerogram which was recorded at a distance of 150 km from the epicenter of the 1977 Vrancea (Romania) earthquake, resulting in severe damage to many modern buildings in Bucharest. Furthermore, stations located on the lake bed zone of Mexico City during the 1985 Michoacan earthquake, with an epicentral distance of about 350 km, caused severe damage to low-rise modern buildings. The senior author made these observations: Although the recorded EQGMs were periodical (practically harmonic) with periods higher than 1.5 seconds and with PGAs up to 0.23g, from the point of view of their effect to buildings with relatively low yield strength capacities, these EQGMs were of the impulsive type, i.e., a series of reversal acceleration pulses.

In view of the results obtained in the above studies and their publication and oral presentation to the earthquake community, it has been very surprising that until 1991, the effects of impulsive types of EQGMs have not been incorporated in seismic code provisions for the practical analysis and design of civil engineering structures, even for those located in the near-field of the source (exceptions have been for the design of special facilities such as dams (Bolt, 1997). The 1991 UBC earthquake requirements for seismic isolated structures introduced near-source factors related to the proximity of the building or structure to known faults with established magnitudes and slip rates in determining the seismic coefficient.

For the response analysis as well as the design of conventional building structural systems it took additional dramatic records with severe pulses that were obtained in the Northridge (1994) and the Kobe (1995) earthquakes to convince the experts (researchers and practitioners) that in the very near field, strong shaking and pulses were more likely to be the rule rather than the exception (Jennings, 1997; Bolt, 1997). Thus the 1997 UBC introduced near-source factors into its earthquake design regulations for buildings using conventional structural systems. Although the introduction of these factors in the code seismic regulation has been a step forward toward the recognition of the importance of the effects of impulsive type of EQGMs, some concerns remain about the reliability of the required procedures, particularly in the following two areas: (1) That the occurrence of these pulses has been limited to sites located within 15 km of the known seismic source and (2) that it is doubtful that the effects of these pulses on the building response can be obtained by simply increasing the required base shear which is determined using as a base a LEDRS.

REFERENCES

Ambraseys, N. (1964), "The Skopje Earthquake of July 26, 1963", *Proceedings*, Skopje International Seminar on Earthquake Engineering, Skopje, Yugoslavia.

Anderson, J.C., and Bertero, V.V. (1987), "Uncertainties in Establishing Design Earthquakes," *Journal of Structural Engineering*, Vol. 113, No. 8, pp. 1709–1724, ASCE, Reston, VA.

Bertero, V.V., et al. (1976) "Establishment of Design Earthquakes—Evaluation of Present Methods," *Proceedings*, International Symposium on Earthquake Structural Engineering, University of Missouri-Rolla, St. Louis, Missouri, Vol. 1, pp. 551–580.

Bolt, B. A. (1975), "San Fernando Earthquake, 1971: Magnitudes, Aftershocks and Fault Dynamics," Chapter 21. Bulletin 196. California Division of Mines and Geology. Sacramento.

Bolt, B. A. (1997), "Discussion of Enduring Lessons and Opportunities Lost from the San Fernando Earthquake of February 9, 1971," by Paul C. Jennings, *Earthquake Spectra*, Vol. 13, No. 3, pp. 545–547, EERI, Oakland, CA.

Cloud, W.K., and V. Perez (1967), "Accelerograms-Parkfield Earthquake," *Bulletin of the Seismological Society of America*, 57(6), pp. 1179–1192.

Despeyroux, J. (1960), "The Aqadir Earthquake of February 29th, 1960. Behavior of Modern Buildings during the Earthquake," *Proceedings*, Second World Conference on Earthquake Engineering," Tokyo and Kyoto, Japan, pp. 21–542.

Housner, G.W., and D.E. Hudson (1958), "The Port Hueneme Earthquake of March 18, 1957," *Bulletin of the Seismological Society of America*, 48(2), pp. 163–168.

Jennings, P.C. (1997), "Enduring Lessons and Opportunities Lost from the San Fernando Earthquake of February 9, 1971," *Earthquake Spectra*, Vol. 13, No. 1 pp. 25–53, EERI, Oakland, CA.

Minami, J.K. (1965), "Relocation and Reconstruction of the Town of Barce, Cyrenaica, Libya, Damaged by the Earthquake of 21 February, 1963," *Proceedings* , Third World Conference on Earthquake Engineering, pp. 96–108, Aukland and Wellington, New Zealand.

Rosenblueth, E., and J. Prince (1965), "El Temblor de San Salvador, 3 de Mayo, 1965: Ingenieria Sismica," *Rev. Soc. Mexican Ing. Sism. 3(2)*, pp. 33–60.

Singh, J.P. (1985), "Earthquake Ground Motions: Implications for Designing Structures and Reconciling Structural Damage," *Earthquake Spectra*, 1(2), pp. 1709–1724, EERI, Oakland, CA.

UBC(1991-1997), *Uniform Building Code*, International Conference of Building Officials (ICBO), Whittier, CA.

APPENDIX B

CONCEPTUAL DESIGN VS ORIGINAL KAJIMA BUILDING COMPARISON

CONCEPTUAL DESIGN - ORIGINAL KAJIMA BUILDING COMPARISON

	Conceptual	Kajima
Total Mass (ton.)	26095	29711
T1 (sec)	1.75	2.15
T2 (sec)	0.62	0.70
Shear Base Capacity (Constant Load Pattern) (kN)	78991	62652
Shear Base Capacity (Linear Load Pattern) (kN)	61244	48576
First story mechanism (kN)	104798	72109
Shear Base Capacity (Constant Load Pattern) (Weight)	0.31	0.21
Shear Base Capacity (Linear Load Pattern) (Weight)	0.24	0.17
First story mechanism (Weight)	0.41	0.25

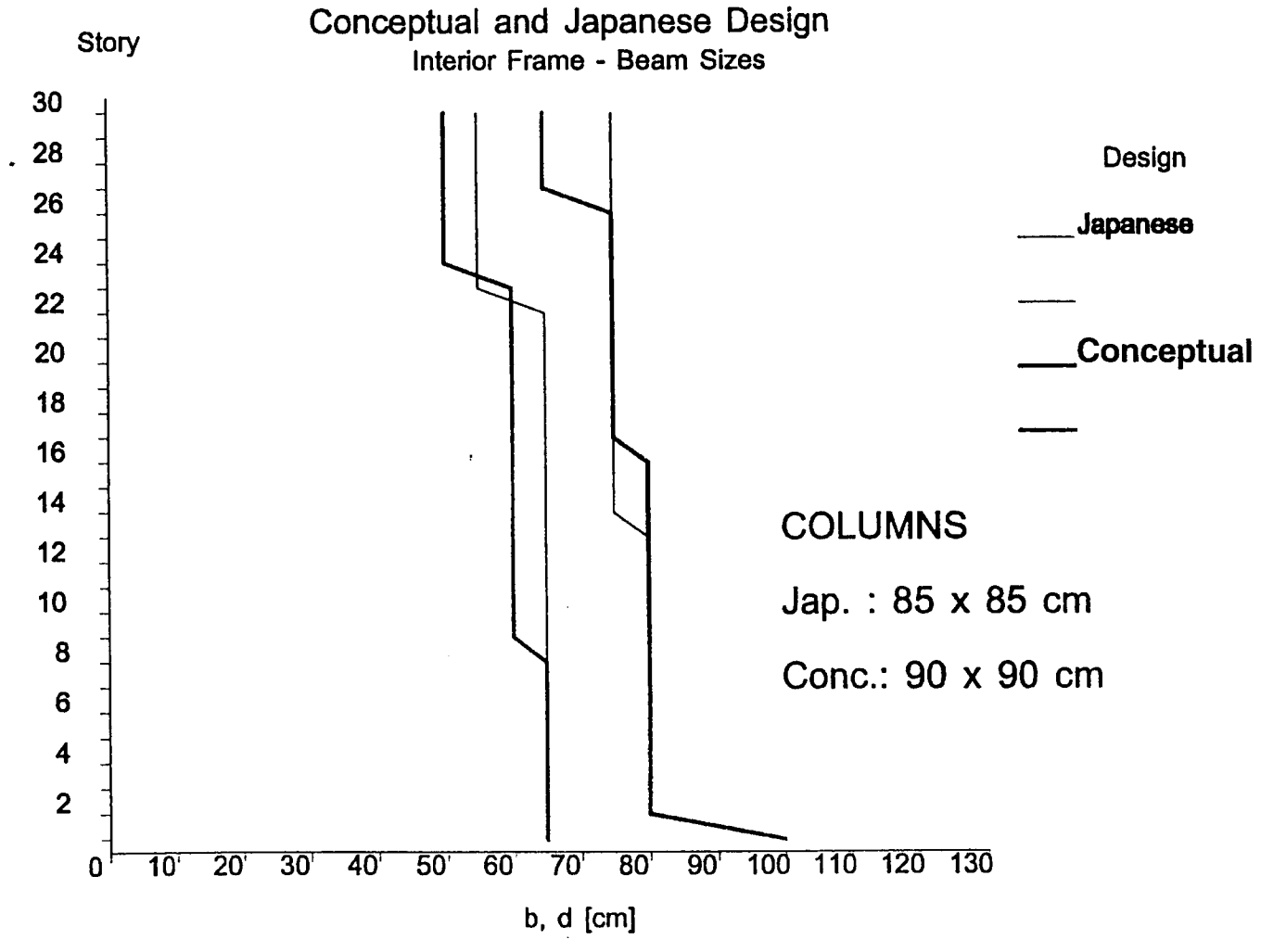
Conceptual and Japanese Design
Interior Frame - Beam Sizes
Story
30
28
26
24
22
20
18
16
14
12
10
8
6
4
2
0
10
20
30
40
50
60
70
80
90
100
110
120
130
b, d [cm]
Design
Japanese
Conceptual
COLUMNS
Jap. : 85 x 85 cm
Conc.: 90 x 90 cm

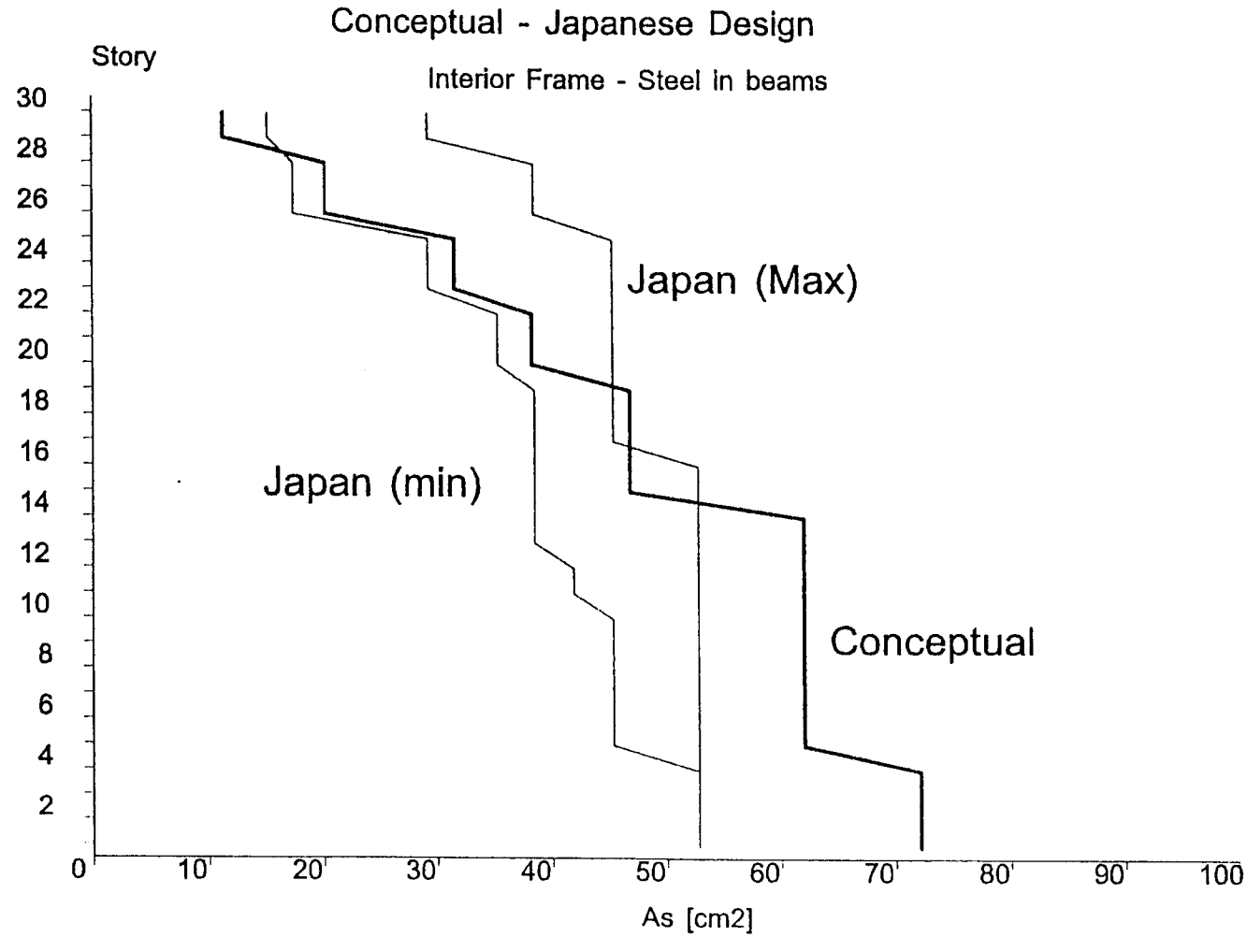
Conceptual - Japanese Design
Interior Frame - Steel in beams
Story
30
28
26
24
22
20
18
16
14
12
10
8
6
4
2
0
10
20
30
40
50
60
70
80
90
100
As [cm2]
Japan (Max)
Japan (min)
Conceptual

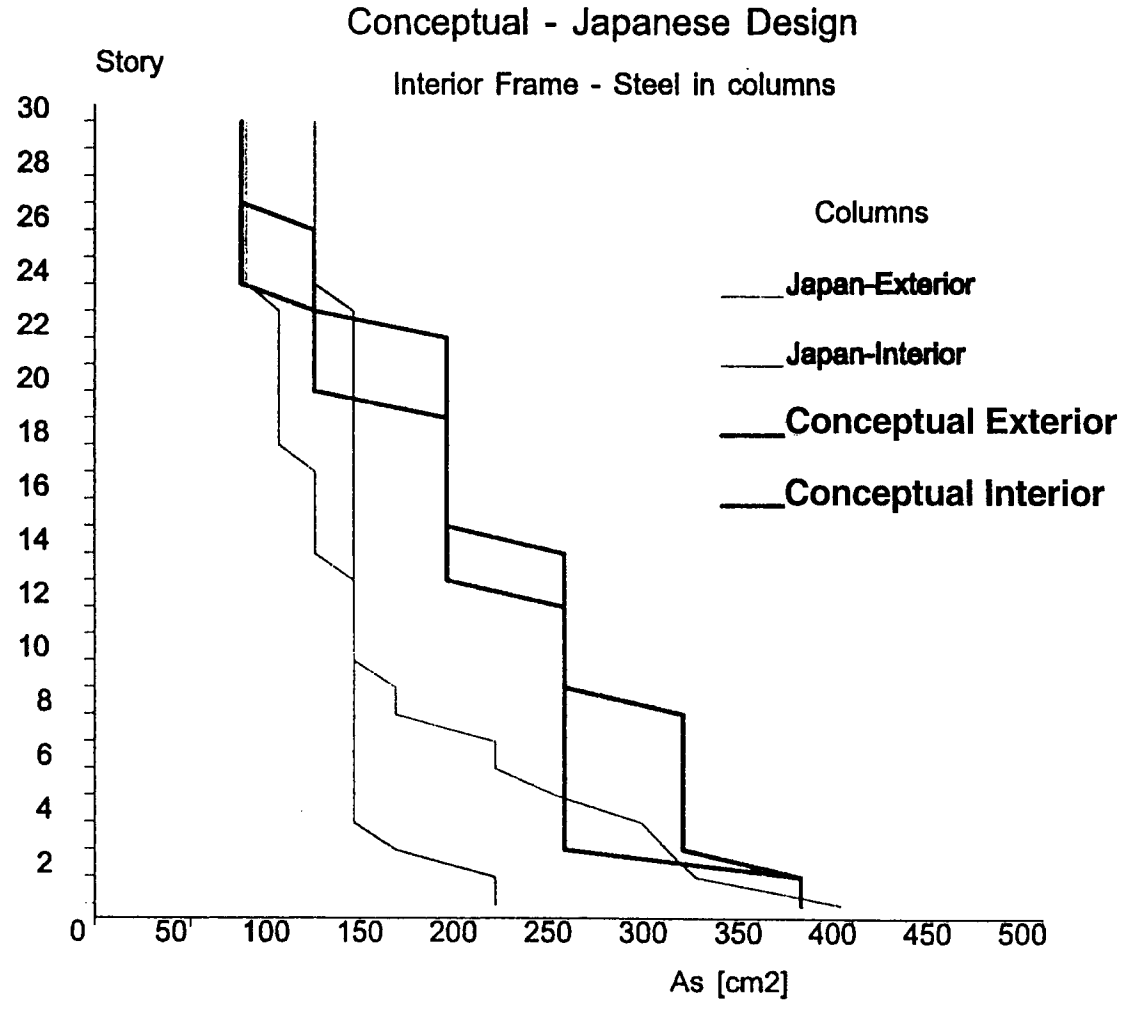
Conceptual - Japanese Design
Interior Frame - Steel in columns
Story
30
28
26
24
22
20
18
16
14
12
10
8
6
4
2
0
50
100
150
200
250
300
350
400
450
500
As [cm2]
Columns
Japan-Exterior
Japan-Interior
Conceptual Exterior
Conceptual Interior

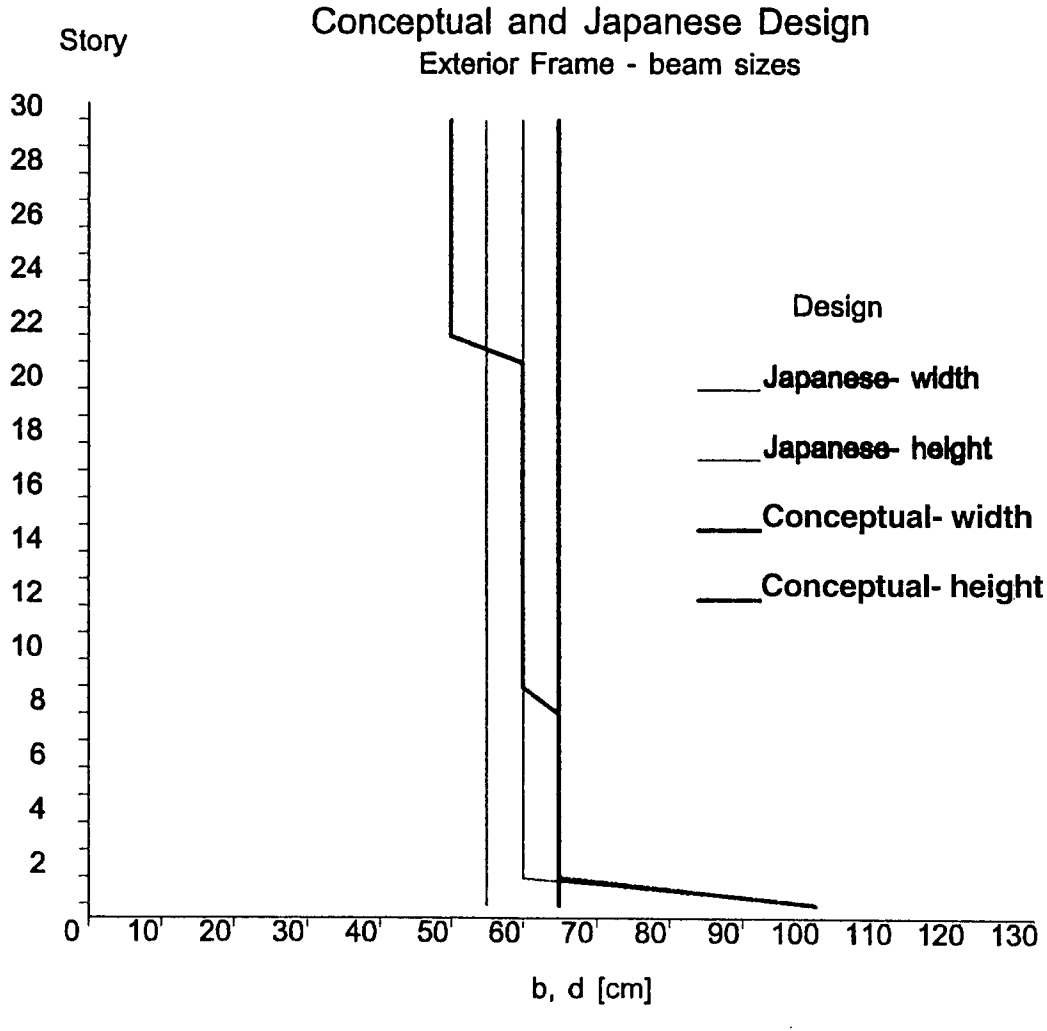

Columns
Conceptual (all)
90 x 90 cm

Japan (exterior)
85 x 85 (1-22)
80 x 80 (23 -30)

Japan (interior)
85 x 85 (1)
80 x 85 (2 - 22)

75 x 80 (23 - 30)

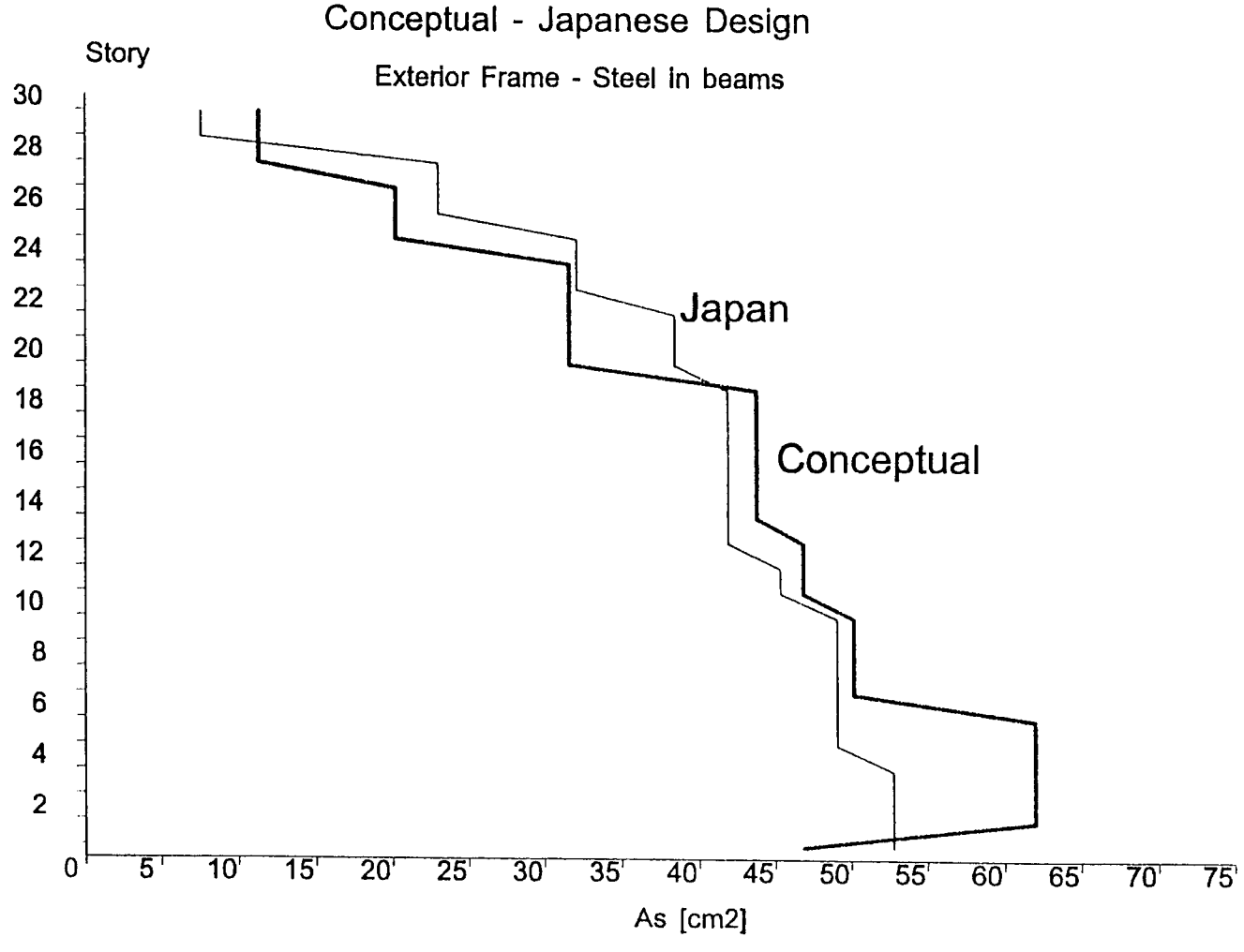
Conceptual - Japanese Design
Exterior Frame - Steel in beams
Story
30
28
26
24
22
20
18
16
14
12
10
8
6
4
2
0
5
10
15
20
25
30
35
40
45
50
55
60
65
70
75
As [cm2]
Japan
Conceptual

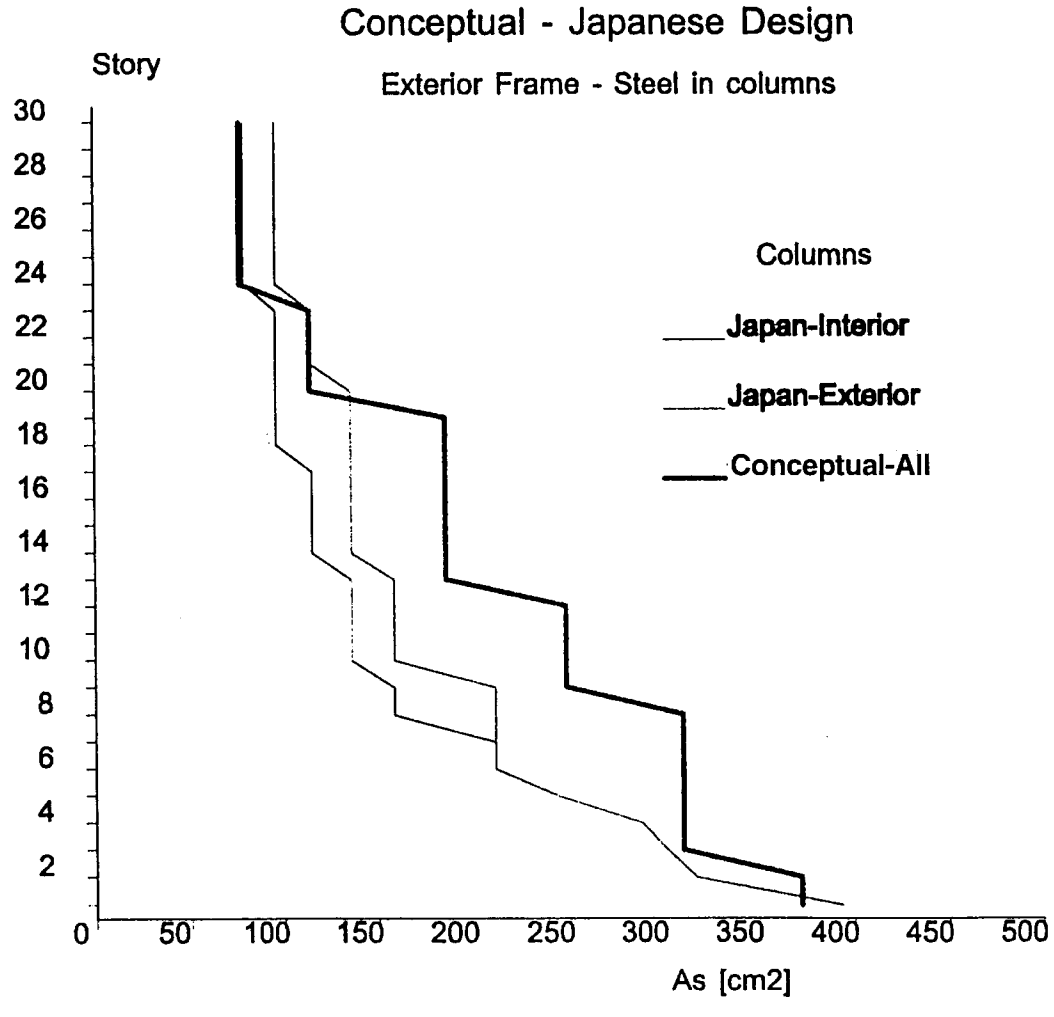
Conceptual - Japanese Design
Exterior Frame - Steel in columns
Story
30
28
26
24
22
20
18
16
14
12
10
8
6
4
2
0
50
100
150
200
250
300
350
400
450
500
As [cm2]
Columns
Japan-Interior
Japan-Exterior
Conceptual-All

PEER REPORTS

PEER reports are available from the National Information Service for Earthquake Engineering (NISEE). To order PEER reports, please contact the Pacific Earthquake Engineering Research Center, 1301 South 46th Street, Richmond, California 94804-4698. Tel.: (510) 231-9468; Fax: (510) 231-9461.

PEER 2000/01 *Further Studies on Seismic Interaction in Interconnected Electrical Substation Equipment.* Armen Der Kiureghian, Kee-Jeung Hong, and Jerome L. Sackman. November 1999. $20.00

PEER 1999/14 *Seismic Evaluation and Retrofit of 230-kV Porcelain Transformer Bushings.* Amir S. Gilani, Andrew S. Whittaker, Gregory L. Fenves, and Eric Fujisaki. December 1999. $26.00

PEER 1999/11 *Performance Evaluation Database for Concrete Bridge Components and Systems under Simulated Seismic Loads.* Yael D. Hose and Frieder Seible. November 1999. $20.00

PEER 1999/09 *Performance Improvement of Long Period Building Structures Subjected to Severe Pulse-Type Ground Motions.* James C. Anderson, Vitelmo V. Bertero, and Raul Bertero. October 1999. $26.00

PEER 1999/08 *Envelopes for Seismic Response Vectors.* Charles Menun and Armen Der Kiureghian. July 1999. $26.00

PEER 1999/07 *Documentation of Strengths and Weaknesses of Current Computer Analysis Methods for Seismic Performance of Reinforced Concrete Members.* William F. Cofer. November 1999. $15.00

PEER 1999/06 *Rocking Response and Overturning of Anchored Equipment under Seismic Excitations.* Nicos Makris and Jian Zhang. November 1999. $15.00

PEER 1999/05 *Seismic Evaluation of 550 kV Porcelain Transformer Bushings.* Amir S. Gilani, Andrew S. Whittaker, Gregory L. Fenves, and Eric Fujisaki. October 1999. $15.00

PEER 1999/04 *Adoption and Enforcement of Earthquake Risk-Reduction Measures.* Peter J. May, Raymond J. Burby, T. Jens Feeley, and Robert Wood. $15.00

PEER 1999/03 *Task 3 Characterization of Site Response General Site Categories.* Adrian Rodriguez-Marek, Jonathan D. Bray, and Norman Abrahamson. February 1999. $20.00

PEER 1999/02 *Capacity-Demand-Diagram Methods for Estimating Seismic Deformation of Inelastic Structures: SDF Systems.* Anil K. Chopra and Rakesh Goel. April 1999. $15.00

PEER 1999/01 *Interaction in Interconnected Electrical Substation Equipment Subjected to Earthquake Ground Motions.* Armen Der Kiureghian, Jerome L. Sackman, and Kee-Jeung Hong. February 1999. $20.00

PEER 1998/08 *Behavior and Failure Analysis of a Multiple-Frame Highway Bridge in the 1994 Northridge Earthquake.* Gregory L. Fenves and Michael Ellery. December 1998. $20.00

PEER 1998/07 *Empirical Evaluation of Inertial Soil-Structure Interaction Effects.* Jonathan P. Stewart, Raymond B. Seed, and Gregory L. Fenves. November 1998. $26.00

PEER 1998/06 *Effect of Damping Mechanisms on the Response of Seismic Isolated Structures.* Nicos Makris and Shih-Po Chang. November 1998. $15.00

PEER 1998/05 *Rocking Response and Overturning of Equipment under Horizontal Pulse-Type Motions.* Nicos Makris and Yiannis Roussos. October 1998. $15.00

PEER 1998/04 *Pacific Earthquake Engineering Research Invitational Workshop Proceedings, May 14–15, 1998: Defining the Links between Planning, Policy Analysis, Economics and Earthquake Engineering.* Mary Comerio and Peter Gordon. September 1998. $15.00

PEER 1998/03 *Repair/Upgrade Procedures for Welded Beam to Column Connections.* James C. Anderson and Xiaojing Duan. May 1998. $33.00

PEER 1998/02 *Seismic Evaluation of 196 kV Porcelain Transformer Bushings.* Amir S. Gilani, Juan W. Chavez, Gregory L. Fenves, and Andrew S. Whittaker. May 1998. $20.00

PEER 1998/01 Unassigned.